BRITISH THESIS SERVICE

DX236631

EVOLUTION OF PARTICLE SIZE DISTRIBUTION IN SUSPENSION POLYMERISATION REACTIONS

By

Fatemeh Jahanzad

A Doctoral Thesis

Submitted in partial fulfilment of the requirements for the award of the

Doctor of Philosophy of the Loughborough University

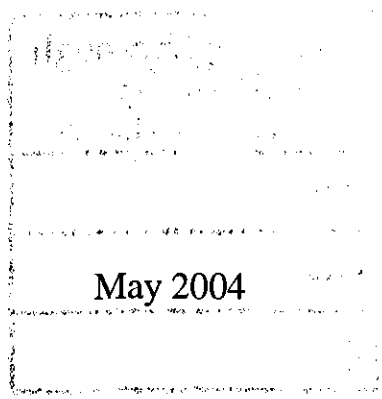

May 2004

to my great family ...

specially to my husband, Shahriar, for his love, friendship, support and patience

and to my parents for their love, support and encouragement throughout my studies

ACKNOWLEDGEMENTS

I wish to express my sincere gratitude to my supervisor, Professor B.W. Brooks, for his valuable help and guidance. I would also like to offer my sincerest thanks and appreciation to my husband, Dr Shahriar Sajjadi, for his support, help, and consultation.

Grateful appreciation is extended to Professor Wakeman, Head of the Department of Chemical Engineering, and to Professor Rielly my director of research.

It is pleasing to acknowledge the help of Mr A. Milne the laboratory technician and Mr Frank Page the operator of scanning electron microscope.

I also value the provision given to me by Loughborough University in funding my studentship.

TABLE OF CONTENTS

ABSTRACT

Suspension polymerisation processes are commercially important for the production of polymer beads having wide applications. Polymers produced by suspension polymerisation can be directly used for particular applications such as chromatographic separations and ion-exchange resins. Particle Size Distribution (PSD) may appreciably influence the performance of the final product. Therefore, the evolution of PSD is a major concern in the design of a suspension polymerisation process.

In this research, methyl methacrylate (MMA) has been used as a model monomer. A comparative study of MMA suspension polymerisation and MMA/water dispersion was carried out, for the first time, to elaborate the evolution of mean particle size and distribution. Polyvinyl alcohol (PVA) and Lauroyl Peroxide (LPO) have been used as stabiliser and initiator, respectively. Polymerisation experiments were carried out using a 1-litre jacketed glass reactor equipped with a turbine impeller and a condenser. The stabiliser, initiator and chain transfer concentrations, inhibitor concentration and type, reaction temperature, impeller speed, and monomer hold up were used as variables. A mathematical model was developed to predict the kinetics of polymerisation as well as the evolution of PSD by population balance modelling. The experimental results were compared with the model predictions.

From the comprehensive experimental results, the characteristic intervals of a typical suspension polymerisation were realised as:

1) *Transition stage* during which PSD narrows dramatically and drop size decreases exponentially due to higher rate of drop break up in comparison with drop coalescence until a steady state is reached. The importance, and even the existence, of the transition stage have been totally ignored in the literature. The results indicate that increasing the impeller speed, and PVA concentration will lead to a shorter transition period. Also increasing the rate of reaction, via increasing initiator concentration, and reaction temperature will shorten this period.

2) *Quasi steady-state stage* during which the rate of drop break up and drop coalescence are almost balanced leading to a steady-state drop size and distribution. The occurrence of this stage is conditional. Low impeller speed and PVA concentration may remove the quasi steady-state stage completely and drops may start growing considerably after a sharp decrease in size during the transition stage.

3) *Growth stage* during which the rate of drop break up considerably falls below the rate of drop coalescence due to the viscosity build up in drops leading to drop enlargement and PSD broadening. Results show that the onset of the growth stage may not be fixed and it depends on the balance of the forces acting on drops. The onset of the growth stage in terms of time was advanced with decreasing stirring speed and PVA concentration and increasing monomer hold up. Under a static steady state, which is formed when a high concentration of PVA is used, there is almost no growth.

4) *Identification stage* during which a solid-liquid suspension is attained and the PSD and mean particle size remain unchanged afterwards. The onset of this stage appears to be fairly constant for different formulations.

The developed model could fairly predict the rate of polymerisation. It was also capable of predicting the evolution of particle size average and distribution qualitatively in the course of polymerisation. The results can be used as a guideline for the control of particle size and distribution in suspension polymerisation reactors. A more quantitative exploitation of the model has been left for a future research.

INTRODUCTION

Suspension polymerisation is widely used in industry to produce polymer beads for a variety of applications such as vinyl chloride homo- and copolymers, styrene homopolymers including general purpose, expandable, and, high impact polystyrene and co- or ter-polymers (such as poly(styrene-acrylonitrile), and poly(acrylonitrile-butadiene-styrene), and methyl methacrylate homo- and coplymers. Apart from these commodity products, there are "high value added" products, such as high surface area polystyrene and polyacrylate-based beads with applications in chromatographic separation media as ion exchange resins and as supports for enzyme immobilisation. With the increasing growth of biotechnology, and the increasing importance of immobilised substrates, demands are steadily growing for the large-scale production of base support materials.

For many applications beads with consistent quality and a size distribution as narrow as possible are required. Despite the fact that suspension polymerisation is a rather old technology, much was not known about this process until the 1990s when the importance of this process for production of polymer bead supports was realised. There are thus considerable incentives for understanding suspension polymerisation processes.

The literature related to the suspension polymerisation is not vast, and several controversial issues are still being studied, and universally accepted conclusions are scarce. A major property of the suspension resulting from a suspension polymerisation is the size of particles. Control of the bead particle size, which is the key to guarantee the quality of bead products, is becoming of great industrial importance, as the production of an increasing number of products involves suspension polymerisation processes. The qualitative understanding of the quantities, which control both the average particle size and the PSD, is quite important. The objective of this research work is to investigate the effect of various reaction and mixing parameters on the evolution of particle size and size distribution in suspension polymerisation reactors.

CHAPTER ONE

LITERATURE REVIEW

INTRODUCTION

The term "suspension polymerisation" describes a process in which monomer is dispersed in the water phase, with the aid of mixing and suspending agents (stabilisers), and transformed to polymer "bead" or "pearl" particles. Suspension polymerisation produces polymer beads, typically with the diameter in the range of 10 μm to 5 mm.

Suspension polymerisation has the following advantages compared with the other free-radical polymerisation processes (bulk, solution, and emulsion): easy heat removal and temperature control; low dispersion viscosity; low levels of impurities in the polymer product (compared with emulsion polymerisation); low separation costs (compared with emulsion polymerisation); and final product in particle form. On the other hand, among the disadvantages of suspension polymerisation one may refer to lower productivity for the same reactor capacity (compared with bulk); wastewater problems; polymer build-up on the reactor wall, baffles, agitators, and other surfaces; no commercial continuous process operability yet; and difficulty in producing homogenous copolymer composition with suspension versus emulsion polymerisation because of the lower interfacial area (particle/water).

Traditionally, a number of important commercial resins are manufactured by this process, including poly(vinyl chloride) (PVC) and copolymers, styrene resins (general purpose polystyrene, expandable polystyrene (EPS), high impact polystyrene (HIPS), poly(styrene-acrylonitrile) (SAN), poly(acrylonitrile-butadiene-styrene) (ABS), styrenic ion-exchange resins, poly(methyl methacrylate) (PMMA) and copolymers, poly(vinyl acetate), etc.

High surface area polystyrene and polyacrylate-based beads have become increasingly important in chromatographic separation media (e.g.; as ion exchange resins and as

supports for enzyme immobilisation) as sorbents both for liquid and gas phase streams and have found a wide demand in the areas of interpenetrating polymer networks, thermally and chemically resistant materials and optical materials. With the increasing growth of biotechnology, and the increasing importance of immobilised substrates, demands are steadily growing for the large-scale production of base support materials. For such applications beads with consistent quality and a size distribution as narrow as possible are required. Despite the fact that the first suspension polymerisation reaction was carried out some 80 years ago, much was not known about this process until the 1990s when the importance of this process for production of polymer bead supports was realised.

Inverse (or reversed-phase) suspension polymerisation processes have been developed to polymerise polar monomers, such as acrylamide (e.g., Dimonie et al., 1982; Lee et al., 2001). The so-called water-in-oil suspension polymerisation comprises an aqueous solution, containing the hydrophilic monomer(s) and initiator(s), which is dispersed in a nonpolar hydrocarbon media and polymerised. The use of perflourocarbon fluids has extended the scope of the suspension polymerisation method to monomers and initiators that can not be used due to their high solubility and reactivity in conventional suspension media (Zhu, 1996).

In a suspension polymerisation process, monomer is initially dispersed in the water phase, with the aid of mixing and suspending agents (stabilisers), to form a liquid-liquid dispersion. Subsequent polymerisation inside drops transforms the liquid monomer drops into solid polymer particles. Therefore, the study of liquid-liquid dispersion seems to be the first step toward the understanding of the major mechanisms involved in a typical suspension polymerisation reactor. On the other hand, the kinetics of polymerisation reactions and the continuous variation of intrinsic properties of drops affect the particle size and particle size distribution dramatically.

In order to study the variations of particle size and particle size distribution in a suspension polymerisation process one should have an understanding of liquid-liquid dispersions and the effects of different mixing parameters on drop size and drop size distribution, on one side, and the kinetics of the polymerisation reactions and effect of

varying viscoelastic properties of drops on the particle size, on the other side, and the interactions between these two phenomena.

In this chapter the main features of liquid-liquid dispersions are discussed first. Then an overall view of the kinetics of polymerisation reactions and effects of these reactions on the nature of the drops are presented. In the last section of this chapter a brief review of the mathematical modelling of liquid-liquid dispersions and suspension polymerisation reactors are presented. The reader should note that some literature review has been given in the "introduction" of the result sections in chapter 3. Those reviews are not repeated here.

1.1 LIQUID-LIQUID DISPERSION

Liquid-liquid dispersions play an important role in many industrial processes including heterogeneous chemical reactions, extraction, emulsion and suspension polymerisation, and emulsion preparation. Stirred tanks represent the most popular equipment to carry out these operations. The geometry and scale of the vessel and impeller, agitation rate and physical properties of the mixed phases, determine the drop breakage and coalescence rates and resulting drop size distributions.

Dispersing a liquid into another immiscible liquid with the help of agitation makes drops of dispersed liquid (dispersed phase) suspended in the continuous liquid (phase). Liquid-liquid dispersions are extremely unstable and separate into two phases if agitation is ceased. To acquire a sufficient stability, a third component, called a *surfactant* or *emulsifier* is required. Surfactants will reduce the interfacial tension and assist the drop break up. Furthermore, they hinder drop coalescence by adsorption on the surface of drops. In the terminology of the suspension polymerisation technology, these materials are usually referred to as *stabilisers*.

Liquid-liquid dispersions can be in laminar, intermediate or turbulent regions depending on the intensity of energy dissipation rate or the intensity of the agitation. The value of tank Reynolds' Number (Re_T) is a criterion used to measure the intensity of agitation. For $Re_T > 10^4$ the liquid-liquid dispersion is considered to be under turbulent conditions. For most suspension polymerisations processes this condition is valid and so only the turbulent flow and its features are discussed here. Drop break up and coalescence in

stirred tanks with a turbulent flow are of prime importance because of their drastic influence on the size of drops.

In this section the concepts corresponding to liquid-liquid dispersions (break up, coalescence, mean drop size and drop size distribution) are discussed and then a brief review of the role of stabilisers in liquid-liquid dispersions is presented.

1.1.1 Turbulent flow

Turbulent flow in a stirred tank is an irregular condition of flow in which various components show a random variation with time and space so that statistically distinct average values can be determined (Hinze, 1987). The fluctuations of velocity due to a random character of a turbulent flow will result in a range of frequencies. It is assumed that the fluid eddies are sized from large to small. Large eddies transfer their kinetic energy to the smaller ones until the kinetic energy is transferred to the smallest eddies. The transfer takes place without energy dissipation. But the smallest eddies dissipate the kinetic energy as heat to overcome the viscous forces. The macroscale of turbulence, l, is defined as the scale of large eddies and is approximated by the width of the impeller. The microscale of turbulence η is defined as the scale of the smallest or maximum energy dissipation eddies (Kolmogoroff, 1941).

The relative velocity fluctuation components are defined as root mean square values in three space coordinates. If the volume under consideration is small enough compared to the macroscale of turbulence, l, the local isotropy can be considered and so the relative velocity between two points in a very small volume is independent of the radius vector of two points (Kolmogoroff, 1941; Shinnar and Church, 1960).

For high levels of turbulence, high tank Reynolds number (Re_T>10^4), the range of energy containing eddies (large eddies) and the range of maximum dissipation eddies (the smallest eddies) are sufficiently far apart ($l \gg \eta$) and the smallest eddies are independent from the large eddies. For this case Kolmogoroff (1941) postulated that the turbulence is statistically in equilibrium and uniquely determined by the energy dissipation per unit mass (ε) and kinematic viscosity (ν). This range is called the universal equilibrium range and is subdivided to two subranges: the inertial subrange where the velocity fluctuation for two points with distance d ($u^2(d)$) is independent of ν and solely dependent on ε,

$$u^2(d) = C_1 \varepsilon^{2/3} d^{2/3} \qquad (1.1.1)$$

and the viscous subrange where the velocity fluctuation is dependent on both ε and ν (Shinnar and Church, 1960).

$$u^2(d) = C_2 (\varepsilon / \nu) d^2 \qquad (1.1.2)$$

C_1 and C_2 in equations 1.1.1 and 1.1.2 are universal constants.
The microscale of turbulence, η, is given by equation 1.1.3 and has been experimentally verified (Shinnar and Church, 1960).

$$\eta = (\nu^3 / \varepsilon)^{1/4} \qquad (1.1.3)$$

The energy dissipation throughout the vessel is not uniform. It has been found that most of the energy is dissipated in the impeller zone rather than in the rest of the vessel (circulation zone) (Rushton et al., 1950; Tavlarides and Stamatoudis, 1981). Rushton et al. (1950) showed that for a high tank Reynolds number ($Re_T > 10^4$) the average energy dissipation rate per unit mass, ε, is independent of the property of the liquid and a function only of the vessel and impeller geometries. In this case:

$$\varepsilon = k_\varepsilon N_I^3 D_I^2 \qquad (1.1.4)$$

where N_I and D_I are the agitation speed and agitator diameter, respectively. k_ε is a constant that depends on geometries of tank and agitator.

1.1.2 Drop Break up

In a liquid-liquid dispersion under turbulent flow conditions, drop break up and coalescence occur continuously. Drop break up is the result of the collision of eddies with drops. Eddies with a scale smaller or the same size as the drop diameter may break the drop when they collide with the drop. Eddies with a scale larger than the drop diameter cannot break the drop and move it when they collide (Shinnar, 1961).

If the average diameter of drops is much larger than the microscale of turbulence but still much smaller than the macroscale of turbulence ($l \gg d \gg \eta$), the system is in inertial subrange. Under such conditions equation 1.1.1 is valid and drops break up due to velocity fluctuations. For drop diameters smaller than η, break up is the result of viscous shear forces (Shinnar, 1961).

Whether or not a drop can be broken depends on the relative magnitude of the restoring forces and the external deforming forces. In other words, a drop can be broken only when it gains enough energy to compensate for the interface energy increase due to an increase in the total surface area and viscous energy of drop. The main external deforming forces are turbulent pressure fluctuations and viscous stress and the restoring forces are mainly due to the interfacial tension and internal viscous stress. Under the condition of inertial subrange ($l \gg d \gg \eta$), the external viscous stress is negligible compared to turbulent pressure fluctuations. Hinze (1955) introduced two dimensionless groups to account for the force balance when both interfacial tension and dispersed phase viscous forces contribute to drop stability. One is a generalised Weber group, *We*, which is the ratio of turbulent energy to interfacial energy, and the other is a viscosity group, *Vi*, which is the ratio of internal viscous energy to interfacial energy of a drop with diameter *d*:

$$We = \rho_c u^2(d) d / \sigma \tag{1.1.5}$$

$$Vi = \frac{\mu_d}{\sqrt{\rho_d d \sigma}} \tag{1.1.6}$$

where μ_d is the dispersed-phase viscosity, and σ is the interfacial tension. Hinze (1955) further postulated that a drop would break up at a critical Weber number which increases with *Vi* number according to the following equation:

$$We = C_3[1 + f(Vi)] \tag{1.1.7}$$

where f is a function of *Vi*.

Maximum stable drop size. According to equation 1.1.7, for the case of negligible dispersed-phase viscosity, C_3 is the critical value of *We* for inviscid dispersions, leading to the determination of the maximum stable drop size (d_{max}), above it the drop will definitively break up. Equation 1.1.8 is a well-known expression for the maximum stable drop diameter for inviscid, low hold up dispersions (negligible coalescence):

$$\frac{d_{max}}{D_I} = K_1 We^{-3/5} = K_2 N_I^{-1.2} \tag{1.1.8}$$

where K_1 and K_2 are constants (Shinnar, 1961).

For non-negligible values of *Vi*, Calabrese et al. (1986) derived the following equation for maximum stable drop size, where K_3 and K_4 are constants:

$$\frac{\rho_c \varepsilon^{2/3} d_{max}^{5/3}}{\sigma} = K_3 \left[1 + K_4 \left(\frac{\rho_c}{\rho_d} \right)^{1/2} \frac{\mu_d \varepsilon^{1/3} d_{max}^{1/3}}{\sigma} \right] \tag{1.1.9}$$

Arai et al. (1977) derived the maximum stable drop size by considering the Voigt model that simultaneously takes the interfacial tension (restoring force) and viscous dissipation into account. Further works (Lagisetty et al. 1986; Koshi et al. 1988a and 1988b; Gandhi and Kumar, 1990) improved this model by incorporating the power law models for viscous fluids, and the effect of surfactant on the maximum stable drop size. Koshi et al. (1988b) were the first who considered the viscoelastic feature of the dispersed phase and proposed a model to predict the maximum stable drop size. They showed that some of the kinetic energy of the eddy is restored by the elastic mode of the viscoelastic fluid and so more energetic eddies or larger eddies are needed, in comparison to a purely viscous fluid, to break a drop.

1.1.3 Drop Coalescence

The coalescence phenomenon is more complex than break up, since it involves not only the approach of two drops, but also the drainage and eventual rupture of the intervening liquid film, in which the physical properties of fluids and interface play an important role. The rate of droplet coalescence is controlled by liquid drainage in the film between approaching droplets, and more significantly, the rigidity of the two corresponding

oil/water interfaces, since this controls the damping of thermally or mechanically induced oscillation in the film thickness.

Drop coalescence rate can be expressed by the product of drop collision frequency and coalescence probability or efficiency. Collision frequency of drops has been treated in a similar way to the collision frequency of ideal gas molecules (kinetic theory of gases) (Howarth, 1964; Abrahamson, 1975; Coulaloglou and Tavlarides, 1977). The proposed correlation for collision frequency is presented in Chapter 4.

Coalescence probability or coalescence efficiency has been the subject of many investigations (Coulaloglou and Tavlarides, 1977; Ross et al., 1978; Sovova, 1981a; Valadez-Gounzález, 1988; Alvarez et al., 1991; 1994; Liu and Li, 1999). Coalescence efficiency depends on the physical and rheological properties of two phases as well as interface properties. When two drops collide due to the turbulent flow they stay together for a short time before they separate. Meanwhile, a film of continuous phase is trapped between the two drops and it should be drained and ruptured before coalescence can occur. The contact or interaction time of colliding drops (t_i) and the coalescence time (t_c), or the time required for film drainage and rupture, are important parameters characterising the process of coalescence. The larger the ratio of t_c to t_i, the less the probability of coalescence. The coalescence efficiency (λ_c) can be defined as (Coulaloglou and Tavlarides, 1977; Ross et al., 1978; Chesters, 1991):

$$\lambda_c = \exp(-t_c / t_i) \qquad (1.1.10)$$

Assuming that the eddies in the inertial subrange are responsible for the motion of drops, Levich (1962) estimated the average contact time between two equal-size drops in turbulent flow as:

$$t_i \propto d^{2/3} \varepsilon^{-1/3} \qquad (1.1.11)$$

Coulaloglou and Tavlarides (1977) derived expressions for coalescence efficiency of deformable and rigid drops. For deformable drops they predicted that coalescence efficiency favours the coalescence of the small drops. Later Sovova (1981a) proposed an expression for λ_c which promotes coalescence of larger drops for deformable drops.

He used the ratio of interfacial energy over the energy of collision for calculating the coalescence efficiency.

In pure dispersions, in the absence of any stabiliser, the oil/water interfaces are mobile when the dispersed phase viscosity is small. In the presence of stabiliser the interfacial mobility is retarded. Liu and Li (1999) have proposed correlations for coalescence time for mobile and immobile systems for Newtonian fluids. They showed that for mobile interfaces the coalescence time is shorter than that for immobile interfaces. In other words, the rate drop coalescence for immobile interfaces (dispersion with stabiliser) is smaller than mobile interfaces (pure system). Liu and Li (1999) also derived the coalescence efficiency, using equation 1.1.10, and found that any increase in turbulence intensity increases the coalescence time and so decreases the coalescence efficiency.

Hashim (2001) studied the effect of viscosity of dispersed phase on the rate of coalescence. He showed experimentally that increasing the dispersed-phase viscosity decreases the rate of coalescence. However, he has found that at higher agitation speeds any increase in dispersed-phase viscosity causes an increase in the rate of coalescence.

The group of Alvarez (Valadez-Gounzález, 1988; Alvarez et al., 1991; 1994) were the first who proposed a model for drop coalescence in suspension polymerisation considering rheological (viscoelastic) behaviour of polymers. More details of their model are presented in the modelling section of this chapter and also chapter 4.

Minimum stable drop size. The minimum stable drop size (d_{min}) in a liquid-liquid dispersion has been estimated from the condition that the turbulent energy imposed on a pair of drops is not enough, when they contact, to prevent their adhesion and, finally, coalescence (Shinnar and Church, 1960):

$$\frac{d_{min}}{D_I} = K_5 We^{-3/8} = K_6 N_I^{-0.75} \qquad (1.1.12)$$

where K_5 and K_6 are constants.

In a turbulence-stabilised dispersion all drops are larger than d_{min} and smaller than d_{max}. According to equations 1.1.8 and 1.1.12, both d_{max} and d_{min} decrease with increasing agitation speed (or energy dissipation rate), although d_{max} decreases more rapidly than

d_{min}. Church and Shinnar (1961) showed that after a critical value of energy dissipation rate (ε_{max}), d_{min} becomes larger than d_{max} and the dispersion is unstable. Under this condition turbulence is unable to prevent coalescence and drops coalesce and break up rapidly.

Zhou and Kresta (1998) showed that the microscale of turbulence (η) can not be a proper estimation for the minimum drop size in liquid-liquid dispersions, due to satellite formation through drop break up. A significant number of drops (up to 30%) smaller than η were measured by them for various reactor and agitator geometries. Zhou and Kresta (1998) found that with increasing agitation speed the minimum drop size approaches the microscale of turbulence, since coalescence becomes more significant.

Liu and Li (1999) proposed correlations for minimum stable drop size for mobile and immobile interfaces for Newtonian fluids. They found that an important difference between the two limiting cases, i.e., drops with mobile interfaces and those with immobile interfaces, lies in the effect of dispersed-phase viscosity. Increasing the viscosity of dispersed phase in mobile-interface systems leads to partial immobility of the interface and so decreases the probability of coalescence. For immobile interfaces the minimum stable drop diameter is independent of dispersed-phase viscosity for low hold up and a weak function of it for high hold up systems.

1.1.4 Evolution of drop size average and distribution

1.1.4.1 Definitions

Drop size average and distributions are two important parameters, which quantify the properties of a dispersion/suspension. Before proceeding, it is essential that these properties are defined.

Mean drop Size. Several mean drop size can be defined for a drop size distribution. For example number (d_n), volume (d_v), and weight (d_w) average drop sizes are defined as follows:

$$d_n = \frac{\sum N_i d_i}{\sum N_i} \qquad (1.1.13)$$

$$d_v = \left(\frac{\sum N_i d_i^3}{\sum N_i} \right)^{1/3} \tag{1.1.14}$$

$$d_w = \frac{\sum N_i d_i^4}{\sum N_i d_i^3} \tag{1.1.15}$$

where N_i is the number of drops with diameter d_i. In liquid-liquid dispersions the most useful mean drop size is the surface average diameter or the Sauter mean diameter (d_{32}) since it is directly related to the dispersed-phase volume fraction (ϕ_d) and the interfacial area per unit volume of continuous phase (a):

$$d_{32} = \frac{\sum n_i d_i^3}{\sum n_i d_i^2} = \frac{6\phi_d}{a(1-\phi_d)} \tag{1.1.16}$$

From the commercial point of view, weight average size seems to be the most important one because it reflects the average size of larger particles, which are usually considered as the main product. In many suspension polymerisation processes, small particles, though important in terms of surface area, are not considered economically valuable and are discharged into the wastewater during washing and/or screening.

Drop size distribution (DSD): A major property of dispersions is the size distribution of the drops, in addition to the average size of drops. In fact, the average drop size is calculated from the full drop size distribution. The drop size distribution in a mixing vessel is largely dependent on the micro- and macro-size turbulent motions and flow patterns in the mixing vessel because the mutual relation between energy dissipation rate, residence time of drops at a certain location in the vessel, and the rates of drop break up and coalescence decides the drop size distribution. From measurements of DSD, and the time evolution of this property, mechanistic information can be gained about the mechanism of drop break up and coalescence (Shinnar, 1961; Nishikawa et al., 1991).

Data for drop size distribution may be illustrated using either differentiated size distribution (fraction of drops with diameter between d and $d+\Delta d$), or cumulative size

distribution (fraction of drops with diameter $\leq d$). The fraction of drops can be either volume fraction, number fraction, or weight fraction. Volume density distribution and diameter density distribution have also been defined by dividing the fraction of drops in a certain size by the bin volume (Δv) and bin diameter (Δd), respectively. As a result, a density distribution is normalised and its surface area is equal to 1.

1.1.4.2 Average Drop Size

The formation of dispersions is governed by two competing processes; drop break-up and drop coalescence. Initially, the bulk of the liquid in the dispersed phase breaks up to produce smaller drops and, simultaneously, the drops coalesce to form larger drops. The drop breakage rate dominates the drop coalescence rate in the initial stage of stirring, which causes drop sizes to decrease with time (Narsimhan et al.,1980). As stirring proceeds, the drop breakage rate decreases while drop coalescence rate increases. Ultimately, a steady state is reached where the rate of both processes become equal, and a steady-state drop size distribution is established. Hong and Lee (1983) indicated that the average drop size during the initial period of mixing decreases and that the minimum transition time depends on the mixing and system's physical properties.

Most of the research work on liquid-liquid dispersions have focused on the steady-state size of drops. Shinnar (1961) proposed that for systems where drop size is controlled by break up, $d_{32} \approx d_{max}$, whereas for systems where drop size is controlled by coalescence, $d_{32} \approx d_{min}$. Sprow (1967) showed that Sauter mean diameter is proportional to maximum stable drop size in dilute dispersions:

$$d_{32} = Cd_{max} \qquad (1.1.17)$$

where C has been found experimentally in the range of 0.38 to 0.70 for various systems (Zhou and Kresta, 1998). However, Pacek et al. (1998) performed a number of dispersion experiments in a specific reactor/agitator geometry and showed that C, in equation 1.1.17, decreases with increasing agitation speed and so d_{32} is not a constant fraction of d_{max} in dilute dispersions. It has been shown that d_{32} can be correlated with the maximum energy dissipation rate, rather than the mean rate of dissipation rate, and the circulation time (Zerfa and Brooks, 1996; Pacek et al., 1998).

In liquid-liquid dispersions the mean drop diameter at steady state increases with increasing dispersed-phase viscosity, hold up, and interfacial tension (Doulah, 1975; Park and Blair, 1975; Delichatsios and Probstein, 1976; Lagisetty et al., 1986; Calabrese et al., 1986; Nishikawa et al., 1987; Gandhi and Kumar, 1990; Kumar et al., 1991) and decreasing agitation speed (Shinnar, 1961; Sprow, 1967; Johnson, 1980; Chatzi and Kiparissides, 1994; Lazrak et al., 1998, Maggioris et al., 2000; Yang et al., 2000).

1.1.4.3 Drop Size Distribution (DSD)

Hong and Lee (1983) indicated that the average drop size during the initial period of mixing decreases exponentially while the size distribution changes less drastically from wide to narrow. The size distribution of drops at the steady state does not vary with time. Many investigators have studied drop size distributions in liquid-liquid dispersions (Chen and Middleman, 1967; Van Heuven and Hoevenaarj, 1969; Brown and Pit, 1974; Chatzi and Kiparissides, 1992; 1994; 1995; Calebrese et al., 1986; Nishikawa et al, 1991; Zhou and Kresta, 1998; Pacek et al., 1998). They have reported that the volume drop size distribution can be represented by a normal, log-normal, or gamma distribution, or a combination of normal distributions to cover all drop size ranges including small, intermediate and large sizes.

Bimodal drop size distributions have been reported by a number of investigators (Ward and Knudsen, 1967; Brown and Pitt, 1972; Konno et al., 1982; Hong and Lee, 1985; Laso et al., 1987; Chatzi et al., 1991; Villalobos, 1993; Pacek et al., 1998). Non-homogeneity of turbulent flows and formation of satellite drops via drop break up have been mentioned as possible reasons of bimodality of the drop size distributions (Chatzi and Kiparissides, 1991; Vivaldo-Lima et al., 1997).

Nonhomogenous environments: It has been shown that in a stirred tank, coalescence and drop break up occur in different regions of the reactor. Coalescence is found to occur predominantly in the region of circulating flow (where the shear stress is least), whereas droplet break up is found to occur mainly in regions of high shear, such as in the vicinity of the agitator (Coulaloglou and Tavlarides, 1976; Clark, 1988). This nonhomogeneity is at least one of those factors that are responsible for bimodal particle size distributions in suspension polymerisation processes (Vivaldo-Lima et al., 1997).

Mechanism of drop break up: Another factor that can be responsible for bimodality of particle size distribution is simply the drop break up mechanism. The mechanism of drop break up is affected by the size of the mother drop, the agitation speed and the viscosity of the drop (Kuriyama et al., 1995). For dispersions with a low-viscosity dispersed phase it has been found that drops *burst* and several smaller drops are obtained (Ali et al., 1981; Chang et al., 1981). Chatzi and Kiparissides (1992; 1994; 1995) proposed a model in which the drops break up into daughter drops and a number of satellite drops with a large ratio of daughter to satellite drop volume. This model could predict their experimental results very well.

With increasing the viscosity of the drop, the number of drops formed by breaking of a mother drop increases and broadens in the size range. This is because the mechanism of drop break up shifts from *bursting* towards *stretching* as the resistance to break up increases. As a result a broad/bimodal drop size distribution is obtained (Ali et al., 1981; Chang et al., 1981; Calabrese et al., 1986a; Kuriyama et al., 1995). In drop break up through *stretching*, the drop is stretched and forms a dumbbell-like shape and then breaks to two large daughter drops (stripping of the two ends of the dumbbell) and several satellite droplets (fragmentation of the liquid thread connecting the daughter drops).

Calabrese et al. (1986a) observed that with increasing drop viscosity, the size of largest drops increased while their number decreased, and the size of the smallest drops decreased while their number increased. They assumed that at higher drop viscosities ($\mu_d > 1$ Pa.sec) an extreme form of stretching may predominate by which the fracture of highly elongated dumbbells produces satellite droplets. Alternatively, break up may only occur close to impeller surfaces and may therefore be more erosive (stripping of small satellite droplets from the mother drop).

The effects of mixing variables on the size distribution of drops and their averages have been extensively studied. In liquid-liquid dispersions drop size distribution become narrower and shifts to a smaller size range with an increase in the agitation speed, and temperature and decreasing the interfacial tension and dispersed-phase hold up (Ross et al., 1978; Chatzi et al., 1991; Chatzi and Kiparissides, 1994; Pacek et al., 1998). An increase of agitation speed or a decrease of interfacial tension causes a reduction of the

minimum transition time, and thus allowing the system to approach equilibrium faster (Chatzi et al., 1991). Drop size distribution broadens with an increase in the dispersed-phase viscosity (Calabrese et al., 1986).

1.1.5 Stabilisers and Stabilisation

Suspending agents or stabilisers play a very important role in stabilisation of polymer particles in suspension polymerisation reactors. Stability of the dispersion is one of the most important physical properties required for industrial suspension processes. The majority of stabilisers used in suspension polymerisation processes are either water-soluble polymeric materials or inorganic particles. Suspending agents adsorb at the monomer/water interface and thus, enhance the stability of drops against coalescence. Water-soluble stabilisers also facilitate the drop break up by reducing the interfacial tension. Surfactants are sometimes added in low concentrations in particular to aid the initial dispersion process, but may have some stabilising function as well. In some commercial suspension polymerisation processes a combination of two suspending agents is performed to provide enough dispersing power.

Polymeric Stabilisers: Polymeric suspending agents stabilise the dispersion by a steric stabilisation mechanism. The mechanisms involved in steric stabilisation are very complicated and a universal theory has not yet been established (Vivaldo-Lima et al. 1997). In oil/water dispersions, steric stabilisation is achieved by adsorbing a polymer to the surface of drops. The polymer (stabiliser) should become firmly anchored by adsorption of its hydrophobic segments ("trains") that have a high affinity for the interface. The hydrophilic segments of polymer ("loops" and "tails") become highly solvated and swollen by the aqueous phase. The interpenetration of solvated polymer sections upon approach of the drops, leads to an increase in interparticle osmotic pressure and a decrease in the configurational entropy of the polymer. Both lead to particle repulsion and colloid stability (Wedlock, 1992).

Typical polymeric stabilisers are PVA, poly(vinyl pyrrolidone) (PVP), and cellulose ethers. The stabilising properties of such water-soluble polymers are influenced by various factors including molecular weight, copolymer composition and structure such as blockiness and the presence and positioning of any branching (Goodall and Greenhill-Hooper, 1990; Mendizabal et al., 1992).

Several investigators have studied PVA as a suspending agent in suspension polymerisation processes (Goodall and Greenhill-Hooper, 1990; Castellanos et al., 1991; Mendizabal et al., 1992; Chatzi and Kiparissides, 1994; Zerfa, 1994; Zerfa and Brooks, 1996; Olayo et al., 1998; Lazrak et al., 1998; Yang et al., 2000). It has been proved experimentally that the molecular weight, degree of hydrolysis and the method of manufacturing of PVA affect the dispersing power of this dispersant.

It has been reported that interfacial tension between the dispersed phase and the aqueous solution of PVA increases with increasing degree of hydrolysis and molecular weight of PVA. Moreover, interfacial tension between the dispersed phase and the aqueous solution of PVA decreases with increasing the water solubility of the dispersed phase (Castellanos et al., 1991; Mendizabal et al., 1992). The thickness of the PVA adsorbed layer on drops increases with increasing molecular weight of PVA. High degree hydrolysed PVAs (>96%), regardless of molecular weight, yield unstable dispersions. Polymerisations using these PVAs yield shapeless bulk polymer. That is because they are too hydrophilic to adsorb strongly enough at monomer-water interfaces to form a coherent film to prevent drop coalescence. Partially hydrolysed PVAs (88%) with low molecular weight (<70,000) yield very stable dispersions (non-reacting suspensions). But polymerisation using these PVAs yields big polymer lumps that are formed by very small particles. These PVAs are more surface active per unit weight than their higher molecular weight counterparts. So they are prone to adsorb more strongly and faster than the higher molecular weight ones. On the other hand, because of their low molecular weight, the thickness of the adsorbed layer is very small and so during the polymerisation, the drops can approach each other closely enough for the adsorbed polymer segments to interact and entangled (bridging). The result is the formation of polymer lumps. Partially hydrolysed PVAs (88%) with high molecular weight (>70,000) yield moderately stable dispersions. Polymerisation using these PVAs carries on without any problem and polymer beads are obtained. These are the best kind of PVAs and can be used as stabilising agents in suspension polymerisation. For partially hydrolysed PVAs, as the molecular weight increases the concentration required to give stable drops during the polymerisation becomes smaller (Castellanos et al., 1991; Mendizabal et al., 1992).

For more water soluble monomers, such as MMA and acrylonitrile, even low molecular weight PVA (partially hydrolysed) gives moderately stable dispersions and polymerisation leads to small lumps or even beads of polymer (Castellanos et al., 1991; Mendizabal et al., 1992).

Inorganic particles. Many different types of inorganic particles have been used in this context, including hydroxyapatite or tricalcium phosphate (TCP), calcium carbonate, barium sulphate, and aluminium oxide/hydroxide. The presence of these particles on the surface of monomer droplets decreases the rate of coalescence by hindering the approach of other monomer droplets. Models for the stabilisation of drops by inorganic particles have been reported (Wang and Brooks, 1992 and 1993). Addition of surfactant may increase the efficiency of the particles as stabilisers. Inorganic stabilisers, such as TCP, can be made *in situ* in suspension polymerisation processes (Sajjadi and Fazeli, 1994; Jahanzad and Sajjadi, 2000). Unlike polymeric stabilisers, inorganic particles usually can be removed after the polymerisation completed by washing with acid or base. Moreover they are generally cheaper than polymeric stabilisers.

1.2 SUSPENSION POLYMERISATION

In suspension polymerisation processes the initiator is soluble in monomer phase and polymerisation occurs in monomer droplets. Calculations show that the monomer droplets are large enough to contain a very large number of free radicals (~ 10^8 mol/l) (Kalfas and Ray, 1993) and so this is a bulk polymerisation carried out in individual droplets.

Several detailed and complete reviews on suspension polymerisation have been published (Brooks, 1990; Yuan et al., 1991; Arshadi, 1992; Hamielec and Tobita, 1992; Vivaldo-Lima et al., 1997; Dowding and Vincent, 2000). A number of investigators have studied suspension polymerisation processes from different points of view. For example, water solubility of monomer and mass transfer (Kalfas et al., 1993: Zhang and Ray, 1997), bifunctional initiators (Villalobos et al., 1993), dependence of polymer molecular weight on particle size (Bhargava et al., 1979), and effect of ultrasonic irradiation on particle size and its distribution (Hatate al., 1985) have been studied.

The production of unsaturated polyesters particles (Narkis, 1979), hollow polymer beads (Jo et al., 1996), and particles with core-shell morphology (Cunningham et al., 2000) through suspension polymerisation have been also reported.

In comparison with the quantity of studies on the kinetics of polymerisation and the properties of final polymer particles in suspension polymerisation processes, less attention has been paid to the study of evolution of particle size and particle size distribution in these processes. The main reason for this is the complexity of the phenomena (drop break up and coalescence rates and drop viscosity build up) affecting the particle size.

1.2.1 Kinetics of free-radical polymerisation

The reaction kinetics of suspension polymerisation are reasonably well understood and are the same as those of bulk polymerisation (Munzer and Trommsdorff, 1977).

The mechanism of free-radical bulk polymerisation of monomer M in the presence of thermal initiator I and chain transfer agent S can be schematically shown as follows:

Initiation:

$$I \xrightarrow{k_d} 2\dot{R}_0 \qquad r_d = 2k_d[I] \qquad (1.2.1a)$$

$$\dot{R}_0 + M \xrightarrow{k_i} \dot{R}_1 \qquad r_i = k_i[I][M] \qquad (1.2.1b)$$

Propagation or chain growth:

$$\dot{R}_n + M \xrightarrow{k_p} \dot{R}_{n+1} \qquad r_p = k_p[\dot{R}][M] \qquad (1.2.2)$$

Chain transfer to:

monomer: $\dot{R}_m + M \xrightarrow{k_f} P_n + \dot{R}_1 \qquad r_f = k_f[M][\dot{R}] \qquad (1.2.3a)$

chain transfer agent: $\dot{R}_n + S \xrightarrow{k_s} P_n + \dot{R}_1 \qquad r_s = k_s[S][\dot{R}] \qquad (1.2.3b)$

Termination:

disproportionation: $\dot{R}_n + \dot{R}_m \xrightarrow{k_{td}} P_n + P_m \qquad r_{td} = k_{td}[\dot{R}]^2 \qquad (1.2.4a)$

combination: $\overset{\circ}{R}_n + \overset{\circ}{R}_m \xrightarrow{k_{tc}} P_{n+m}$ $r_{tc} = k_{tc}[\overset{\circ}{R}]^2$ (1.2.4b)

where $\overset{\circ}{R}_n$ and P_n denote the free-radical and dead polymer molecules with chain length n (degree of polymerisation), respectively. r and k represent the rate and the rate constant for each reaction, respectively, with the subscript indicating the type of the reaction. [] denotes the concentration.

The rates of initiator consumption (equation 1.2.1a) and initiation (equations 1.2.1a and 1.2.1b) can be written as below:

$$\frac{1}{V}\frac{d([I]V)}{dt} = -k_d[I] \tag{1.2.5a}$$

$$R_I = 2fk_d[I] \tag{1.2.5b}$$

where V is the total volume of reaction mixture and f is the initiator efficiency. The overall rate of polymerisation, R_p, or the rate of monomer consumption, is:

$$R_p = -\frac{1}{V}\frac{d([M]V)}{dt} = (k_p + k_f)[M][\overset{\circ}{R}] \tag{1.2.6}$$

According to equation 1.2.4 the overall rate of termination reactions is:

$$R_t = r_{tc} + r_{td} = (k_{td} + k_{tc})[\overset{\circ}{R}]^2 = k_t[\overset{\circ}{R}]^2 \tag{1.2.7}$$

where k_t is the overall termination rate constant ($k_t = k_{td} + k_{tc}$). Assuming QSSA for the rate of radical formation, the radical concentration can be obtained as $[\overset{\circ}{R}] = (2fk_dI/k_t)^{1/2}$ from equations 1.2.5b and 1.2.7. Then R_p can be rewritten as:

$$R_p = (k_p + k_f)[M]\left(\frac{2fk_d[I]}{k_t}\right)^{1/2} \tag{1.2.8}$$

Monomer conversion (x) is defined as:

$$x = \frac{[M]_0 V_0 - [M]V}{[M]_0 V_0} \tag{1.2.9}$$

where $[M]_0$ is the initial monomer concentration. Since the density of monomer is generally less than corresponding polymer, a volume contraction factor (ε_p) is defined as:

$$\varepsilon_p = (\rho_p - \rho_m)/\rho_p \tag{1.2.10}$$

where ρ_m and ρ_p are densities of monomer and polymer, respectively. Accordingly, the variation of reaction volume can be written as:

$$V = V_0(1 - \varepsilon_p x) \tag{1.2.11}$$

where V_0 is the initial volume of monomer.

The instantaneous number-average degree of polymerisation ($X_{n,in}$), which is the average number of monomer units in a polymer chain formed at time t, can be obtained from the following equation:

$$X_{n,in} = \frac{R_p}{R_I} = \frac{(k_p + k_f)[M]}{(2fk_d[I]k_t)^{1/2}} \tag{1.2.12}$$

1.2.2 Diffusion-controlled Reactions

There are some important effects in free-radical polymerisation which can affect the kinetics and polymer molecular weight during the course of the polymerisation. They are briefly discussed here.

Diffusion-controlled termination: In free-radical polymerisation, in the medium conversion region, there is an "autoacceleration effect" or "gel effect" which leads to a

decrease of k_t and so increases the overall rate of polymerisation and polymer molecular weight (see equations 1.2.8 and 1.2.12). This effect is due to entanglements between long free-radical chains because of increasing polymer concentration (conversion). This hinders the free radicals in approaching, reacting with each other, and terminating and so the termination reactions become diffusion controlled. The polymer concentration and molecular weight are the most important factors that affect the onset and intensity of the gel effect. Using a chain transfer agent reduces, and control, the polymer molecular weight and so reduces the importance of the gel effect (Odian, 1991; Rempp and Merrill, 1991).

Diffusion-controlled Propagation: There is another important effect in free-radical polymerisation that may occur at high conversion region. If the reaction temperature is below the glass transition temperature (T_g) of the polymer being produced, the propagation reactions become diffusion controlled as the glassy state is approached at high conversions. In the glassy state even the motion of small molecules of monomer is restricted and the propagation reactions ceases to occur. This sets a limiting conversion on the polymerisation process. This phenomenon is called "glass effect" (Odian, 1991; Rempp and Merrill, 1991).

Diffusion-controlled initiation: The rate of initiator decomposition might be also affected at high conversions. The decomposition of initiator molecules into two primary radicals takes place in an environment consisting of monomer molecules. When two primary radicals are produced, they are kept close together by the surrounding monomer molecules for a very short time before they can move away. In this very short time they can react with each other and form the initial initiator molecule or other stable compounds that cannot be decomposed. The latter case decreases the efficiency of the initiator to produce free radicals. This effect is referred to as the "cage effect". This effect causes the initiator efficiency, f, to be lower than unity (in the range of 0.4 to 0.8 depending on the properties of initiator and monomer). During polymerisation in which the viscosity of the reaction media increases, f decreases due to the intensifying of the cage effect. This can decrease the rate of polymerisation (see equation 1.2.8) at high conversions (Odian, 1991; Rempp and Merrill, 1991). However, the cage effect might not limit the final conversion for suspension polymerisation reactions because a small

part of the radicals enter the particles from the water phase, depending on the initiator concentration in the water phase (Cunningham, 1999).

1.2.3 Heterogeneous Nature of Suspension Polymerisation

Suspension polymerisations occur in heterogeneous monomer-water dispersions. The kinetics of suspension polymerisation, however, have been considered to be similar to the free radical bulk polymerisation (Munzer and Trommsdorff, 1977). This assumption is based on the fact that the locus of polymeriastion in suspension polymerisation is in the monomer drops. While this assumption seems to be sound for many cases as long as the kinetics of the oil phase is concerned, it may not be sufficient under all circumstances.

Emulsion Particles: The formation of emulsion particles in suspension polymerisation reactions has been realized for a long time (Almog and Levy, 1980; Adams et al., 1990; Cunningham, 1999). These particles are the result of a homogenous nucleation mechanism occurring in the aqueous phase (Fitch et al., 1969). Because of segregation of radicals in these particles, they usually have a higher molecular weight than the particles formed with suspension polymerisation. To address such a phenomenon, the kinetics of the water phase should be also considered in parallel to that of the oil phase. Another route by which the emulsion particles can be formed is by the partial dissolution of monomer/polymer droplets (Azad and Fitch, 1978). Dissolusion of monomer droplets by molecular diffusion occurs faster for smaller droplets because of their higher monomer fugacity, which in turn is due to their small radius of curvature and therefore higher surface energy. Because of the formation of polymer in the droplets, the droplets do not completely disappear and so colloidal-sized particles are formed. These small particles have the same molecular weight as larger suspension particles.

Monomer Partitioning: When the solubility of the monomer in the aqueous phase is negligible (as it is for styrene, for example), quantitative predictions are possible for suspension polymerisation using the same kinetic model used for the corresponding homogeneous (bulk) polymerisation. However, in the case of monomers with a moderate to high water solubility in the aqueous phase, quantitative agreement between the experimental results and the model prediction are usually lacking. This is because

some of the monomer resides in the water phase and do not get involved in the polymerisation reaction. As polymerisation proceeds in the drops, monomer transfers from the aqueous phase into the drops to compensate the monomer that has replenished. Kalfas et al (1993) carried out a series of suspension homo- and copolymerisations of monomers with different water solubility. Their results showed that mass transfer limitations in suspension polymerisation of partially water-soluble monomers (MMA, vinyl acetate and acrylonitrile) at low monomer-to-water ratios is considerable and leads to a lower final conversion in comparison with higher monomer-to-water ratios. Later Zhang and Ray (1997) showed that the aqueous-phase mass transfer is not the limiting resistance, and the intraparticle diffusion may cause limitations on monomer transport.

1.2.4 Particle Size Average and Distribution

Suspension polymerisation reactions generally produce particles with a broad size or bimodal distribution. Bead particles are usually the intended product from a suspension reactor, with diameters in the range of 10 μm to 5 mm. In principal, the size of particles in suspension polymerisation is determined by a balance between the rate of drop break up and coalescence, similar to that in a simple dispersion process. The major difference is that in the polymerising drops, the drop properties are not constant and vary with time.

Without the presence of a stabiliser, the polymerising drops would agglomerate after a certain degree of polymerisation. As polymerisation proceeds in the drops, the viscosity of the drops increases correspondingly. For example, in suspension polymerisation of styrene, the dispersed droplets reach a critical viscosity of about 100 cp at about 30% conversion from which droplet coalescence overcomes the droplet breakage. As a result the mean particle size starts to increase (Church, 1966; Arai et al., 1977; Konno et al., 1982; Villalobos et al., 1993). Particle growth stops at a secondary critical viscosity (10^6 cp) reached at about 70% conversion because coalescence becomes less likely for highly elastic collisions. The period during which particles grow is usually called the "sticky stage" (Villalobos et al;1993). By the combined action of stabilisers and turbulent agitation, agglomeration can be prevented until individual droplets are transformed into solid spherical particles (Church and Shinnar; 1961). The type and

concentration of suspending agent plays an important role in prevention of coalescence between polymerising drops. Regarding recent applications of suspension polymerisation products, the major aim in this process is the formation of as uniform as possible dispersion of monomer drops in the aqueous phase with controlled coalescence of these drops during the polymerisation process. This indicates that the kinetics of polymerisation together with mixing and surface phenomena associated with stabilisation of drops are quite important in elucidation of polymer bead formation in suspension polymerisation reactions.

To understand drop size variations in suspension polymerisations, reports on liquid-liquid dispersions with high viscosity dispersed phase are quite useful. With increasing viscosity of the disperse phase in a liquid-liquid dispersion, the rate of drop break up decreases due to higher resistant forces (Koshi et al., 1988b). When the viscosity of the dispersed phase is high the rate of drop break up is determined by resisting viscous forces and independent of interfacial-tension forces (Calabrese et al., 1986; Koshy et al., 1988b).

Koshy et al. (1988b) were the first accounted for the effect of elasticity increase on the rate of drop break up. They showed that the drop break up for a viscoelastic fluid needs more energetic eddies or larger eddies in comparison to a purely viscous fluid due to the restoring some of the kinetic energy of the eddies by the elastic mode of the viscoelastic fluid. Mighri et al. (1998) also showed experimentally that drop resistance to deformation and break up increases with increasing drop elasticity.

Increase in the viscosity of dispersed phase in mobile-interface systems leads to partial immobility of the interface and so decreases the efficiency of coalescence (Liu and Li, 1999). This results in a decrease in the rate of drop coalescence with an increase in the viscosity of the drop.

In a suspension polymerisation the viscoelastic properties of the dispersed phase (drops) increase with time, especially during the gel effect, as the result of conversion of monomer to polymer. Experimental evidence shows that particle size increases significantly during the gel effect in suspension polymerisation processes (Konno et al., 1982, Zerfa and Brooks, 1996; Lazrak et al., 1998; Yang et al., 2001). Viscosity increase in the polymerising drops affects inversely the rates of drop break up and

coalescence but affects break up more than coalescence and so the mean drop size increases during the gel effect or "sticky stage", as the theoretical predictions shows (Alvarez et al., 1994).

1.2.4.1 The origin of satellite particles

In the final product of a suspension polymerisation process, bead particles are usually accompanied by a few orders of magnitude larger number of very small satellite particles and emulsion particles. As mentioned earlier (section 1.1.5.3) in liquid-liquid dispersions nonhomogeneity of turbulent flows and mechanism of drop break up may be responsible for the formation of small drops and for the bimodality of drop size distribution. In a suspension polymerisation reactor in addition of the above factors (Vivaldo-Lima et al., 1997), satellite particles could be the result of the following factors:

Change in the mechanism of drop break up: The mechanism of drop break up is strongly affected by the viscosity of the drop. As previously mentioned (section 1.1.5.3) with an increase in the drop viscosity the mechanism of drop break up shifts from bursting towards stretching and erosion. At very high viscosities of dispersed phase (polymer/water dispersions with high ratio of μ_d/μ_c) it has been found recently that drop deformation and break up consisted in erosion at the drop surface. Clouds of very small ribbons and sheets were developed around the drop then stretched and finally broken into very small droplets (Mighri and Huneault, 2002).

Emulsion particles: As mentioned earlier (section 1.2.3) emulsion particles are formed in the aqueous phase in suspension polymerisation of monomers with moderate to high water solubility. Although these particles are very small they may coagulate due to instability.

1.2.5 New developments

The inadequacy of traditional suspension polymerisation process to produce polymers of narrow particle size distribution motivates more attempts to develop new methods for producing monodisperse polymer particles by suspension polymerisation. Some of these attempts include: 1- using an encapsulation step of monomer droplets (Matsumoto

et al., 1989) previous to the polymerisation step (which can then be carried out in suspension without using stabilisers), 2- proposal of a circular loop reactor to carry out the suspension polymerisation, which was reported to be superior for the production of the polymer (polystyrene) particles of uniform size than the conventional suspension polymerisation process (Tanaka and Hosogai, 1990), 3- development of a method for the production of large monosized spherical polymer particles made by passing the monomer under pressure through a nozzle coupled to an energised piezoelectric crystal (Colvin et al., 1990), 4- carrying out the suspension polymerisation (of MMA) in a "gelled" solution of water and agarose (which immobilises the polymerising drops all along the reaction) (Polacco et al., 1994).

In a new technique, a new kind of reactor called oscillatory-baffled reactor has been studied extensively for suspension polymerisation (e.g., Ni et al., 1998; Ni et al., 1999; Ni et al., 2001), and for mixing behaviour (e.g., Ni et al., 1998; Ni et al., 2003).
Another technique has been developed to use membranes as a novel emulsification technique to produce monodisperse drops. Subsequent suspension polymerisation produces monodisperse polymer particles. Shirazu porous glass (SPG) membranes (e.g., Omi et al., 1994; Yuyama et al., 2000; Ma et al., 2003) have been used for this purpose. Very recently polytetraflouroethylene (PTFE) membranes have been used for producing monodisperse oil in water emulsions (Yamazaki et al., 2002; Yamazaki et al., 2003).

1.3 Modelling of Suspension Polymerisation

Suspension polymerisation processes can be classified in several levels on which modelling is important. These levels are microscale chemical kinetics (polymerisation reactions), mesoscale physical phenomena (interphase equilibrium, interphase and intraphase heat and mass transfer, fluid mechanics and micromixing, break up/coalescence phenomena, polymer morphology), and the macroscale reactor phenomena (macromixing, overall energy and material balances, particle population balances, heat and mass transfer from the reactor, reactor dynamics and control) (Vivaldo-Lima et al., 1997). Usually, separate models are required at each level, and simplified versions of the smaller scale models are incorporated as the scale grows larger.

In suspension polymerisation processes microscale chemical kinetics are reasonably well understood. The macroscale has been considered independently from the other scales, so that effective interconnection has not been obtained to date. The least developed issues in the suspension polymerisation processes is mesoscale (breakage/coalescence phenomena) and its relation with rheological behaviour of the polymerising mass, the kinetics of polymerisation, non-homogenous flow and rate of energy dissipation in the reactor. However, the modelling of break up and coalescence processes in liquid-liquid dispersions has been the subject of many investigations during the last 50 years (e.g.; Shinnar and Church, 1960; Valentas and Amundson, 1966; Coulaloglou and Tavlarides, 1976; 1977; Calabrese et al., 1986; Chatzi and Kiparissides, 1992; 1995; Tsouris and Tavlarides, 1994).

The first attempt to model the particle size distribution in suspension polymerisation reactors was done by Mikos et al. (1986). They assumed that if the drops become stabilised from the early reaction, the final size distribution of particles is governed by the initial distribution, taking into account the contraction of monomer when it is converted to polymer. So Mikos et al. (1986) did not consider the effect of kinetics of polymerisation and viscosity build up in the polymerising drops. Their report of PSD modelling of suspension polymerisation is based on a purely dispersion mechanism.
To date, a few studies have been reported on the modelling of suspension polymerisation reactions that combine the kinetics of polymerisation and the dynamics of the dispersion. The break through in modelling of suspension polymerisation reactions was reported by a Mexican group (Valadez-Gounzález 1988; Alvarez et al. 1991; 1994) and then followed by other research groups (Vivaldo-Lima et al., 1998; Maggioris et al., 1998 and 2000; Chen et al., 1999; Machado et al., 2000).

One of the most complex features of liquid-liquid dispersions is the nonhomogeneity of the turbulent flow. It has been shown that in a stirred tank, coalescence and drop break up occur with different magnitudes in different regions of the reactor (Coulaloglou and Tavlarides, 1976). Coalescence is found to occur predominantly in the region of circulating flow, whereas droplet break up is found to occur mainly in the vicinity of the agitator. However, most of the modelling attempts have been made with the assumption of homogeneity of the vessel content. In liquid-liquid dispersions the inherent nonhomogeneity of turbulent flow makes the modelling very difficult. Tsouris and

Tavlarides (1994) have developed a model that assumes a homogeneous environment but accounted for the nonhomogeneity of the tank by using two energy dissipation rates at the impeller and circulation zones. Recently, two-compartment models have been presented that consider two zones, the impeller zone and the circulation zone. Two population balances have been proposed for the two zones; taking into account the exchange flow between the two compartments (Nambiar et al., 1994; Alexopoulos et al., 2002). Two-compartment model has also been used for suspension polymerisation processes (Vivaldo-Lima et al., 1998; Maggioris et al., 1998; 2000). The parameters for the two-compartment models are compartment ratio of energy dissipation rates, compartment volume ratio and exchange flow rate. They have been determined through computational fluid dynamics (CFD) simulations (Bourne and Yu, 1994). Alopaeus et al. (1999) proposed a multi-block (multi-compartment) model for stirred tanks. They divided the stirred tank into eleven sub-regions. However, they have not discussed the advantages of their model over two-compartment models.

The two- or multi-zones models are also known as "compartment mixing models" (Cui et al., 1996). As a matter of fact, these modelling approaches can be considered as simplifications, or approximations, of a rigorous three-dimensional CFD calculation (Mann et al., 1995).

1.3.1 Free-Radical Polymerisation

1.3.1.1 Modelling of the Kinetics

Several models have been proposed for predicting the kinetics and polymer molecular weights in free-radical polymerisation; among them the method of instantaneous properties (Marten and Hamielec, 1979) and the method of moments (Chiu et al., 1983) are the most important models. In the method of instantaneous properties, the instantaneous molecular weights of the polymer are integrated to give the cumulative molecular weights. In the method of moments, the cumulative molecular weights are directly obtained by integration of the moment equations. The method of instantaneous properties is presented here, while the method of moments will be discussed in detail in Chapter 4.

In the method of instantaneous properties instantaneous number-average ($X_{n,in}$) and weight-average ($X_{w,in}$) degree of polymerisation, which are defined as the properties of the polymer chains produce at time t, are presented by following equations:

$$X_{n,in} = \frac{1}{\tau + \beta/2} \tag{1.3.1}$$

$$X_{w,in} = \frac{2(\tau + 3/2\beta)}{(\tau + \beta)^2} \tag{1.3.2}$$

$$\tau = \frac{(2fk_d[I]k_{td})^{1/2}}{k_p[M]} + k_f/k_p + k_s[S]/k_p[M],\ \beta = \frac{(2fk_d[I]k_{tc})^{1/2}}{k_p[M]} \tag{1.3.3}$$

The parameter τ represents the importance of disproportionation termination reactions and chain transfer reactions in the molecular weight of polymer. While the parameter β reflects the role of the combination termination reactions in the polymer molecular weight.

The cumulative number-average and weight-average degree of polymerisation, which are defined as the properties of all polymer chains produce until time *t*, can be obtained by integration of equations 1.3.1 and 1.3.2 over the reaction time.

$$X_n = \int_0^t X_{n,in}\,dt \tag{1.3.4}$$

$$X_w = \int_0^t X_{w,in}\,dt \tag{1.3.5}$$

Average polymer molecular weights are easily calculated by multiplying of the average degrees of polymerisation by the molecular weight of the monomer.

1.3.1.2 Modelling of Diffusion-controlled Reactions

The variations of termination and propagation rate constants during the gel and glass effects have been predicted by several semi-empirical relationships. Three of the most applied correlations in this regard have been proposed originally by Marten and Hamielec (1979) based on free volume theory, Tulig and Tirrel (1981) based on the reptation theory, and Chiu et al. (1983) based on random walking statistics. Here the

model of Marten and Hamielec (1979) is presented. The model of Chiu et al. (1983) will be discussed in Chapter 4.

Marten and Hamielec (1979) proposed correlations for the variation of k_t and k_p during the gel and glass effects, respectively. These correlations are on the base of the molecular weight of the polymer formed during the reaction and the free volume of the reaction mixture, which varies with the monomer conversion. They defined a parameter (K) for any polymerisation system, which can be calculated for every increment in conversion as follows:

$$K = M_w^m \exp(A/V_f) \tag{1.3.6}$$

$$V_f = [0.025 + \alpha_m (T - T_{gm})]\phi_m + [0.025 + \alpha_p (T - T_{gp})]\phi_p \tag{1.3.7}$$

where V_f is the free-volume of the monomer/polymer solution, T is reaction temperature (K), α is the thermal expansion coefficient, and m and A are adjustable parameters. Subscripts m and p denotes monomer and polymer, respectively.

The critical value of K (K_{cr}) for the onset of the gel effect for any specific monomer, is a function of temperature only. When the value of parameter K reaches its critical value, the gel effect begins and k_t will decrease according to the following correlation:

$$k_t = k_{t0} (M_{wcr} / M_w)^n \exp(-A(1/V_f - 1/V_{fcr1})) \tag{1.3.8}$$

where M_{wcr} and V_{fcr1} are the values of polymer weight-average molecular weight and free-volume at the onset of gel effect and n is an adjustable parameter.

Marten and Hamielec (1979) proposed the following equation for the decrease in k_p with conversion during glass effect:

$$k_p = k_{p0} \exp(-B(1/V_f - 1/V_{fcr2})) \tag{1.3.9}$$

where V_{fcr2} is the free-volume of system at onset of glass effect and B is an adjustable parameter.

1.3.1.3 Modelling of the Rheological Properties

It is apparent that the rheological properties of drops change with time as polymerisation proceeds in the drops. As the drops become more viscous, their tendency to break up is depressed. The coalescence efficiency may be also affected by the drop rheological properties. Therefore, appropriate correlations are required to allow for the variation in drop properties with polymer concentration or conversion in the drops.

Baillagou and Soong (1985a) proposed the following equation to calculate viscosity of monomer/polymer solution (μ) based on free-volume and coil-coil interaction theories:

$$\mu(M, c_p, T) = \mu_m(T) + KM_w^n c_p^m \exp(B/V_f) \tag{1.3.10}$$

where c_p is polymer concentration, M_w is polymer molecular weight. K, B, m, and n are adjustable parameters.

Alvarez et al. (1990,1994) calculated the zero-shear viscosity using free-volume theory:

$$\mu = CT^m D^n \tag{1.3.11}$$

$$D = \exp\left(\frac{-2.3\phi_m}{A + B\phi_m}\right) \tag{1.3.12}$$

where μ is the zero-shear viscosity, A is a temperature-dependent parameter, and B and C are constants.

Another correlation for prediction of variation of zero-shear viscosity, with temperature, conversion and polymer molecular weight in free radical bulk polymerisation of MMA, has been given by Stuber (1986):

$$\eta_s = F\zeta \tag{1.3.13}$$

$$F = 0.00216[1 + 0.125(c_p M_w)^{0.5} + 3.75\times10^{-11}(c_p M_w)^{3.4}] \tag{1.3.14}$$

$$\zeta = \exp[(600+80c_p+c_p^2)(1/T-1/465.15)+1.2\times10^{-5}c_p^3] \qquad (1.3.15)$$

where c_p is polymer weight percent, and M_w is polymer weight-average molecular weight (thousands).

1.3.2 Particle Size Distribution

The modelling of break up and coalescence processes in liquid-liquid dispersions has been the subject of many investigations during the last 50 years (e.g.; Shinnar and Church, 1960; Valentas and Amundson, 1966; Coulaloglou and Tavlarides, 1976; 1977; Calabrese et al., 1986; Chatzi and Kiparissides, 1992 and 1995; Tsouris and Tavlarides, 1994). In this section, the main features of these models are discussed.

1.3.2.1 Population Balance Equation (PBE)

By assuming homogeneous isotropic turbulence, implying perfect macromixing and statistical homogeneity of the vessel content, the population balance approach is usually used for tracing the destruction and re-creating of individual identities of drops by dynamic processes of break up and coalescence. The evaluation of drop volume distribution can be described by the following integro-differential equation:

$$\frac{dF(v,t)}{dt} = \int_{v}^{v_{max}} b(v')\beta(v',v)u(v')F(v',t)dv' - b(v)F(v,t) + \int_{v_{min}}^{v/2} c(v-v',v')F(v-v',t)F(v',t)dv' - F(v,t)\int_{v_{min}}^{v_{max}-v} c(v,v')F(v',t)dv' \qquad (1.3.16)$$

where $F(v,t)$ is the drop volume distribution (the number of drops with volume v at time t), v_{min} and v_{max} are the minimum and maximum drop volumes, respectively, which can exist in the dispersion. $b(v)$ and $c(v,v')$ are the rates of drop break up and coalescence, respectively.

$\beta(v',v)$ is the probability of forming a drop with volume v from breakup of a drop with volume v' or, in other words, the daughter drop volume distribution, which can be assumed approximately by a normal distribution about a mean value $\bar{v}$, since it is the combined result of a large number of independent random events:

$$\beta(v',v) = 1/(\sigma_v\sqrt{2\pi})\exp\{-(v-\bar{v})^2/(2\sigma_v^2)\} \quad (1.3.17)$$

Assuming that 99.6% of the droplets lie inside the interval $[\bar{v} \pm 3\sigma_v]$, then the standard deviation, σ_v, is defined as follows:

$$\sigma_v = \bar{v}/3 = v'/(3u(v')) \quad (1.3.18)$$

$u(v')$ is the average number of daughter droplets formed by breaking of a drop with volume v'.

The steady state drop size distribution for a liquid-liquid dispersion can be obtained by applying $dF(v,t)/dt = 0$ to equation 1.3.16:

$$F(v)[b(v) + \int_{v_{min}}^{v_{max}} c(v,v')F(v')d(v')] = \int_{v}^{v_{max}} b(v')\beta(v',v)u(v')F(v')d(v') + \int_{v_{min}}^{v/2} c(v-v',v')F(v-v')F(v')d(v') \quad (1.3.19)$$

1.3.2.2 Drop Break up

The application of population balance equation to liquid-liquid dispersion systems requires that the break up frequency of droplets with a certain size be known. Valentas and Amundson (1966) assumed that the rate of break up is proportional to the droplet surface area. Ross et al. (1978) calculated the break up rate by drawing an analogy between droplet break up and molecular decomposition. Coulaloglou and Tavlarides (1977) obtained two expressions for break up rate, $b(d)$, using two different approaches. In one approach they assumed that a drop breaks if its turbulent kinetic energy is greater than the drop surface energy. In this case break up rate was derived in terms of the fraction of drops with turbulent kinetic energy greater than a critical value and the time elapsed between the beginning of a drop deformation and its break up:

$$b(d) = C_1 N_I (D_I / d)^{2/3} \exp\left\{- C_2 \sigma / \left(\rho_d d^{5/3} N_I^2 D_I^{4/3}\right)\right\} \quad (1.3.20)$$

where C_1 and C_2 are constants. In another approach break up of a drop is caused from a collision with a turbulent eddy. If the turbulent kinetic energy imparted to the drop is greater than the drop surface energy, the drop deforms and breaks. The break up rate is then determined by the fraction of these collisions for a random motion of drops and eddies, and by the break up time:

$$b(d) = C_1 N_I (D_I / d)^{2/3} (2/\pi) \Gamma\left\{3/2, C_2 \sigma / \left(\rho_d d^{5/3} N_I^2 D_I^{4/3}\right)\right\} \quad (1.3.21)$$

According to Narsimhan et al. (1979), the break up of a drop exposed to a turbulent field is due to its oscillation resulting from the relative velocity fluctuations imposed by the arrival of eddies at the surface of the drop. So the rate of break up depends on the average number of eddies arriving at the surface of the drop per unit time and on the probability that an arriving eddy will have energy greater than or equal to the minimum increase in surface energy of the drop required for break up:

$$b(d) = C_1 erfc\left\{C_2 (\sigma / \rho_d)^{1/2} / \left(d^{5/6} N_I D_I^{2/3}\right)\right\} \quad (1.3.22)$$

Valadez-Gounzález (1988) proposed a model for the break up rate with two efficiency terms; energy and time efficiencies (λ_e and λ_t). He assumed that a minimum amount of energy for (at least) a minimum period of time should be provided to a droplet to break it up. He proposed that the rate of break up should be given as follows:

$$b(v) = \omega_b(v) \lambda_t(v) \lambda_e(v) \quad (1.3.23)$$

where ω_b is collision frequency of eddies with droplets. The time efficiency was proposed to be a function of the time required for a deformed polymer droplet to flow a distance equal to its original radius and the time where enough energy to break the droplet is available. The energy efficiency is obtained from an energy balance considering the surface energy (the energy required to overcome interfacial tension) and the energy required to promote the viscous internal flow. To account for the monomer/polymer flow, he used a power law viscosity model and assumed the flow to

be equivalent to the flow of a monomer/polymer mixture through a circular duct of diameter equal to the droplet diameter and a pressure drop on the order of magnitude of the available kinetic energy. On the basis of these assumptions Valadez-Gounzález (1988) obtained expressions for collision frequency and time and energy efficiencies with five adjustable parameters.

Alvarez et al. (1991 and 1994) used the same approach as Valadez-Gounzález (1988), but instead of using a power law viscosity model, they assumed the polymer flow to behave as a Maxwell fluid and only one break up efficiency was used. The efficiency expression they obtained has only two adjustable parameters. The proposed equations for break up rate distribution have been presented in details in Chapter 4. Alvarez et al. (1994) showed theoretically that with an increase in the viscoelasticity of the drop the rate of break up is reduced due to increased resistance of drops for being broken.

Chatzi and Kiparissides (1992) assumed the break up rate to depend on the average number of eddies arriving on the surface of the drop per unit time and on the probability that the arriving eddy will have energy greater than or equal to break a droplet of diameter *d*. They indeed used the same principle as Valadez-Gounzález (1988) but only considered surface energy to be overcome, so their model is limited to low dispersed phase viscosity. Chatzi and Kiparissides (1992) considered that a mother drop breaks up to one daughter and several satellite drops and presented the following correlation for break up frequency:

$$b(d) = C_I erfc\left[\frac{C(\sigma/\rho_d)^{1/2}}{d^{5/6}N_I D_I^{2/3}}\right], \qquad C = C_{II}\left[\frac{N_{da}x^{2/3} + N_{sa}}{N_{da}x + N_{sa})^{2/3}} - 1\right]^{1/2} \qquad (1.3.24)$$

where C_I and C_{II} are constants, N_{da} and N_{sa} are the number of daughter and satellite drops, respectively, and x is the ratio of volume of daughter to volume of satellite drops. This concept allows the prediction of bimodal distributions, which is common in suspension polymerisations in small reactors (Konno et al., 1982; Villalobos, 1993). Although there is experimental evidence that drops break up into a large number of daughter drops of different sizes (Tavlarides and Stamatoudis, 1981), in most modelling attempts this number is assumed to be fixed and usually equal to 2 (e.g., Coulaloglou

and Tavlarides, 1976; 1977; Delichatsios and Probstein, 1976; Alvarez et al., 1991; 1994).

Recently a review of models for drop break up in liquid-liquid dispersions has been published (Lasheras et al., 2002).

1.3.2.3 Drop Coalescence

Coalescence has been modelled assuming that the suspended droplets move randomly and their collision frequency is similar to the collision frequency of ideal gas molecules (kinetic theory of gases) (Howarth, 1964; Abrahamson, 1975; Coulaloglou and Tavlarides, 1977; Das et al., 1987). Coulaloglou and Tavlarides (1977) proposed equation 1.3.25 for collision frequency of drops with diameters d_u and d_v, $\omega_c(d_u,d_v)$, where k_c is a constant.

$$\omega_c(d_u,d_v) = k_c \frac{\varepsilon^{1/3}}{1+\phi_d}(d_u^2 + d_v^2)\sqrt{(d_u^{2/3} + d_v^{2/3})} \qquad (1.3.25)$$

Shinnar and Church (1960) stated that coalescence will not happen if the kinetic energy of the oscillations imposed to the drops by turbulent pressure fluctuations is greater than the energy of the adhesion between two drops. Based on this idea, Coulaloglou and Tavlarides (1977) derived the coalescence efficiency (λ_c) for deformable and rigid drops as follows:

$$\lambda_c(d_u,d_v) = \exp\left\{-k_c(\mu_c\rho_c N_I^3 D_I^2/\sigma^2)(d_u d_v/(d_u+d_v))^4\right\} \text{(deformable drop)} \quad (1.3.26a)$$

$$\lambda_c(d_u,d_v) = \exp\left\{-k_c\mu_c/[N_I D_I^{2/3}(d_u+d_v)^{4/3}]\right\} \quad \text{(rigid drops)} \quad (1.3.26b)$$

Howarth (1964) considered coalescence as a "single-shot" process. If the velocities of two colliding drops are greater than a critical value they coalesce immediately. Sovova (1981a; 1981b) proposed an expression for coalescence efficiency by considering that the drops follow the motion of eddies having the same scale to their size. Drop coalescence occurs if the turbulent energy of collision of the drops is greater than their surface energy. The fraction of "energetic collisions" has been derived as:

$$\lambda_c(d_u,d_v)=\exp\left\{-k_c\sigma(d_u^2+d_v^2)(d_u^3+d_v^3)/[\rho_d N_I^2 D_I^{4/3} d_u^3 d_v^3 (d_u^{2/3}+d_v^{2/3})]\right\} \quad (1.3.27)$$

The group of Alvarez (Valadez-Gounzález, 1988; Alvarez et al., 1991 and 1994) also used the kinetic theory of gases for calculating collision frequency but they proposed different expressions for coalescence efficiency that take into consideration the rheological changes of polymerising drops. Valadez-Gounzález (1988) proposed this efficiency to depend on a deformation efficiency, a film drainage efficiency, and a time for deformation efficiency. The expressions for these efficiencies were developed using a power law rheological model. Alvarez et al. (1991) proposed that the overall coalescence efficiency is the product of four efficiencies, namely, an efficiency for drop-drop approach, a deformation efficiency, a film drainage efficiency before the film is broken, and a film drainage efficiency once it has been broken. They also considered the effect of the suspending agent on the coalescence by using a Maxwell fluid model to characterise the rheological behaviour of the drops. Later, Alvarez et al. (1994) considered only two efficiency terms, the deformation efficiency and the film drainage efficiency. The details of their model are presented in chapter 4.

1.3.4 CONCLUSIONS

It is understood from the literature review that the kinetics of polymerisation and drop break up and coalescence play important roles in the determination of the size of polymer beads in suspension polymerisation processes. Despite many relevant publications, in particular after 1990, the effects of the kinetics of polymerisation reactions and rheological properties of polymerising drops on the rates and mechanisms of drop break up and coalescence are not well elucidated. The following general conclusions may be drawn from the literature review regarding suspension polymerisation:

1- In a liquid-liquid dispersion, there is a transition period during which the average drop size exponentially decreases with time until it reaches a steady-state value. For a suspension polymerisation, generally it is accepted that the drop size reaches a steady-state in the initial stage of mixing before polymerisation proceeds much (a low viscosity build up in the drop). If the polymerisation reaction proceeds fast compared with the stabilisation of the dispersion, it is possible that the initial drop sizes never decreases to the steady state value and starts enlarging from the start of the polymerisation.

2- The occurrence of the quasi steady-state in the size of particle in suspension polymerisation is still in question.

3- The role of satellite particles in the stability of particles and evolution of particle size has not been elucidated.

4- The effects of chain transfer agents, on particle size average and distribution in suspension polymerisation processes have not been studied.

5- Recent modellings of suspension polymerisation reactions have used the application of CFD. This technique gives a better possibility for investigating the inhomogeneities in the reaction vessel.

OUTLINE OF THE RESEARCH

The objective of this research is to investigate the evolution of particle size distribution in suspension polymerisation reactors. In order to elaborate on the kinetics of polymerisation and particle size evolution, appropriate kinetic and population balance models are also developed. The experimental results are tested against the mathematical model predictions.

Methyl methacrylate was chosen as the model monomer to study the effects of different operation and formulation parameters on the evolution of the drop/particle size average and distribution as well as the reaction kinetics. The distinctive feature of this research is that corresponding non-reacting MMA/water dispersions are also carried out to unravel the importance of the forces influencing the dynamics of dispersion processes. The comparative study of reacting and non-reacting dispersion systems will be seen to provide valuable information regarding drop behaviour in suspension polymerisation reactions.

A widely used stabiliser, Polyvinyl alcohol (PVA) with a hydrolysis degree of 88%, was selected for this research. Lauroyl peroxide (LPO), which has low water solubility, was selected as an initiator. The advantage of using LPO is that the formation of emulsion particles will be limited.

Three categories of variables can be found for a suspension polymerisation. The first category includes those parameters that affect the properties of the water phase such as stabiliser concentration and type. The second category contains those parameters that affect the kinetics of polymerisation such as initiator and chain transfer types and concentrations. The third category includes those parameters that affect the mixing conditions of the dispersion/suspension such as impeller type and speed, tank geometry and baffling. Some variables may be classified under more than one category. The variables selected for this research, which are from the three categories, are suspending agent (PVA) concentration, initiator (LPO) concentration, chain transfer agent (*n*-DDM) concentration, monomer hold up, inhibitor type and concentration, reaction temperature, and agitation speed.

CHAPTER TWO

EXPERIMENTAL PROCEDURES

2.1 MATERIALS

Distilled water was used as the continuous phase. Methyl methacrylate (MMA) (analytical grade, Aldrich) was distilled at reduced pressure. Polyvinyl alcohol (PVA) (M_w = 85000-146000, degree of hydrolysis = 87-89%, Aldrich), lauroyl peroxide (LPO) (97%, Aldrich), *normal*-dodecyl mercaptan (*n*-DDM) (98+%, Aldrich), hydroquinone (HQ) (99%, Aldrich) and 4-*tert*-butylcatechol (TBC) (97%, Aldrich) were used without any further purification.

Auxiliary chemicals including sodium lauryl sulphate (SLS), acetone, and methanol were analytical grade obtained from Aldrich and were used as received.

2.2 EXPERIMENTAL

Set up: Experiments were carried out using a 1-litre jacketed glass reactor with an internal diameter of 10 cm equipped with a four-bladed flat turbine-type impeller with a width of 5.0 cm, a standard four-baffle plate with the width of 1/10 of vessel diameter located at 90° intervals, an overhead reflux condenser, a thermocouple, a sampling device, a port for nitrogen purge, and an inlet for feeding ingredients (*Figure 2.1*). The temperature of the vessel content was controlled within ± 1.0°C of the desired reaction temperature (mostly 70°C) by pumping water at an appropriate temperature through the reactor jacket. The temperature of the vessel contents was continuously monitored by a thermocouple. An adjustable impeller-speed motor with a display was used. Agitation speed was adjusted at the desired level before the start of each experiment.

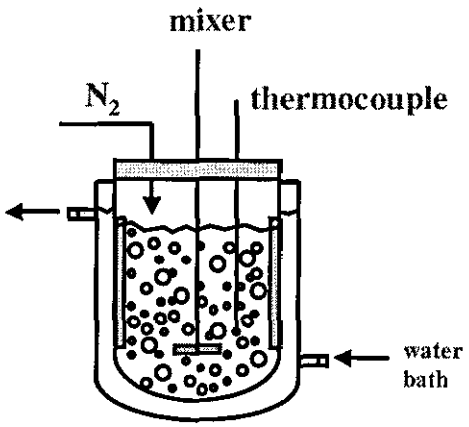

Figure 2.1 Schematic experimental set up

Procedure: For suspension polymerisation experiments, nitrogen purging was carried out for 30 minutes before the monomer phase was added. The PVA solutions were made by dissolving PVA granules in the distilled water. The mixture was kept stirred at 50°C for at least a few hours and then the solution was stored for further use. For each experiment, the required amount of PVA solution was added to the reactor containing pre-weighed amount of distilled water and then the temperature was raised to the reaction temperature. The dispersed phase was weighed, sealed and heated to the reaction temperature. The initiator was dissolved in the monomer phase, just prior to the addition of the monomer to the reaction vessel. Samples were withdrawn at the desired time intervals from the reaction vessel using a hypodermic syringe. The total volume of the mixture in the reactor was always kept constant at 700 cm^3 for all the experiments.

2.3 MEASUREMENTS

The kinetics of polymerisation was monitored by measuring the conversion by a gravimetric method. The evolution of drop size distributions was monitored by using laser diffraction and optical microscopy. The interfacial tension of the dispersions was measured by the Du Nouy ring technique. The concentration of monomer in the water phase was obtained using gas-liquid chromatography. The experimental reproducibility is briefly discussed in Appendix A.

2.3.1 Conversion

Monomer conversion was measured gravimetrically. Small quantities of the dispersion were withdrawn from the reactor and transferred into the small weighed aluminium foil dishes. The samples, contained in the dishes, were weighed and then quenched by adding cold acetone. The dishes were kept in the vacuum oven at 50°C for at least 18 hours. Monomer, acetone, and water were driven off by drying to constant weight in the vacuum oven. Then the dishes were weighed again to calculate the monomer conversion using the following expression:

$$conversion = \frac{\frac{weight.residue}{aliquot.weight} - solid.fraction}{monomer.fraction} \qquad (2.1)$$

The solid fraction accounts for the weight fraction of initiator and stabiliser, and any other solid additive such chain transfer agent and inhibitor, in the reactor. The monomer fraction accounts for the weight fraction of monomer in the reactor.

2.3.2 Drop/Particle Size Distribution

Several techniques have been developed for drop size measurements of liquid-liquid dispersions and emulsions. Optical microscopy seems to be one of the oldest techniques used for drop size measurements in liquid-liquid dispersions. Traditionally, optical microscopy has been used for off-line measurements. In several reports, vessels with a special on-line photomicrographic set-ups have been designed to obtain size distributions of the dispersed phase drops during mixing (Park and Blair, 1975; Hong and Lee, 1983; Chatzi and Lee, 1987; Coulaloglou. and Tavlarides, 1976 and 1977; Konno et al, 1983; Konno et al., 1988; Borwankar et al., 1986; Clark, 1988). Pacek et al. (1994) developed a *video-microscope-computer* technique for on-line monitoring of the drop size and size distribution as well as the structure of the drops. Hocq et al. (1994) and Bae and Tavlarides (1989) used *a capillary method* for drop-size measurement. Tsouris and Tavlarides (1994) used *a laser capillary* technique which is able to measure bivariate distributions of drop size and drop concentration by monitoring the intensity of the laser light penetrating the walls of the capillary glass tube along with the sampled drops and continuous phase are forced to pass. Hong and Lee (1983) used a *light transmission method.* Alopaeus et al. (2002) used *a laser beam*

reflectance measurement device that is based on a rapidly rotating laser beam. The laser beam randomly measures chord length of passing drops, and the measured distribution of chord length is then converted into a drop size distribution. Zhou and Kresta (1998) used an *aerometrics phase doppler particle analyser* (PDPA) to measure the size of drops. The technique requires the transparency of the dispersion in addition to the transparency of both phases. Another technique which is widely used for liquid-liquid and solid-liquid dispersions is the *laser diffraction technique* (Chatzi et al., 1991). This technique is based on the measurement and interpretation of the angular distribution of light diffracted by the drops and uses the Fraunhofer diffraction theory.

In this research we used two off-line techniques: laser diffraction and optical microscopy. Because of the presence of the stabiliser, the dispersions were sufficiently stable to allow reliable size measurements to be made with off-line techniques. The advantages of laser diffraction are its speed and that it does not need any calibration. Its drawback is that it requires the samples to be diluted. The advantage of the optical technique is visual observation of drops and their shape, and that under normal circumstances samples can be directly used for measurements. Its demerit is that it is very tedious and there is always the possibility that representative samples for measurement cannot be obtained. This is particularly true for broad size distributions because of the natural tendency of operators to size larger and more distinct drops. The combination of the two techniques proved to be very efficient.

2.3.2.1 Laser diffraction particle sizer

In this research, a laser diffraction technique has been selected as the main method for drop/particle size measurement. A laser diffraction particle sizer (Malvern, Coulter LS130), based on Fraunhofer diffraction, was used for PSD/DSD measurements. For a brief description of the method see Appendix B.

Prior to any measurement, the sample cell of the instrument was thoroughly cleaned and filled with an aqueous solution of sodium lauryl sulphate (SLS; 0.2 g/l) to prevent coalescence of the droplets. In order to avoid irreproducibility, the sampling point was fixed at 2 cm distance from the impeller shaft and 3 cm below the suspension level. Samples were withdrawn at desired time intervals. A drop of each sample was immediately transferred to the sample cell. The cell contents were mixed gently by a magnetic stirrer, provided in the cell, to prevent coalescence of droplets during the

measurement. Sampling and size measurements were continuously carried out in the course of the process (non-reacting dispersion or suspension polymerisation).

Particle/drop sizing required the dispersion to be highly diluted in water whereupon the monomer in the monomer drops or unreacted monomer inside the particles may diffuse out of the particles, depending on the water solubility of the monomer. Water-solubility of MMA at 25°C is around 15 g/litre. A simple mass balance shows that dilution of samples with 10^2 times volume of water would be enough to drain almost all MMA monomer out of particles/drops. To avoid underestimation of drop sizes, the distilled water used for the dilution of the samples, was saturated with the monomer prior to preparation of the surfactant solution.

Typical PSD Calculation

The particle sizer Coulter LS130 has 84 channels (bins) which accommodate size range that change logarithmically. These channels cover the size range of 0.43-822 μm.

The output of the particle sizer is in terms of volume of drops in each bin size. This can be easily transformed to volume frequency distribution (f_v), defined as:

$$f_v(d_i) = \frac{V_i}{\sum V_i} \tag{2.2}$$

where V_i is the volume of drops with a diameter between d_i and $d_i+\Delta\ln(d_i)$. Considering that $V_i = N_i v_i$, where N_i is the number of drops with diameter between d_i and $d_i+\Delta\ln(d_i)$, the number frequency distribution (f_n) can be calculated as follows:

$$f_n(d_i) = \frac{N_i}{\sum N_i} \tag{2.3}$$

$$f_n(d_i) = \frac{f_v(d_i)/d_i^3}{\sum f_v(d_i)/d_i^3} \tag{2.4}$$

It should be noted that both f_v and f_n are normalised in terms of a logarithmic scale of size; $\ln(d)$. The distribution in terms of normal scale of size, d, is more convenient for

practical applications. The normalised distributions in terms of d can be calculated using the following equation:

$$F(d_i) = \frac{f_v(d_i)}{\Delta d_i} \tag{2.5}$$

$F(d_i)$ is called "diameter density distribution", which has the dimension of inverse length unit (μm^{-1}) and satisfies the normalisation condition:

$$\sum_{d_{min}}^{d_{max}} F(d_i)\Delta(d_i) = 1 \tag{2.6}$$

where d_{min} and d_{max} are the diameters of the smallest and the largest drops that exist in the vessel, respectively.

Application of density distributions facilitates the comparative study of drop size distributions of different samples. In this way all size distributions are normalised and can be compared easily with each other on a single graph.

Table 2.1 indicates a typical result from the particle sizer. The sample used was withdrawn from a MMA suspension polymerisation run at the beginning of the polymerisation. A quick look at the data in this table reveals that they represent a bimodal distribution. The maximum of the first peak is at about 2.6 μm and that of the second one is at about 77 μm (the data related to the peaks are written in bold). Generally most size distributions obtained in this research presented a bimodal distribution including a main or primary peak at a larger diameter range and a secondary peak in a diameter range lower than 10 μm. The formation of tiny droplets have been attributed to nonhomogeneity of turbulent flows in stirred tanks, drop break up mechanism (breaking into daughter drops and large number of small satellite droplets), and viscosity build up in the drops (in the case of suspension polymerisation). Detailed discussions regarding the formation of satellite droplets are presented in Chapter 1.

For simplicity, hereafter the drops included in the main or primary peak are called "daughter drops". Those drops, which usually form the secondary peak and are smaller

than 10 μm, are called "satellite droplets". These terminologies are used throughout this text.

Table 2.1 Typical results obtained from the Laser sizer (Coulter LS130).

d_i (μm)	V_i (μm^3)	d_i (μm)	V_i (μm^3)	d_i (μm)	V_i (μm^3)	d_i (μm)	V_i (μm^3)
0.42922	0	2.9045	141.4	19.654	116.1	133	1128
0.47013	0	3.1813	136	21.528	132	145.68	891.5
0.51495	0	3.4846	128.1	23.58	155.8	159.56	677.3
0.56403	0.1884	3.8168	118.3	25.828	197.1	174.77	468.7
0.6178	2.219	4.1806	107.3	28.29	263	191.43	293.7
0.67669	6.115	4.5791	95.8	30.986	352.5	209.68	173.2
0.7412	10.54	5.0156	84.58	33.94	459.4	229.67	84.77
0.81185	16.82	5.4937	74.24	37.175	585.6	251.56	21.94
0.88924	25.02	6.0174	65.52	40.719	753	275.54	1.32
0.974	35.04	6.591	59.29	44.601	998.1	301.81	0
1.0668	46.32	7.2193	55.61	48.852	1355	330.58	0
1.1685	58.62	7.9074	53.7	53.509	1831	362.09	0
1.2799	71.87	8.6612	52.9	58.61	2389	396.61	0
1.4019	85.49	9.4868	52.86	64.197	2938	434.41	0
1.5356	99	10.391	53.41	70.316	3352	475.82	0
1.682	111.7	11.382	54.94	**77.019**	**3510**	521.18	0
1.8423	123	12.467	58.44	84.36	3359	570.86	0
2.0179	132.3	13.655	64.93	92.402	2946	625.28	0
2.2102	139.1	14.957	74.81	101.21	2399	684.88	0
2.4209	143	16.382	87.59	110.86	1863	750.17	0
2.6517	**143.8**	17.944	101.8	121.43	1436	821.67	0

Figures 2.2 and *2.3* show the drop size distributions of data given in Table 2.1 in terms of logarithmic and normal scale of drop diameter, respectively. The volume fraction of the droplets below 10 μm (secondary peak) is 0.06 while the number fraction of these small droplets is 0.99. This implies that in terms of volume, the satellite droplets contain only 6 % of the whole volume of drops. But in terms of number, 99 % of drops have a diameter smaller than 10 μm. Similar results have been observed with samples from all non-reacting or reacting dispersions in the context of this study. This difference in the distribution of drops indicate how significant is to use an appropriate distribution for any intended use.

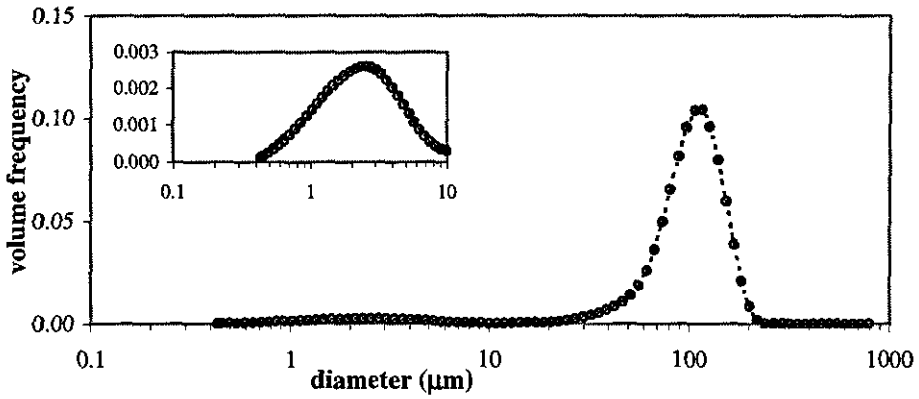

Figure 2.2 Drop size distribution for typical data given in Table 2.1. The small figure shows a close up of the peak in the diameter range of below 10 μm.

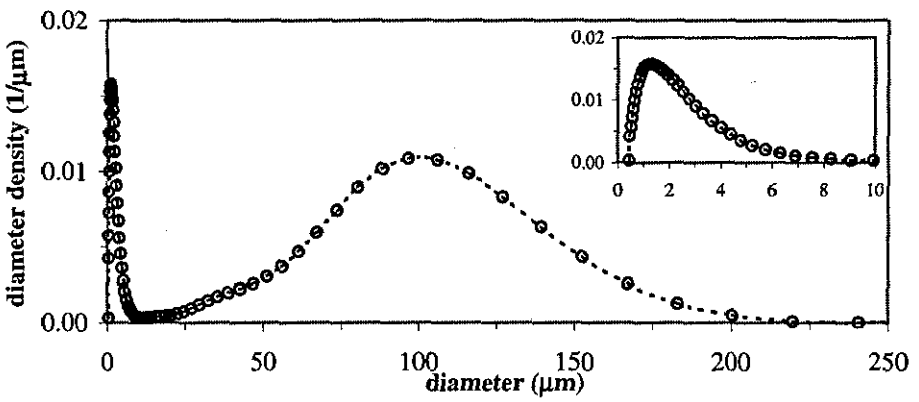

Figure 2.3 Diameter density distribution for typical data given in table 2.1. The small figure shows a close up of the peak in the diameter range of below 10 μm.

The Sauter mean diameter of particles (drops) was calculated using the following equation:

$$d_{32} = \frac{\sum_{i=1}^{\infty} N_i d_i^3}{\sum_{i=1}^{\infty} N_i d_i^2} = \frac{\sum_{i=1}^{\infty} f_n(d_i) d_i^3}{\sum_{i=1}^{\infty} f_n(d_i) d_i^2} = \frac{\sum_{i=1}^{\infty} f_v(d_i)}{\sum_{i=1}^{\infty} f_v(d_i)/d_i} \qquad (2.7)$$

We have used the above equation to determine the Sauter mean diameter of the drops in the whole diameter range, for the drops with diameter above 10 μm, and also for

satellite droplets with diameter below 10 μm. Table 2.2 compares the Sauter mean diameter for the above three groups of drops for the data in Table 2.1. It is obviously seen that the presence of a large number of satellite droplets has a great effect on the Sauter mean diameter.

Table 2.2 Sauter mean diameter for different size classes of drops presented in Table 2.1.

	whole range (D'_{32})	$d > 10$ μm (D_{32})	$d < 10$ μm (d_{32})
Sauter mean diameter (μm)	22.94	62.73	2.27

In order to track the variations in the mean drop size of the daughter drops, the satellite droplets, and the whole population of drops in the course of a reacting/non-reacting dispersion process, the Sauter mean diameter has been separately calculated for these populations. The corresponding Sauter mean diameters are labelled as: daughter drops (D_{32}), satellite droplets (d_{32}), and the whole drops (D'_{32}).

2.3.2.2 Optical Microscopy

As a complementary method, the particle/drop size was also measured using an optical microscope connected to a camera and a graphic printer. Several photographs were taken from each sample and 350-500 drops were counted. The number frequency distribution obtained was used to calculate the other distributions and the Sauter mean diameter.

A comparison of the resulted DSD from the two methods for a typical sample is illustrated in *Figure 2.4*. Good agreement is observed between the results of the two methods. Some differences can be seen, however, in the small-size range. These differences can be explained in view of the accuracy of each technique in measuring the small-size portion of the drops and their inherent measurement errors. In the laser diffraction method, the size range is discretised on the logarithmic diameter scale, which places more weight on the small-size droplets. On the other hand, the actual determination of drop sizes by photography may result in significant errors, especially for small drops that cannot be distinguished very clearly (Mlynek and Reshnik, 1972;

Chatzi et al., 1989). Laso et al. (1987) comment on the tendency of the observer to preferentially count larger drops while neglecting smaller ones. As a result, the error associated with the measurement of small droplets is higher than that for the large drops. The laser diffraction method has been used as a fast and accurate technique suitable for on- and off-line measurements, which allows determination of multimodal drop size distributions with increased sensitivity especially in measuring the small diameter drops (Chatzi et al., 1991).

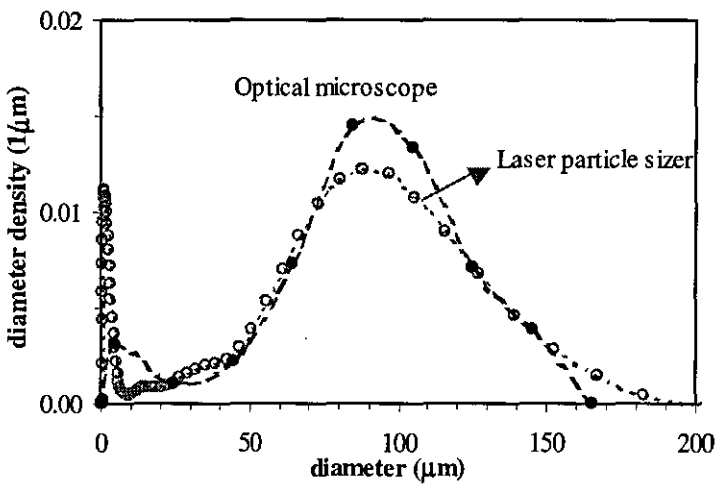

Figure 2.4 Comparison between the results obtained by optial microscope and laser particle sizer (Coulter LS130) for the same sample (polymer particles).

Generally the measurement of very small drops/particles was very difficult to carry out using optical microscopy. In some cases large particles were surrounded with a large number of small particles. These small particles could be observed clearly especially during the suspension polymerisation processes and in particular in the final stage of the polymerisation when they become solid. These drops/particles were in the diameter range of below 10 μm. Evidence of presence of these small drops/particles are shown as appropriate.

2.3.3 Interfacial Tension

Interfacial tensions between MMA and aqueous solutions of PVA (the grade used in this study) were measured using a Du Nouy ring tensiometer. The principles of this method have been presented in Appendix C. No correction was made on the reading.

15 cm^3 of different aqueous solutions of PVA (0.25, 0.5, 1.0, 2.0, 4.0, and 10.0 g/l) were prepared and transferred into small glass dishes. 15 cm^3 of MMA was added very gently through the sidewall of the dish to lie as a layer on top of the aqueous phase. Samples were allowed for 30 min to reach the thermodynamic equilibrium before any surface tension was recorded. Measurement was repeated three times for each sample. The average value was reported as the interfacial tension. The surface tension of pure water was measured to check the reliability of the tensiometer.

2.3.4 Aqueous-phase Monomer Concentration

Monomer concentration in the aqueous phase was measured using a Gas-Liquid Chromatograph (Pye Unicam 304-FID GLC). A brief description of gas-liquid chromatography (GLC) has been presented in Appendix D.

A general-purpose capillary column, wall coated-fused silica-CP-SIL5, was used. The detector used was flame ionization one (FID). The advantage of this detector is that it does not detect water, in addition to its high sensitivity. The carrier gas was helium (He). The GLC measurements were carried out at the following conditions: column temperature of 40°C, injector and detector temperature of 125 and 130°C, respectively; the flame fuel gases hydrogen and air at 17.0, and 10.0 kg/cm^2, respectively, and the carrier gas He at the flow rate of 18 ml/min. Samples of 1 µl were injected to the column. For each sample, two injections were carried out and the average value was used. In the case of a large discrepancy between the output values, the injection was carried out for the third time and the average of all three injections was used.

Calibration: Methanol (Me) was used as the internal standard to avoid the effect of variation in sample volume to the injection port. In order to calculate the concentration of MMA in the sample, a calibration curve is required.

The calibration curve for GLC measurement was prepared using the following expression:

$$\frac{W_{MMA}}{W_{Me}} = F_r \frac{A_{MMA}}{A_{Me}} \qquad (2.8)$$

where W_{MMA} and W_{Me} are the weight of MMA and the standard, Me, in the sample, and A_{MMA} and A_{Me} are surface areas of the MMA and the standard in the chromatographs, respectively. F_r is the response factor of MMA compared to the internal standard.
10 standard solutions of MMA, Me, and water (with known concentrations) were prepared and injected into the GLC. The addition of water was made to obtain samples similar to those from the dispersions. Using the surface areas of MMA and Me in the obtained chromatographs, and the weight ratios of the MMA and Me in the samples, the calibration curve shown in *Figure 2.5* was drawn, according to the above equation. The slope of this graph shows the value of response factor, F_r = 0.84, which remains constant with concentration ratio of MMA and Me, and also with the concentrations of other ingredients such as water.

Sample preparation: Samples were taken from the reactor at appropriate intervals and kept in capped test tubes for a while to allow for phase separation to occur. Samples from the aqueous phase were withdrawn with a syringe and weighed. A known amount of a Methanol solution (with known concentration) was added to the samples. Using the response factor, and the known values of MMA and Me peak areas and weight of Me in the sample, it is possible to calculate the MMA weight in the sample from which the monomer concentration in the water phase can be calculated.

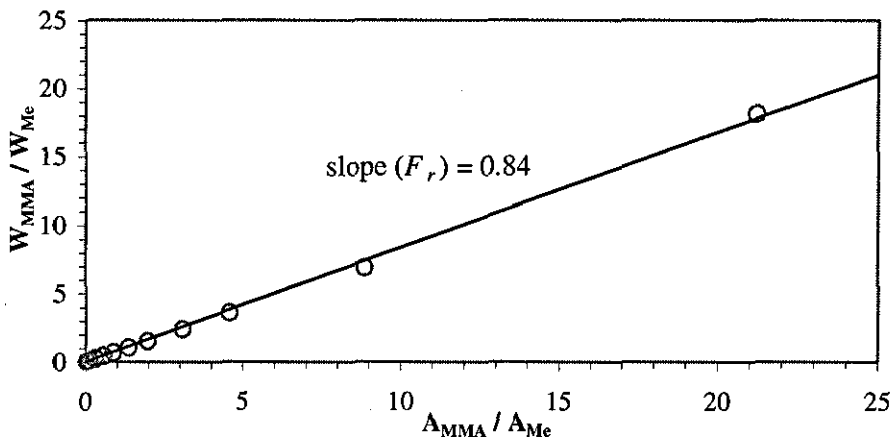

Figure 2.5 Calibration curve for calculating MMA concentration in the aqueous phase using methanol (Me) as the internal standard.

CHAPTER THREE

EXPERIMENTAL RESULTS AND DISCUSSION

INTRODUCTION

The experimental results from the MMA batch suspension polymerisation with PVA as a stabiliser and LPO as an initiator are presented in this chapter. The MMA/water dispersions were also carried out with PVA as stabiliser.

LPO was used to limit the formation of emulsion particles. Experiments with initiators such as azobisisobutyronitrile (AIBN) resulted in the formation of a large number of emulsion particles so were not perused in this research.

Drop size measurements was carried out with laser light diffraction method. The initial results obtained by optical microscopy are given in the first year report and not repeated here. The variables studied in this research are:

1. Suspending agent (PVA) concentration that mainly affects properties of the continuous phase.
2. Initiator (LPO) and chain transfer agent (*n*-DDM) concentrations that affect properties of the dispersed phase.
3. Inhibitor concentration (water-soluble and oil-soluble inhibitors) that may affect properties of both phases.
4. Reaction temperature that affects properties of both phases but mainly the dispersed phase (kinetics of polymerisation).
5. Agitation speed that affects the mixing conditions and directly the drop/particle size.
6. Monomer hold up that affects directly the drop/particle size. It also affects properties of both phases due to monomer partitioning between the two phases.

In the following sections the effects of these variables on the evolution of average particle size and distribution, in both non-reacting dispersion and suspension polymerisation of MMA, are presented.

3.1 EFFECT OF PVA CONCENTRATION

3.1.1 INTRODUCTION

The performance of a stabiliser in terms of its ability to stabilise a droplet is a function of surface coverage of the drop, and diffusion and adsorption characteristics of stabiliser molecules, which is further determined by the molecular properties of the stabiliser. For polymeric stabilisers soluble in the continuous phase, stability of liquid-liquid dispersions was found to increase with both increasing polymer molecular weight and degree of grafting of hydrophobic branches. In this case drop stabilisation is achieved mainly by an increase in the resistance to film thinning thus hindering the coalescence process. This may be achieved through two mechanisms. The first is related to higher viscosity of continuous phase with adding polymeric stabiliser. The other mechanism is what has been called "Marangoni effect". When the intervening film thins, it sweeps along its path the stabiliser molecules adsorbed on the interface, creating a stabiliser concentration gradient and subsequent interfacial tension gradient that opposes the film thinning (He et al., 2002).

PVA, is one of the polymeric water-soluble stabilisers used in suspension and emulsion polymerisation processes. A number of studies have been done on suspension polymerisation using PVA as stabiliser and the effects of its characteristic properties on stabilisation of drops (e.g., Konno et al., 1982; Goodall and Greenhill-Hooper, 1990; Castellanos et al., 1991; Mendizabal et al., 1992; Zerfa, 1994).

Effect of degree of hydrolysis: For PVA, an increase in hydrophobicity represents an increase in the driving force for the molecules to move to and adsorb onto the water/monomer interface, which improves the stability of dispersion. Therefore the lower the degree of hydrolysis for PVA, the higher the driving force for adsorption and the better is drop stability (He et al., 2002). As the degree of hydrolysis increases the interfacial tension increases and larger drops with broader distribution are obtained (Chatzi and Kiparissides, 1994). Using PVAs with a very low degree of hydrolysis (< 80) or molecular weight, however, results in some coagulation and agglomeration of polymer particles and the formation of polymer lumps, while using PVAs with a very high degree of hydrolysis (>90) result in unstable dispersions leading to formation of

shapeless polymer bulk (Castellanos et al., 1991; Mendizabal et al., 1992). PVAs with a very high degree of hydrolysis are too hydrophilic to adsorb strongly enough at monomer-water interfaces to form a coherent film that will inhibit drop coalescence.

Effect of Molecular Weight : The ability of PVAs, of similar degree of hydrolysis, to stabilise dispersions increases with increasing molecular weight. But this influence is more significant for PVAs with a lower degree of hydrolysis (He et al., 2002). The thickness of the PVA adsorbed layer on drops increases with increasing molecular weight of PVA. For low molecular weight PVAs the thickness of the adsorbed layer is very small and so, during the polymerisation, the drops can approach each other closely enough for the adsorbed polymer segments to interact and become entangled (bridging). The result is the formation of polymer lumps.

It has been reported that the best PVA grade for using as a stabilising agent in suspension polymerisation is a PVA with degree of hydrolysis of 80-90 and molecular weight above 70000 (Goodall and Greenhill-Hooper, 1990; Castellanos et al., 1991; Mendizabal et al., 1992). This grade of PVA forms a thicker and stronger layer on the water/monomer interface and has less tendency to desorb, therefore, a similar grade was selected as stabiliser for the current research.

One of the crucial factors in the control of polymer beads formed in suspension polymerisation reactors is the concentration of the stabiliser used. Increasing the concentration of stabiliser in general, and PVA in particular, has been found to increase its ability to stabilise the dispersion due to steric and Marangoni effects. Although it has been also reported that some types of PVAs at high concentrations show a decrease in coalescence time probably caused by partial cancellation of Marangoni effect due to readily available stabiliser molecules in the continuous phase. It has been shown that the increase in viscosity of the continuous phase with increasing PVA concentration does not play a major role in drop stabilisation (He et al., 2002). In an excellent paper, Konno et al. (1982) reported the effect of PVA concentration on the coalescence of dispersed drops in suspension polymerisation of styrene. They, for the first time, monitored the transient drop size during polymerisations and suggested that the coalescence of dispersed drops above the maximum stable drop size is not effectively prevented by the stabiliser. A smaller mean particle size and sharper PSD have been obtained with increasing PVA concentration (Konno et al., 1982). With increasing PVA concentration in a liquid-liquid dispersion, mean drop size decreases and PSD becomes

narrower (Chatzi and Kiparissides, 1994). Chatzi and Kiparissides (1994) have also reported formation of bimodal PSDs suggesting erosive mechanism for drop break up.
In this series of experiments, we study the effect of PVA concentration on the evolution of particle size distribution in MMA suspension polymerisation. Particular attention has been paid to the formation and growth of very small droplets. To underline the characteristic features of drop evolution in suspension polymerisations, or a reacting liquid-liquid dispersion, the results have been compared with those from corresponding non-reacting liquid-liquid dispersion.

3.1.2 EXPERIMENTAL

The materials, experimental procedure and measurements have been described in detail in Chapter 2. All experiments (polymerisations and dispersions) in this series were carried out at 70°C and an agitation speed of 500 rpm. The MMA hold up was 0.20. The LPO concentration (for polymerisation runs) was 1.0 wt% based on the monomer phase. Different PVA concentrations were used in this series.
Two series of experiments were carried out in this study. In one series, the entire required amount of PVA was used in the initial formulation. In another series, a part of PVA was used in the initial formulation and the second part was added during the polymerisation.
Interfacial tensions of MMA/aqueous PVA solutions were measured for different PVA concentrations.

3.1.3 RESULTS AND DISCUSSION

3.1.3.1 Non-reacting MMA/Water Dispersion

Mean Drop Size: The time evolution of the Sauter mean diameter of drops in the MMA-water dispersions with PVA concentrations of 0.2, 0.5, 1.0, 4.0, and 10 g/l is shown in *Figure 3.1.1*. D_{32} and d_{32} are the Sauter mean diameters for drops with diameter higher (daughter drops) and lower (satellite droplets) than 10 μm, respectively. D'_{32} is the Sauter mean diameter of all drops. *Figure 3.1.1a* shows that the drop sizes are exponentially reduced with time until they approach a fairly constant value. Based on these figures, the evolution of drop size can be divided into two stages; *transition* and *quasi steady-state*. During the transitions stage, drops are broken into smaller drops as they pass through the impeller region. A steady state, or a near steady state, was

reached in about 2 hours after which the size of drops did not significantly vary. With increasing PVA concentration, the rate of drop break up increased during the transition period due to a lower interfacial tension. Also the minimum transition time decreases with decreasing interfacial tension (Chatzi et al., 1991). As a result, a shorter transition stage and a lower steady-state D_{32} was achieved with increasing PVA concentration. The difference, however, became less important with increasing PVA concentration. This is backed by a diminishing difference in the interfacial tension (σ) with increasing PVA concentration as can be seen in *Figure 3.1.2.*

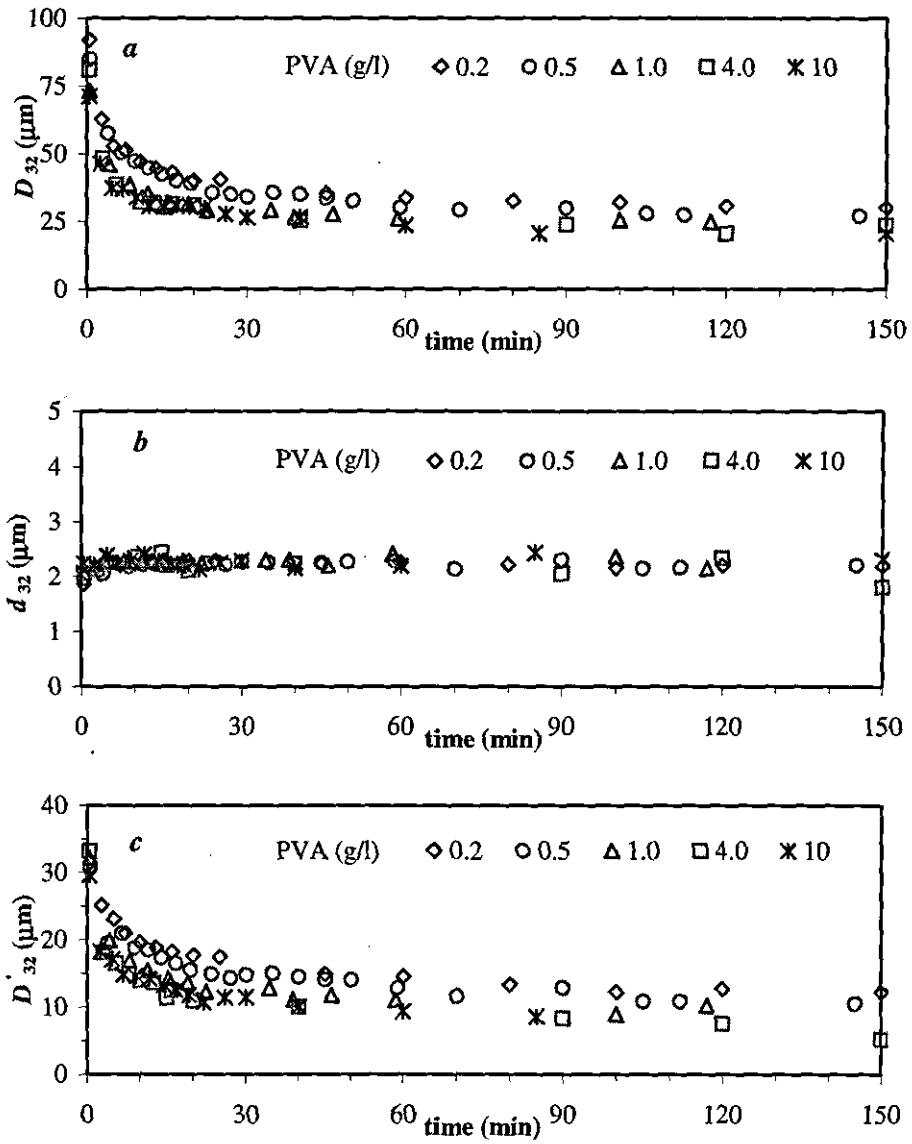

Figure 3.1.1 Time evolution of *a*) daughter drops, *b*) satellite droplets, and *c*) overall Sauter mean diameter with different PVA concentrations.

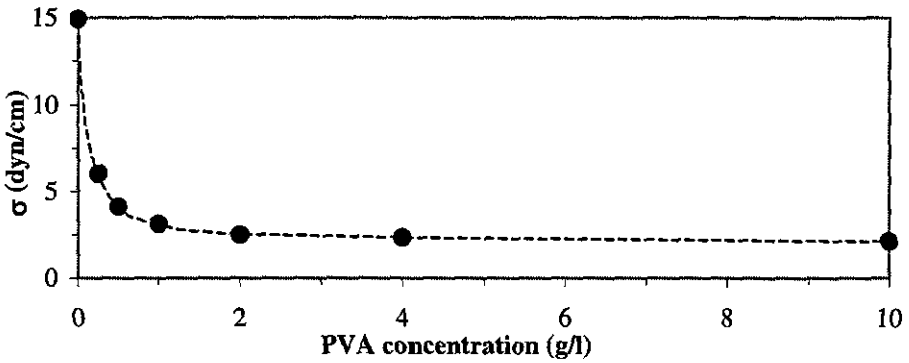

Figure 3.1.2 Variations of interfacial tension with PVA concentration.

According to *Figure 3.1.1b*, the size of satellite droplets does not seem to be affected by the PVA concentration. The time variations of the overall Sauter mean diameter, D'_{32}, (*Figure 3.1.1c*) is similar to D_{32}.

Drop Size Distribution: Figures 3.1.3 to *3.1.5* demonstrate the time evolution of drop size distribution for dispersions with 0.2, 1.0, and 10.0 g/l PVA. The micrographs for a typical run is shown in *Figure F.1* (Appendix F). The size distribution of daughter drops continuously narrowed and shifted to a smaller size with time. It is quite interesting to note that size distributions never reached a real steady-state distribution. Even after 150 min, the size distribution was still narrowing with time, but with a much lower rate. For practical applications, however, the average size of drops may be considered constant.

The results indicate that a large number of satellite droplets are formed. The mechanism of formation of these droplets is discussed in chapter one. *Figure F.2* (Appendix F) shows micrographs of drops sorrounded with numerous satellite droplets. The formation of stalite droplets was also observed for the styrene/water dispersion in the presence of PVA, but to a lesser extent (Appendix E). In *Figure 3.1.6*, the variation of the volume fraction of the satellite droplets (f_{vs}) is plotted against time for different PVA concentrations. The general trend observed from the family of curves shown in *Figure 3.1.6* is that the overall volume of the satellite droplets increases with time and PVA concentration and reaches a plateau at a later time.

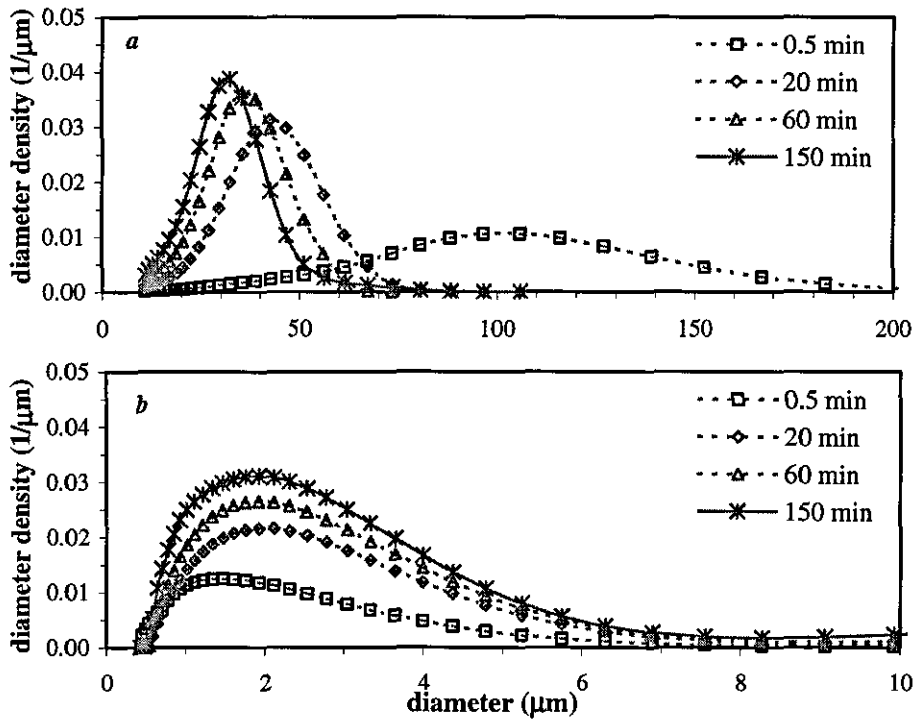

Figure 3.1.3 Time evolution of *a*) daughter, and *b*) satellite drop size distributions in dispersoin with PVA = 0.20 g/l.

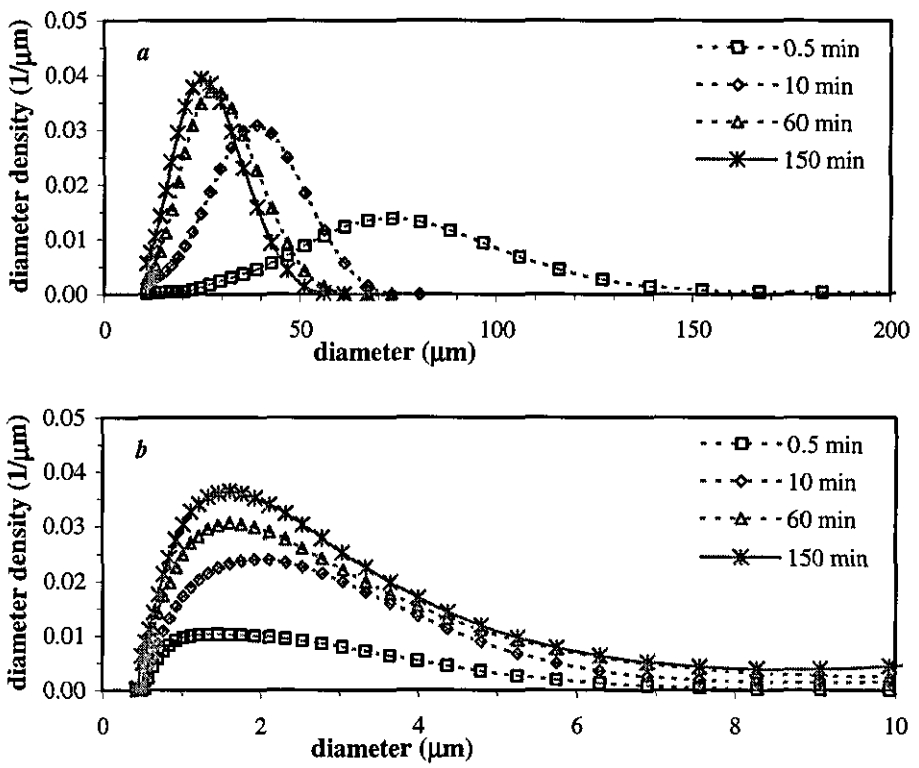

Figure 3.1.4 Time evolution of *a*) daughter, and *b*) satellite drop size distributions in dispersoin with PVA = 1.0 g/l.

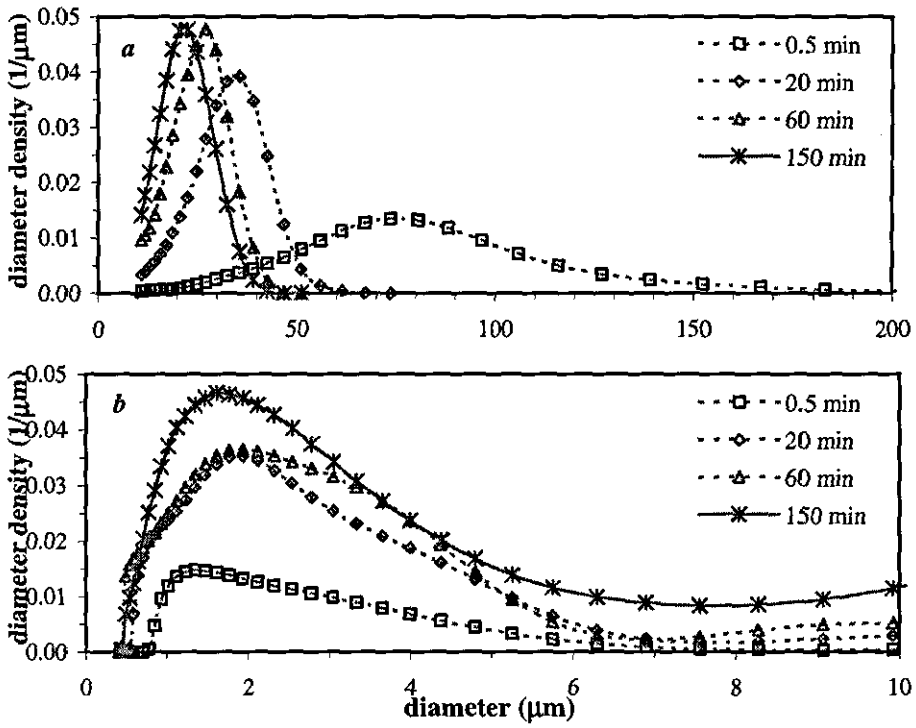

Figure 3.1.5 Time evolution of *a*) daughter, and *b*) satellite drop size distributions in dispersoin with PVA = 10 g/l.

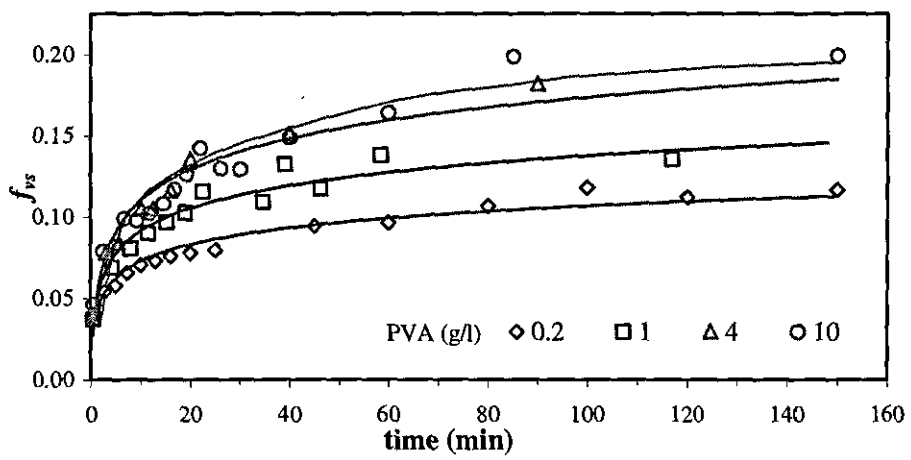

Figure 3.1.6 Time variation of volume fraction of satellite droplets in dispersions with different PVA concentrations.

3.1.3.2 MMA Suspension Polymerisation

3.1.3.2.1 One-Shot (Batch) Addition of PVA

Rate of Polymerisation: Figure 3.1.7 shows the conversion-time variation for runs with PVA concentrations of 0.1, 0.2, 0.5, 1.0, and 4.0 g/l (conversion was not measured for PVA = 10 g/l). As it is seen from this figure all the data points fall on the same curve indicating that PVA concentration does not affect the rate of polymerisation. It is also evident that the rate of polymerisation shows a drastic increase around the conversion of 0.40 because of the gel effect. The onset of the gel effect was reached in about 60 min. Within the next 10 min, the conversion reached a value as high as 0.9. Events in the time interval of 60-70 min, therefore, have a crucial effect on the PSD evolution because of the viscosity increase in the particles in association with the gel effect.

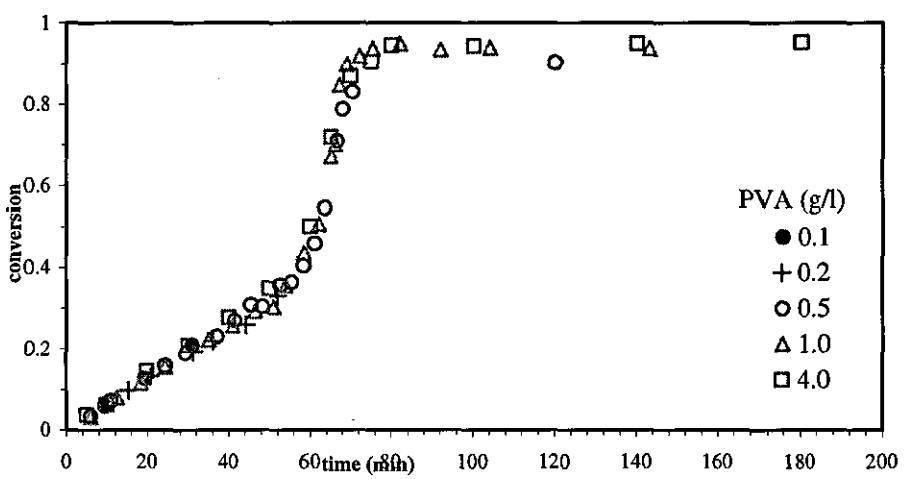

Figure 3.1.7 Conversion-time variations for runs with different PVA concentrations (for other conditions see section 3.1.2).

Mean Particle Size: Figure 3.1.8 illustrates the variations of the Sauter mean diameter of daughter drops, satellite droplets and the whole population of drops with time. In order to correlate the time evolution of drops to the kinetics of polymerisation and the status of the reaction system, the variations in Sauter mean diameter of daughter drops with conversion is shown in *Figure 3.1.8d.* The average drop size initially decreased with time (this may be again called *transition stage*), reached a plateau, and then either remained practically constant or increased with time depending on the PVA

concentration.

The pattern of variation in drop size with time after the end of the transition stage can be characterised by up to three intervals depending on the polymerisation conditions. The first interval is the *quasi steady-state stage* during which a rather constant drop size is maintained by balanced rates of drop break up and coalescence despite an increase in the drop viscosity. The occurrence of a steady state for suspension polymerisation is not always certain because of kinetic events occuring in the polymerising drops. Note that even for the dispersion processes there is some reduction in the size of drops with time during the so called quasi steady state. Unlike the dispersion process without polymerisation, the overall size of drops at the plateau showed a mixed behaviour with increasing PVA concentration because of the formation of satellite droplets. In the case of the PVA concentration of 0.1 g/l, the steady state was never reached and drops grew continuously, after the first reduction, until mass coagulation of particles occurred 20 min after the start of the polymerisation (see *Figures 3.1.8a* and *3.1.8c*). For PVA concentration of 0.2 g/l, the steady state lasted for 40 min and after that drops started growing very steeply. For PVA concentration of 0.5 g/l, the quasi steady state lasted for 50 min and then drops grew slowly. For PVA concentrations of 1.0 g/l and more, the polymerisations produced almost the same trend of constant drop size until approximately 62 min. Generally, the duration of the steady-state was prolonged with increasing PVA concentration.

As the drop viscosity increases, a point is reached where drops can not be easily broken up but they can still undergo coalescence. As a result, drops start growing by coalescence. This interval can be called the *growth stage*. This stage has been called the *sticky stage* in the literature perhaps because of the impression that drop coalescence increases with the drop viscosity due to increasing drop tackiness. However, the present author believes that this is a misleading title because, during this interval, particles are usually more stable against coalescence than in the earlier stage. The viscosity increase in the drops reduces the rate of drop break up more significantly than drop coalescence resulting in an increase in the size of particles. Drops with less coverage with the stabiliser are more susceptible to coalescence after a collision due to a weaker surface protection. The higher the PVA concentration, the later was the onset of the growth stage, and the less was the particle enlargement during the growth stage due to higher surface coverage ratio of particles. This can be readily realised from *Figure 3.1.8.*

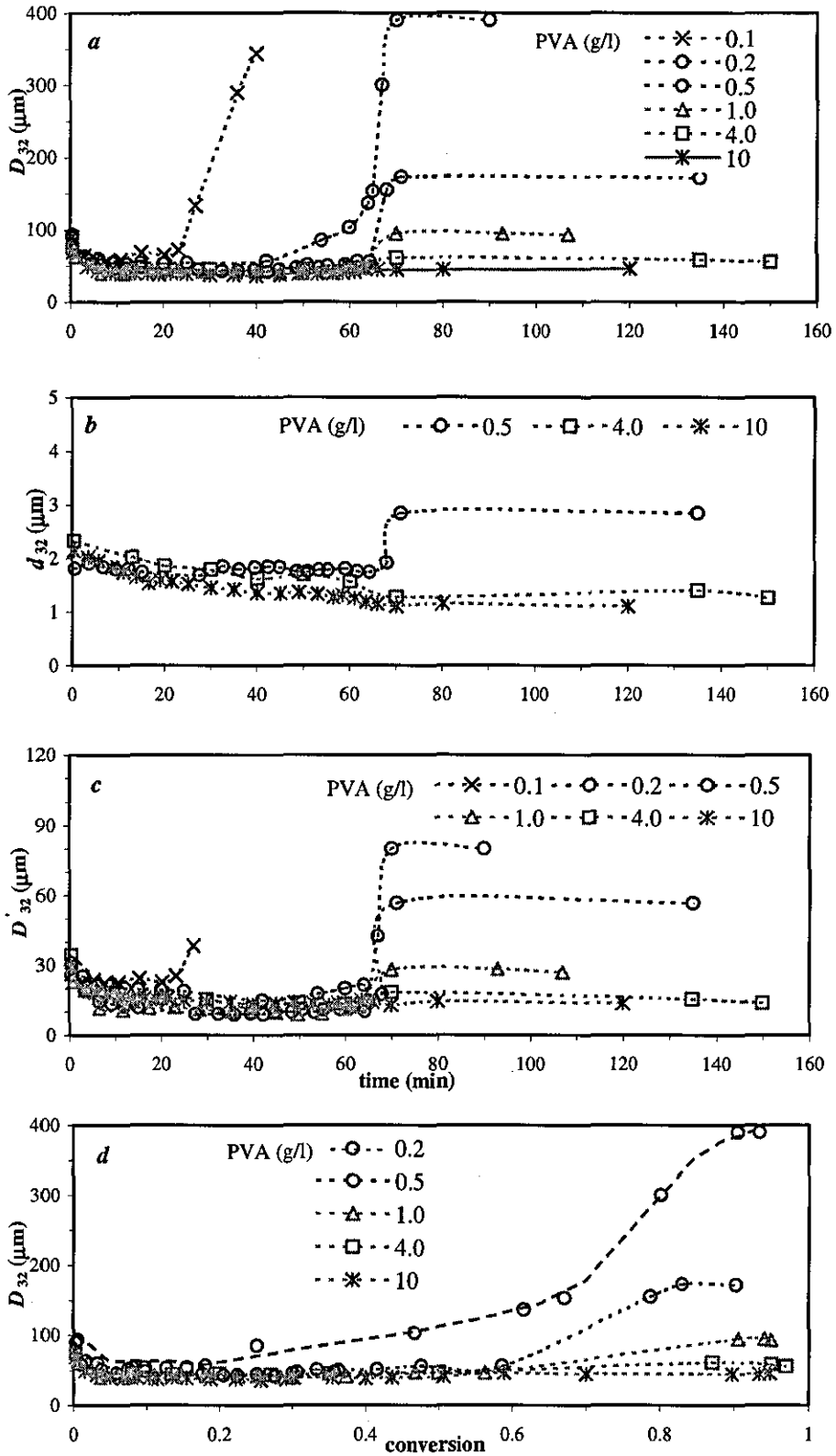

Figure 3.1.8 Variations of Sauter mean diameter of *a*)daughter, *b*)satellite and *c*)all drops with time and *d*)daughter drops with conversion for different PVA concentrations.

At the end of the growth stage, drops have a very high viscosity and behave like solid particles. These drops cannot coalesce with each other and they keep their identity for the remainder of the process. This has been called the *identification point* (Alvarez at al., 1994). Variations in average drop size occur in both the transition stage and the growth stage but sizes remain almost constant during the steady state and during the *identification stage* (i.e., after the indentification point is reached); although some limited flocculation may occur during the *identification stage*.

Particle Size Distribution: Figures 3.1.9 to *3.1.14* show the time evolution of PSD for the PVA concentrations of 0.1, 0.2, 0.5, 1.0, 4.0, and 10.0 g/l, respectively. The peak for daughter drops, or bead particles, which covers the particle size > 10 μm, have been clearly illustrated in *Figures 3.1.9a* to *3.1.14a*. The peak for satellite droplets, which appeared under 10 μm, has been clearly shown in *Figures 3.1.9b* to *3.1.14b*. *Figure F.3* (Appendix F) shows typical SEM micrographs of particles and satellite particles. In some instances the surface of large particles are covered with small particles indicating the importance of particle flocculation in the system under study. The flocculation of small satellite particles with themselves and large particle was also observed.

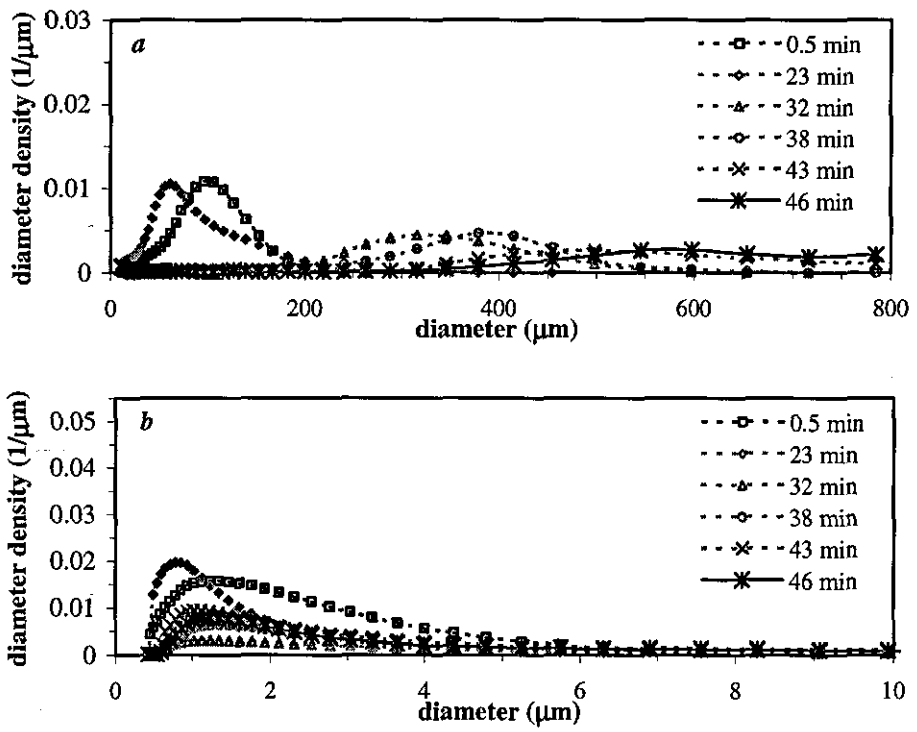

Figure 3.1.9 Time evolution of *a*) daughter, and *b*) satellite drop size distributions in the run with PVA = 0.10 g/l.

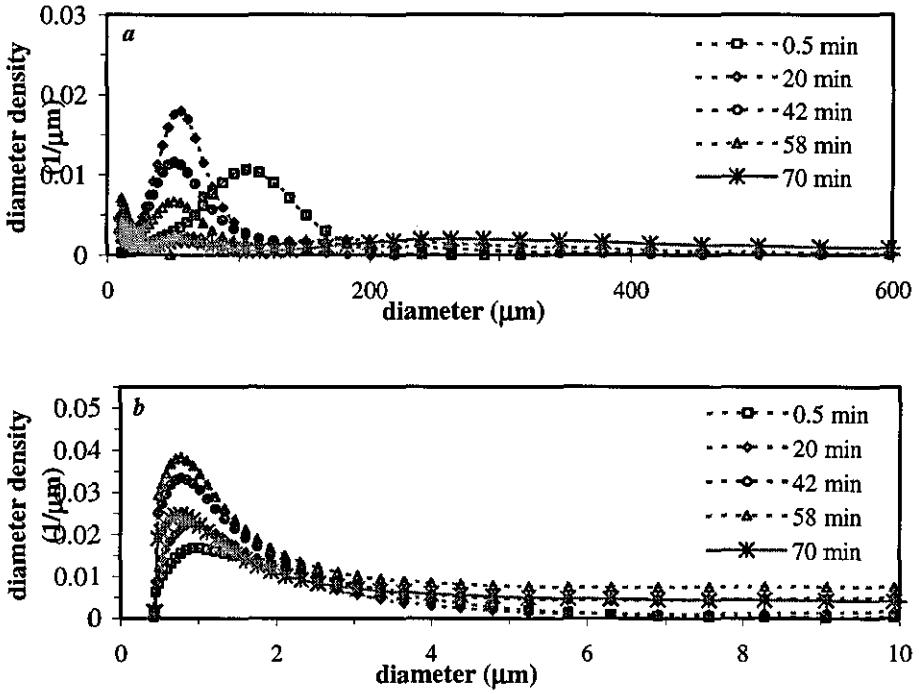

Figure 3.1.10 Time evolution of *a*) daughter, and *b*) satellite drop size distributions in the run with PVA = 0.20 g/l.

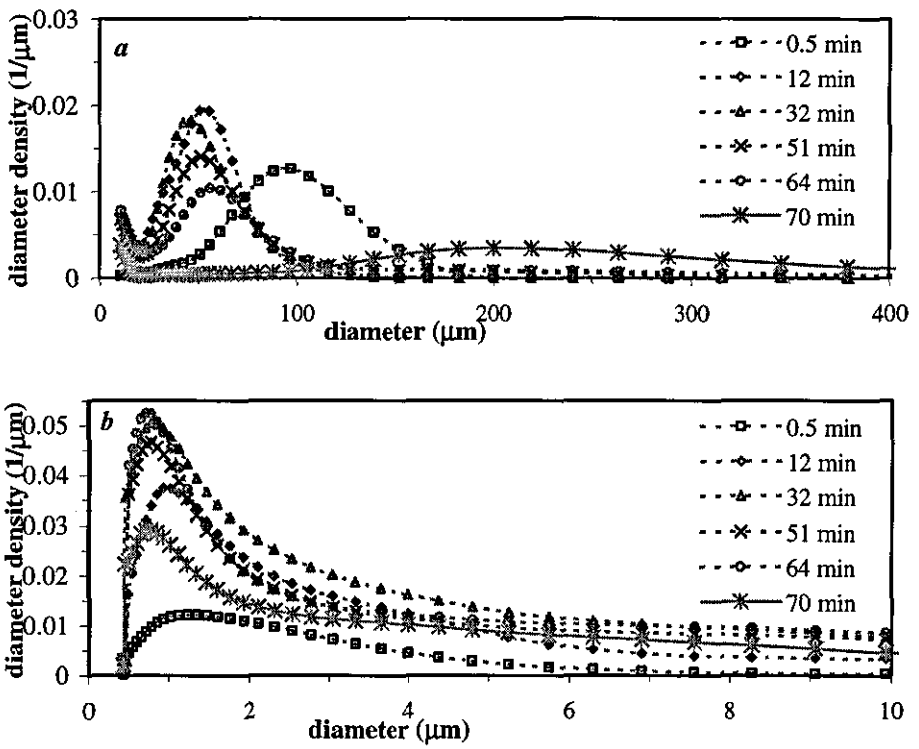

Figure 3.1.11 Time evolution of *a*) daughter, and *b*) satellite drop size distributions in the run with PVA = 0.50 g/l.

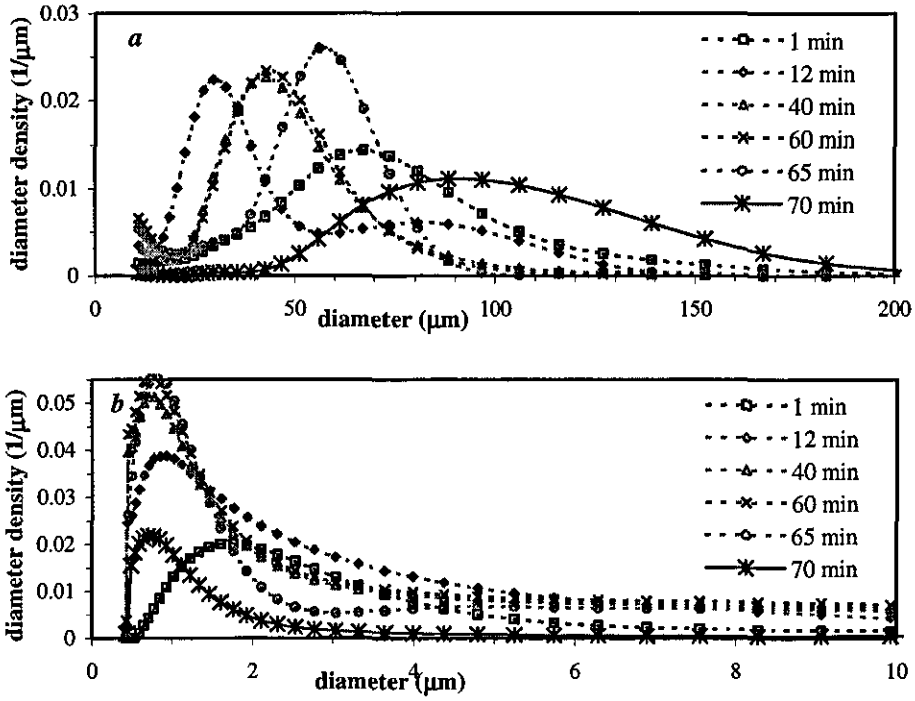

Figure 3.1.12 Time evolution of *a*) daughter, and *b*) satellite drop size distributions in the run with PVA = 1.0 g/l.

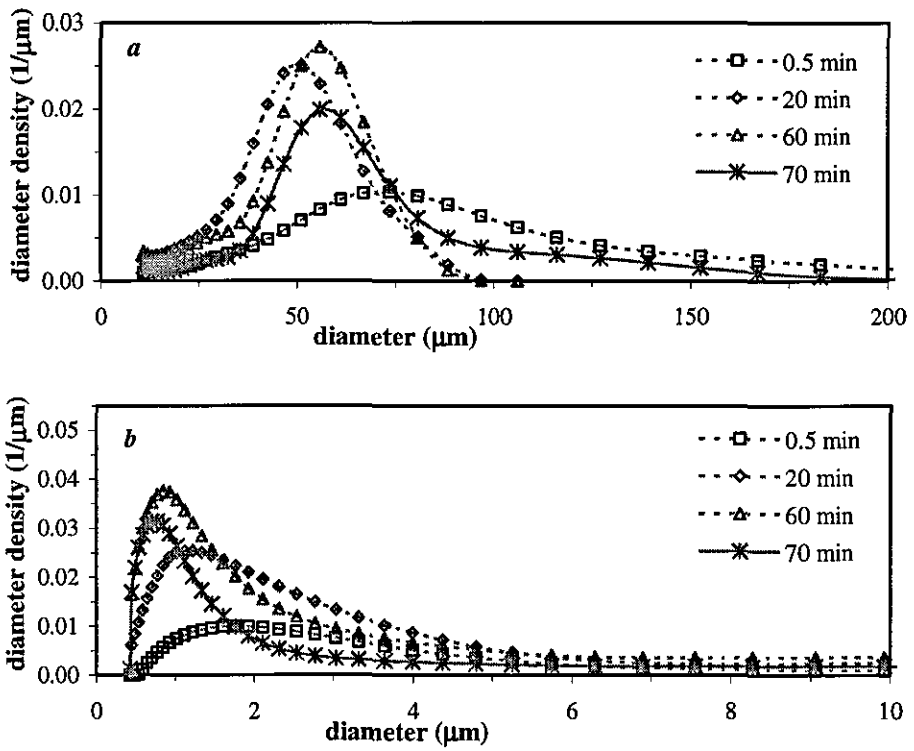

Figure 3.1.13 Time evolution of *a*) daughter, and *b*) satellite drop size distributions in the run with PVA = 4.0 g/l.

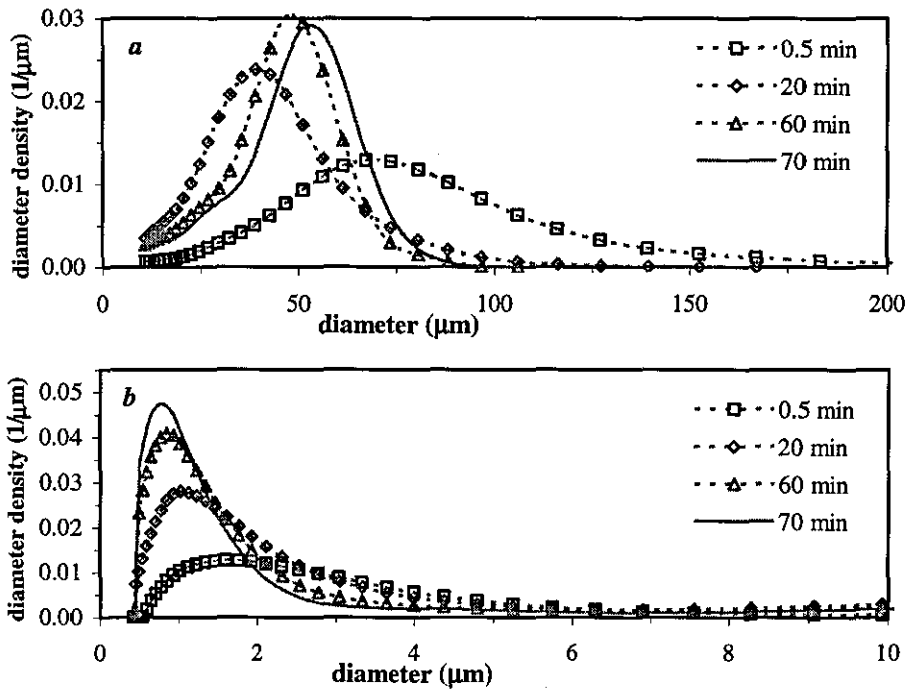

Figure 3.1.14 Time evolution of *a*) daughter, and *b*) satellite drop size distributions in the run with PVA = 10 g/l.

The evolution of satellite droplets is discussed below. Generally, satellite droplets were continuously formed during polymerisation by break up of daughter drops up to 60 min from the start of polymerisation as can be observed in *Figures 3.1.9b* to *3.1.14b*. Satellite particles were also observed in the suspension polymerisation of a sparingly water-soluble monomer (styrene) with PVA as a stabiliser (Appendix E). *Figure 3.1.15* clearly shows that, however, satellite droplet formation was less prevalent at the higher PVA concentrations so that for the PVA concentration of 10 g/l, the volume fraction of the satellite droplets reached a constant value early in the reaction. An interesting result is that the order of satellite formation takes an opposite trend to that observed for the dispersion process in which satellite formation increased with PVA (see *Figure 3.1.6*). One possible explanation for this is as the polymerising drops becomes smaller with increasing PVA concentration, their stability is increased and their vulnerability to break up is reduced because of their viscosity cohesive force. As a result the formation of satellite droplets is hindered. Whereas at a lower PVA concentration, where the polymerising drops are large as well as unstable, the more viscous drops are more

favourably broken up into satellite droplets because of shift in the mechanism of the drop break up with drop viscosity. At intermediate PVA concentrations, i.e. 1.0 g/l PVA, the evolutions of droplet volume fractions for the non-reacting dispersion and suspension polymerisation processes are comparable.

In contrast to *Figure 3.1.1b* which shows a constant d_{32} for the satellite droplets formed in the dispersion process, as seen in *Figure 3.1.8b*, d_{32} of those droplets formed in the suspension polymerisation decreased at higher PVA concentrations but remained constant at a lower PVA concentration. It seems that the viscosity build up in drops will change the mechanism of drop break up from bursting to stretching so that more satellite droplets are formed. It has been reported that the rate of drop break up at a high viscosity becomes independent of interfacial tension (Calabrese et al., 1986; Koshy et al., 1988b). *Figure 3.1.15* reveals that the volume fraction of satellite droplets reaches a maximum around 45-50 min from the start of the polymerisation and suddenly decreases after that. At a low to medium PVA concentration, where drops are not sufficiently stabilised against coalescence, satellite droplets are removed from the suspension by coalescence with daughter drops and between themselves during the growth stage. With increasing PVA concentration, more of the satellite droplets could be preserved in the suspension. For a PVA concentration of 4.0 g/l, see *Figure 3.1.13b* and *Figure 3.1.15*, only a small fraction of satellite droplets were lost during the growth stage. Interestingly, for the PVA concentration of 10.0 g/l, see *Figure 3.1.14b* and *Figure 3.1.15*, almost all satellite droplets remained in the reaction medium.

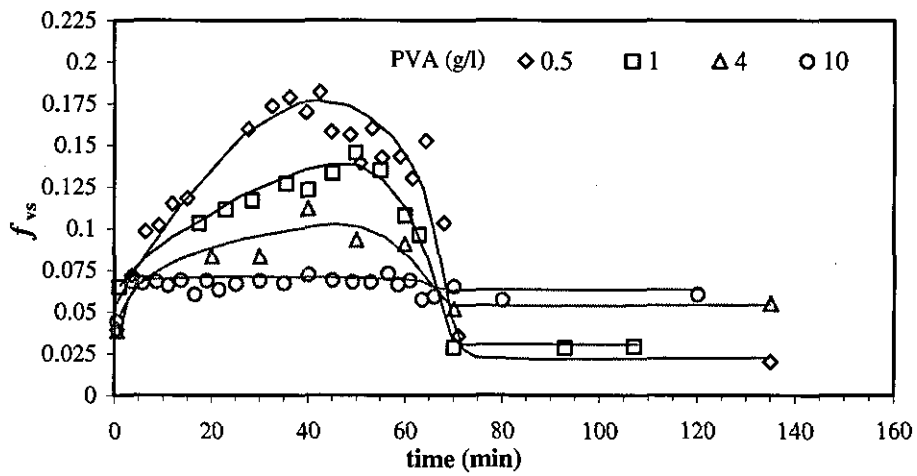

Figure 3.1.15 Time variation of volume fraction of satellite droplets in polymerisations with different PVA concentrations.

Generally the evolution of the PSD of daughter drops followed a similar pattern to that of the Sauter mean diameter. The size distribution of daughter drops initially narrowed and shifted to a lower value of drop size with time (transition stage). The evolution of the size distribution after the transition stage showed a quasi steady state and a growth stage with magnitudes depending on the PVA concentration. Note that the fact that the PSD curves include two peaks and a constant Sauter mean diameter does not necessarily mean a constant PSD for either type of drops, but only for the overall PSD. During the quasi steady state, the PSD of daughter drops moved slightly to the higher range, because of a decreasing rate of drop break up due to increasing drop viscosity. However this was simultaneously compensated for by the formation of large number of satellite droplets leading to a rather constant overall Sauter mean diameter. The PSDs remained unchanged after 70 min when the identification point was reached.

3.1.3.2.2 Two-Stage Addition of PVA

Three experiments were carried out semi-batchwise at initial PVA concentrations of ($[PVA]_0$=) 0.1, 0.15, and 0.25 g/l. The total PVA concentration was kept constant at 0.5 g/l. The remainder of the PVA (to make the final PVA concentration equal to 0.5 g/l) was added to the reaction vessel in one shot after 50 minutes from the start of the polymerisations. The desired amount of PVA was added as a 1.0 wt% PVA aqueous solution. In a further experiment the remainder of the PVA was fed to the reaction vessel continuously with a dosing pump. In that experiment an initial PVA concentration of 0.25 g/l was used and the rest of the PVA (in the form of a 0.5 wt% PVA aqueous solution) was added with a pump during the reaction until t = 50 minute.

Rate of Polymerisation: Figure 3.1.16 shows the conversion-time for runs with different initial charges of PVA. The overall rate of polymerisation was not affected by the addition procedure, as was expected.

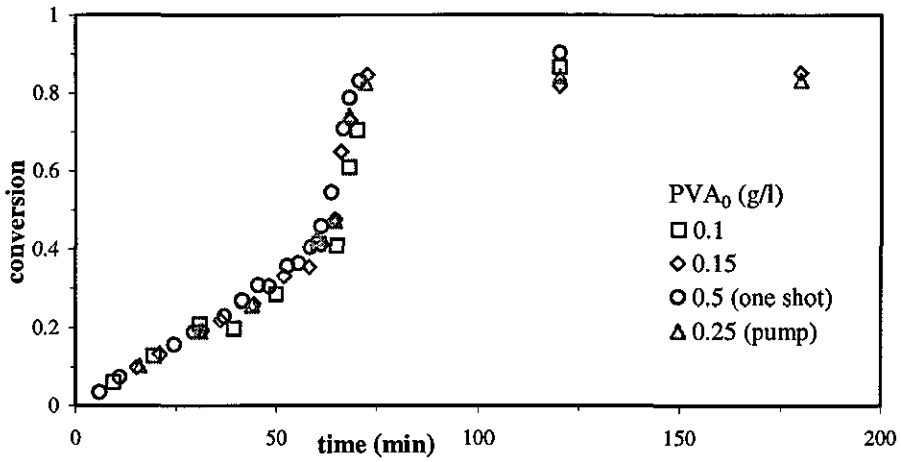

Figure 3.1.16 Conversion-time variations for one shot and two shot PVA additions. (for other conditions see section 3.1.3.2.2).

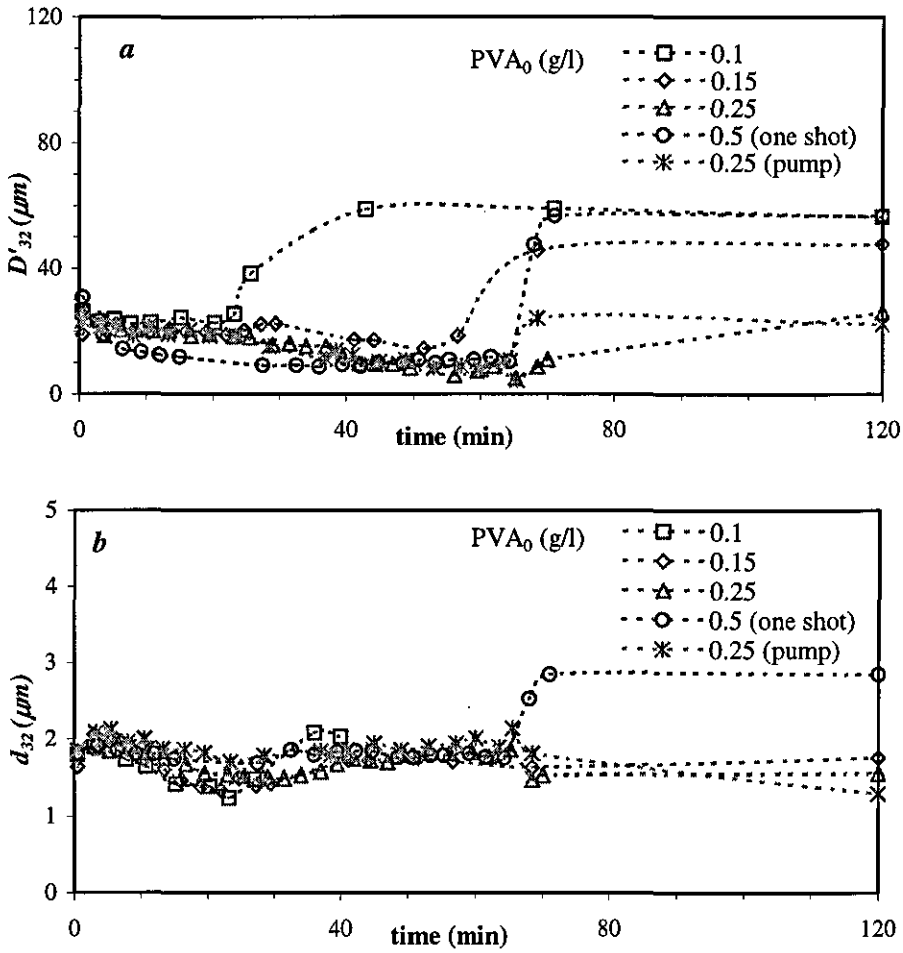

Figure 3.1.17 Variations of Sauter mean diameter of *a*) all drops and *b*) satellite droplets with time.

Mean Particle Size: Figure 3.1.17 shows the variations of overall Sauter mean diameter (D'_{32}) with time for this series. Generally, the application of a higher concentration of PVA resulted in a longer steady-state period. For $[PVA]_0 = 0.1$ g/l, there was a short steady-state period and drops enlarged 20 min after the start of the polymerisation leading to a significant growth in the size of particles. The addition of the remainder of the PVA improved the stability of particles and maintained their size in the course of polymerisation (for this experiment the size of particles exceeded the operational size range of the particle sizer after 45 min, so photographs were taken from the samples using an optical microscope and the particle size average was determined by counting about 300 particles). For the higher initial charge of PVA, drops showed a rather long steady-state period. The growth stage started after about 62 min from the start of the polymerisation. The interesting result is that by post-addition of the stabiliser, it is possible to control the size of final particles within a rather wide range. Furthermore, it is possible to produce finer particles with the same overall concentration of the stabiliser. From *Figure 3.1.17*, it is conjectured that there could be a critical concentration of PVA for any polymerisation condition, $[PVA]_0 > 0.15$ g/l for the current study, above which two-stage addition of stabiliser will result in the formation of smaller particles in comparison with those from the corresponding batch process.

Particle Size Distribution: Figure 3.1.18 compares the final PSDs for this series. Delayed addition of the PVA stabiliser will remove the possibility of grafting PVA molecules on the PMMA particles which has been found to occur in emulsion polymerisation of MMA (Okaya et al., 1999; Kim et al., 2003). Therefore with holding a fraction of the stabiliser for the later stage of the polymerisation, can reduce the size of final particles.

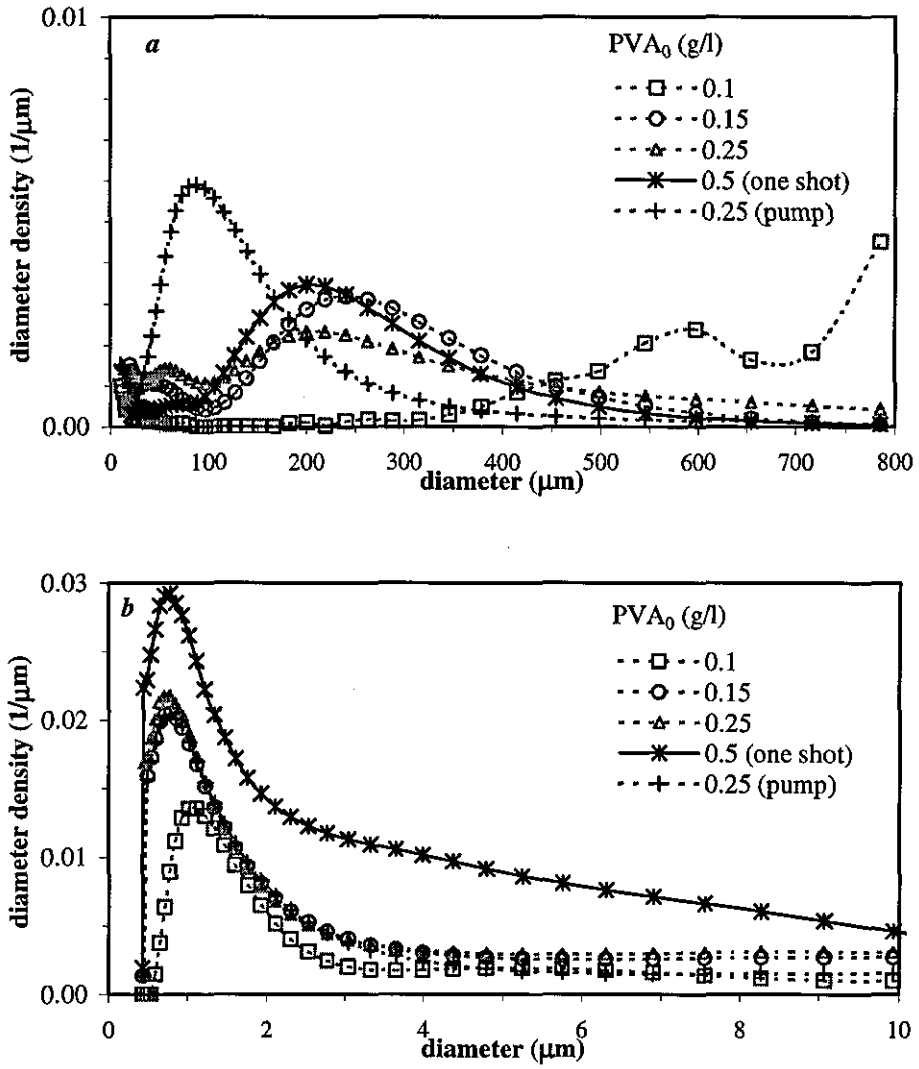

Figure 3.1.18 Final *a*) daughter, and *b*) satellite PSDs for the runs with different PVA addition policy (final PVA concentration= 0.5 g/l).

Figures 3.1.19 to *3.1.22* show the evolution of drop/particle size distribution for this series of experiments.

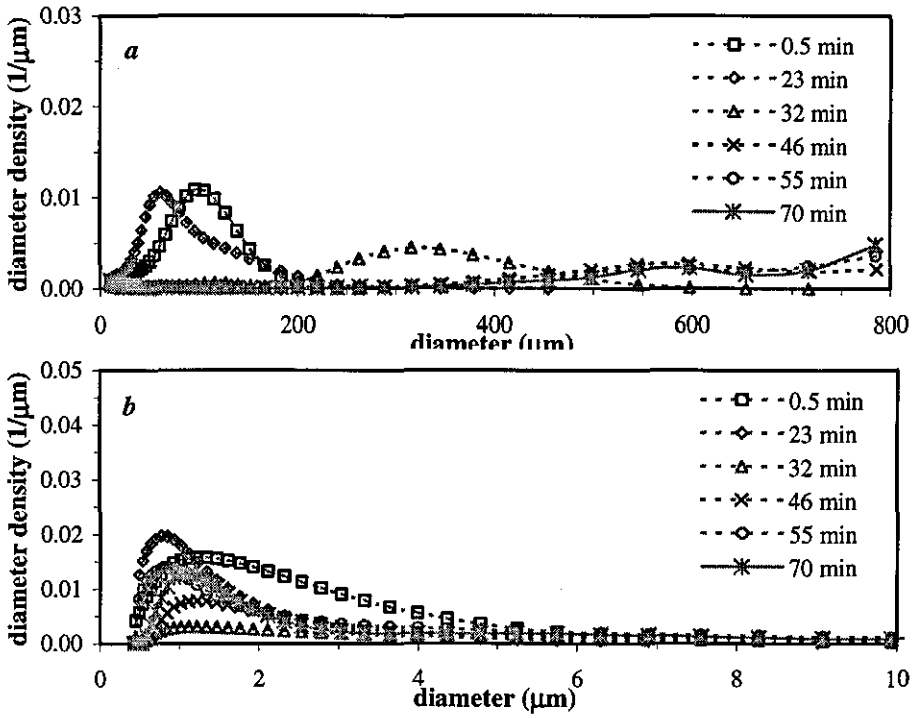

Figure 3.1.19 Variations of a) daughter, and b) satellite PSD with time for the run with two-shot adding of PVA, initially 0.1 finally 0.5 g/l.

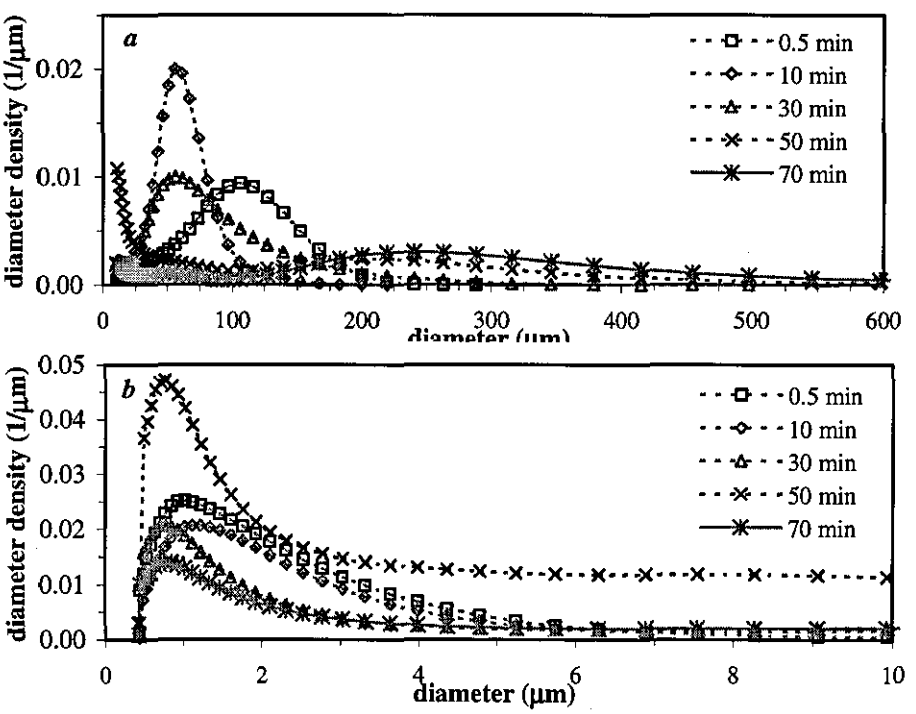

Figure 3.1.20 Variations of a) daughter, and b) satellite PSD with time for the run with two-shot adding of PVA, initially 0.15 finally 0.5 g/l.

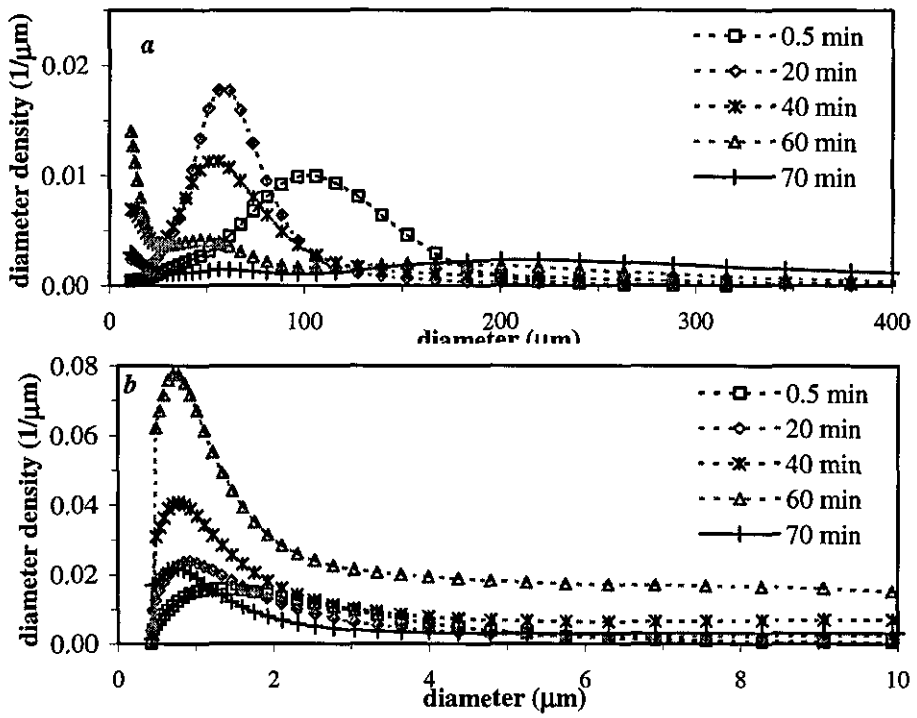

Figure 3.1.21 Variations of a) daughter, and b) satellite PSD with time for the run with two-shot adding of PVA, initially 0.25 finally 0.5 g/l.

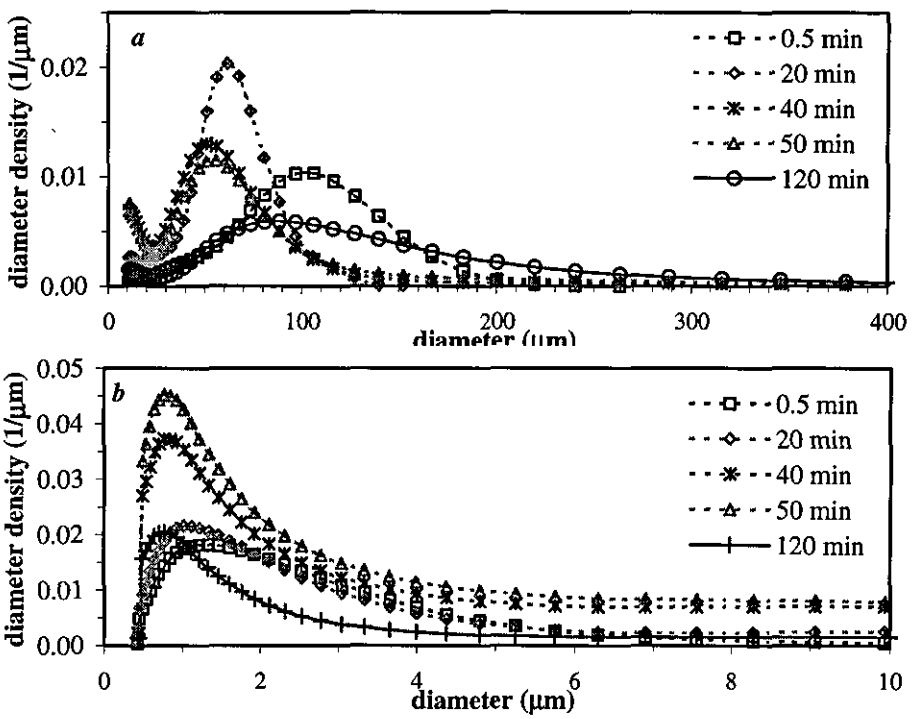

Figure 3.1.22 Variations of a) daughter, and b) satellite PSD with time for the run with pump addition of PVA, initially 0.25 finally 0.5 g/l.

3.1.3.3 Suspension Polymerisation versus Non-reacting Dispersion

Mean Drop/Particle Size: In *Figure 3.1.23* the time variations of the Sauter mean diameter of daughter drops in reacting and non-reacting systems are compared for different PVA concentrations used in this study (0.2, 0.5, 1.0, 4.0, and 10.0 g/l). For all PVA concentrations, at first D_{32} decreases exponentially for both the reacting and non-reacting systems. However, it seems that while the size of drops in the dispersion continues to decrease with time, the drops in the suspension polymerisation reach practically a constant value shortly after the start of the polymerisations. The difference between the steady-state drop sizes in the two systems grows with time. This implies that the viscosity build up in drops during the early minutes of polymerisation enhanced drop stability against break up (Dowding et al., 2000). It has been reported that during the initial period of a typical suspension polymerisation, in which the viscosity of the monomer/polymer mixture in the drops has not increased considerably, a steady-state drop size distribution may be established at which the rates of drop break up and coalescence are balanced (Konno et al., 1982). Mikos et al (1986) assumed that if the drops become stabilised from the early stages of the reaction, the final size distribution of particles is governed by the initial distribution of the non-reacting dispersion at the steady state. The results suggest that even a small increase in the viscosity of drops during the early minutes of reaction is sufficient to slow down the rate of drop break up and increase the steady-state size of drops.

With increasing PVA concentration, particle growth and PSD broadening occurred only to a limited extent in the suspension polymerisation. As a result the evolution of drop size average and size distribution in suspension polymerisations follow similar trends to those in the corresponding dispersions at a high stabiliser concentrations, as shown in *Figure 3.1.23* for the PVA concentration of 10.0 g/l. The experimental data from Konno et al. (1982) for the suspension polymerisation of styrene with 10 g/l PVA provides further evidence for such a claim. Although the size measurements with optical microscopy, as used by Konno et al.(1982), may not be sufficiently sensitive to detect small variations in particle size.

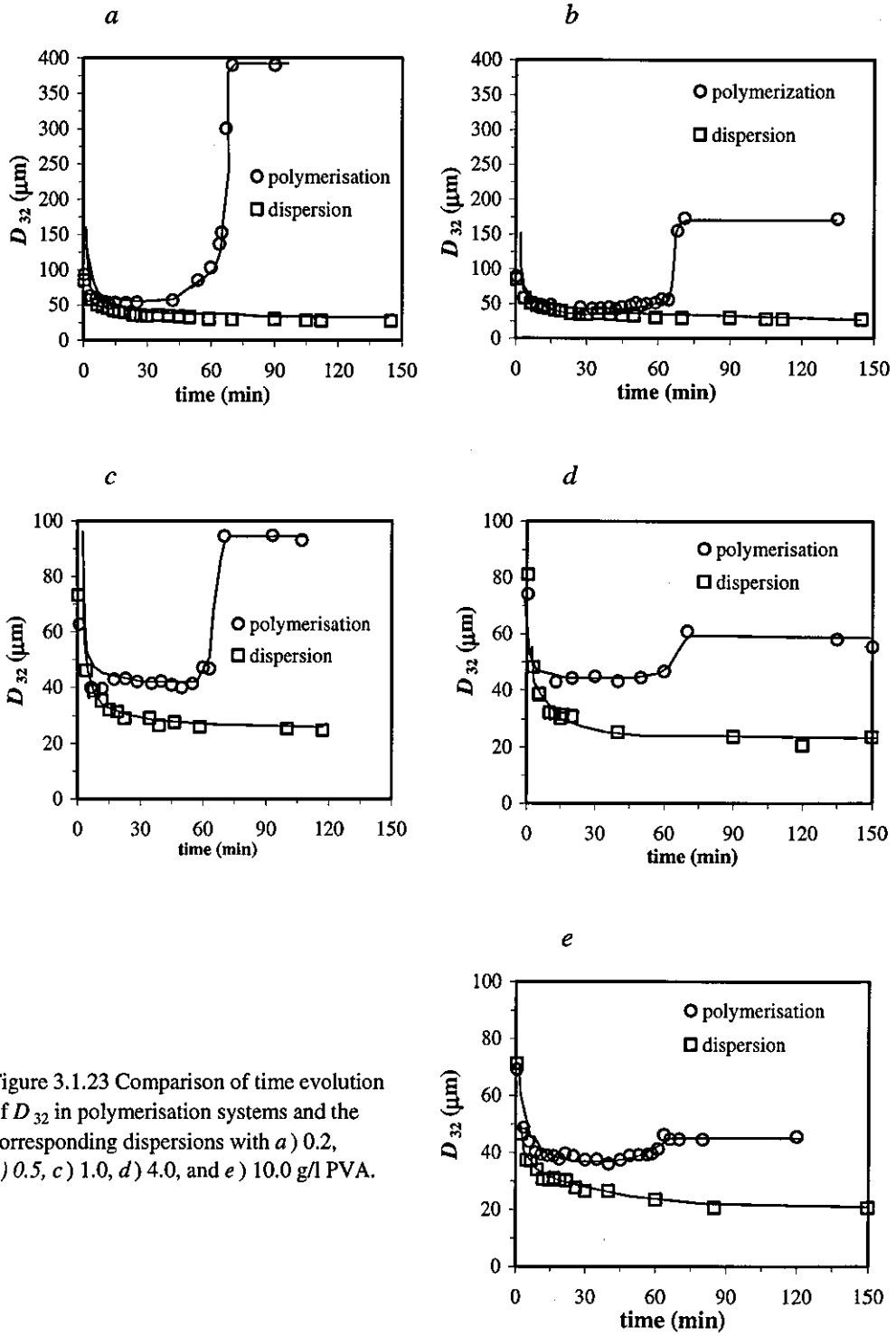

Figure 3.1.23 Comparison of time evolution of D_{32} in polymerisation systems and the corresponding dispersions with *a*) 0.2, *b) 0.5, c*) 1.0, *d*) 4.0, and *e*) 10.0 g/l PVA.

Drop/Particle Size Distribution: In *Figure 3.1.24* the evolution of drop size distributions in the reacting and non-reacting systems are compared for different PVA concentrations used in this study. The size distributions from both systems in the first minute of the runs during which polymerisations have not appreciably progressed, whatever the PVA concentration is, coincided with each other. Later, during the transition period, the size distributions diverged with a degree depending on the PVA concentration. While both narrowed significantly with time, until a steady-state value was reached. The final size distributions approached each other with increasing PVA concentrations.

The variations of the D_{32} versus PVA concentration for final drops from the dispersion process (steady-state value), the steady-state drops from the suspension polymerisation, and the final particles from polymerisation process are plotted in *Figure 3.1.25*. The steady-state size of particles from suspension polymerisations is consistently larger than that from corresponding dispersions, indicating the importance of the kinetic events occurring during the transition period. It can be also seen from this figure that D_{32} of polymer particles approaches that of drops in the corresponding dispersions with increasing PVA concentration.

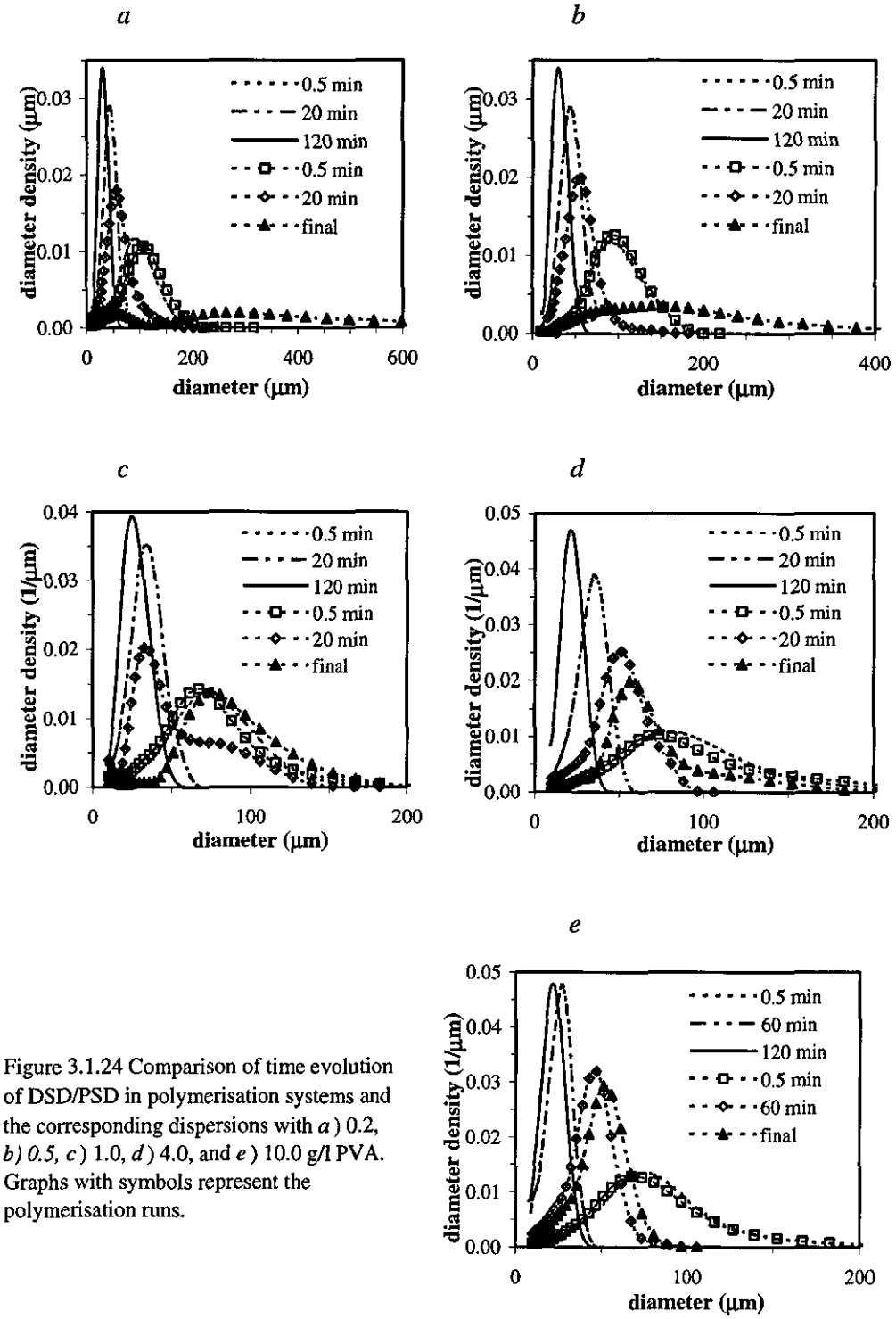

Figure 3.1.24 Comparison of time evolution of DSD/PSD in polymerisation systems and the corresponding dispersions with *a*) 0.2, *b*) 0.5, *c*) 1.0, *d*) 4.0, and *e*) 10.0 g/l PVA. Graphs with symbols represent the polymerisation runs.

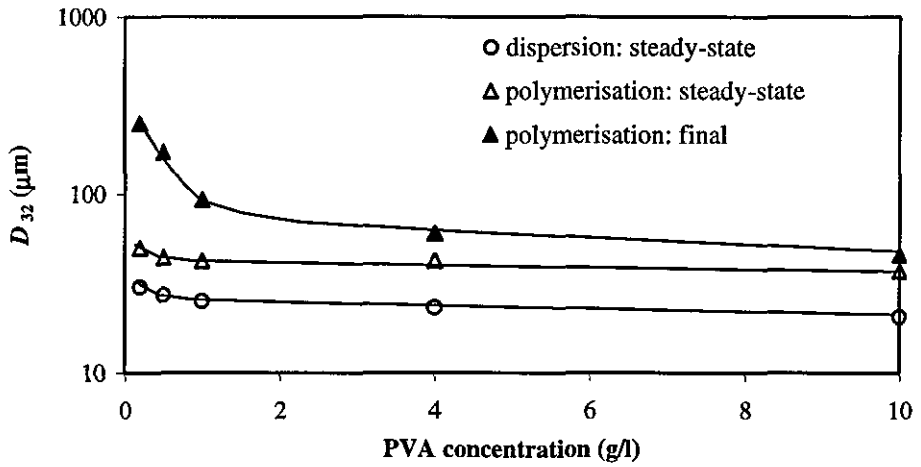

Figure 3.1.25 Effect of PVA concentration on steady-state and final D_{32} in polymerisation systems and the corresponding dispersions.

3.1.4 CONCLUSIONS

- From the experimental results of this series of experiments, the characteristic intervals of a typical suspension polymerisation were realised as follows:

  Transition Stage; during which PSD narrows dramatically and drop size decreases exponentially due to higher rate of drop break up in comparison with drop coalescence.

  Quasi Steady-State Stage; during which the rate of drop break up and drop coalescence are almost balanced leading to a quasi steady-state drop size and distribution.

  Growth Stage; during which the rate of drop break up falls considerably below the rate of drop coalescence due to the viscosity build up in drops leading to drop enlargement and PSD broadening.

  Identification stage; during which a solid-liquid suspension is attained and the PSD and mean particle size are unchanged.

- For simple liquid-liquid dispersions only the transition and steady-state stages exist. *Figures 3.1.26* and *3.1.27* show a typical variation of Sauter mean diameter of drops with time in the four intervals of suspension polymerisation

and in the two intervals of dispersion, respectively. The boundaries of the intervals have been shown on these figures.

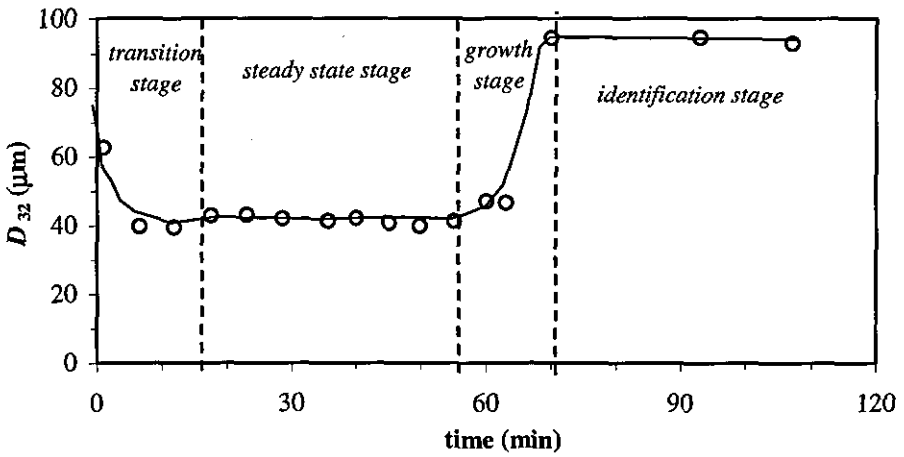

Figure 3.1.26 Characteristic intervals in time evolution of Sauter mean diameter in a typical suspension polymerisation of MMA (ϕ_d = 0.2, [PVA] = 1 g/l, N_I = 500 rpm, T=70°C).

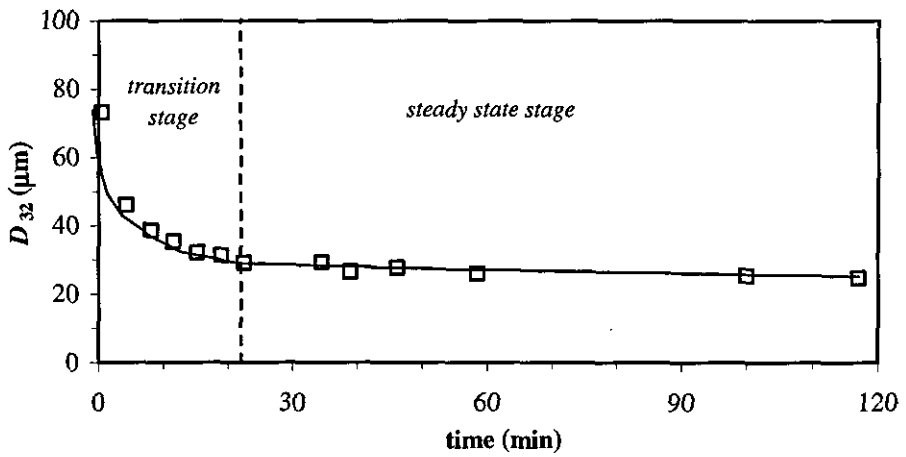

Figure 3.1.27 Characteristic intervals in time evolution of Sauter mean diameter in a typical dispersion of MMA/W (ϕ_d = 0.2, [PVA] = 1 g/l, N_I = 500 rpm, T = 70°C).

- The volume fraction of the satellite droplets (f_{vs}) formed in the MMA/Water dispersions increased with time and with PVA concentration. In the MMA suspension polymerisation, f_{vs} increased with time but decreased with PVA concentration.

- The boundaries of the intervals can be distorted with variation in the stabiliser concentration. In a non-reacting dispersions shorter transition stage and lower steady-state drop size are obtained for higher stabiliser concentration. In a suspension polymerisation, with a low stabiliser concentration, the transition stage is longer, the steady-state stage is very short and the growth stage is advanced. At a high stabiliser concentration, the steady state, growth and identification stages overlap so that the drops formed after transition stage are maintained in the reaction medium and are gradually converted to polymer beads with little interaction with other particles. The results suggest that the *critical viscosity* or *conversion* at which growth stage starts is not a constant and depends on the polymerisation conditions. For suspension polymerisation of styrene, for example, it has been reported that the dispersed droplets reach a critical viscosity of about 100 cp at about 30% conversion from which droplet coalescence overcomes the droplet breakage (Villalobos et al; 1993).

- The significance of the transition stage has hardly been recognised in the literature. It was shown that there is a difference between the drop sizes from the two processes during the transition period. This implies that the viscosity build up in drops during the early minutes of polymerisation is an important kinetic event and that its effect on the evolution of drops cannot be ignored.

- From the results, two types of steady state can be suggested. The steady state drop size distribution in liquid-liquid dispersions will mainly depend on the relative magnitude of the rates of drop break up and coalescence. At steady state, when the rates of drop break up and coalescence are balanced, coalescence removes as many drops from the dispersion as are made via the break up mechanism. This has been called a *dynamic steady state* where individual drops do not retain a unique identity but undergo continuous break up and coalescence. The runs carried out at low PVA concentrations present that type of steady state. With increasing drop viscosity, the rate of drop break up will be reduced and the growth stage starts. *Figures 3.1.23a - 3.1.23c* represent such conditions. If drops are reduced to a size that cannot be further broken by

agitation and if they are also sufficiently protected against drop coalescence, then drops do not undergo any transformation during mixing and with increasing drop viscosity so that *static steady state* may be established. Static steady state can actually be achieved, or approached, if a high concentration of stabiliser, for example, is used. The resulting drops from such dispersions would be very small. *Figure 3.1.23e* shows that the increase in drop size is very small in the growth stage for the polymerising drops with PVA concentration of 10 g/l despite the large increase in the drop viscosity.

3.2 EFFECT OF INITIATOR AND CHAIN TRANSFER AGENT CONCENTRATIONS

3.2.1 INTRODUCTION

The kinetics of polymerisation can play an important role in the evolution of particle size and size distribution in a typical suspension polymerisation reaction. The viscosity of drops and its variation with time is in fact a reflection of the rate of polymerisation inside drops. In this part we attempted to alter the time variation of drop viscosity by changing the formulation variables; namely initiator and chain transfer agent concentrations. With increasing initiator concentration, the concentration of propagating radicals increases leading to a boost to the rate of polymerisation reaction. The chain transfer agent does not affect the radical concentration, but increases their mobility, through reducing the viscosity of the reaction medium, and thus facilitates radical termination. This can result in a lower rate of polymerisation at high conversions where termination reactions are usually diffusion controlled. The initiator and chain transfer agent concentrations are ideal variables for this case study, because they are used in a very small amount so that the oil phase and interfacial properties of the dispersions are not appreciably affected by their presence.

The rate of polymerisation reaction is highly affected by the reaction temperature. However, the interfacial properties of the stabiliser are also affected. Therefore, the temperature effect was excluded from this section and will be discussed separately. The effects of the concentration of the initiator, lauroyl peroxide (LPO), and the concentration of the chain transfer agent, *n*-dodecyl mercaptan (*n*-DDM), on the evolution of PSD in the suspension polymerisation of MMA are discussed here.

3.2.2 EXPERIMENTAL

The materials, experimental procedure and measurements have been described in detail in Chapter 2. All experiments in this series were carried out at 70°C and agitation speed of 500 rpm. MMA hold up was 0.20 and PVA concentration was 1.0 g/l. For the

experiments with *n*-DDM as variable, the LPO concentration was kept constant at 1.0 wt% based on the monomer phase.

3.2.3 RESULTS AND DISCUSSION

3.2.3.1 Initiator Concentration

Suspension polymerisations of MMA with LPO concentrations of 0.25, 1.0, and 4.0 wt% were carried out. No chain transfer agent was used in this series.

Rate of Polymerisation: Figure 3.2.1 shows the conversion-time variations for the runs with different LPO concentrations. The overall rate of polymerisation increased with LPO concentration. The rate of polymerisation in a typical free radical polymerisation is given by equation 1.2.8 (chapter 1) which is repeated here:

$$R_p = (k_p + k_f)[M]\left(\frac{2fk_d[I]}{k_t}\right)^{1/2} \qquad (3.2.1)$$

The above equation shows that, in agreement with the experimental data at low conversions, R_p will theoretically increase with $[I]^{1/2}$. The onset of the gel effect was also affected by the LPO concentration. Generally the onset of the gel effect is affected by two factors; the volume fraction of polymer in the mixture (or conversion) and the molecular weight of the polymer produced (Marten and Hamielec, 1979; 1982).

The number-average molecular weight of polymer is given by equation 1.3.1 (chapter 1) which can be written as follows:

$$\frac{1}{X_n} = \frac{(2fk_d[I]k_{td})^{1/2}}{k_p[M]} + \frac{(2fk_d[I]k_{tc})^{1/2}}{2k_p[M]} + k_f/k_p + k_s[S]/k_p[M] \qquad (3.2.2)$$

The above equation indicates that, in the absence of any chain transfer reaction, X_n is proportional to $[I]^{-1/2}$. *Figure 3.2.1* shows that for the LPO concentrations of 0.25, 1.0, and 4.0 wt% the gel effect starts at conversions of 0.35, 0.40, and 0.45, respectively. With increasing the LPO concentration shorter polymer chains were produced and the gel effect was postponed to higher conversions. The rate of the polymerisation reaction

during the gel effect increased significantly with LPO concentration, as was expected. Generally, a higher final conversion was achieved with increasing LPO concentration.

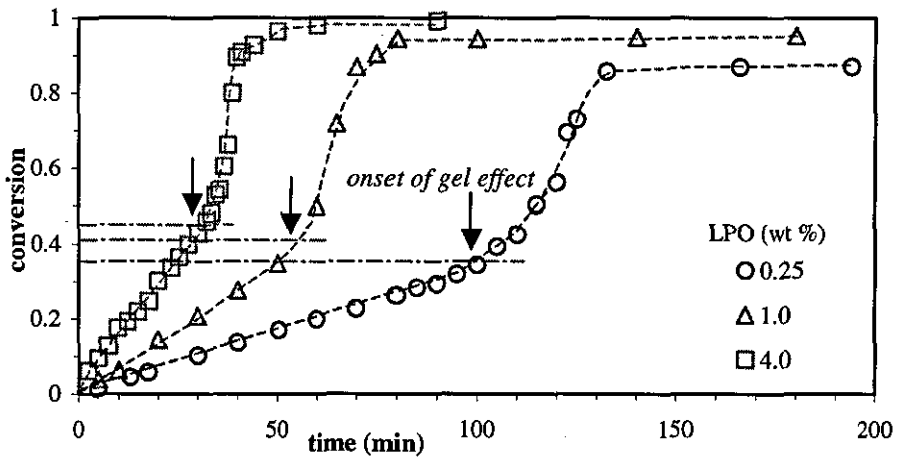

Figure 3.2.1 Conversion-time variations for MMA suspension polymerisations with different LPO concentrations (for other conditions see section 3.2.2).

Mean Drop Size: Figure 3.2.2 illustrates the variations of Sauter mean diameter of daughter drops (D_{32}) with time and conversion. *Figure 3.2.2a* shows that during the transition stage, the size of drops was initially reduced to a low value for all LPO concentrations used. Interestingly, the largest decrease in the average size of drops during this stage was obtained for the lowest LPO used. Obviously this is due to a lower rate of viscosity build up in the drops containing a lower concentration of LPO. A larger increase in the rate of viscosity build up, associated with a higher rate of polymerisation for the higher LPO concentration, damps the rate of drop break up so that the rate of drop break up and drop coalescence is balanced earlier. This results in a larger drop size in the beginning of the quasi steady-state stage. During this stage drops underwent a slight size increase with time. The slope depended on the rate of viscosity build up (rate of polymerisation) in the drops. A higher initiator concentration resulted in a larger rate of polymerisation and thus a higher rate of viscosity increase. The quasi-steady state lasted longer for the lower LPO concentration.

Note that time is not a good representative of the status of the polymerising drops when they contain different concentrations of the initiator. The evolution of D_{32} can be better explained if the comparison is made at a constant conversion. *Figure 3.2.2b* reveals that growth stage started at the lowest conversion, for the lowest LPO concentration. This is

because of the formation of high molecular weight polymer with decreasing LPO concentration, as previously explained. Because of a higher viscosity of drops with a lower LPO concentration (at a constant conversion), the balance between drop break up and drop coalescence is perturbed. Generally, particle growth started earlier than the gel effect became operative, however, it became very intensive (during the growth stage) after the gel effect started. The duration of the growth stage was longer for the run with the lower LPO concentration simply because of a lower rate of polymerisation that allowed more particles to coalescence (see *Figure 3.2.2a*). During this period the particles were more likely to coalescence with each other. As a result, the size of final particles increased with decreasing LPO concentration. This accords with the data reported by Lazrak et al (1998) on the MMA suspension polymerisation with benzoyl peroxide as initiator and theoretical prediction of Alvarez et al. (1994).

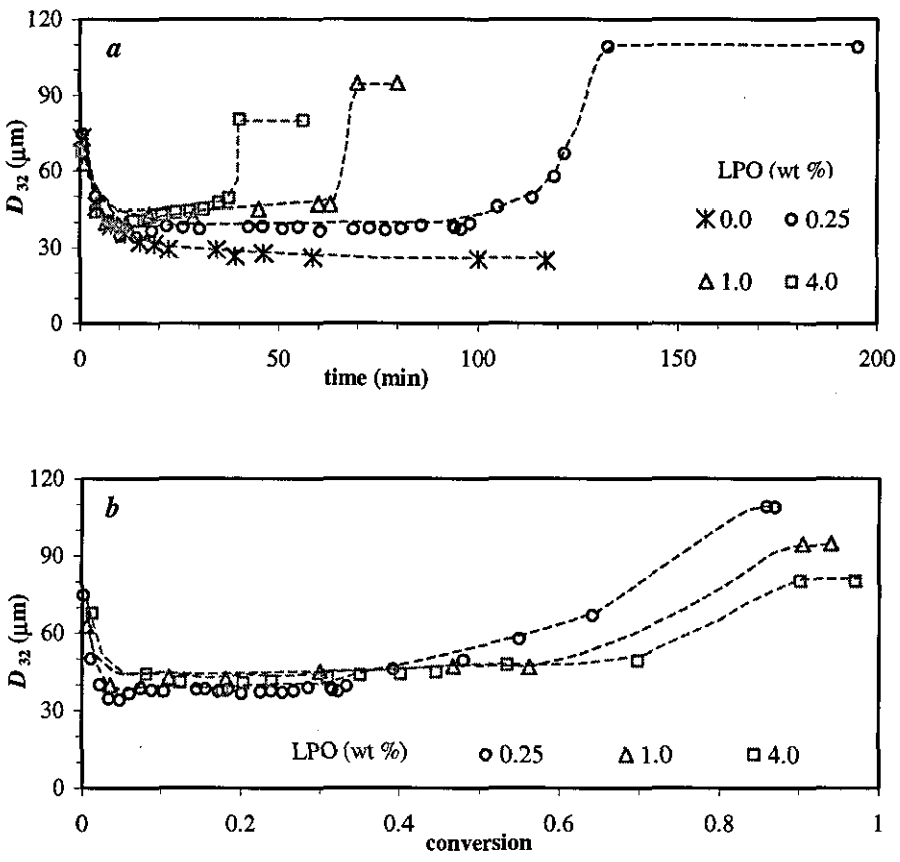

Figure 3.2.2 Variations of Sauter mean diameter of daughter drops with *a*) time, and *b*) conversion for suspension polymerisations with different LPO concentrations (the data for the corresponding dispersion, without LPO, is also inclusded in *a*).

Particle Size Distribution: Figures 3.2.3 and *3.2.4* indicate the time evolution of PSD for the runs with LPO concentrations of 0.25 and 4.0 wt%, respectively (the time evolution of PSD for 1.0 wt% LPO has been previously shown in *Figure 3.1.12*). As it can be seen, with decreasing the LPO concentration, larger particles formed and broader particle size distribution were obtained.

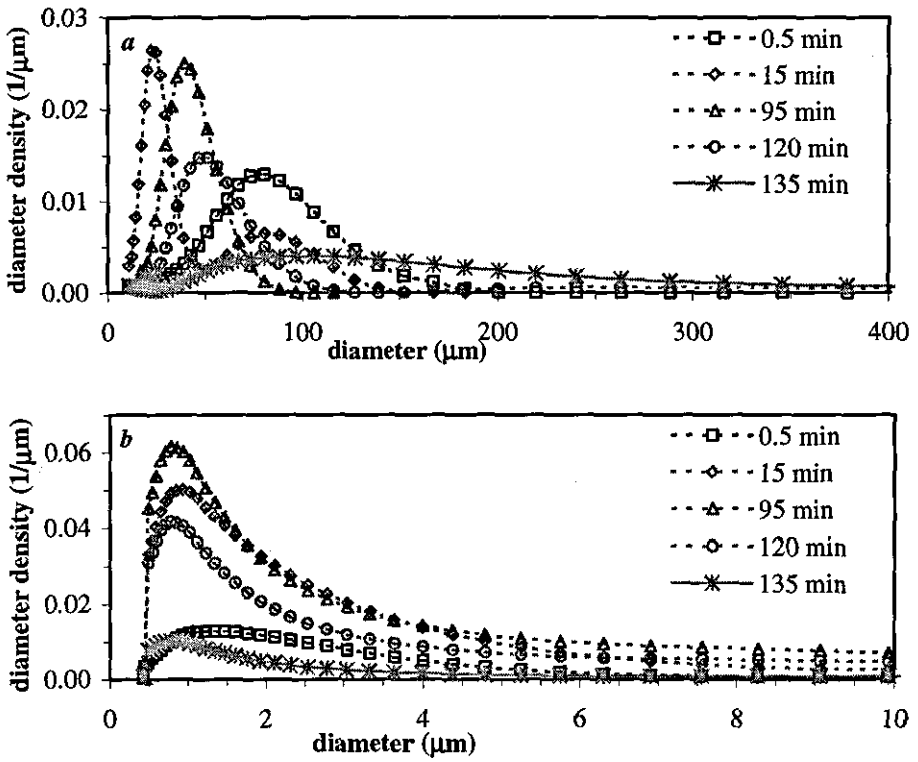

Figure 3.2.3 Time evolution of *a*) daughter, and *b*) satellite PSDs for the run with LPO = 0.25 wt%.

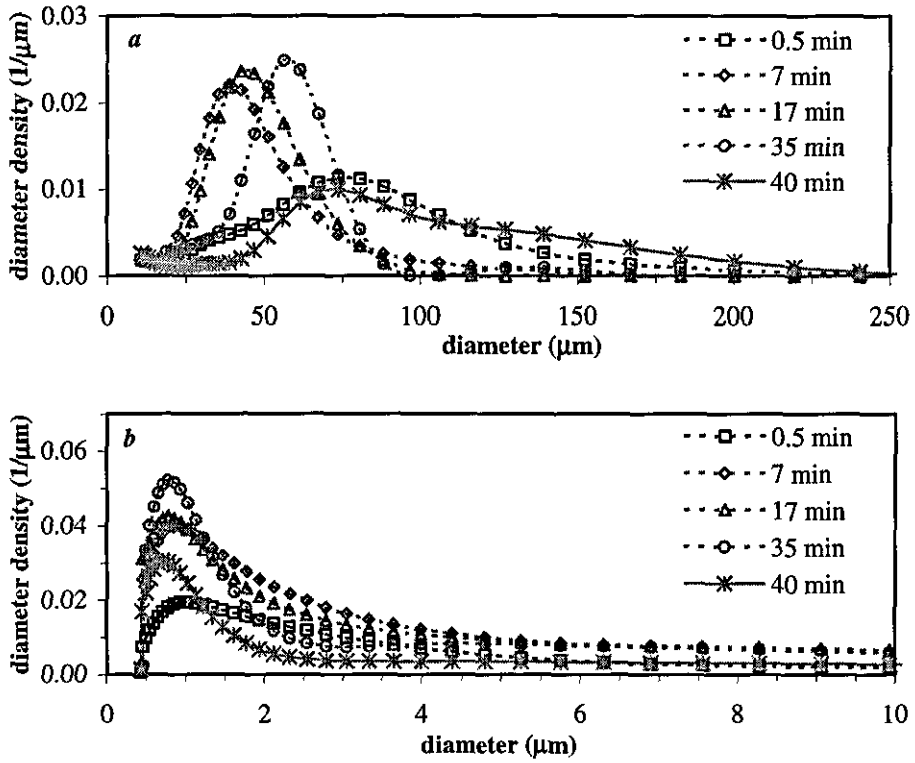

Figure 3.2.4 Time evolution of *a*) daughter, and *b*) satellite PSDs for the run with LPO = 4.0 wt%.

An important observation was that more satellite droplets were produced in the course of reaction with decreasing LPO concentration simply because of prolonged reaction time. In section 3.1.3.1 we showed that the number of satellite droplets in the non-reacting MMA dispersion, which behaves similar to a polymerisation with a very low amount of initiator, increased continuously with time. A longer steady-state stage allows the satellite droplets to be formed in a larger number. *Figure 3.2.5* illustrates the time variation of f_{vs}. The initial rate of satellite formation seems to be the same for all runs. According to this figure for the run with 0.25wt% LPO concentration, satellite droplets are continuously formed up to 95 min, which is shortly before the onset of the growth stage. For the runs with LPO concentration of 1.0 and 4.0 wt%, the formation of satellite droplets continued during the steady-state stage that lasted up to 50, and 30 min, respectively. It can be stated that the formation of satellite droplets correlates with the duration of the steady-state stage.

As the growth stage started and intensified due to the gel effect, the events changed and most of the satellite droplets were lost by coagulation (or flocculation) with other drops.

The extent of disappearance of the satellite droplets during the growth stage was high for the runs using low LPO concentrations because of a long mixing time required to reach the identification point. As a result, final suspensions with high LPO concentration contained more satellite particles as shown in *Figure 3.2.6b*.

Figure 3.2.6a shows a comparison between final PSDs of the daughter drops. With increasing LPO concentration PSD becomes narrower and moves towards smaller particle sizes as was explained before.

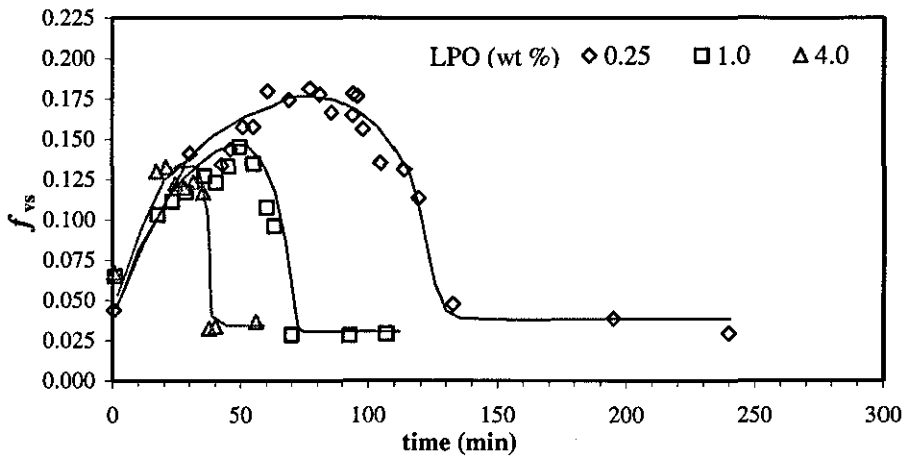

Figure 3.2.5 Time variation of volume fraction of satellite droplets in polymerisations with different LPO concentrations.

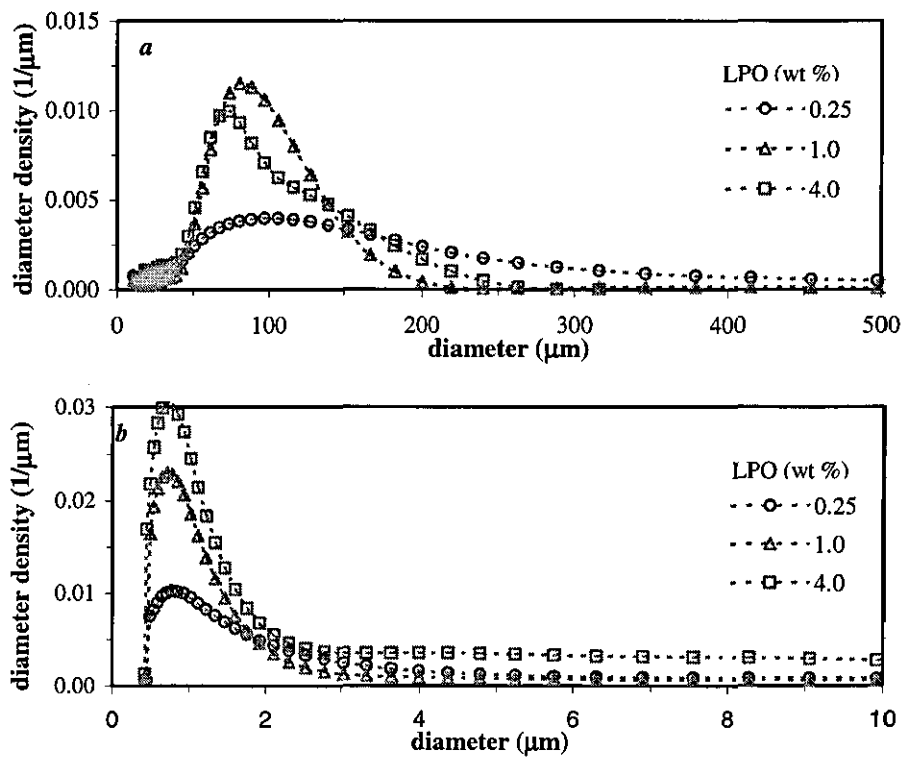

Figure 3.2.6 Final *a*) daughter, and *b*) satellite PSDs for runs with different LPO concentrations.

3.2.3.2 Chain Transfer Agent Concentration

Three experiments were carried out with *n*-DDM concentrations of 0.0, 0.25, and 1.0 wt% based on monomer phase.

Rate of Polymerisation: Figure 3.2.7 illustrates the conversion-time variations for these runs. The rate of polymerisations for the region of $x < 0.40$ are almost identical for all runs, indicating chain transfer to *n*-DDM does not affect the inherent kinetics of polymerisation. The kinetic chain length of polymer in the presence of a chain transfer agent is determined by equation 3.2.2 where [*S*] represents the chain transfer agent concentration. In the initial stage of polymerisation where k_t is very high, X_n is controlled by termination reactions. A difference in the rate of polymerisation is developed for $x > 0.40$ when the gel effect is operative at the condition of this study. During the gel effect k_t is so reduced that X_n is controlled by the chain transfer agent concentration ($1/X_n = k_{n\text{-DDM}}[n\text{-DDM}]/k_p[M]$). A higher chain transfer agent concentration, thus, results in a lower molecular weight of polymer being formed. The decrease in the rate of polymerisation with increasing *n*-DDM concentration occurs because the gel effect is suppressed due to the reduction in polymer molecular weight. A similar observation was reported for styrene/acrylonitrile suspension copolymerisation with *n*-DDM as chain transfer agent and TCP as suspending agent (Jahanzad and Sajjadi, 2000). The onset of the gel effect was postponed to the conversion of 0.55 for the run using 0.25wt% *n*-DDM. For the run with *n*-DDM concentration of 1.0 wt%, a very mild and short gel effect was observed around the conversion of 0.70.

Mean Drop Size: The variations in Sauter mean diameter of daughter drops with time and conversion are shown in *Figure 3.2.8*. The duration of the transition stage was not appreciably affected by the *n*-DDM concentration. In the initial stage of polymerisation the evolution of viscosity of drops is similar for all runs because the molecular weight of polymer is controlled by the termination reactions. As a result, the drops have the same size during the transition stage for *n*-DDM different concentrations.

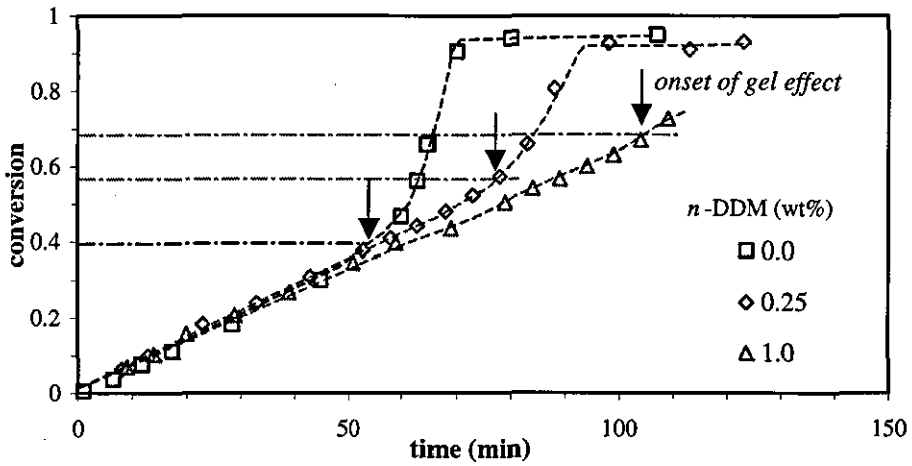

Figure 3.2.7 Conversion-time variations for runs with different *n*-DDM concentrations (for other conditions see section 3.2.2).

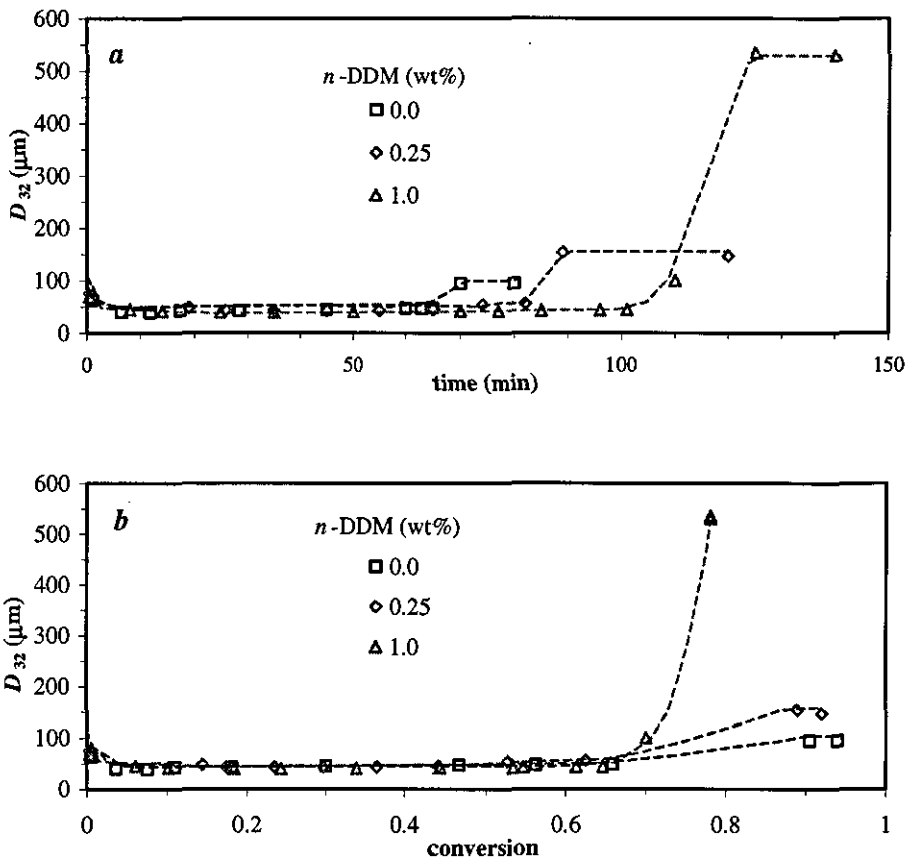

Figure 3.2.8 Variations of Sauter mean diameter of daughter drops with *a*) time, and *b*) conversion for runs with different *n*-DDM concentrations.

The onset of the growth stage was reached earlier in terms of time with decreasing *n*-DDM concentration. In terms of conversion, however, the growth stage started at the critical conversion of $x = 0.65$, independent of the chain transfer concentration. This means that the molecular weight of the polymer did not appreciably affect the onset of the growth stage. We showed before that the onset of the growth stage is displaced with variation in the LPO concentration. It should be noted that the molecular weight of the polymer formed up to the intermediate conversion ($x = 0.40$) is expected to be constant for the runs with different *n*-DDM concentrations, as explained above. Application of a higher *n*-DDM concentration, more than the range used here, can reduce the molecular weight of the polymer formed in the early stage of reaction and affect the drop size evolution in the corresponding stage.

The steady-state stage was prolonged with increasing *n*-DDM concentration (see *Figure 3.2.8a*). During the growth stage, drops enlarged with time with a rate depending on the *n*-DDM concentration. For the run with no *n*-DDM, the growth stage was very short, of the order of 5 min, so that particles grew a little during this stage. For *n*-DDM concentration of 0.25wt% the growth stage was passed in 10 min, long enough to increase the size of particles almost two fold. For the run with 1.0 wt % *n*-DDM, the growth stage lasted for a long time. When the conversion of 0.80 was reached, at 125 min, gross coagulation occurred and led to the formation of large flocculated particles. The results indicate that the duration of the growth stage is of crucial importance in the stability of suspension polymerisation reactors. The presence of *n*-DDM in suspension polymerisation of MMA destabilises the particles through prolonging the growth period or coalescence-controlled period for particles.

Particle Size Distribution: The time evolution of particle size distributions for the runs in the presence of *n*-DDM is illustrated in *Figures 3.2.9* and *3.2.10*. Similar trends, as previously explained, occur for all polymerisations. The initial distributions were rather broad but they became narrower with time. The application of *n*-DDM reduced the population of satellite droplets. The evolution of satellite droplets can be observed in *Figures 3.2.9b* and *3.2.10b*. Final PSDs have been illustrated in *Figure 3.2.11*. Generally, the size of final particles increased with *n*-DDM concentration. Correspondingly, a broader distribution was obtained with increasing *n*-DDM concentration. A larger population of satellite droplets was obtained at a lower *n*-DDM concentration.

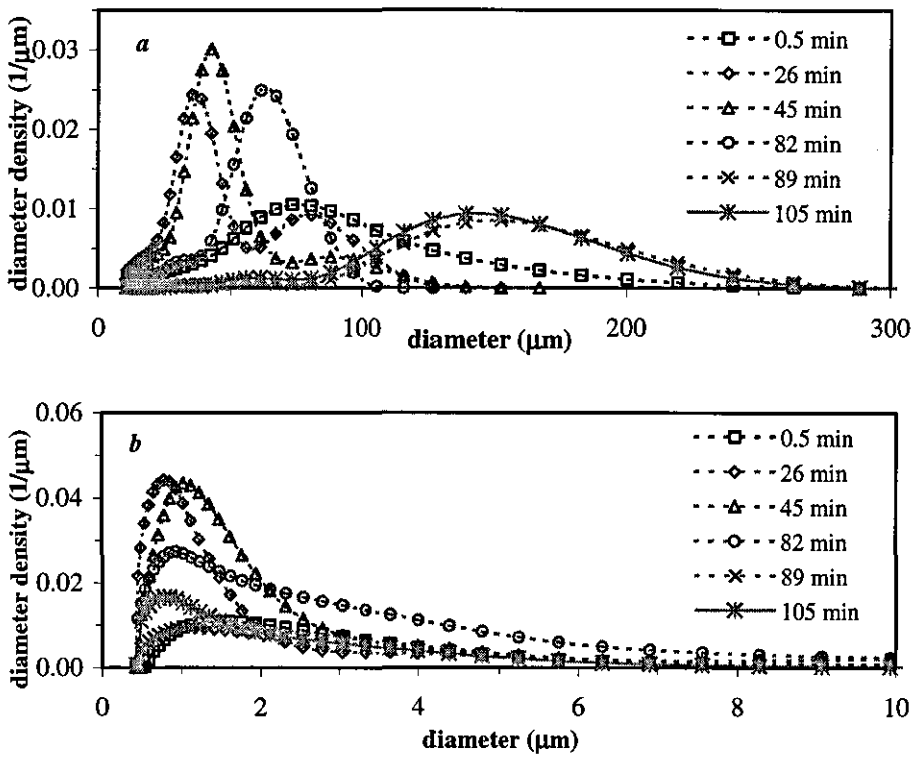

Figure 3.2.9 Time evolution of *a*) daughter, and *b*) satellite PSDs for the run with *n*-DDM = 0.25 wt%.

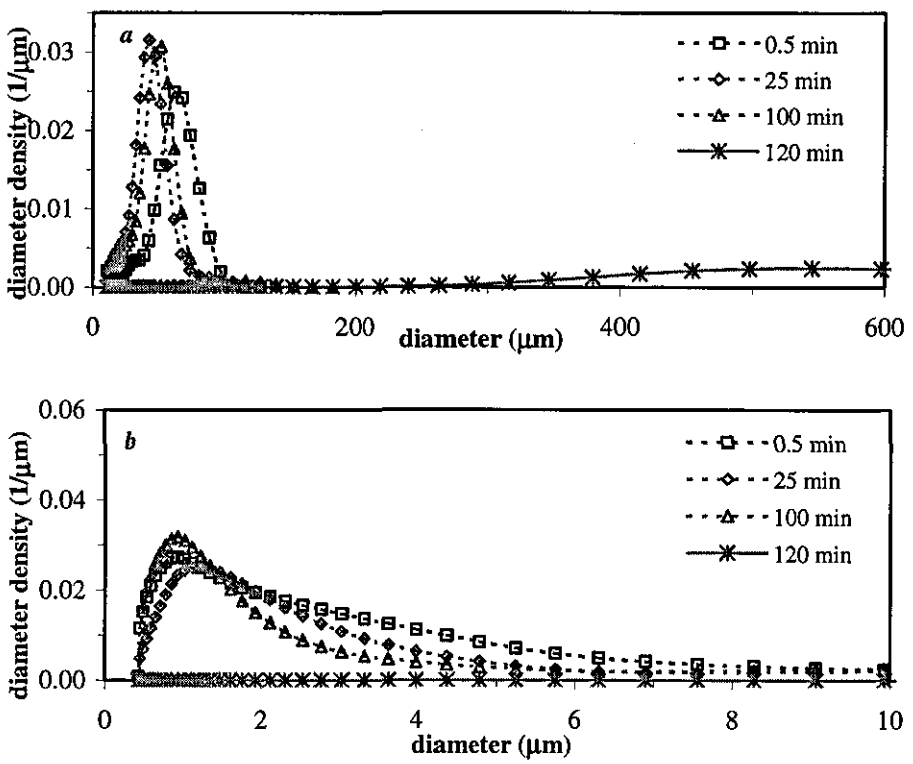

Figure 3.2.10 Time evolution of *a*) daughter, and *b*) satellite PSDs for the run with *n*-DDM = 1.0 wt%.

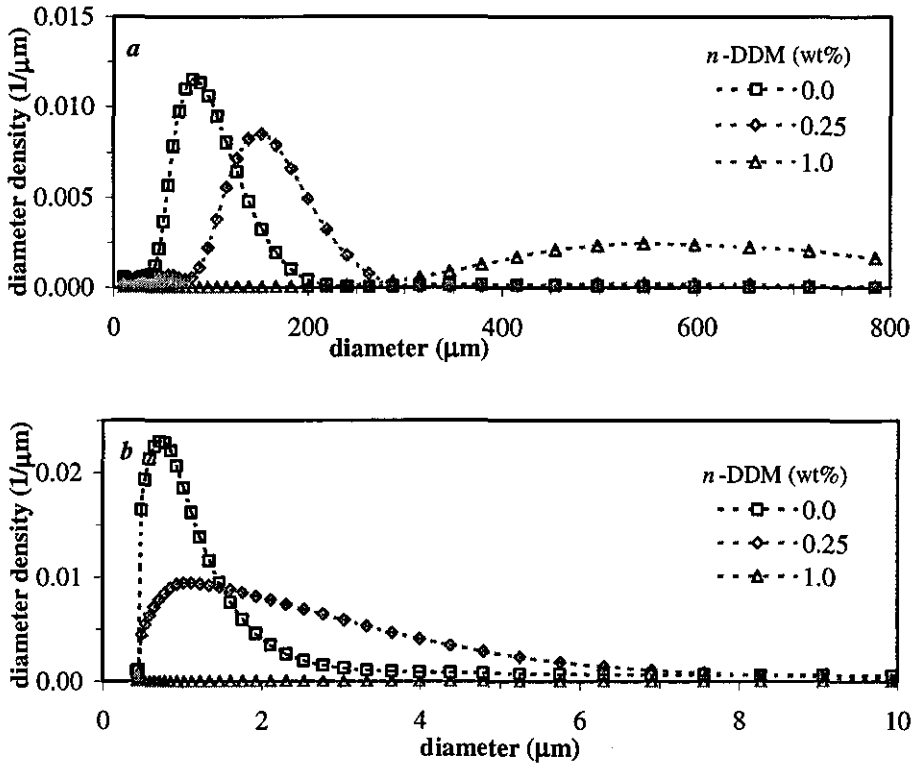

Figure 3.2.11 Final *a*) daughter, and *b*) satellite PSDs for the runs with different *n*-DDM concentrations.

3.2.4 CONCLUSIONS

The main conclusions are:

- Decreasing initiator concentration lowers the rate of viscosity build up in drops and, thus, enhances drop reduction in the transition stage. As the initiator concentration is reduced to a low value, the pattern of size variation of drops accords with that from non-reacting dispersions during this stage.

- As a result of delayed balance between drop break up and coalescence, a lower steady-state size of drops was obtained with decreasing initiator concentration.

- Drops with a higher viscosity (at the same conversion), formed by application of a lower initiator concentration, revealed more instability and started to grow

earlier in terms of conversion. As a result larger particles were obtained with decreasing initiator concentration.

- The effect of chain transfer concentration on the evolution of the drop size average could be seen as its reflection on the viscosity of the polymer formed. With a high chain transfer agent concentration the rate of polymerisation was inversely affected (in intermediate conversion) and larger particles were obtained mainly due to flocculation. The application of chain transfer agent, however, broadened the range of conversion during which the quasi steady state could be operative. The balance between drop break up and coalescence could be maintained further with a decline in the drop viscosity due to the formation of low-molecular-weight polymer formed by application of chain transfer agent.

3.3 EFFECT OF INHIBITION

3.3.1 INTRODUCTION

A significant portion of the petrochemical industry is based on the production and utilisation of polymerisable monomeric compounds. Certain of these readily polymerisable monomers are particularly reactive because their molecules contain an activated ethylenic bond, i.e., a non-aromatic carbon-carbon double bond that is activated by conjugation with other multiple bonds between adjacent atoms. Examples of polymers produced from such monomers are polystyrene and polymethyl methacrylate. The presence of activated ethylenic unsaturation in the readily polymerisable monomers enables polymerisation of the monomers to be conducted under rather mild but carefully controlled conditions.

However, the readily polymerisable monomers often undergo undesirable polymerisation, e.g., polymerisation prior to the time polymerisation is intended, as during the production, purification, storage or handling of the monomers, when exposed to free radicals resulting from the presence of other free radical sources. This premature free-radical polymerisation can have significant consequences since the polymer formed tends to foul or even plug the mechanical equipment used in the production, purification, handling or even storage of the monomer unless precautions are taken to inhibit or prevent the polymerisation. Premature polymerisation typically produces a polymer product of inferior quality and can be a safety hazard if operating equipment becomes plugged. To prevent or at least retard premature free-radical polymerisation of readily polymerisable monomers it is conventional to add to the monomer a small but effective amount of an antioxidant or inhibitor. Many, if not most, of the conventional polymerisation inhibitors are complex organic compounds containing functional groups with atoms of oxygen, nitrogen or sulfur.

Studies on suspension polymerisation kinetics in academia are usually carried out with high-purity grade monomers. In industrial practice, however, it is impractical to purify raw materials and commercial monomers, which contain inhibitors, are usually used. The addition of inhibitors increases the shelf life of monomers by suppressing their

polymerisation. These substances (inhibitors) act by reacting with the initiating and propagating radicals and converting them either to non-radical species or radicals of reactivity too low to undergo propagation. Such polymerisation suppresses are classified according to their effectiveness. Inhibitors stop every radical and polymerisation is completely halted until they are consumed (induction or inhibition period). At the end of this period, polymerisation proceeds at the same rate as in the absence of inhibitor (ideal inhibitor behaviour).

Retarders are less efficient and stop only a portion of the radicals. In that case, polymerisation occurs, but at a slower rate and without an induction period (ideal retarder behaviour). A single substance may function either as inhibitor or retarder or both, depending on its concentration, so that distinction between inhibitors and retarders becomes a matter of degree (Odian, 1991). Quinones and catechols are two important classes of inhibitors. They represent water-soluble and oil-soluble inhibitors, respectively.

It has been found that quinones act as retarders in bulk polymerisation of MMA initiated by benzoyl peroxide and azobis-isobutyronirile (Mark, 1967). Bezoquinone interferes only slightly in the initiation reactions at 60°C but reacts with the growing chain radicals. This retarded free-radical product disappears by termination with ordinary growing chain radicals. It has also been found that the retarded free-radical product attack on monomer, resulting in limited copolymerisation of MMA and benzoquinone. The absence of an appreciable concentration of stabilised radicals formed by direct interaction of quinone molecules and initiator fragments indicates the operation of a different retarding mechanism in systems containing quinones such as bezoquinone and hydroquinone. The same results were found for styrene polymerisation initiated by benzoyl peroxide (Mark, 1967).

In order to study the effect of inhibitor on the evolution of particle size and its distribution in suspension polymerisation of MMA a series of experiments with oil-soluble and water-soluble inhibitors were carried out.

3.3.2 EXPERIMENTAL

The materials, experimental procedure and measurements have been described in details in Chapter 2. Hydroquinone (HQ), 99%, and 4-*tert*-butylcatechol (TBC), 97%, both from Aldrich were used as inhibitors without further purification.

In one experiment suspension polymerisation of MMA was carried out using the MMA monomer as received (un-purified monomer containing 10-100 ppm monomethyl ether hydroquinone).

Experiments were performed with different concentrations of the oil-soluble inhibitor (TBC) and water-soluble inhibitor (HQ). The base formulation for this series contained 1.0 g/l of PVA and 1.0 wt% of LPO. The reaction temperature was 70°C. An agitation speed of 500 rpm was used for the experiments with TBC. The experiments with HQ were carried out at the agitation speed of 300 rpm.

3.3.3 RESULTS

3.3.3.1 Effect of Non-removed Inhibitor in the Monomer

In all experiments carried out in this research we removed the inhibitor from the monomer via reduced-pressure distillation. In order to study the effect of impurities in the monomer on the kinetics of polymerisation and particle size, in one experiment we used the monomer (MMA containing 10-100 ppm monomethyl ether hydroquinone) as received without further treatment.

Rate of Polymerisation: *Figure 3.3.1* shows the conversion-time variations for the experiment with the un-purified monomer in comparison with the corresponding polymerisation run with the purified monomer. The presence of inhibitor in the monomer inhibited the polymerisation reaction, as was expected, and also retarded the rate of polymerisation. The retardation effect on the rate of polymerisation was more apparent after the onset of the gel effect.

Mean Particle Size: *Figure 3.3.2* illustrates the time evolution of D_{32} for this series. Interestingly, the run with un-purified monomer resulted in smaller polymer beads. A smaller steady-state D_{32} was obtained for un-purified monomer because of lower viscosity in comparison with that for the purified monomer at the initial stage due to the induction period observed for the un-purified monomer. During the growth stage the

steep growth observed for the purified monomer drops was reduced to a mild growth for the un-purified monomer drops.

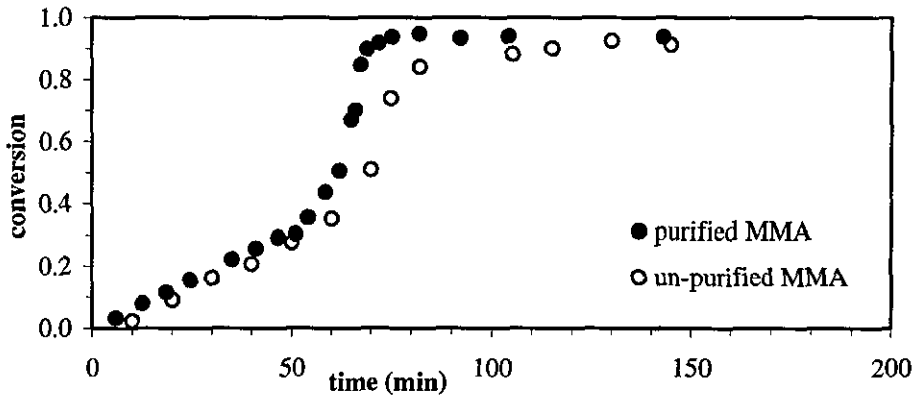

Figure 3.3.1 Conversion-time variations in suspension polymerisation of MMA with purified and un-purified monomer (for other conditions see section 3.3.2).

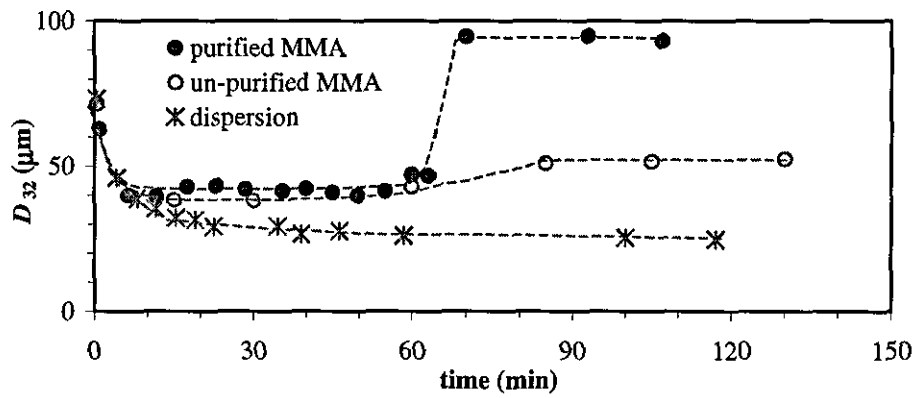

Figure 3.3.2 Time evolution of D_{32} in suspension polymerisation of MMA with purified and un-purified monomer and in the coresponding dispersion.

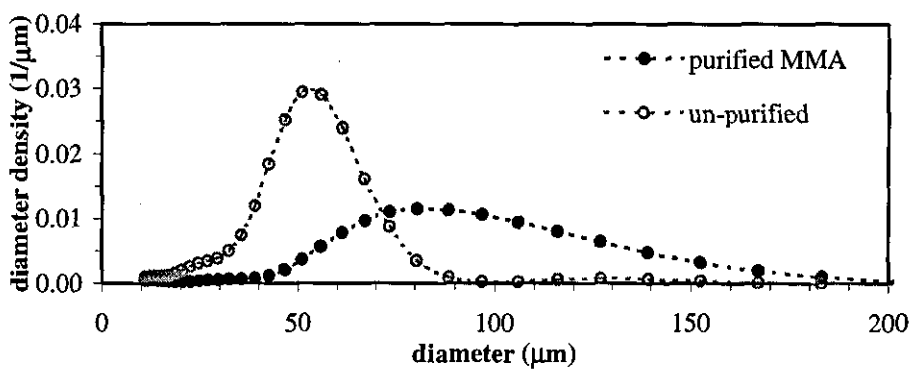

Figure 3.3.3 Final PSDs in suspension polymerisation of MMA with purified and un-purified monomer.

Particle Size Distribution: *Figure 3.3.3* illustrates the final PSDs for this series. The run with un-purified monomer showed a sharper PSD.

The enhanced stability of drops/particles that resulted from use of un-purified monomer caused us to look at the effect of inhibition on particle size and PSD in a more systematic way. A series of experiments was launched in which the monomer was distilled to remove the unwanted inhibitor. In these experiments a specified amount of an oil-soluble or water-soluble grade of inhibitor was added to the monomer phase or the water phase, respectively.

3.3.3.2 Effect of oil-soluble inhibitor

Rate of Polymerisation: *Figure 3.3.4* shows the conversion-time results for the runs with 0.0, 0.1, and 0.4 g of TBC. The presence of TBC in the monomer phase not only delayed the start of polymerisation but also reduced the rate of polymerisation. The latter effect was more apparent for the run with 0.4 g TBC.

Mean particle size: *Figure 3.3.5* shows the evolution of D_{32} for the runs with different amounts of TBC. Generally, the application of TBC resulted in smaller polymer beads. The presence of TBC in the monomer drops inhibits the polymerisation reaction during the early stage of the mixing so that the suspension polymerisation reaction behaves as a simple liquid-liquid dispersion. As a result, the early evolution of D_{32} of drops coincided with that of the corresponding non-reacting MMA-water dispersion. Once the inhibition period elapsed and the polymerisation started, drops became more resistant to drop break up and their size reduction slowed down. As a result, the steady-state drop size was established at a lower value with increasing TBC concentration. The size of drops showed a small increase during the quasi-steady state. Drops showed a mild growth at the times of 65 and 90 min for the runs with the TBC loading of 0.1 and 0.4 g, respectively, according to their onset of the gel effect. The final size of particles obtained with the monomer containing TBC were much smaller than that with pure monomer.

Particle Size Distribution: *Figure 3.3.6* shows the final PSDs of this series. Application of TBC resulted in a sharper size distribution, as well as a smaller mean size of particles.

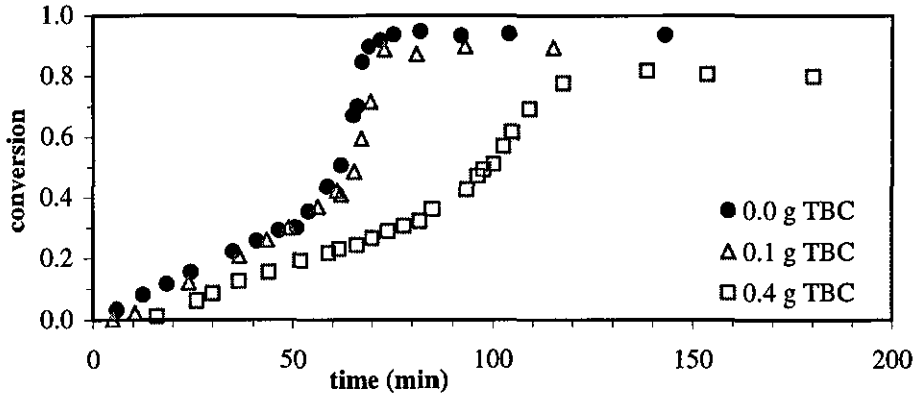

Figure 3.3.4 Conversion-time variations in suspension polymerisation of MMA with different TBC concentrations (for other conditions see section 3.3.2).

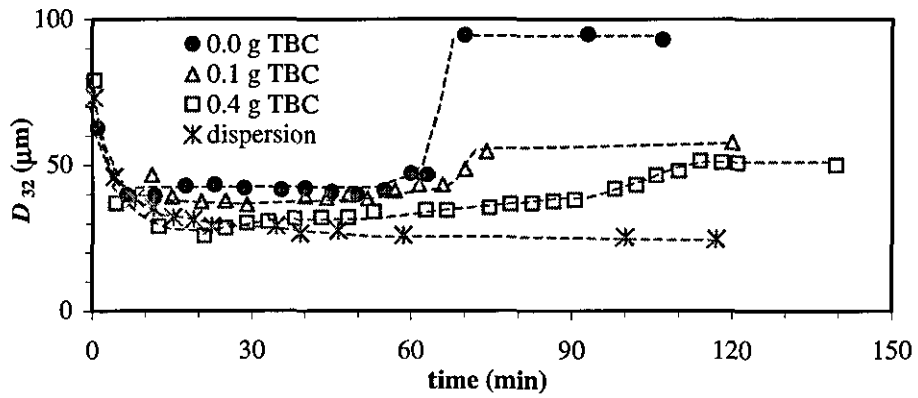

Figure 3.3.5 Time evolution of D_{32} in suspension polymerisation of MMA with with different TBC concentrations and in the corresponding dispersion.

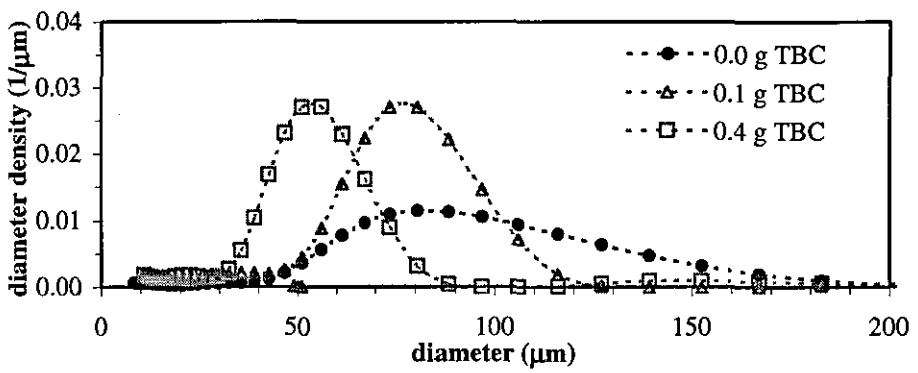

Figure 3.3.6 Final PSDs in suspension polymerisation of MMA with different TBC concentrations.

3.3.3.3 Effect of water-soluble inhibitor

Rate of Polymerisation: The conversion-time histories for this series with 0.0, 0.1 and 0.4 g of HQ in the water phase are shown in *Figure 3.3.7*. The run with the higher quantity of HQ showed a longer induction period and a depressed rate of polymerisation in the later stages of polymerisation.

Mean Particle Size: The application of HQ resulted in smaller polymer beads as shown in *Figure 3.3.8*. HQ affected the evolution of drop size during the transition stage in the same way as TBC. The presence of HQ in the water phase almost suppressed the size variation of drops/particles during the growth stage. The drop size variations with time for the runs using different amounts of HQ are quite similar, despite a significant effect of HQ on the rate of polymerisation as depicted in *Figure 3.3.7*.

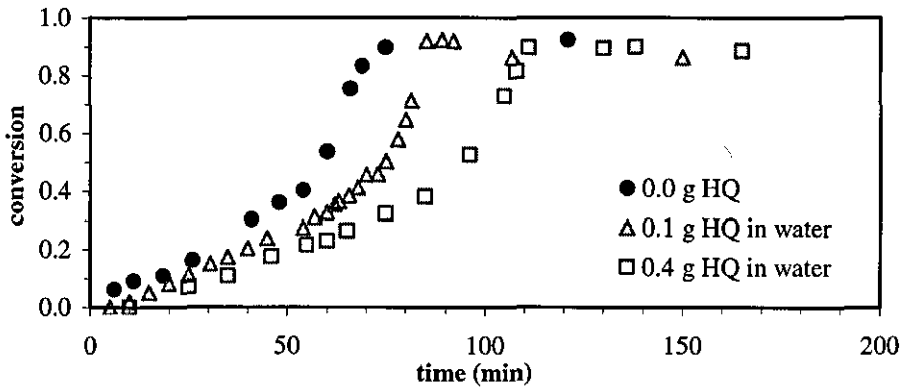

Figure 3.3.7 Conversion-time variations in suspension polymerisation of MMA with different amounts of HQ added into the aqueous phase (for other conditions see section 3.3.2).

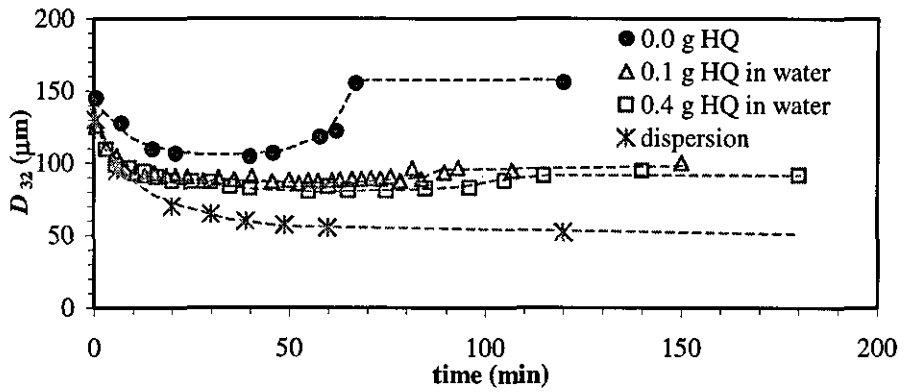

Figure 3.3.8 Time evolution of D_{32} in suspension polymerisation of MMA with different amounts of HQ added into the aqueous phase and in the corresponding dispersion.

Particle Size Distribution: *Figure 3.3.9* shows the final PSDs of this series. The presence of HQ in the water phase improved the stability of the polymerising drops and resulted in a narrower particle size distribution as well as a smaller average particle size.

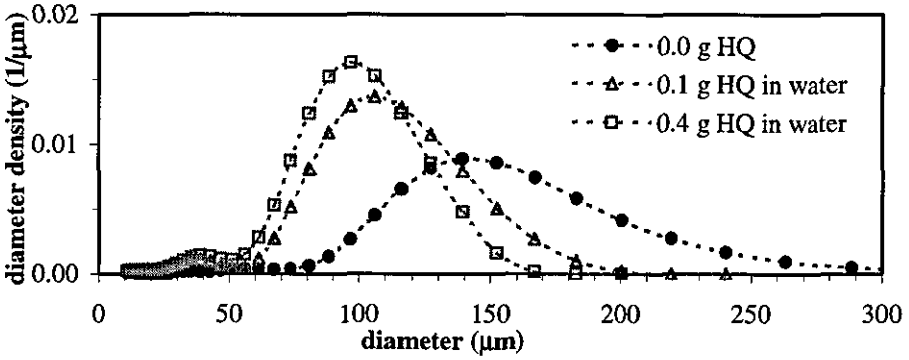

Figure 3.3.9 Final PSDs in suspension polymerisation of MMA with different amount of HQ added into the aqueous phase.

3.3.4 DISCUSSION

In a typical free-radical polymerisation chain growth continues until the radical is terminated or transferred to another substance. If an inhibitor exists, primary radicals will be converted to unreactive forms:

$$\textit{Inhibition:} \qquad \overset{\circ}{R}_0 + Z \xrightarrow{k_z} \textit{inactive product} \qquad (3.3.1)$$

where Z and k_z represent the inhibitor and the inhibition rate coefficient, respectively. So an inhibitor depresses the rate of polymerisation by reducing the concentration of active radicals.

For an ideal inhibitor, polymerisation does not start before all the inhibitor molecules have been consumed. If the activity of the inhibitor is not high, chains can grow before they react with an inhibitor molecule. In such a case, the term retardation can better describe the chemistry of the process:

$$\textit{Retardation (ideal):} \qquad \overset{\circ}{R}_n + Z \xrightarrow{k_z} P_n + \textit{inert product} \qquad (3.3.2)$$

$$\textit{Retardation (non-ideal):} \qquad \overset{\circ}{R}_n + Z \xrightarrow{k_z} \overset{\circ}{Q}_n \qquad (3.3.3)$$

where $\dot{Q}$ is a radical with reduced activity. While retardation may not affect the number of radicals, it will affect the reactivity of the radicals formed and thereby reduces the rate of polymerisation. An important point is that a retarder can act as a chain transfer agent by terminating active growing radicals (Huo et al., 1987; Penlidis et al, 1988).

Now we attempt to describe the role of the inhibitors used in the suspension polymerisations according to their solubility in the two phases. In suspension polymerisation, the locus of polymerisation reaction is, in fact, in the monomer drops or the monomer phase. Although HQ is water soluble, it partitions into both water and monomer phases. A closer look at *Figure 3.3.7* reveals that the inhibition period for HQ is rather short. Note that the highest amount of HQ used is 0.0036 mol (0.4 g), which is almost equivalent to the total amount of the initiator available in the monomer phase (0.0035 mol). However, the inhibition period observed for this run was around 10 min. After this inhibition time, when all, or a part of the HQ dissolved in the oil phase is consumed, the polymerisation starts. During the polymerisation period, as HQ is consumed in the oil phase via reaction with initiator radicals, HQ dissolved in the water phase diffuses into the monomer phase until all of the HQ is consumed. The retardation effect of HQ, in the aftermath of the inhibition, also depends on the diffusion rate of HQ from the water phase to the oil phase, which is influenced by the agitation speed and the viscosity of the polymerising drops.

TBC is an oil-soluble substance, thus, TBC molecules tend to stay in the monomer phase and react with the initiator derived free radicals. When the concentration of the TBC dissolved in the monomer phase is reduced to a certain value by reaction with the free radicals generated in the monomer phase, polymerisation starts (see *Figure 3.3.4*). There are several reports in the literature indicating that inhibitors, such as TBC, do not behave ideally as inhibitors and act as chain transfer agents as well as retarders and reduce the polymer molecular weight (Huo et al., 1987; Cunningham et al., 2000, Bevington et al., 2002 and 2003).

It can be concluded that both of the inhibitors used affected the rate of polymerisation. However, from the data presented in *Figures 3.3.4* and *3.3.7*, it is apparent that TBC inhibited the polymerisations in a more drastic way than HQ. This was easily explained

by favoured dissolution of TBC in the monomer phase. Both inhibitors retarded the rate of polymerisation significantly with an increase in the inhibitor concentration.

The application of inhibitors changed the magnitude of drop size variations. A higher inhibitor concentration gave a longer inhibition period, a more severe drop break up rate, and finally a lower steady-state drop size (see *Figures 3.3.5* and *3.3.8*). The results also indicate that the presence of an inhibitor in the system damps the variation of drop size during the growth stage. HQ appears to be more efficient in the prevention of drop coalescence and production of small polymer beads in comparison with TBC. It is interesting to note that the presence of even 100 ppm of a monomethyl ether hydroquinone in the un-purified monomer was sufficient to greatly reduce the final particle size (see *Figure 3.3.2*).

Figure 3.3.10 shows the evolution of the volume fraction of satellite droplets (f_{vs}) for the runs with purified and un-purified monomer. *Figure 3.3.11* demonstrates the evolution of f_{vs} for the runs with HQ. Both quinone-type inhibitors hindered formation of satellite particles (see *Figure F.4,* Appendix F). The mechanisms suggested for the formation of satellite droplets/particles have been mentioned in chapter 1. A very brief description is given here.

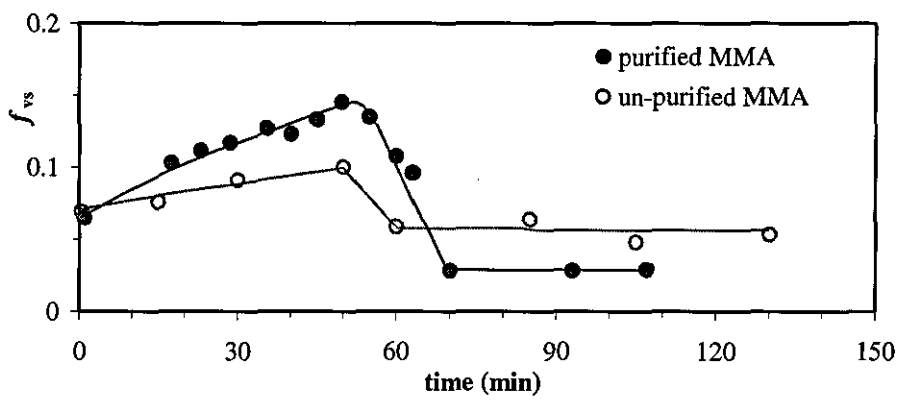

Figure 3.3.10 Time evolution of volume fraction of satellite droplets in polymerisation of MMA with purified and un-purified monomer.

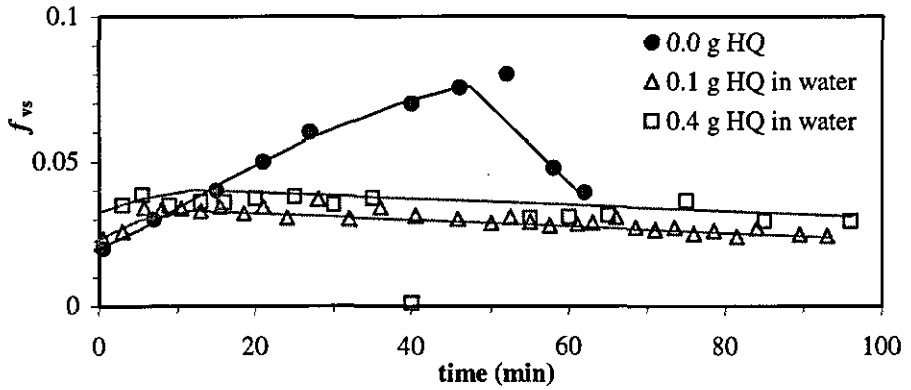

Figure 3.3.11 Time evolution of volume fraction of satellite droplets in polymerisation of MMA in the presence of HQ.

Satellite droplets are usually assumed to be formed as a result of a drop breakage mechanism. It has been suggested that drops break up into daughter drops and a large number of satellite drops (Chatzi and Kiparissides, 1992). Satellite droplets could be formed due to the nonhomogeneities of mixing. Drops in the zone close to the impeller may break up into very small droplets. The size of satellite droplets formed by these mechanisms is usually around d_{min} (larger than a few microns). Dispersion/emulsion polymerisation mechanism can also produce small particles. It is known that emulsion particles can be formed in suspension polymerisation reactions (Cunningham, 1999). For MMA monomer with relatively high water solubility (16 g/l at 70°C), the formation of emulsion particles could be quite significant. Emulsion particles are formed by a homogeneous nucleation mechanism (Fitch et al, 1969) in large numbers. The free radicals generated in the water phase propagate with the dissolved monomer to reach a critical size after which they become insoluble in the water phase and precipitate to form primary polymer particles. These tiny particles adsorb emulsifier/stabiliser from the continuous phase and after some coagulation with other particles, depending on the concentration of stabiliser and agitation speed, will eventually form stable polymer particles. The newly formed particles will compete with monomer drops for adsorption of stabiliser. By adsorption of stabiliser, the amount of stabiliser available to the drops is diminished leading to a decreased stability of drops with a subsequent intensive growth by coalescence.

A point worthy of attention is that the volume fraction of satellite particles maintained in the suspension in the runs with HQ inhibitor because of enhanced stability of the suspension (*Figure 3.3.11*). Whereas the runs with the pure monomer ended up with a loss of satellite particles as a result of an extensive flocculation/coagulation of satellite particles during the growth stage. The results suggest that the formation of large number of satellite droplets/particles could be the reason why particles grow appreciably in the absence of an inhibitor. The growing free radicals generated in the water phase by the decomposition of the dissolved initiator will be terminated by reaction with inhibitor molecules dissolved in the water phase before they can reach the critical size to form primary particles. Application of water-soluble inhibitors as a means to reduce the formation of dispersion/emulsion particles has been reported, but not compared and/or analysed, in the literature (e.g., Okubo et al., 1997; Ma et al., 2003). Such a conclusion, however, is not evident for TBC as the cessation in the formation of satellite particles was not evident in the results obtained with this inhibitor (not shown). Although TBC is an oil-soluble inhibitor, its solubility in the water phase, 0.2 wt% at 25°C (Sax and Lewis, 1989), should be sufficient to prevent aqueous-phase polymerisation. This assumption may look more plausible if we note that the concentration of the free–radicals generated in the water phase is very low. This is because LPO is also an oil-soluble initiator and its solubility in the water phase is limited. The reduction in the size of particles with TBC concentration may have an origin in the drop viscosity.

The importance of the Emulsion/Dispersion Particles

In order to verify and estimate the contribution of emulsion particles to instability of the suspensions, we performed a dispersion polymerisation with the aqueous phase that had the same formulation as that in the suspension polymerisation.

The reaction temperature and PVA concentration were kept at 70°C and 1 g/l, respectively. The impeller speed was 500 rpm. The water phase was saturated with the monomer (MMA) and the initiator (LPO). Considering that the water solubility of MMA is 16 g/l at 70°C, we used 8.96 g MMA for 560 g of aqueous phase (i.e., 1 g/l PVA solution). LPO is an oil soluble initiator, but it is dissolved in the water phase to a limited extent. The melting point of LPO (54°C) is lower than the reaction temperature (70°C) and so the undissolved LPO remains as small droplets in the aqueous phase. Precautions were taken to remove suspended droplets of MMA and LPO from the

aqueous phase. The dispersion polymerisation was carried out for 3 hr. The solution became bluish after about 30 min indicating that polymer particles were being formed. In fact this observation showed that the infinitesimal amount of dissolved LPO in water provided a sufficient number of radicals in the water phase to induce homogeneous nucleation. After 3 hr, the remainder of the monomer containing 1.0 wt% LPO, was added to the reactor and the suspension polymerisation started. For simplicity we may refer to this process as a hybrid of dispersion-suspension polymerisation in which the formation of emulsion/dispersion particles was enhanced as will be discussed later.

Rate of Polymerisation: *Figure 3.3.12* shows the conversion-time variation for the conventional suspension polymerisation of MMA and the corresponding dispersion-suspension polymerisation. Time zero for the latter process is the time that suspension polymerisation started. As seen from this figure, all the data points fall on the same curve. The inset in this figure shows the variation of conversion in dispersion polymerisation of MMA during the first 3 hr of dispersion-suspension polymerisation.

Mean Particle Size and Particle Size Distribution: *Figure 3.3.13* illustrates the variations of Sauter mean diameter of drops (D_{32}) with time and conversion for the two processes. The mean size of particles obtained as a result of dispersion polymerisation was about 20 μm. *Figure 3.3.14a* shows that the particles formed by this mechanism have a broad distribution. Most of the particles obtained by this mechanism are smaller than 10 μm. This indicates that particles formed by this mechanism can be correctly labelled as satellite particles. It should be noted that the primary particles formed by homogeneous nucleation in the aqueous phase are usually small but they may coagulate due to instability.

The measuring device used in this research was not able to detect particles smaller than 0.40 micron. So the contribution of particles smaller than 0.40 micron to the instability of the suspension was not accounted for.

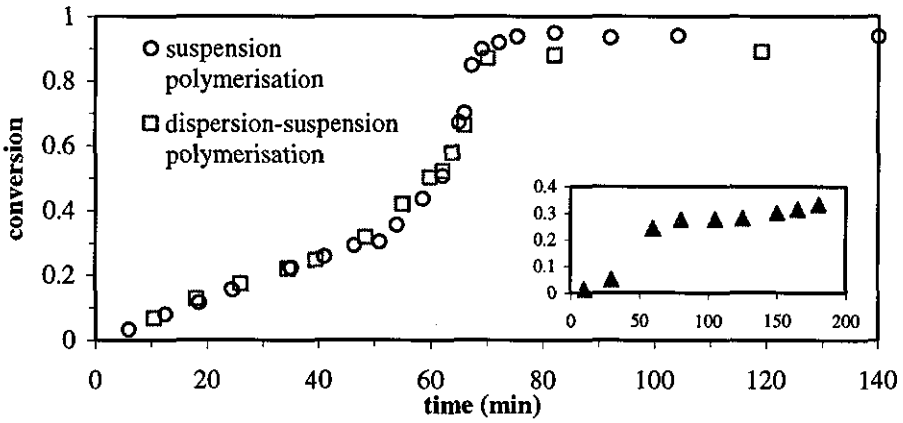

Figure 3.3.12 Conversion-time variations in suspension polymerisation of MMA and the corresponding disp-susp polymerisation (for the conditions see section 3.3.4). The small graph shows the conversion-time variations for the dispersion polymerisation.

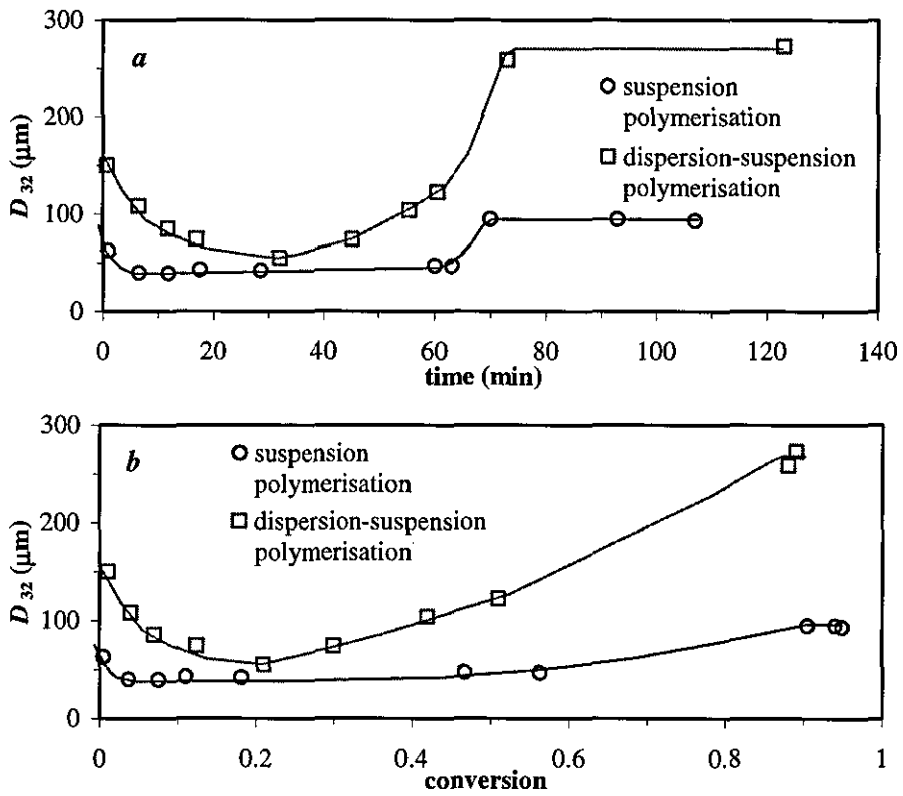

Figure 3.3.13 Evolution of D_{32} in suspension polymerisation of MMA and the corresponding dispersion-suspension polymerisation with *a*) time, and *b*) conversion.

When the second stage (suspension polymerisation) started, the size of drops of added monomer decreased according to the typical pattern in a transition stage (*Figure 3.3.13*). However, the rate of reduction in drop size is rather low in comparison with that of suspension polymerisation. This could be due to a higher interfacial tension of

monomer/water interface as a result of emigration of the stabiliser molecules from the water phase to the surface of emulsion particles. After sometime with continuation of a period of mixing, the size of drops fell to a value close to the steady-state value for the drops in the suspension polymerisation. Eventually a point was reached when drop size showed a rapid increase in size. Larger particles were obtained from the dispersion-suspension polymerisation in comparison with those from the suspension polymerisation. Note that this experiment sets the maximum contribution of the dispersion/emulsion particles to the suspension polymerisation. This is because in a suspension polymerisation, both suspension and dispersion polymerisation occur simultaneously and competitively. The primary particles formed via the dispersion polymerisation may collide and coalesce with drops, before they become stable.

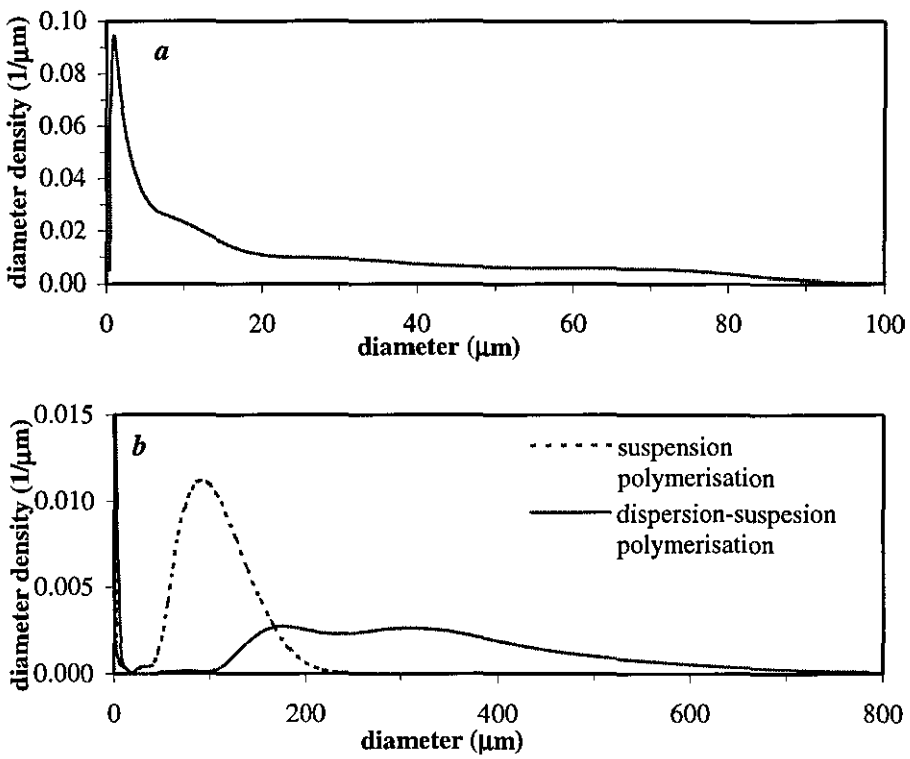

Figure 3.3.14 Final PSD for *a*)dispersion polymerisation, and *b*)dispersion-suspension polymerisation and conventional suspension polymerisation of MMA.

The role of the dispersion particles in the overall evolution of particles can be summarised as a sink for the stabiliser, which causes the large particles to grow to a great extent as a result of their low coverage by the stabiliser. However, the author is

not certain that this is the only factor that destabilises the dispersions, at least for TCB. Further study on the subject is left for future research.

The PSDs of final particles from the dispersion-suspension polymerisation and conventional suspension polymerisation are shown in *Figure 3.3.14b*. The instability of polymerising drops in the dispersion-suspension polymerisation, caused by the formation of large number of satellite particles, led to an evolution of broad size distribution of particles.

3.3.5 CONCLUSIONS

The main conclusions specific to this series are:

- Because of the heterogeneous nature of suspension polymerisation reactions, the retardation effect of water-soluble inhibitors may be enhanced because of continuous diffusion from the water phase to the monomer phase.
- The presence of inhibitor retarded the rate of polymerisation and viscosity increase in drops, and thus facilitated drop break up so that smaller drop size was achieved at the end of transition stage.
- The quasi steady-state drop size was lowered and approached that of monomer/water dispersion with increasing inhibitor concentration.
- The application of inhibitors damped the growth stage and resulted in smaller polymer beads. A possible reason for an enhanced stability of drops, in the presence of an inhibitor, was found to be due to the cessation of formation of emulsion/dispersion particles.
- The results from dispersion-suspension polymerisation process indicate that dispersion/emulsion particles diminished the availability of the stabiliser to the drops by adsorbing it. This slowed down the drop breakage rate during the transition stage and established a higher steady-state drop size (if any) in comparison with the conventional suspension polymerisation. Too many satellite particles would destabilise the suspension and cause an imbalance in the break up and coalescence rates so that particles continuously grow with the progress of reaction (no quasi-steady state) and larger particles are obtained in comparison with the conventional suspension polymerisation.

3.4 EFFECT OF TEMPERATURE

3.4.1 INTRODUCTION

In a suspension polymerisation the variation in reaction temperature will affect the properties of both monomer and oil phases. The effect of an increase in temperature on the dispersed phase is a higher rate of polymerisation, two- to threefold rate increase for a 10°C temperature increase (Odian, 1991), nothing certain can be said about its effects on the properties of the water phase, which mainly depends on how PVA distributes between the two phases at higher temperatures. Therefore, the results on the temperature effects were not lumped with those that affect either of the two phases.

In this part of the thesis, the effects of temperature on the PSD evolution in the suspension polymerisation of MMA have been studied. The results have been also compared with those from corresponding non-reacting MMA/water dispersions.

3.4.2 EXPERIMENTAL

The materials, experimental procedure and measurements have been described in detail in Chapter 2. All experiments in this series were carried out at the agitation speed of 300 rpm. MMA hold up was 0.20. LPO and PVA concentrations were 1.0 wt% (based on monomer) and 1.0 g/l (based on water), respectively.

3.4.3 RESULTS AND DISCUSSION

3.4.3.1 Non-reacting Liquid-Liquid Dispersion

Non-reacting dispersions of MMA in water were carried out at different temperatures of 50, 60, 70, and 80°C.

Mean Drop Size: The time variation of Sauter mean diameter of daughter drops at different temperatures is illustrated in *Figure 3.4.1*. The drop size variations during transient stage were almost the same for the different temperatures. Generally, the drop size did not vary much with temperature (except for the drop size at 50 °C which showed slightly a higher value than the others).

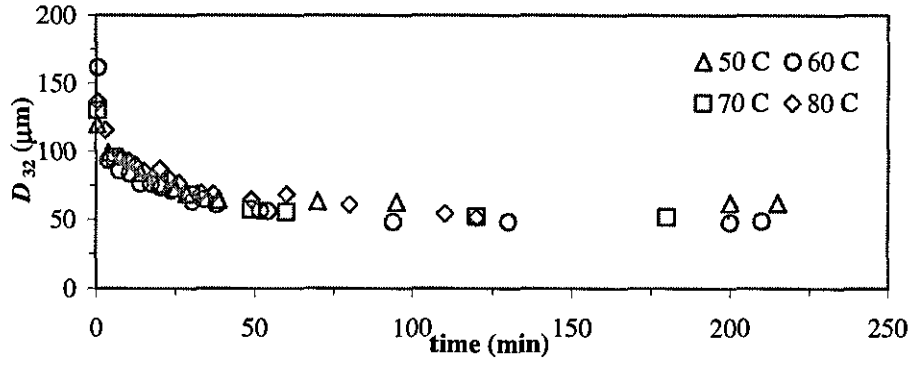

Figure 3.4.1 Time variations of Sauter mean diameter of daughter drops for dispersions at different temperatures (for the other conditions see section 3.4.2).

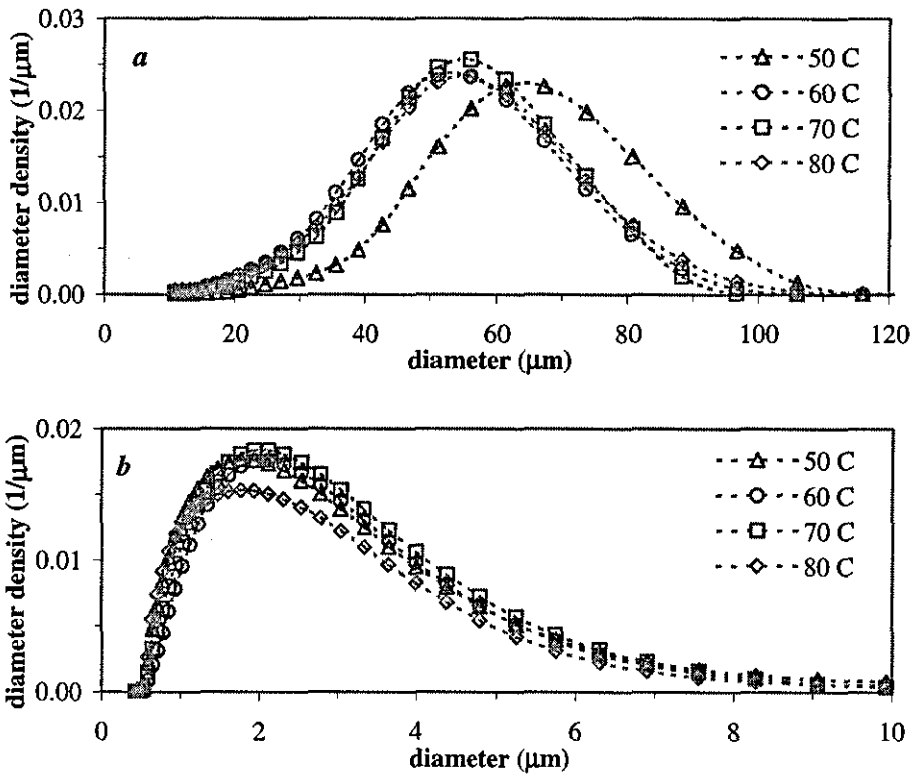

Figure 3.4.2 Final *a*) daughter, and *b*) satellite drop size distributions for dispersions at different temperatures.

Drop Size Distribution: Figure 3.4.2 shows that the final DSDs in the dispersions are quite similar at different temperatures. Lazrak et al. (1998) showed that the interfacial tension between MMA and aqueous PVA solution, with the same specification as that used in this study, decreases with a temperature increase. Therefore, a temperature increase may be expected to facilitate the rate of drop break up and thus, decrease the size of drops. From the results, however, it is apparent that temperature did not affect the balance of the drop break up and coalescence significantly so that D_{32} remained unaffected by temperature variations within the range 60-80°C.

The time evolutions of DSDs at each temperature have been illustrated in *Figures 3.4.3* to *3.4.6*. The DSDs continuously narrowed with time until a quasi steady state reached after some time. *Figure 3.4.7* illustrates the time evolution of the volume fraction of the satellite droplets (f_{vs}). Satellite droplets were continuously formed during the transition stage. However, no precise distinction can be found between f_{vs} – time curves for different temperatures.

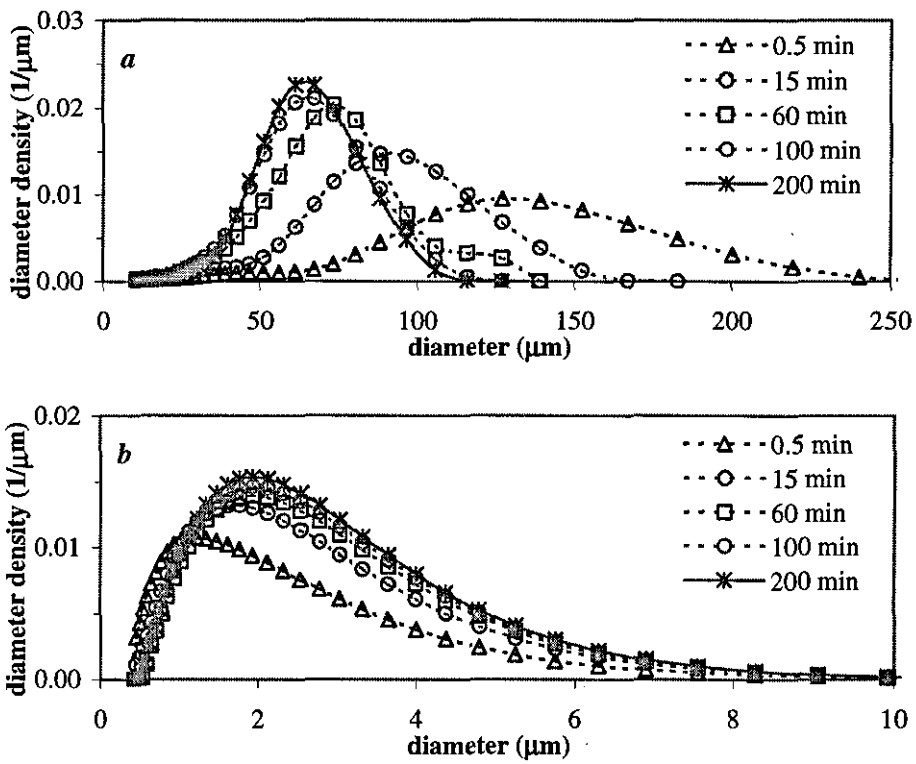

Figure 3.4.3 Time evolution of *a*) daughter, and *b*) satellite drop size distributions for the dispersion at 50°C.

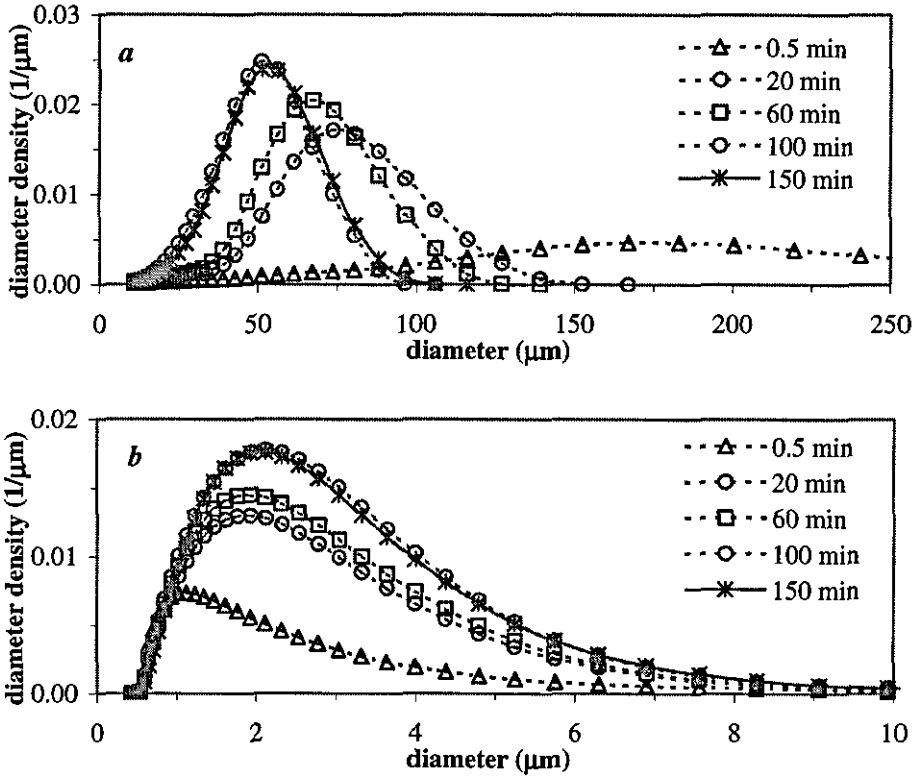

Figure 3.4.4 Time evolution of *a*) daughter, and *b*) satellite drop size distributions for the dispersion at 60°C.

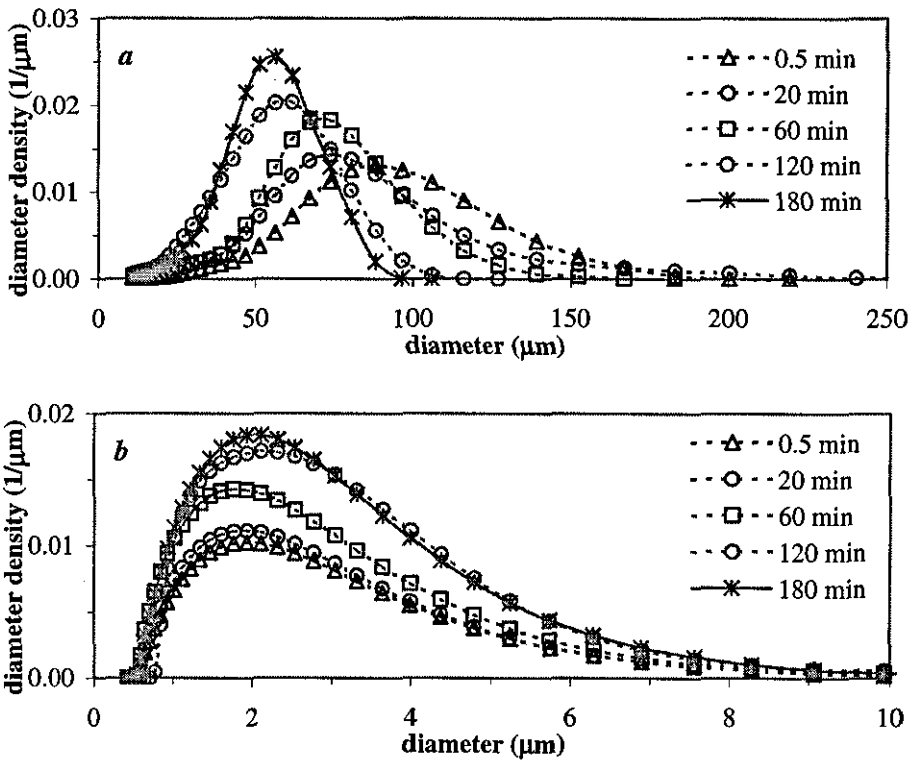

Figure 3.4.5 Time evolution of *a*) daughter, and *b*) satellite drop size distributions for the dispersion at 70°C.

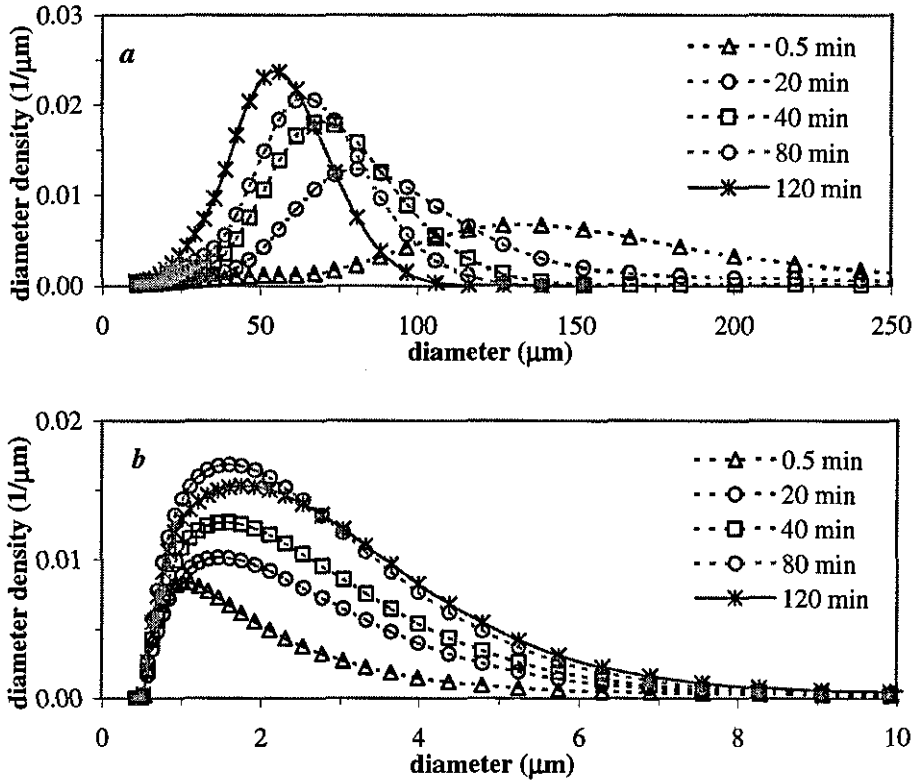

Figure 3.4.6 Time evolution of *a*) daughter, and *b*) satellite drop size distributions for the dispersion at 80°C.

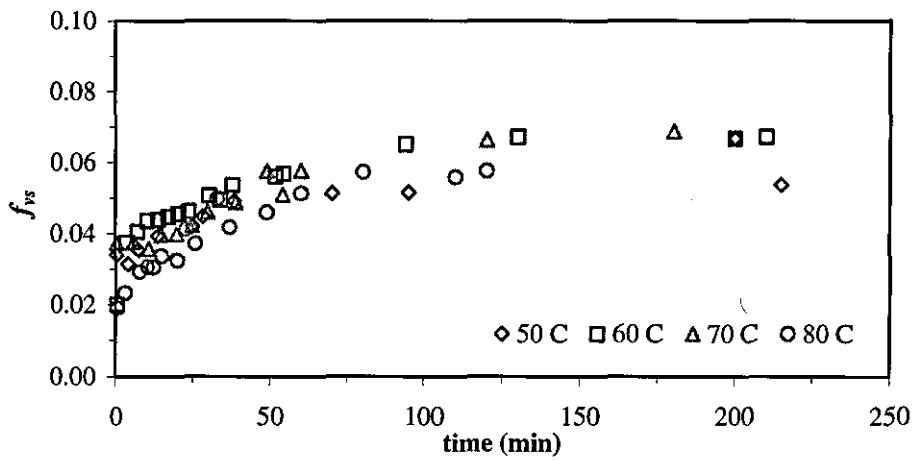

Figure 3.4.7 Time variation of volume fraction of satellite droplets in dispersions at different temperatures.

3.4.3.2 Suspension Polymerisation

The suspension polymerisations of MMA were carried out at temperatures of 50, 60, 70, and 80°C.

Rate of Polymerisation: The conversion-time variations for the runs at different temperatures are depicted in *Figure 3.4.8.* It is evident from this figure that the rate of polymerisation increases with temperature. By considering the early time data for conversion at each temperature, we can calculate the initial rate of polymerisation. This calculation showed that in the range of temperature studied (50-80°C) the rate of polymerisation increased 2.26 times (on average) for each 10°C increase in the reaction temperature.

The onset of the gel effect was recorded at 210, 100, 55, and 32 min (corresponding to the conversions of 0.30, 0.35, 0.40, and 0.45, respectively) for polymerisations carried out at 50, 60, 70, and 80°C, respectively. A closer look at *Figure 3.4.8* reveals that in terms of conversion, the onset of the gel effect occurred at lower conversions with decreasing temperature because of the high-molecular weight polymer formed at a lower temperature. The duration of the gel effect, however, was shortened with increasing temperature. This implies that the viscosity increase during the gel effect will occur in a short interval of time at high temperatures (at about 5 minute for 80°C, for example).

Mean Particle Size: Figures 3.4.9a and *3.4.9b* show the variations of Sauter mean diameter of daughter drops (D_{32}) with time and conversion, respectively, at different temperatures. The reduction in D_{32} during the transition stage appears to be more appreciable for the lower temperatures; simply because for these runs the viscosity build up in drops was slow and thus, drop break up could continue further. For the higher temperatures, such as 80°C, the rise in drop viscosity depressed the rate of drop break up and caused the transition stage to become short by balancing drop break up and coalescence.

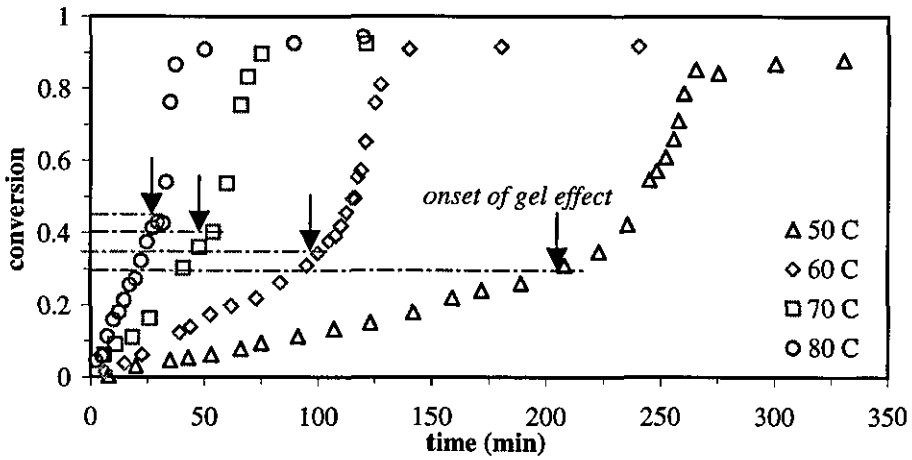

Figure 3.4.8 Time-conversion variations for runs at different temperatures (for the other conditions see section 3.4.2).

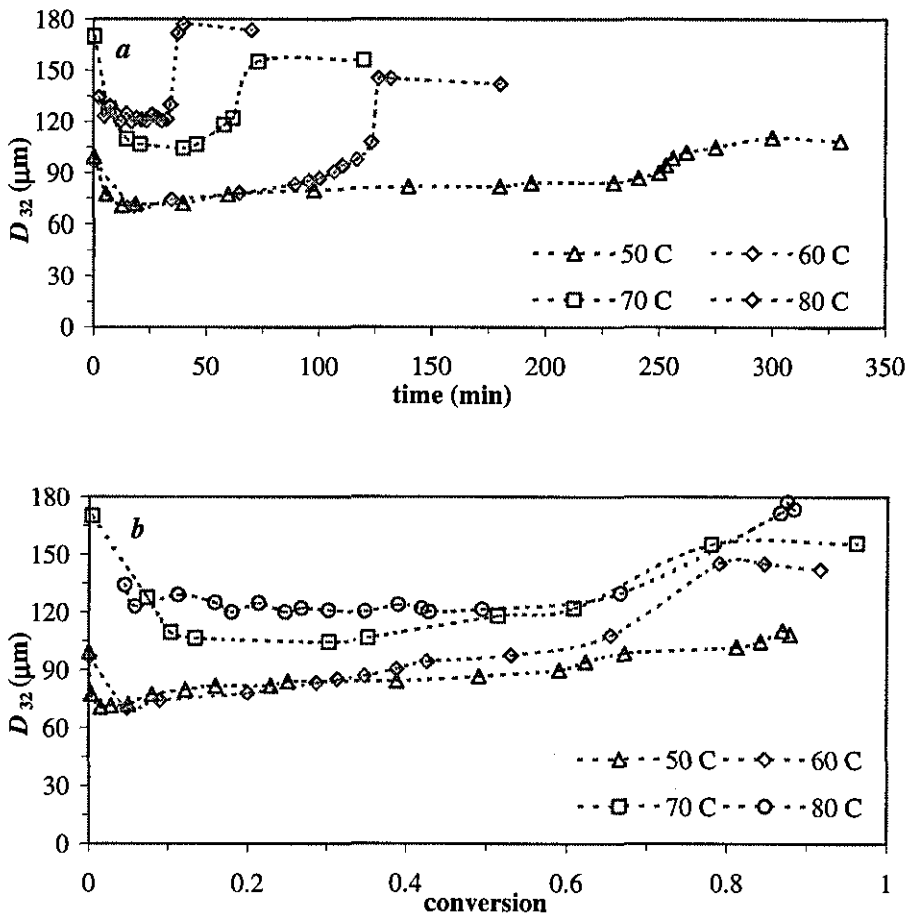

Figure 3.4.9 Variations of Sauter mean diameter daughter drops with *a*) time, and *b*) conversion at different temperatures.

As a result of depressed rate of break up, a higher quasi steady-state drop size was achieved with a temperature increase. It is seen from *Figures 3.4.9a* that D_{32} reveals a mild growth during so called quasi steady-state stage for the lower temperatures (50 and 60 °C). For these runs, in fact, D_{32} started increasing after a few percent conversion (see *Figure 3.4.9b*). It can be stated alternatively that for these runs the steady state was never achieved. For runs with the reaction temperatures of 70 and 80°C, quasi steady states lasted for some time. At 80°C, D_{32} remained constant until a conversion of 0.60. The molecular weight of polymer, and the polymer viscosity, is significantly reduced with increasing temperature. Note that this is a double effect because besides formation of low molecular weight polymers with low viscosity, polymers are less viscous at higher temperatures. It is likely that at high temperatures when the viscosity of the dispersed phase is comparatively low, the balance between drop break up and drop coalescence is maintained to a greater extent resulting in a rather constant D_{32} during quasi steady state. For the lower temperatures, the viscosity build up in drops with conversion is so high that the rate of drop break up is extensively affected as reaction proceeds. As a result, the rate of drop break up falls behind the rate of coalescence. This leads to a constant, though small, rise in the size of particles even during the quasi steady-state stage.

For all runs, a significant rise in the drop size was observed during the gel effect where a massive increase in the drop viscosity occurred within a short period of time. The growth was less significant for the lower temperatures and became steeper with a temperature increase. If the stabiliser performance does not vary with temperature, a possible conclusion emerging from the data obtained on MMA/water dispersions, then a greater particle growth is expected at a lower temperature because of the large surface area of particles formed and also a longer gel effect that allows more coalescence. This is in contrast to the results obtained. Therefore, it seems that the growth of the particles at higher temperatures could be due to loss of stability of the polymerising drops. This implies that PVA becomes less effective in protecting polymerising drops against coalescence with increasing temperature. It has been stated in the literature that there is an overall trend of decreasing drop stability with increasing temperature, though the magnitude of reduction is quite different for different PVAs (Lazrak et al., 1998). It has been shown that this effect is not due to a decrease in viscosity of the continuous phase with increasing temperature (He et al., 2002). The reasons for the loss of particle

stability at higher temperatures are not known. Increased rate of chain transfer to PVA and dissolution of PVA in the monomer phase at higher temperatures are possible two reasons.

Particle Size Distribution: Figure 3.4.10 shows a comparison between the final PSDs. As a general statement, a larger and broader polymer particle and PSD were obtained with increasing temperature. *Figures 3.4.11* to *3.4.14* show the time evolution of the PSDs for the polymerisations carried out at 50, 60, 70, and 80°C. The breadth of distributions narrowed initially, but widened in the course of reaction. A distinctive feature of polymerisation at lower temperatures (50 and 60°C) is the evolution of a bimodal PSD during the polymerisations. The bimodal size distribution of daughter drops occurred during the so-called quasi steady state and lasted till the onset of growth stage. During the growth stage particles coalesced to form a single peak. The formation of bimodal PSDs at lower temperatures is thought to be due to the shift in the drop break up mechanism from uni-sized to multi-sized drops with increasing drop viscosity (Kuriyama et al., 1995).

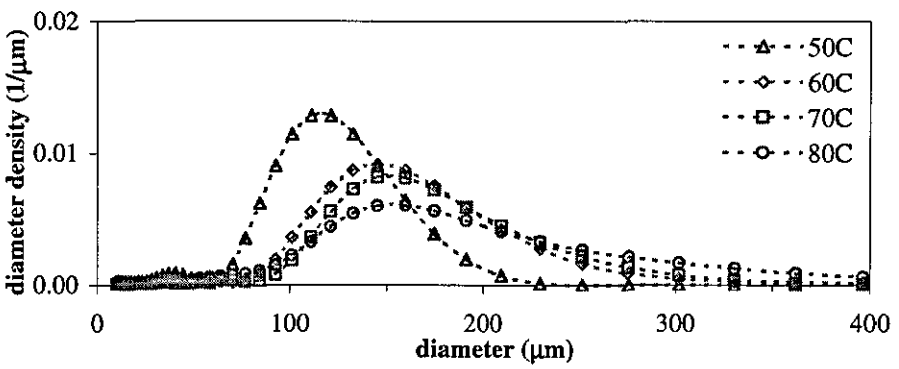

Figure 3.4.10 Final PSDs for runs at different temperatures.

The evolution of satellite droplets is also illustrated in *Figures 3.4.11b* to *3.4.14b*. Satellite droplets were continuously formed during polymerisation. The time variation of f_{vs} is shown in *Figure 3.4.15*. Satellite particles were generated at a greater rate with increasing temperature. For the lower temperatures, satellite particles remained in suspension by the end of reaction. For the higher temperature (80°C), however, satellite particles were lost by coalescence with large particles in association with the low stability of the suspensions. However, all runs ended with almost the same value of f_{vs}.

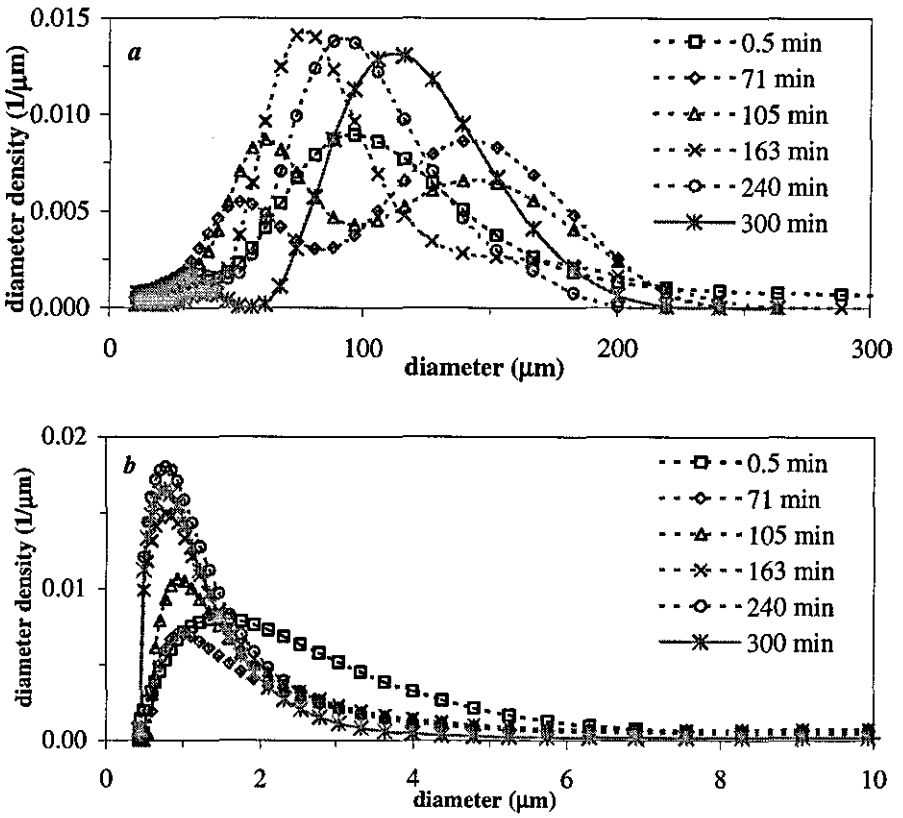

Figure 3.4.11 Time evolution of *a*) daughter, and *b*) satellite PSDs for run at 50°C.

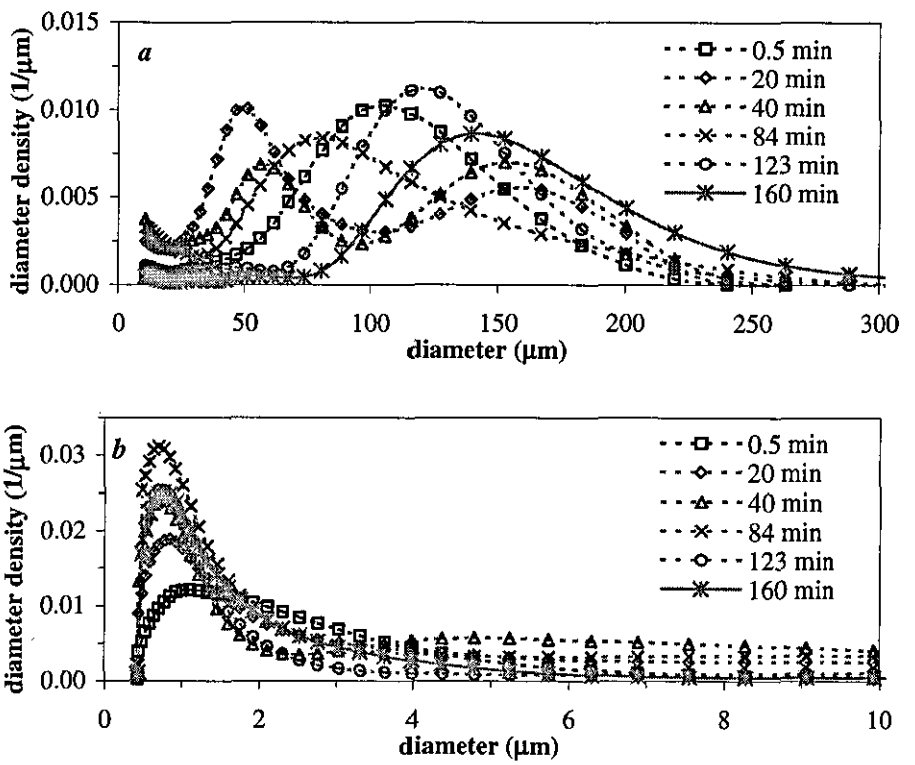

Figure 3.4.12 Time evolution of *a*) daughter, and *b*) satellite PSDs for run at 60°C.

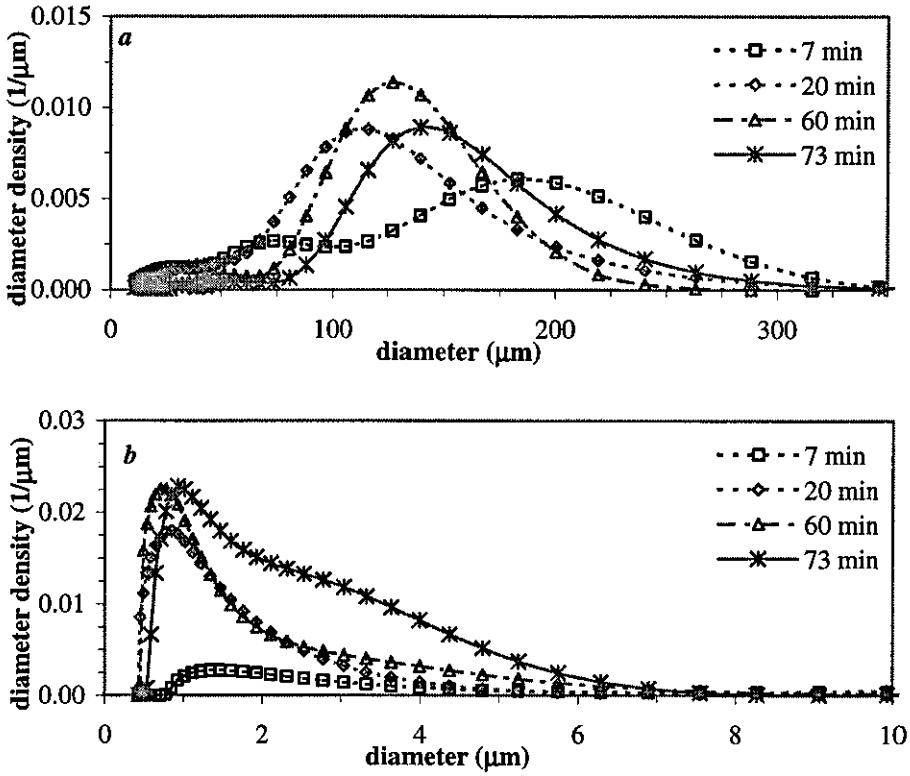

Figure 3.4.13 Time evolution of *a*) daughter, and *b*) satellite PSDs for run at 70°C.

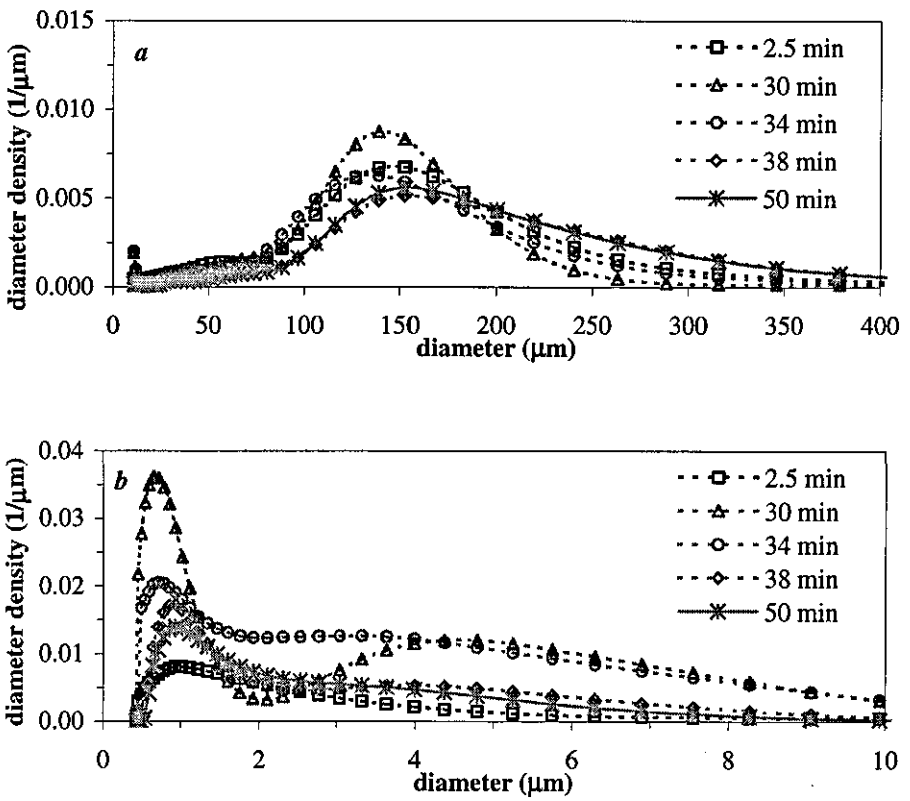

Figure 3.4.14 Time evolution of *a*) daughter, and *b*) satellite PSDs for run at 80°C.

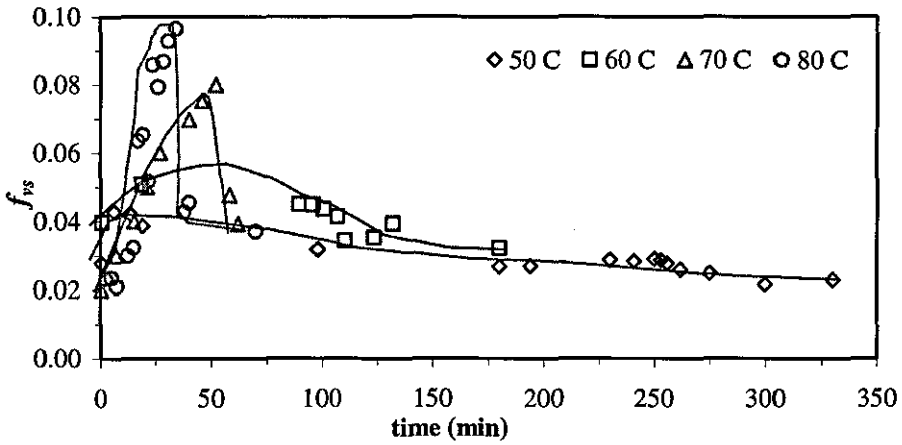

Figure 3.4.15 Time variation of volume fraction of satellite droplets in suspension polymerisations at different temperatures.

3.4.3.3 Suspension Polymerisation versus Non-reacting Dispersion

Mean Drop/Particle Size: Figure 3.4.16 compares the time variation in the Sauter mean diameter of drops from the MMA/water dispersion with that of particles from the MMA suspension polymerisation at the same temperatures. A larger difference between the size of particles and drops was developed at a higher temperature. This can be partly attributed to the higher rate of reaction and viscosity build up in the polymerising drops, which establishes an early quasi steady state by reducing the rate of drop break up. The loss of stability of polymerising drops against coalescence at higher temperatures seems to be the second factor, which contributes to such a difference.

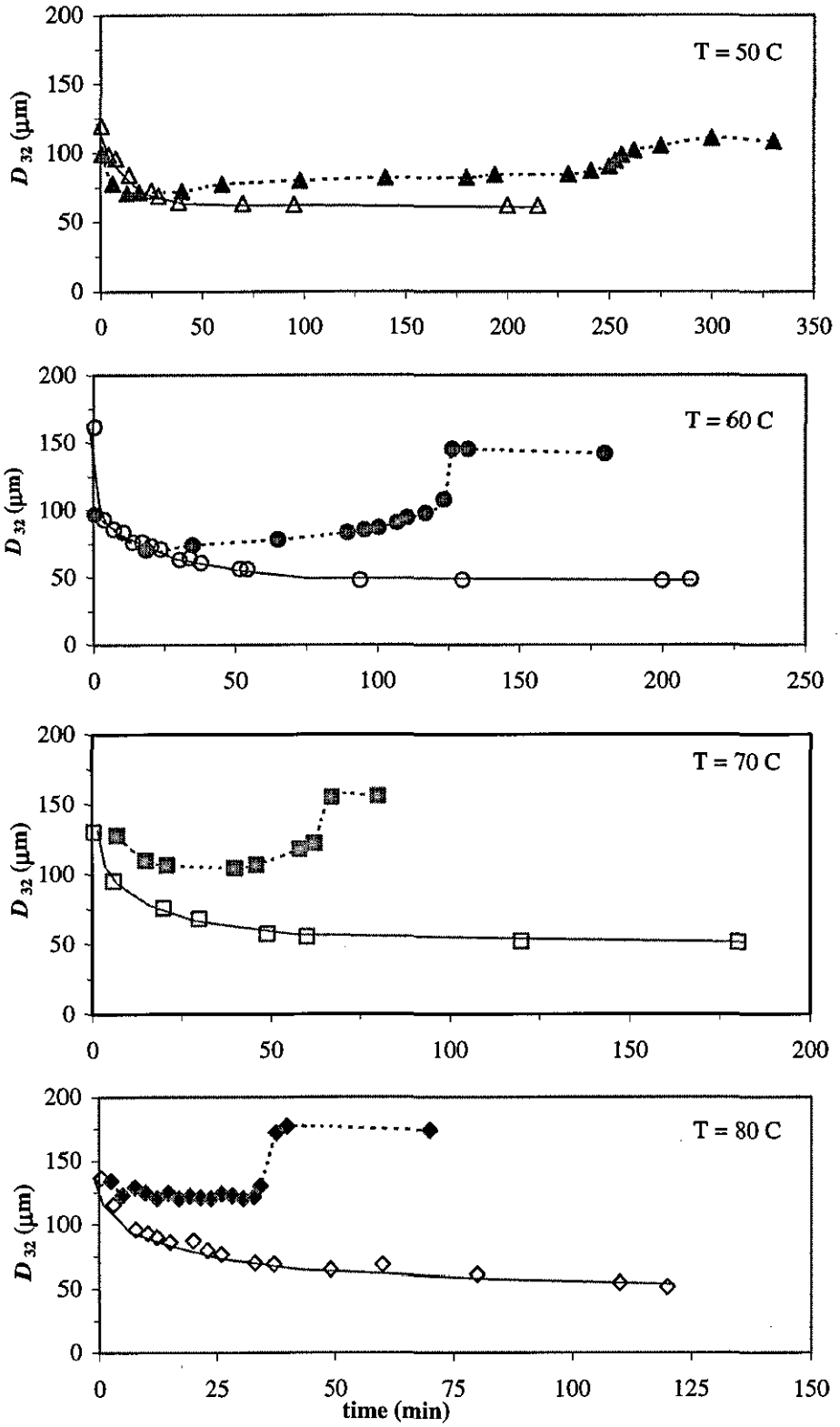

Figure 3.4.16 Comparison of time variations of D_{32} for dispersions (empty symbols) and corresponding suspension polymerisations (full symbols) at different temperatures.

3.4.4 CONCLUSIONS

The reaction temperature was found to play an important role in the determination of the size average and distribution of particles in the suspension polymerisation of MMA. The main conclusions are:

- Increasing the reaction temperature effectively shortened the transition period and resulted in larger drops/particles.

- The balance between drop break up and coalescence during the so-called quasi steady-state stage was better maintained at higher temperatures where the polymer produced had a lower viscosity. At lower temperatures, drop size increased with time during this stage. A real quasi steady-state drop size was only achieved at higher temperatures and within a broader range of conversion.

- The growth stage was less evident at a lower temperature. Whereas a longer growth stage is theoretically expected for a slower rate of polymerisation. Therefore the pattern of size variations with temperature during the growth stage is most likely due to variation in the properties of the aqueous phase.

3.5 EFFECT OF AGITATION SPEED

3.5.1 INTRODUCTION

When two miscible phases are brought into contact by agitation, drops are formed with size depending on, among other variables, the agitation speed. The size of drops is determined by the competition of break up and coalescence. An increase in the agitation speed increases the rate of drop break up and thus favours the formation of smaller drops (Shinnar, 1961; Sprow, 1967; Johnson, 1980; Chatzi and Kiparissides, 1994; Lazrak et al., 1998, Maggioris et al., 2000; Yang et al., 2000). However, at very high agitation speeds the drop size may increase due to an increase in the rate of coalescence because of the very large surface area of drops and reduced effectiveness of the suspending agent molecules on the interface. A U-shape dependence of the mean drop size on the agitation speed has been reported by several investigators (Johnson, 1980; Tanaka and Hosogai, 1990; Chatzi and Kiparissides, 1994; Zhou and Kresta, 1998).

In suspension polymerisations increasing the agitation speed decreases the final polymer particle size (Konno et al., 1982; Kalfas et al., 1993; Lazrak et al., 1998). Yang et al. (2001) have applied a variable agitation-speed method during the suspension polymerisation of styrene to limit the drop size enlargement during the growth stage and control the final polymer particle size.

In this section the effect of agitation speed on the evolution of PSD in the suspension polymerisation of MMA has been studied. The results have been also compared with those from corresponding non-reacting MMA/water dispersions.

3.5.2 EXPERIMENTAL

The materials, experimental procedure and measurements have been described in detail in Chapter 2. All experiments in this series were carried out at 70°C. MMA hold up was 0.20. LPO and PVA concentrations were 1.0 wt% (based on monomer) and 1.0 g/l (based on water), respectively.

3.5.3 Results and Discussion

3.5.3.1 Non-reacting MMA/Water Dispersion

Non-reacting MMA/water dispersions were carried out with agitation speeds of 220, 300 and 500 rpm. The agitation speed of 220 was the minimum agitation speed at which a thorough dispersion could be achieved for monomer hold up of 0.20.

Mean Drop Size: Figure 3.5.1 shows the time evolution of Sauter mean diameter of daughter drops for this series. The transition stage is expected to elapse earlier with a higher agitation speed (Chatzi et al., 1991). Such a pattern could be observed in the data points for the runs with agitation speeds of 300 and 500.

Another series of experiments was carried out with agitation speed as a variable at PVA concentration of 2.0 g/l. The values of steady-state Sauter mean diameter were obtained from each run and are plotted against agitation speed in *Figure 3.5.2*. On a log-log plot, the data are well correlated with a line of slope –1.0 (i.e., $d_{32} \propto N_I^{-1.0}$).

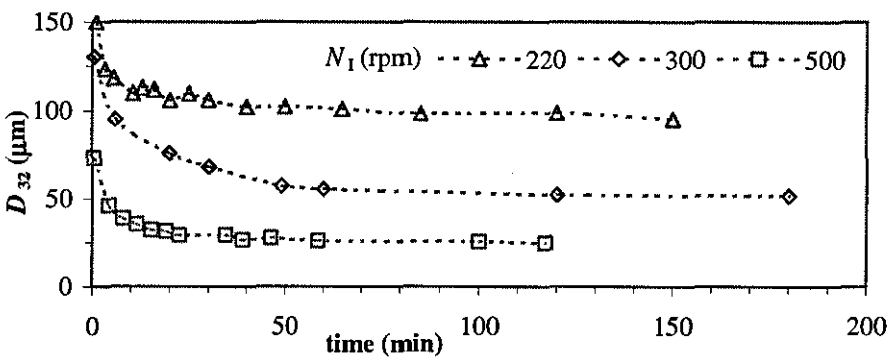

Figure 3.5.1 Variations of Sauter mean diameter of daughter drops with time in dispersions with different agitation speeds (for other conditions see section 3.5.2).

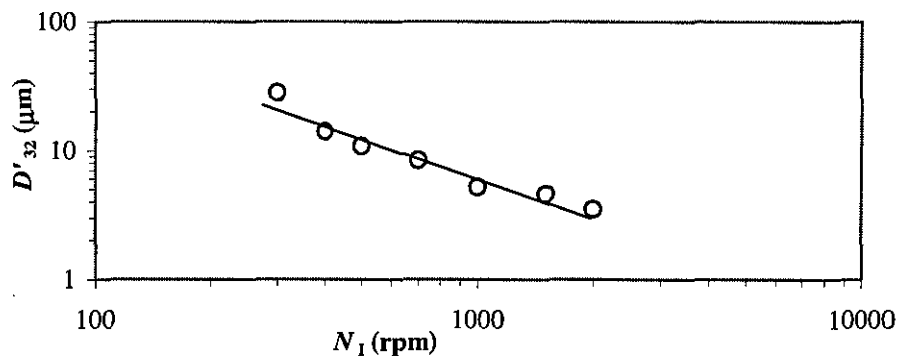

Figure 3.5.2 Variation of steady-state D'_{32} with agitation speed for a series of non-reacting dispersions.

The maximum and minimum stable drop diameters, above or below which drop undergoes break up or coalescence, respectively, have been suggested by Hinze (1955) and Shinnar (1961). Assuming that these boundary values are a linear function of the average size of drops (Sprow, 1967), the following correlations are obtained where K_b and K_c are constants (see equations 1.1.8 and 1.1.12, chapter 1):

$$\frac{d_{32}}{D_I} = K_b N_I^{-1.2} \qquad \textit{Break-up dependent} \qquad (3.5.1)$$

$$\frac{d_{32}}{D_I} = K_c N_I^{-0.75} \qquad \textit{Coalescence dependent} \qquad (3.5.2)$$

From the comparison of the experimental exponent (-1.0) with those above, it can be concluded that both drop break up and coalescence are operative under the condition of this study with the PVA concentration of 2.0 g/l. It is apparent that drop coalescence becomes more predominant as the PVA concentration is reduced (see part 3.1) to 1.0 g/l used for this series.

Drop Size Distribution: In *Figure 3.5.3* the steady-state DSDs (after at least 2 hours from starting the agitation) for this series are shown. *Figure 3.5.4* presents the evolution of drop size distribution with time for the dispersion with the lowest N_I used (220 rpm). Note that the time evolution of DSDs for agitation speeds of 300 and 500 rpm have been previously shown in *Figures 3.4.5* and *3.1.4*, respectively. Daughter drops were continuously reduced in size and narrowed in breadth with time. The shape of DSDs seems to change from a normal distribution at a higher impeller speed to one that is negatively skewed at a lower impeller speed. Volume fraction of satellite droplets (f_{vs}), as shown in *Figure 3.5.5*, increases with time and impeller speed. However, an increase in agitation speed from 220 rpm to 300 rpm did not result in any appreciable increase in f_{vs}.

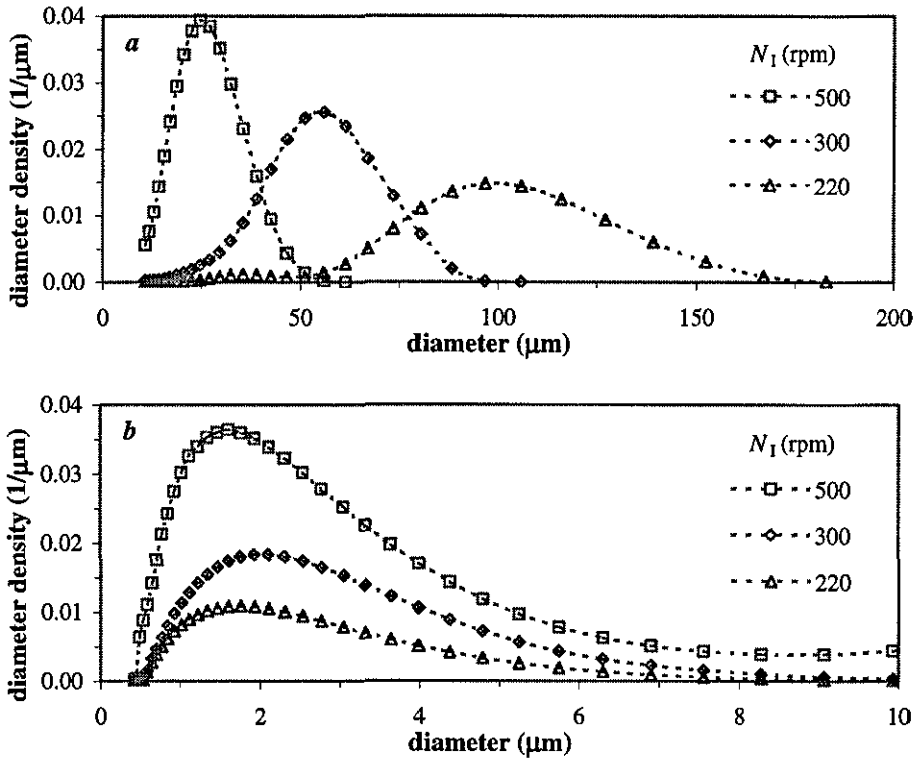

Figure 3.5.3 Final *a*) daughter, and *b*) satellite drop size distributions in dispersions with different agitation speeds.

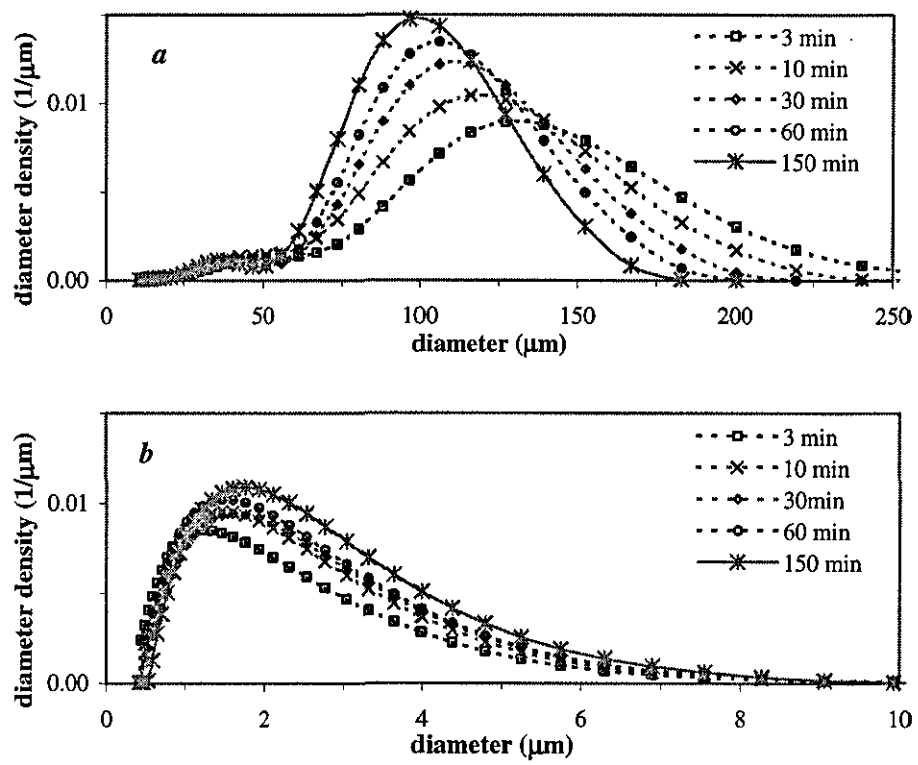

Figure 3.5.4 Time evolution of *a*) daughter, and *b*) satellite drop size distributions for the dispersion with N_I=220 rpm.

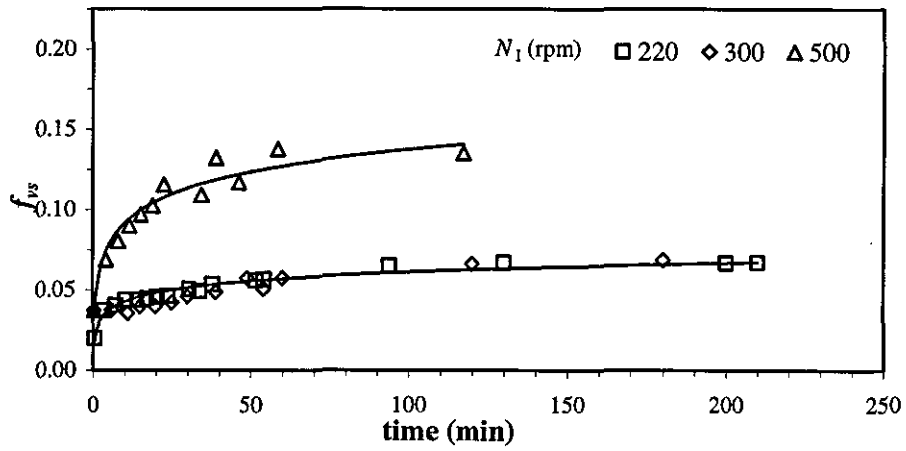

Figure 3.5.5 Time variation of volume fraction of satellite droplets in dispersions with different agitation speeds.

3.5.3.2 Suspension Polymerisation

Suspension polymerisations of MMA were carried out at three agitation speeds of N_I = 220, 300, and 500 rpm.

Rate of Polymerisation: Figure 3.5.6 shows the conversion-time variation for the runs with different impeller speeds. No effect of agitation speed was found on the rate of polymerisation, as was expected.

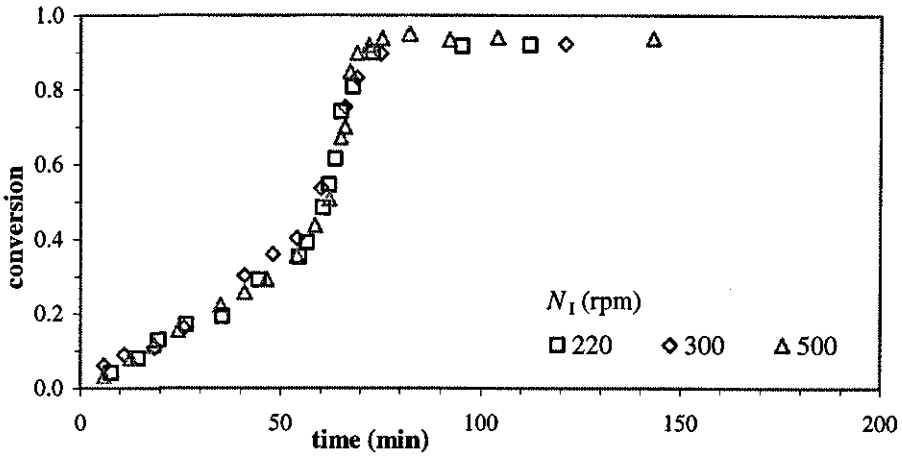

Figure 3.5.6 Conversion-time variations for MMA suspension polymerisation with different agitation speeds (for other conditions see section 3.5.2).

Mean Particle Size: Figure 3.5.7 shows the variations of Sauter mean diameter of daughter drops with time and conversion. Generally, the approach to the steady state lasted longer with an decrease in impeller speed. It is quite interesting to note that the duration of the steady-state stage was shortened with decreasing impeller speed. For N_I = 300 rpm, the steady-state stage was shorter than that for N_I = 500 rpm. For N_I = 220 rpm, the steady-state stage did not exist and the particle growth (growth stage) started just after the transition stage where the minimum appeared. Consequently, the duration of the growth stage was the longest for the lowest agitation speed. The onset of the growth stage occurred approximately at the conversions of about 0.20, 0.40 and 0.60, for N_I = 220, 300, and 500 rpm, respectively. It can be stated that the critical conversion at which the particle growth started, is not a constant and could be affected by the mixing conditions, as well as the viscosity of drops.

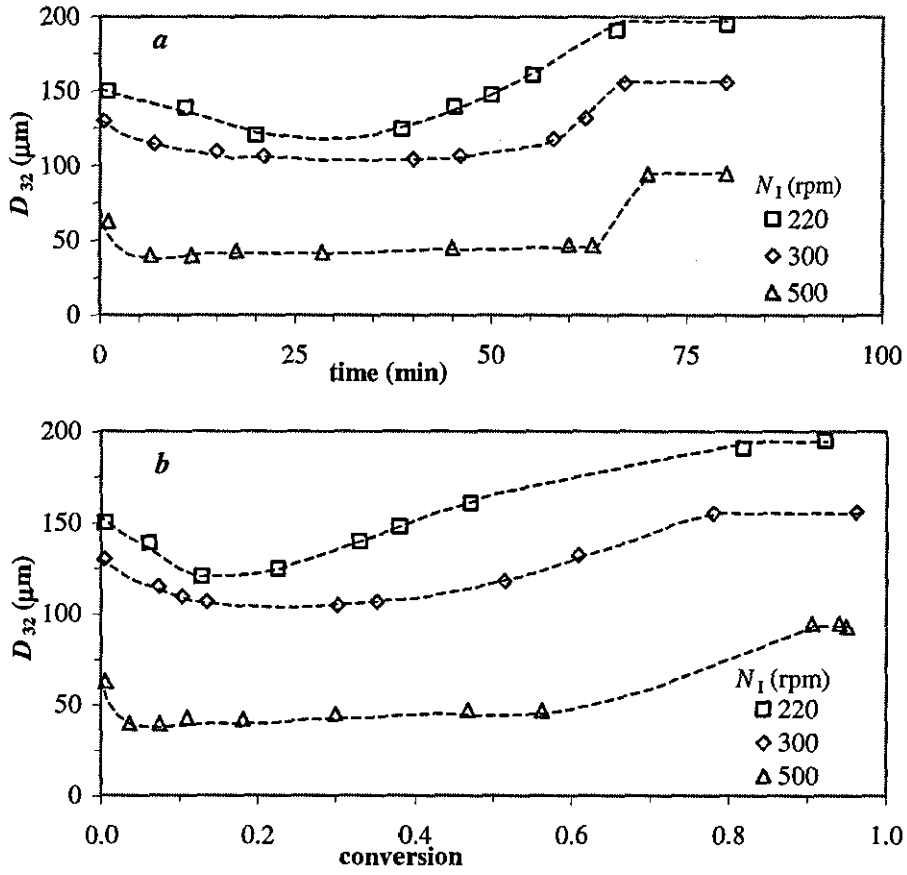

Figure 3.5.7 Variations of Sauter mean diameter of daughter drops with *a*) time, and *b*) conversion for runs with different agitation speeds.

The reason for disappearance of the steady state (for N_I = 220 rpm) is that the rate of drop break up is a strong function of the agitation speed. We should bear in mind that to maintain balance the rate of drop coalescence also increases with agitation speed as more drops are formed. Note that drop/drop collision frequency increases with the agitation speed, but the efficiency of coalescence decreases due to decline in the contact time so that the net result is an increase in the rate of drop coalescence with the agitation speed. The rate of drop break up is highly affected inversely by drop viscosity. At a low agitation speed, with a lower rate of drop break up, an increase in the drop viscosity will lead to an imminent reduction in the rate of drop break up. Therefore, the balance between drop break up and coalescence could not be maintained further and no steady state could be attained. This will result in a gradual enlargement of drops with time and conversion. The balance could be better maintained at higher impeller speed, which allows a quasi-steady state to form.

Particle Size Distribution: Figure 3.5.8 shows a comparison between the PSDs of the final particles for this series. A larger size and a broader distribution were obtained with decreasing impeller speed for daughter particles. *Figure 3.5.9* shows the time evolution of PSD for the experiment with N_I = 220 rpm (the time evolution of PSD for agitation speeds of 300 and 500 rpm have been previously shown in *Figures 3.4.13* and *3.1.12*, respectively). Similar trends to those previously explained for the dispersions, are observed here for the large particles.

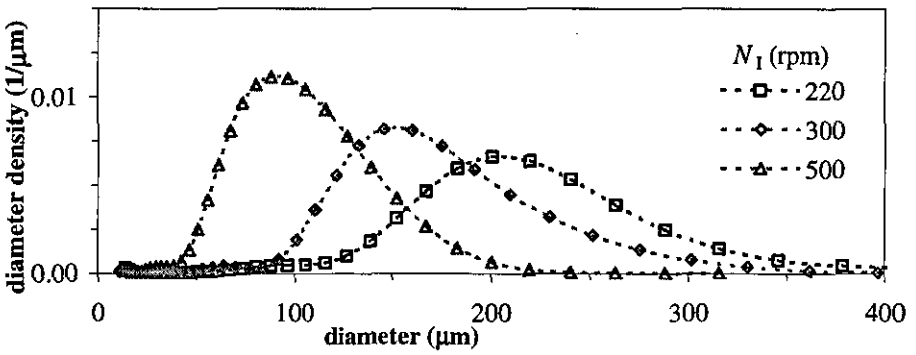

Figure 3.5.8 Final PSDs for runs with different agitation speeds.

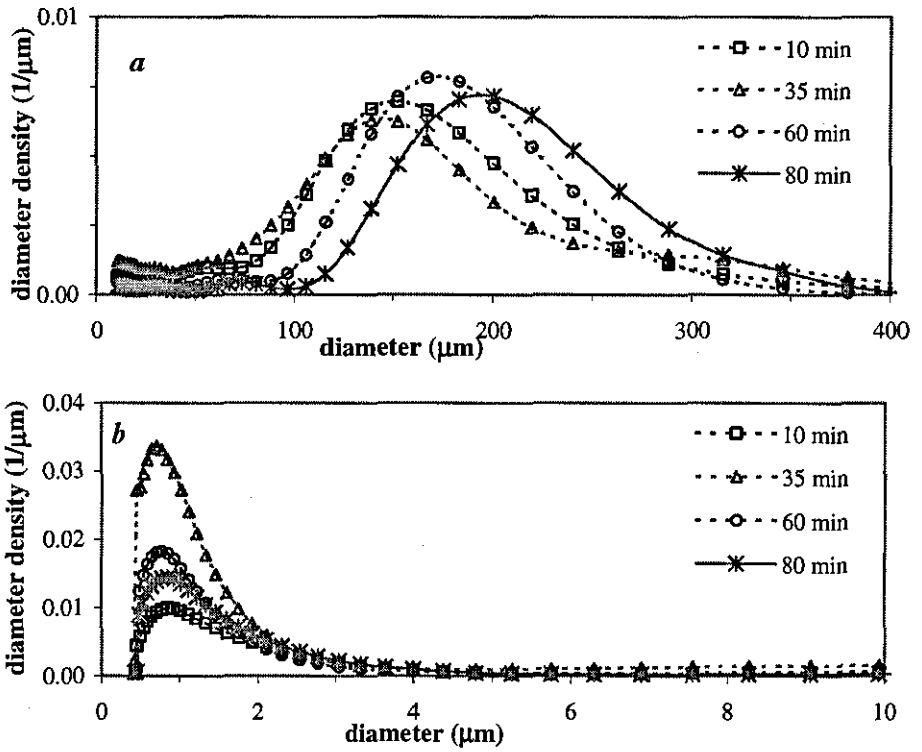

Figure 3.5.9 Time evolution of *a*) daughter, and *b*) satellite PSDs for the run with N_I = 220 rpm.

Figure 3.5.10 shows the time evolution of the volume fraction of satellite droplets (f_{vs}) for the suspension polymerisations with different agitation speeds. The transient formation of satelite droplets increased with stirring speed, similar to the results obtained for the dispersion process. Generally, the formation of satelite droplets/particles can be correlated with the duration of the steady state. The loss of satelite particles occured when particles entered the growth stage. This occured at different time and conversions for different agitation speeds. However, all runs ended more or less with the same volume fraction of the satellite droplets because of coaggulation during the growth stage.

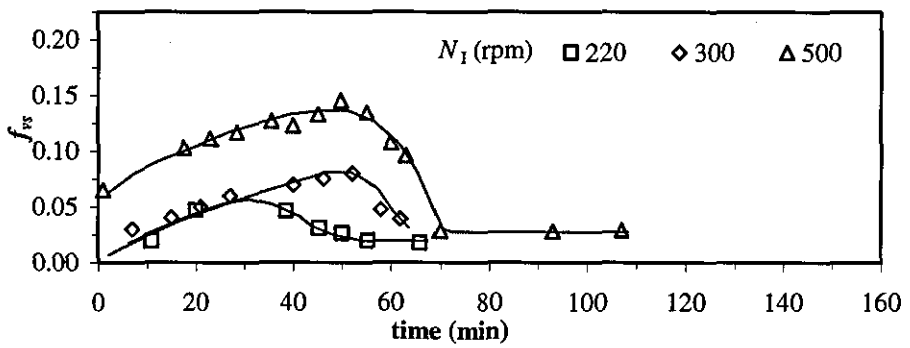

Figure 3.5.10 Time variation of volume fraction of satellite droplets in polymerisations with different agitation speeds.

3.5.3.3 Suspension Polymerisation versus Non-reacting Dispersion

Mean Drop/Particle Size: Figure 3.5.11 compares the time evolution of D_{32} in suspension polymerisations and in the corresponding dispersions for two agitation speeds of 300 and 500 rpm. The approach to steady state was short when a high agitation speed was used. As a result, the evolution of D_{32} during the transition period for both dispersion and polymerisation processes was very similar. In fact, drops are reduced to small sizes quickly enough at a high agitation speed before their viscosity starts to increase appreciably as a result of ongoing polymerisation reaction. However, a difference gradually develops as polymerisation proceeds.

Figure 3.5.12 shows the variations of D_{32} of the final polymer particles from the suspension polymerisations and that of the steady-state drops from the non-reacting dispersions with agitation speed. The difference between drops from the two processes narrows with a stirring speed increase within the range of study.

Drop/Particle Size Distribution: Figure 3.5.13 compares the evolution of size distributions for the two processes for the runs with N_I = 300 and 500 rpm. At the higher agitation speed, the difference between the size distributions of drops from the two processes was small, but later grew with time. For the lower impeller speed, the difference in the size distributions appeared to be appreciable even in the initial stage of mixing. The gap became wider with time.

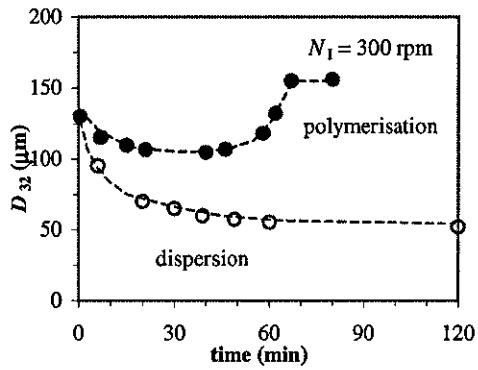

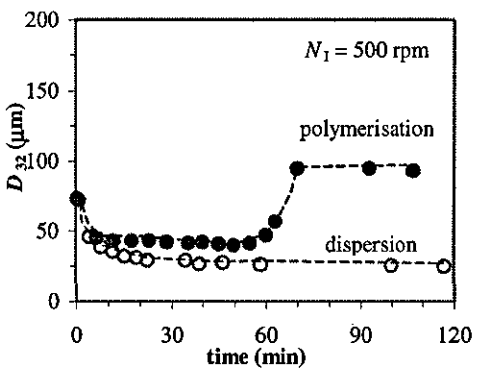

Figure 3.5.11 Time variation of Sauter mean diameter of daughter drops in suspension polymerisations and the corresponding dispersions with different agitation speeds.

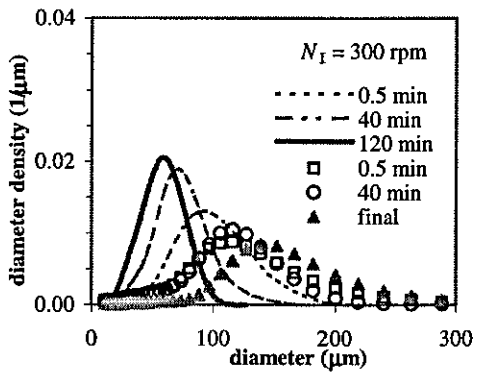

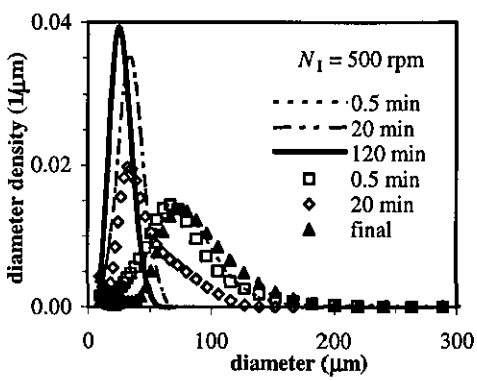

Figure 3.5.13 Comparison of time evolution of DSD/PSD in polymerisation systems and the corresponding dispersions with different agitation speeds. Graphs with symbols represent the polymerisation.

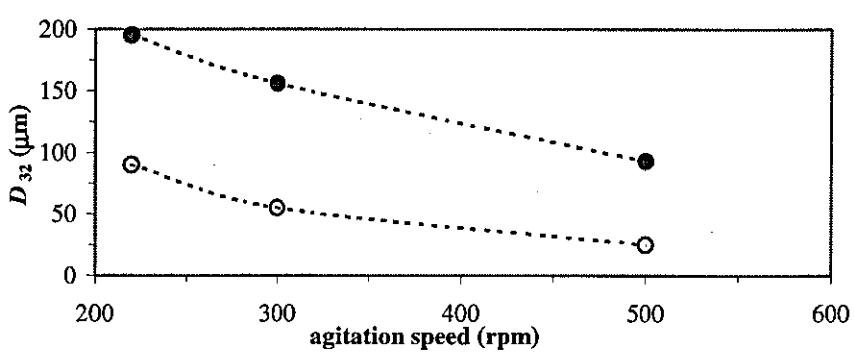

Figure 3.5.12 Variation of Sauter mean diameter with agitation speed for suspension polymerisations (full symbols) and the corresponding dispersions (empty symbols).

3.5.4 CONCLUSIONS

The following major conclusions can be made:

- Drop coalescence was found to be important under the conditions of this study even when a PVA concentration of 2.0 g/l was used.

- For both dispersion and polymerising processes, the size of final drops/particles decreased with an increase in agitation speed within the range studied.

- A high agitation speed decreases the time required to reach the steady state, and thus eliminates or alleviates the influence of viscosity increase, in association with the polymerisation reaction, on the size of drops. This may lead to a similar evolution of drop sizes in a suspension polymerisaion and the corresponding non-reacting dispersion in the early reaction and during the transition stage in particular.

- The duration of the so-called steady-state stage was prolonged with increase in the agitation speed. The rate of drop break up is highly affected by drop viscosity at a low agitation speed. As a result, the quasi steady state could be better maintained at a higher impeller speed. At a low agitation speed, there was no quasi steady state.

3.6 EFFECT OF MMA HOLD UP

3.6.1 INTRODUCTION

It is always desired in industry to increase the output of manufacturing units at minimum cost. In suspension polymerisation processes this target is usually met by increasing the monomer hold up. The increase in monomer hold up, however, destabilises the particles and also increases the possibility of thermal runaway. Therefore, a careful examination of interaction of parameters involved in suspension polymerisation reactors is required.

The maximum stable drop diameter, above which the drop undergoes a break up, for inviscid and low hold up dispersions (negligible coalescence) is (see equation 1.1.8, chapter 1) (Hinze, 1955):

$$\frac{d_{\max}}{D_I} = K_1 We^{-3/5} = K_2 N_I^{-1.2} \qquad (3.6.1)$$

The minimum stable drop diameter below which the drop will coalesce has been shown to be (see equation 1.1.12, chapter 1) (Shinnar, 1961):

$$\frac{d_{min}}{D_I} = K_3 We^{-3/8} = K_4 N_I^{-0.75} \qquad (3.6.2)$$

Any drop within the size range of $d_{min} < d < d_{max}$, thus, is expected to be stable. Sprow (1967) assumed, and also verified within experimentation, that d_{32} is proportional to d_{max}. So:

$$d_{32} = K_5 d_{max} = K_6 We^{-3/5} = K_7 N_I^{-1.2} \qquad (3.6.3)$$

This approach, which correlates d_{32} with the mixing conditions, has been used by many investigators since then. The application of this correlation, however, has been

questioned by some investigators in recent years (Pacek yet al., 1998; Zhou and Kresta, 1998). Generally, in a liquid-liquid dispersion with increasing the volume fraction of dispersed phase (ϕ_d) the mean particle size increases. Increase in ϕ_d increases the dispersion viscosity and thus damps the turbulence of the system, and also increases the collision frequency of dispersed drops. All these result in an increase in mean drop size (Doulah, 1975; Park and Blair, 1975; Delichatsios and Probstein, 1976; Lagisetty et al., 1986; Nishikawa et al., 1987; Kumar et al., 1991). In order to accommodate such an effect in the prediction, a following general form has been used (Calderbank, 1958; Brown and Pitt, 1970; Coulaloglou and Tavralides, 1976; Van Heuven and Beek, 1971; Mlynek and Resnick, 1972; Godfrey and Grilc, 1984; Lagisetty et al., 1986):

$$\frac{d_{32}}{D_I} = a(1 + b\phi_d)We^{-0.60} \qquad (3.6.4)$$

Similar correlations, which used different exponents for ϕ_d, have been also suggested (Nishikawa et al, 1987).

For suspension polymerisation, however, d_{32} is a complex function of mixing conditions as well as the kinetics of polymerisation. Several investigators have studied the effect of monomer hold up in suspension polymerisation on the final polymer particle size (Konno et al., 1982; Kalfas et al., 1993; Alvarez et al., 1994; Lazrak et al., 1998). All studies show that the final average particle size increases with monomer hold up.

In this section the effect of dispersed phase hold up on the kinetics and the evolution of PSD in the suspension polymerisation of MMA has been studied. The results have been also compared with those from corresponding non-reacting MMA/water dispersions.

3.6.2 EXPERIMENTAL

The materials, experimental procedure and measurements have been described in details in Chapter 2. All experiments in this series were carried out at 70°C and agitation speed of 300 rpm. LPO and PVA concentrations were 1.0 wt% (based on

monomer) and 1.0 g/l (based on water), respectively. Different MMA hold ups were used for suspension polymerisation runs (ϕ_d = 0.025, 0.05, 0.10, 0.20, 0.30, and 0.40) and non-reacting dispersion runs (ϕ_d = 0.05, 0.20, and 0.40).

Gas-liquid chromatography was used to determine the equilibrium MMA concentration in the aqueous phase. Details of the measurements are given in Chapter 2.

3.6.3 Results and Discussion

3.6.3.1 Non-reacting Liquid-Liquid Dispersion

Mean Drop Size: Figure 3.6.1 shows the time evolution of the Sauter mean diameter of drops (D_{32}) in non-reacting MMA/water dispersions for different values of ϕ_d. A larger drop size was obtained with increasing ϕ_d due to collisions of drops. The increased rate of drop coalescence balances the rate of drop break up earlier, thus a shorter transition stage was obtained.

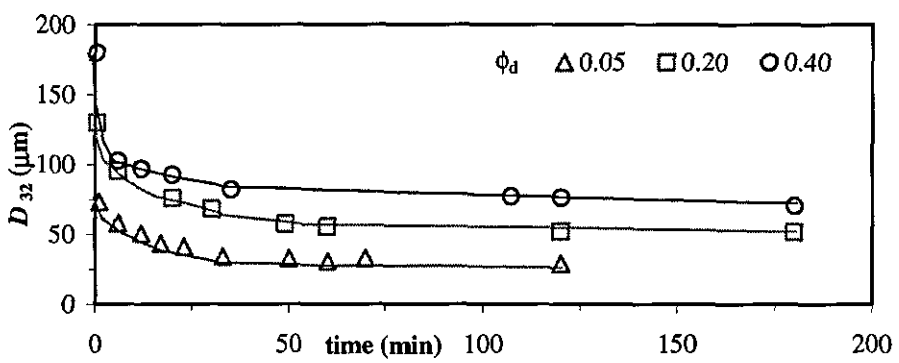

Figure 3.6.1 Time variations of Sauter mean diameter of daughter drops for dispersions with different MMA hold ups (for conditions see section 3.6.2).

If the experimental overall Sauter mean diameter (D'_{32}) is fitted with equation 3.6.4, the values of constants are obtained as follows: a = 0.022, and b = 3.55. The constant a, which depends on the experimental conditions and set up, is within the range given in the literature. According to the literature, a value of b close to 3.0 is representative of turbulence damping (Brown and Pitt, 1974; Doulah, 1975), and a value of b larger than 3 and up to 10 is indicator of coalescence (Davies, 1972; Godfrey et al. 1987; 1989). The result suggests that both turbulent damping and drop coalescence contribute to the rise in the drop size with ϕ_d. This implies that at the stabiliser level used, the dispersion

is within the coalescence operative region, but not the coalescence dominating region, where the size of drops is determined by a dynamic balance between drop break up and coalescence.

A point worthy of attention here is that the interfacial area expands with a rise in the volume fraction of the dispersed phase. At high-dispersed phase volume fractions the collision between drops is frequent. The coalescence efficiency of drops (with a certain size), however, is not affected by the hold-up for pure liquid-liquid dispersions. In the presence of (a fixed concentration of) a stabiliser, drops become less protected with a hold up increase as the coverage of the drops with the stabiliser falls. This may lead to an increase in the coalescence efficiency of drops. This implies that for stabilised dispersions, a rise in the hold up would enhance both the collision rate and the drop coalescence efficiency. However, the effect is still not as extensive as that for pure liquid-liquid dispersions because of the drop stability provided by stabilisers.

Drop Size Distribution: The steady-state drop size distributions are compared in *Figure 3.6.2* for different values of ϕ_d. The application of a larger amount of monomer resulted in the broadening of size distribution of daughter drops in association with an increase in the average size of drops. The population of satellite droplets increased with decreasing monomer hold up. The reduction in the population of the satellite droplets at a high hold up is a result of a high rate of drop collision with subsequent coalescence. However, the rate of droplet coalescence was not high enough to eliminate the peak of satellite droplets.

Figures 3.6.3 and *3.6.4* demonstrate the time evolution of drop size distribution for the dispersions with the maximum and minimum ϕ_d values used; namely 0.05 and 0.40, respectively (the same graph for $\phi_d = 0.20$ has been shown in *Figure 3.4.5*). Similar to the results previously described, the DSDs continuously narrowed and shifted to a lower size with time. The peaks for the satellite droplets were dilated with time indicating that these small droplets were continuously formed during mixing, particularly for lower ϕ_d values where drop break up is dominant.

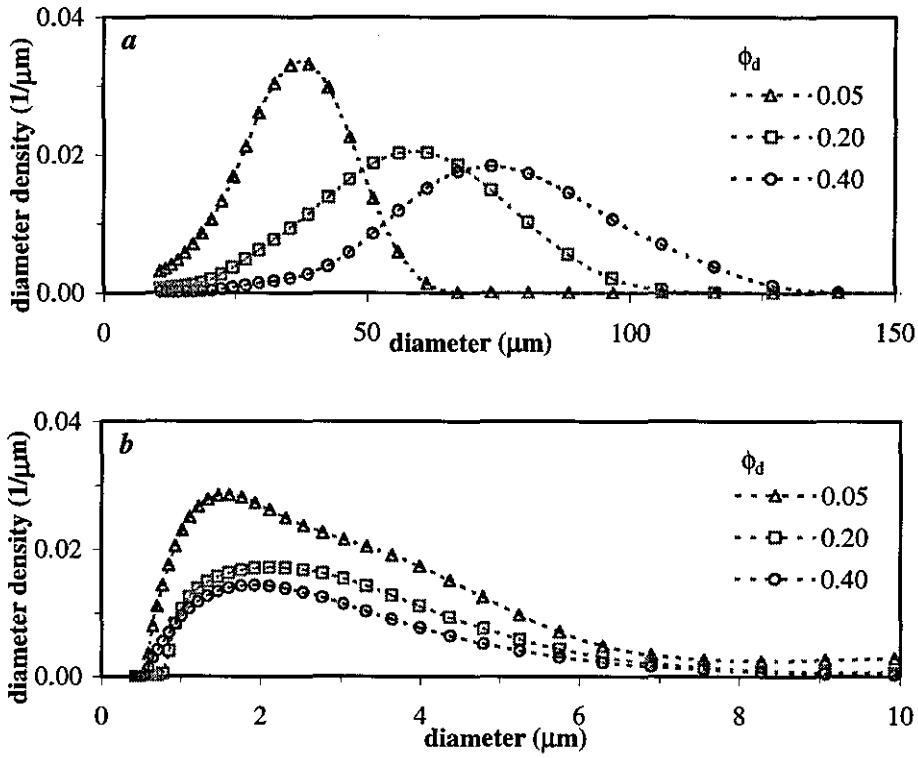

Figure 3.6.2 Steady-state *a*) daughter, and *b*) satellite drop size distributions for dispersions with different MMA hold ups.

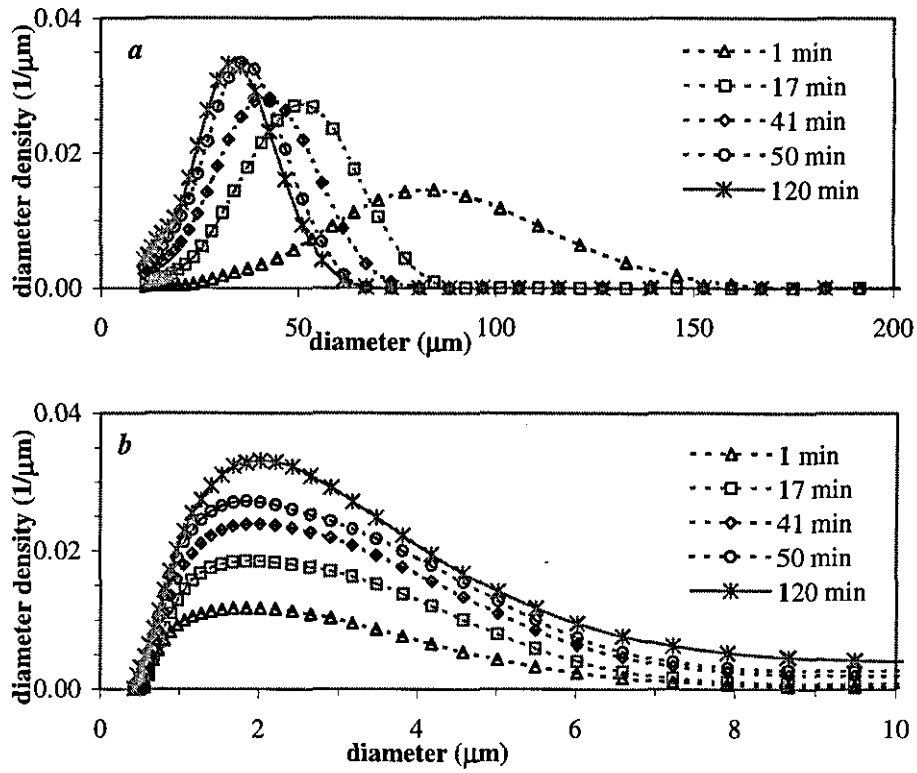

Figure 3.6.3 Evolution of *a*) daughter, and *b*) satellite drop size distributions for the dispersion with $\phi_d = 0.05$.

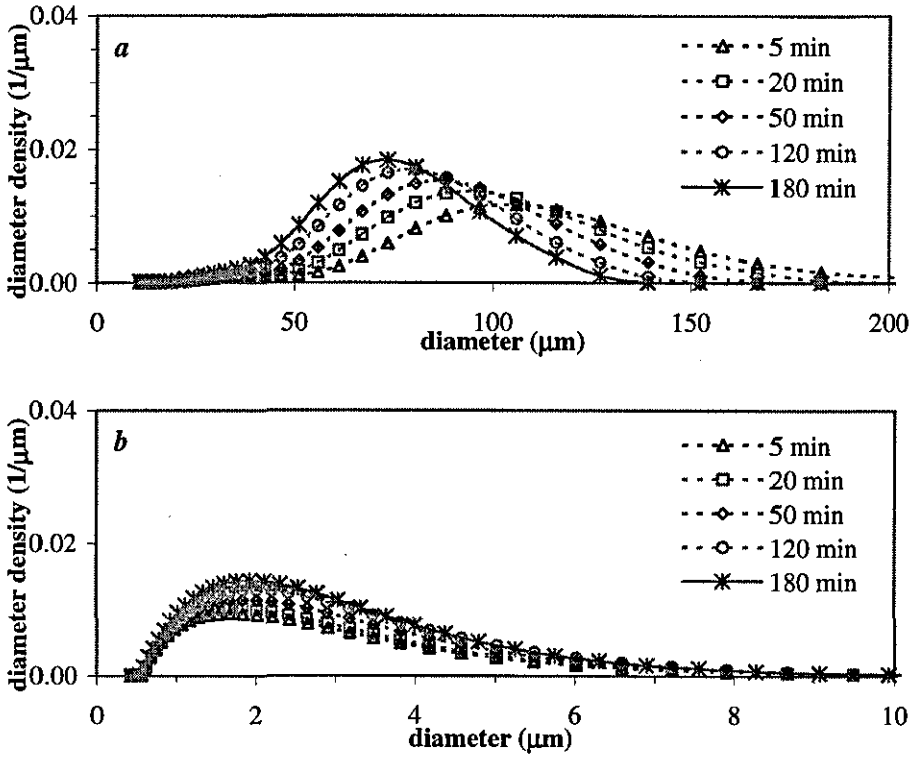

Figure 3.6.4 Evolution of *a*) daughter, and *b*) satellite drop size distributions for the dispersion with $\phi_d = 0.40$.

3.6.3.2 Suspension Polymerisation

In this series suspension polymerisations with different MMA volume fractions (0.025, 0.05, 0.10, 0.20, 0.30, and 0.40) were carried out.

Rate of Polymerisation: Figure 3.6.5 shows the conversion-time variation for the runs with different monomer hold ups. The rate of polymerisation can be better described if the following conversion ranges are considered:

Initial stage: The initial rate of polymerisation shows an increase with increasing monomer hold up. MMA has a high water solubility; 1.6 wt% at 70°C (Kalfas et al., 1993). The initial monomer in the reactor saturates the water phase. This reduces the amount of monomer available in the monomer droplets. Knowing that the locus of polymerisation in suspension polymerisation is in fact the monomer drop phase, and assuming that the polymerisation of MMA in the water phase is negligible, the rate of polymerisation is expected to decrease with decreasing ϕ_d. For $\phi_d = 0.025$, 60% of

the initial monomer is dissolved in the water phase and is absent from the locus of polymerisation. Obviously, the rate of polymerisation was mostly affected for this case. For ϕ_d = 0.05, polymerisation still started with 30% of the initial monomer charge in the water phase, and so the rate of polymerisation was consequently affected. With higher ϕ_d values, the initial rate of polymerisation became less affected by ϕ_d.

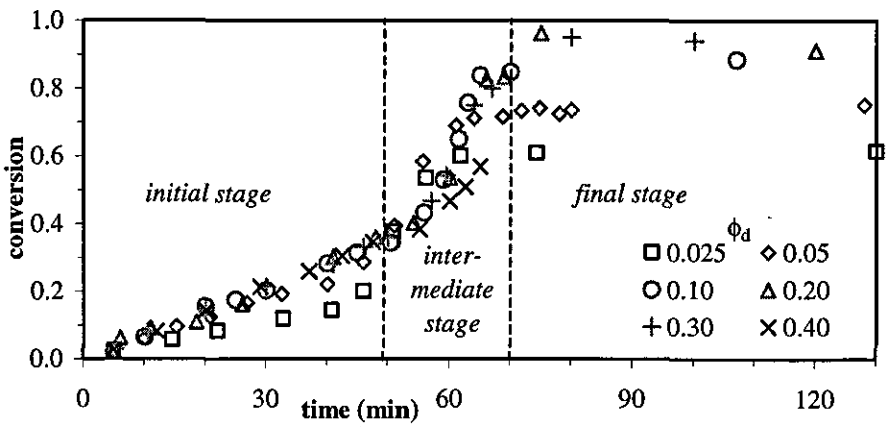

Figure 3.6.5 Conversion-time variations for runs with different MMA hold ups (for other conditions see section 3.6.2).

Intermediate stage: This stage, which covers the gel effect, appears at different conversions according to the ϕ_d used. For the higher values of ϕ_d, the gel effect started at conversion of 0.40, which corresponds to the onset of the gel effect for MMA bulk polymerisation. With decreasing ϕ_d, the onset of the gel effect is shifted towards a lower conversion. For ϕ_d = 0.025, for example, the gel effect started at a conversion of 0.20. It should be noted that the onset of the gel effect depends on the monomer conversion inside the drops and not on the reactor monomer conversion. This means that for all polymerisations, it is expected that the onset of the gel effect occurs at x = 0.40, despite different values for the corresponding overall conversion.

Final stage: Generally a lower final conversion was achieved for the lower ϕ_d. This again is a result of monomer partitioning between monomer drops and water phase. As the polymerisation reaches higher conversions in the particles, however, the monomer dissolved in the water phase slowly diffuses into the polymer particles and

reacts there. This effect is more significant for the lower ϕ_d. The measurement of conversion for ϕ_d =0.40 was hampered by gross coagulation of particles, as is explained later.

Monomer Partitioning: As stated above, monomer partitioning in the water phase may play an important role in the kinetics of polymerisations particularly with low values of ϕ_d. *Figure 3.6.6* shows the variations in MMA concentration in the aqueous phase with time and conversion in the suspension polymerisations with ϕ_d = 0.10 and 0.30. Both systems behaved similarly with no apparent difference. Initially MMA concentration in water gradually decreased with time (and conversion) from about 1.6 wt%, which is the equilibrium solubility of MMA in water at 70°C, because of diffusion of monomer molecules from the water phase into the polymerising drops. Monomer transport occurs to maintain the thermodynamic equilibrium between phases as a result of conversion of monomer to polymer in the polymerising drops. The rate of monomer conversion increased significantly after about 55 minutes (corresponding to a conversion of 0.40) due to the gel effect. As a result, monomer molecules migrated from the water phase to the polymer/monomer drops in order to maintain the equilibrium. This led to a sudden drop in the MMA concentration in the water phase. As the conversion reached higher values, the MMA concentration in the water phase dropped to a value as low as 0.2 wt%. Monomer transport at this stage was quite slow due to solidification of polymer particles.

Mean Particle Size: Figures 3.6.7 compares the variation in the Sauter mean diameter of daughter drops with time and conversion for different values of ϕ_d. The general pattern is that the final size of particles increased with ϕ_d. The extent of variation in D_{32} with ϕ_d is more than what turbulence damping can allow for. This implies that drop coalescence is quite important at the conditions of this study, as confirmed in the experiments with non-reactive MMA/water dispersion system. Now we look at the variations of D_{32} in different time intervals.

A lower average size of particles was obtained at the end of the transition stage for the lower values of ϕ_d, similar to the results shown for non-reacting MMA/water dispersions. This is because the steady-state drop size increases with hold up as a result of increase in drop encounters.

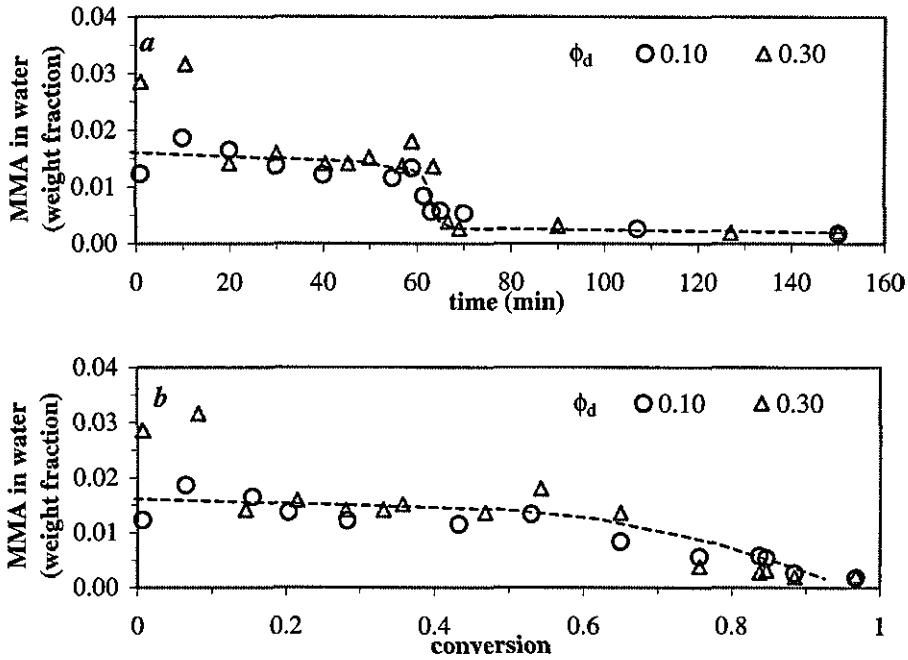

Figure 3.6.6 Variations of MMA concentration in the aqueous phase with *a*) time, and *b*) conversion for suspension polymerisations with two different MMA hold ups.

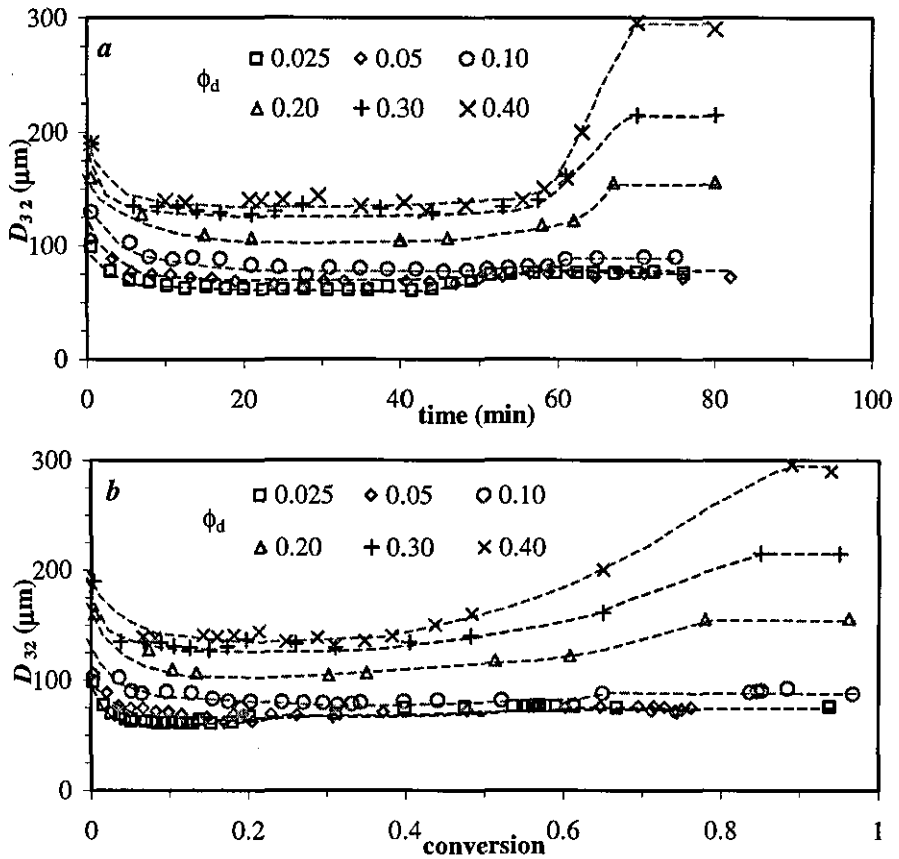

Figure 3.6.7 Variations of Sauter mean diameter of daughter drops with *a*) time, and *b*) conversion for runs with different MMA hold ups.

The drop size showed a slight rise with time with lower values of ϕ_d, but showed an appreciable increase in the beginning of the gel effect for the runs with higher values of ϕ_d. For the lowest values of ϕ_d used, 0.025 and 0.05, the critical conversion at which drop enlargement occurred was around the value of 0.20, which corresponds to the onset of the gel effect for these runs as mentioned above. Except for the two lowest ϕ_d used, the conversion range for the quasi-steady state stage seems to narrow with increasing ϕ_d (see *Figure 3.6.7b*). This implies that with an enhancement of the rate of drop coalescence with a ϕ_d increase, the balance between drop break up and coalescence is perturbed earlier and drops enter the growth phase. The results suggest that the onset of the growth stage is advanced with increasing ϕ_d. For the highest ϕ_d used, 0.40, particle coalescence occurred extensively at $x = 0.45$ leading to the formation of some polymer lumps.

Particle Size Distribution: The PSDs of final particles are compared in *Figure 3.6.8*. For lower ϕ_d values, 0.025 and 0.05, rather sharp final PSDs were obtained. Whereas for the higher values of ϕ_d, 0.20-0.40, positively skewed PSDs were obtained as a result of increased particle coalescence with ϕ_d. Generally, the size distribution broadened with increasing ϕ_d.

Figures 3.6.9 and *3.6.10* show the time evolution of PSD for the runs with extreme ϕ_d values of 0.025 and 0.40, respectively (the same graph for $\phi_d = 0.20$ has been shown in *Figure 3.4.13*). Similar to the results presented before, the PSDs of all suspensions showed a peak for satellite particles. All PSDs continuously broadened with time. A high rate of particle size broadening occurred during the growth stage for all runs with an intensity increasing with ϕ_d. It is quite interesting to note that particle size distribution broadened with time in the course of polymerisation even for the run with $\phi_d = 0.025$.

Figure 3.6.9b shows that for the lower ϕ_d, the PSD peaks for the satellite droplets reached their steady-state configuration quite early. This is because the small monomer drops formed at low ϕ_d values could not be further broken into satellite droplets. At the higher values of ϕ_d, the satellite droplets were continuously formed during polymerisation.

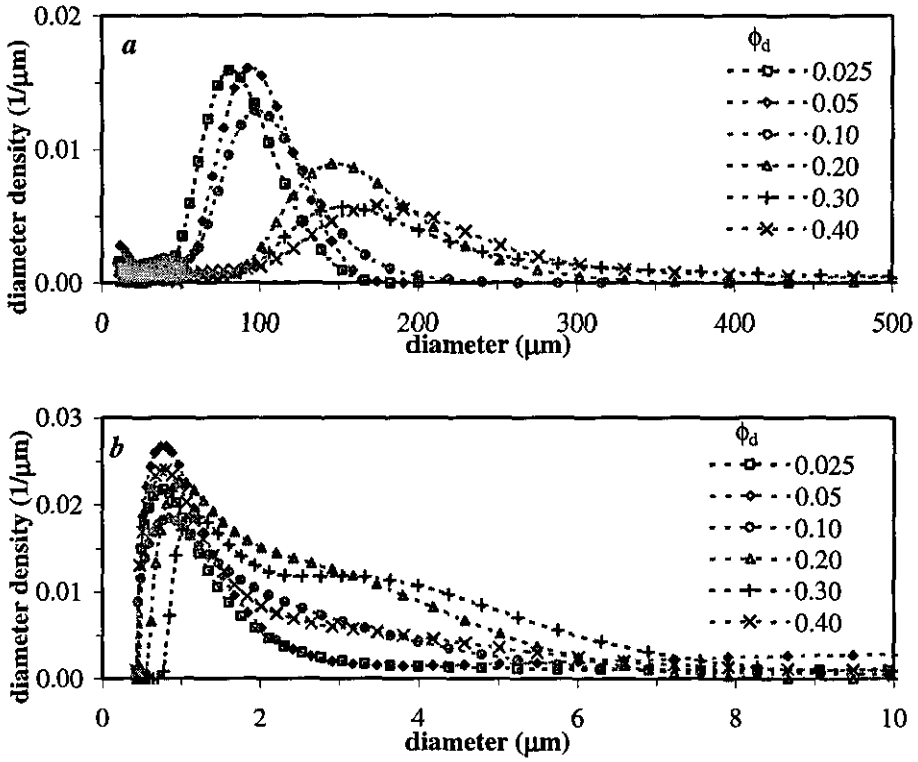

Figure 3.6.8 Final *a*) daughter, and *b*) satellite PSDs for runs with different MMA hold ups.

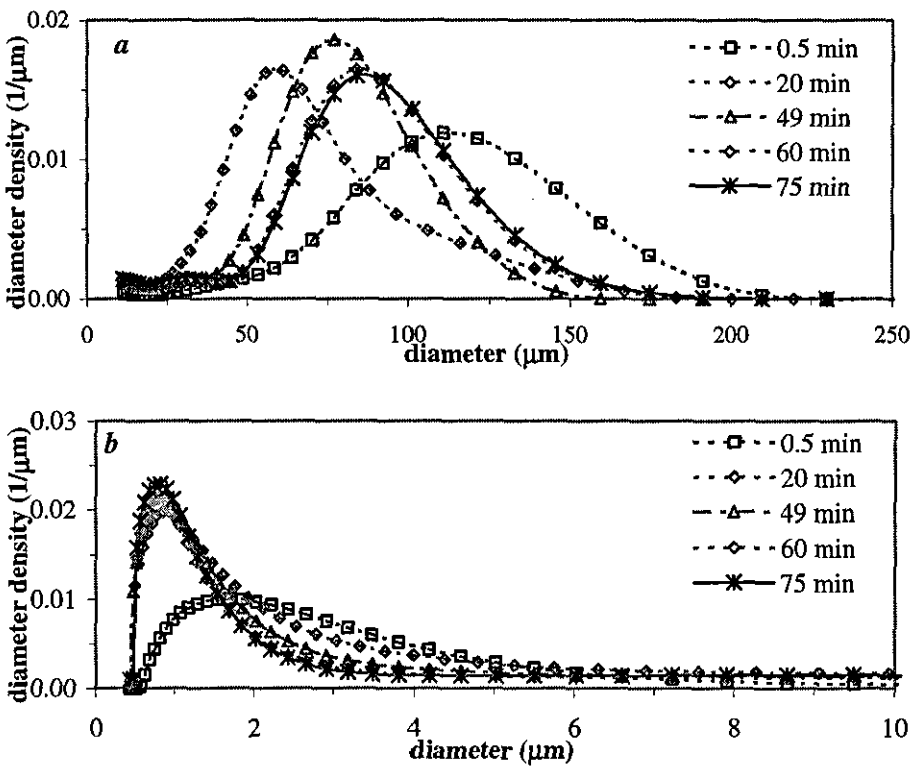

Figure 3.6.9 Variations of *a*) daughter, and *b*) satellite PSDs with time for the run with $\phi_d = 0.025$.

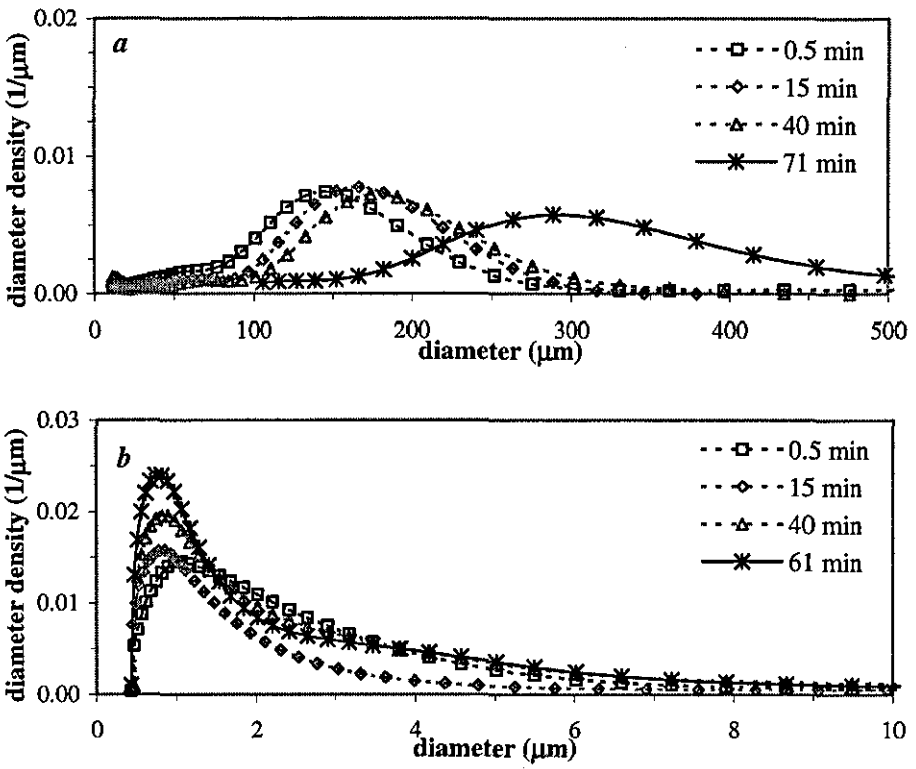

Figure 3.6.10 Variations of *a*) daughter, and *b*) satellite PSDs with time for the run with $\phi_d = 0.40$.

3.6.3.3 Suspension Polymerisation versus Non-reacting Dispersion

Mean Drop/Particle Size: Figure 3.6.11 compares the time evolution of the Sauter mean diameter of daughter drops in suspension polymerisations and the corresponding MMA/water dispersions with different MMA hold ups. The difference between the drop sizes in the two processes developed with time during the transition stage and steady-state stage and reached its maximum at the end.

Figure 3.6.12 compares the final size of particles (or drops) from the two processes. The quasi steady-state size of particles for the polymerisation experiments is also shown on the graph. The difference between the steady-state size of particles and drops, from the two processes, increased gradually with ϕ_d. The difference between the final size of particles and drops, from the two processes, increased with ϕ_d as a result of increasing drop instability in the suspension polymerisation.

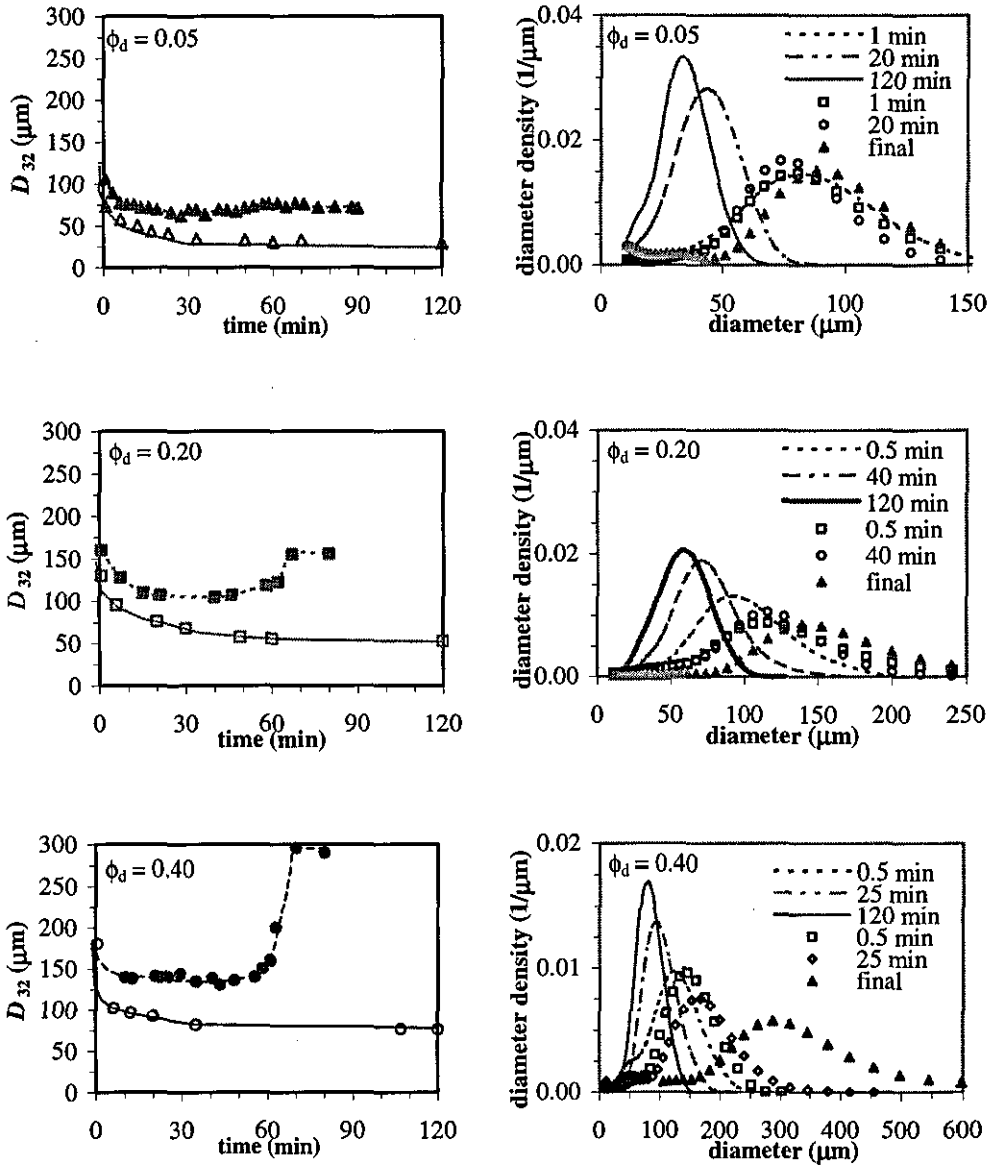

Figure 3.6.11 Comparison of time variations of Sauter mean diameter of daughter drops for dispersions (empty symbols) and corresponding suspension polymerisation (full symbols) with different MMA hold ups.

Figure 3.6.13 Comparison of time evolution of DSD/PSD in polymerisation systems and in the corresponding dispersions with different MMA hold ups. Graphs with symbols represent the polymerisation.

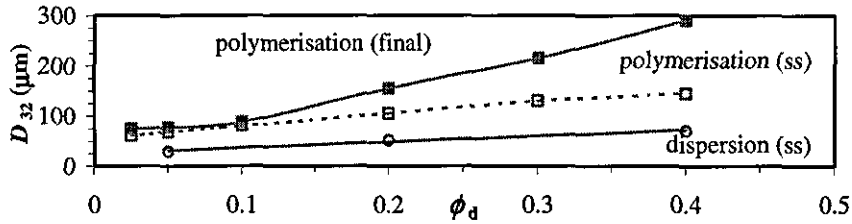

Figure 3.6.12 Variations of final and steady-state D_{32} in suspension polymerisations and steady-state D_{32} in some of the corresponding dispersions with MMA hold up ("ss" stands for "steady-state").

Drop/Particle Size Distribution: Figure 3.6.13 compares the evolution of particle/drop size distribution for ϕ_d values of 0.05, 0.20, and 0.40 in the two processes. The match between the data from the two processes is quite close in the initial stages. As reaction proceeds, the distance between distribution of drops and particles at a fixed time grows. For higher ϕ_d values, the difference escalates as the reaction proceeds to the gel effect region because of the instability caused by frequent collisions of polymerising drops. For lower values of ϕ_d, the difference freezes because of relative stability of the polymerising drops due to more coverage by the stabiliser and also because of less frequent collision.

3.6.4 CONCLUSIONS

The main conclusions are:

- The final size of drops/particles increased with ϕ_d.
- From the variation of the Sauter mean diameter with ϕ_d in the dispersion process, it can be stated that the size of drops is determined by a dynamic equilibrium between drop break up and coalescence. This implies that coalescence occurs in the system under study.
- Changes in the growth stage were more drastic with increasing monomer hold up (at a constant stabiliser concentration in water phase) due to an increased coalescence efficiency and rate of drop encounters leading to higher rate of coalescence.
- The monomer partitioning can affect the kinetics of polymerisation particularly at low values of monomer hold up.
- The boundaries of the so-called quasi-steady state, in terms of time and conversion, vary with monomer hold up. Except for the low values of ϕ_d, where the monomer solubility in the water phase significantly affects the kinetics of the polymerisation, the balance between drop break up and coalescence was maintained longer in terms of conversion with decreasing ϕ_d.
- The difference between the final size average and distribution of drops/particles from dispersion and suspension polymerisation is the least when a low monomer hold up is used.

CHAPTER FOUR

MATHEMATICAL MODELLING

INTRODUCTION

In a suspension polymerisation reactor the evolution of particle size distribution is the result of interactions of the mixing conditions and the kinetics of the polymerisation reactions that lead to the viscosity build up in the polymerising drops. Therefore, mathematical modelling of particle size distribution in suspension polymerisation processes should account for both the mixing parameters and the kinetic and rheological behaviour of the system.

Mathematical modelling of the kinetics of polymerisation reactions has been more understood and investigated in comparison with that of mixing phenomena such as drop break up and coalescence and their relation with viscoelastic properties of drops, non-homogenous flow and with the rate of energy dissipation in the reactor. In this regard modelling of non-homogeneous turbulent flow has become the most challenging aspect of modelling of suspension polymerisation reactors in the recent years. Compartment-mixing models and complex CFD simulations have been used to model the nonhomogeneity of the system (Vivaldo-Lima et al., 1998; Alopaeus et al., 1999; Maggioris et al., 1998 and 2000). For a literature review on modelling of suspension polymerisations see part 3.1, chapter 1.

The model developed in this research consists of two main parts; the kinetic model and the population balance model. The kinetic model predicts the time evolution of conversion and the polymer average molecular weights using the method of moments. The viscosity and the elasticity of the monomer/polymer mixture are predicted using the appropriate correlations. The population balance model assumes, at the first step, a homogeneous environment for simplicity and predicts the drop/particle size distribution and average particle size. The rates of drop break up and coalescence are predicted

using the model presented by Alvarez et al. (1994), which considers the viscoelastic properties of the monomer/polymer mixture assuming a Maxwell body-type fluid.

Other parts of the model include prediction of monomer concentration in the aqueous phase using the Flory-Huggins theory, and the stabiliser partitioning between the aqueous phase and the water/drop interface using Langmuir-type interfacial adsorption for PVA.

In this chapter the different parts of the model are presented first and then the numerical solutions are discussed. The model predictions will be tested against experimental data.

4.1 POPULATION BALANCE MODELLING (PBM)

In the developed model the evaluation of drop volume distribution has been carried out by numerical solution of the population balance equation for dispersed drops, which is an integro-differential equation. The population balance equation may be given in terms of drop volume (see Equation 1.3.16). It is more desirable, however, to write this equation in terms of drop diameter using $dv=(\pi/2)(6/\pi)^{2/3}v^{2/3}d(d_v)$:

$$\frac{dF(d_v,t)}{dt} = (\pi/2)(6/\pi)^{2/3}v^{2/3}\int_{d_v}^{d_{v_{max}}} b(v')\beta(v',v)u(v')F(d_{v'},t)d(d_{v'})$$
$$-b(v)F(d_v,t)+v^{2/3}\int_{d_{v_{min}}}^{d_{v/2}} c(v-v',v')F(d_{v-v'},t)F(d_{v'},t)d(d_{v'}) \qquad (4.1.1)$$
$$-F(d_v,t)\int_{d_{v_{min}}}^{d_{v_{max}}-v} c(v,v')F(d_{v'},t)d(d_{v'})$$

$\beta(v',v)$, the daughter drop volume distribution, can be assumed approximately by a normal distribution about a mean value $\bar{v}$ since it is the combined result of a large number of independent random events (see equation 1.3.17):

$$\beta(v',v) = 1/(\sigma_v\sqrt{2\pi})\exp\{-(v-\bar{v})^2/(2\sigma_v^2)\} \qquad (4.1.2)$$

4.1.1 Break up

The rate of break up of a drop of volume v and diameter d_v can be represented in terms of frequency ($\omega_b(v)$) and efficiency ($\lambda_b(v)$) expressions:

$$b(v) = \omega_b(v)\exp[-\lambda_b(v)] \qquad (4.1.3)$$

Break up frequency

By assuming that drop of diameter d_v breaks only if an eddy with wavelength d_v transfers its energy to the drop, the frequency term will be given by $u(d_v)/ d_v$ where $u(d_v)$ is the relative velocity between two points separated by a distance d_v (Shinnar, 1961):

$$u^2(d_v) = \frac{k_u(\varepsilon d_v)^{2/3}}{(1+\phi_d)^2} \qquad (4.1.4)$$

k_u is constant. The average energy dissipation rate (ε) is given by (see equation 1.1.4, chapter 1):

$$\varepsilon = k_\varepsilon N_I^3 D_I^2 \ , \qquad k_\varepsilon = N_p V_t / D_I^3 \qquad (4.1.5)$$

where N_p is the Power Number (Oldshue, 1983) and V_t is the total volume of the reactor content.

Using equation 4.1.4, the frequency term can be written as follows where k_b is an adjustable parameter:

$$\omega_b(v) = \frac{k_b \varepsilon^{1/3}}{(1+\phi)d_v^{2/3}} \ , \qquad k_b = k_u^{1/2} \qquad (4.1.6)$$

Break up efficiency

Break up efficiency is the ratio of required to available energy. The required energy is the energy to overcome the surface-tension resistance ($e_s=2\sigma/\rho_d d_v$) and viscoelastic resistance (e_v). The available energy is equal to the energy dissipated by a turbulent fluctuation with wavelength d_v, which is $(1/2)u^2(d_v)$ per mass unit.

To calculate e_v, a Maxwell body-type, unidirectional fluid is considered initially at rest and then subjected to a pressure drop ($-e_{ve}\rho_d$) during a fluctuation period $d_v/u(d_v)$. By calculating the required energy, e_v, to displace the fluid as much as d_v within one fluctuation time, the break up efficiency can be obtained using the following equation (Alvarez et al., 1994):

$$\lambda_b(v) = a_b \Omega(d_v) \tag{4.1.7a}$$

$$\Omega_b(d_v) = \frac{6}{\mathrm{Re}(d_v)[1+\mathrm{Re}(d_v)V_e(d_v)]} + \frac{1}{We(d_v)} \tag{4.1.7b}$$

where a_b is an adjustable parameter, $Re(d_v)$ and $We(d_v)$ are the Reynolds and Weber numbers for a drop of diameter d_v, and $V_e(d_v)$ is a dimensionless function that accounts for elasticity:

$$We(d_v) = \rho_d d_v u^2(d_v)/\sigma \ , \qquad \mathrm{Re}(d_v) = d_v u(d_v)/\nu_d \tag{4.1.8a}$$

$$V_e(d_v) = \Theta \exp\left[-\frac{1-\alpha}{2Y_0\,\mathrm{Re}(d_v)}\right] - \frac{1}{12} \ , \qquad Y_0 = \frac{\mu_d^2}{\rho_d E_d d_v^2} \tag{4.1.8b}$$

$$\alpha = \sqrt{1-48Y_0} \ , \qquad \Theta = \frac{Y_0}{\alpha(1-\alpha)}\left[1+\alpha-\frac{(1-\alpha)^2}{1+\alpha}\exp\left(-\frac{1-\alpha}{2Y_0\,\mathrm{Re}(d_v)}\right)\right] \tag{4.1.8c}$$

E_d and ν_d are Young's elasticity modulus and the kinematic viscosity of the dispersed phase ($\nu_d = \mu_d/\rho_d$), respectively. E_d may be considered as a linear function of polymer-monomer conversion (x),

$$E_d = xE_p \tag{4.1.9}$$

where E_p is Young's elasticity modulus of pure polymer.

4.1.2 Satellite Droplets

In order to predict the formation of satellite droplets we may use the correlation presented by Chatzi and Kiparissides (1992) that considers break up of a mother drop to a few daughter drops (N_d) and a number of smaller satellite droplets (N_s) with a volume ratio of daughter to satellite drops of x_{ds}. The number of drops with volume v, $\beta(v',v)u(v')$ (see equation 4.1.1), formed by break up of a drop of volume v', is:

$$\beta(v',v)u(v') = \begin{cases} N_d\beta(v',v) + N_s\beta(v',x_{ds}v), \\ N_d\beta(v',v), \\ 0, \end{cases} \quad \text{if} \quad \begin{cases} v \le v'/(N_d x_{ds} + N_s) \\ v'/(N_d x_{ds} + N_s) < v \le v'/[N_d + (N_s / x_{ds})] \\ v > v'/[N_d + (N_s / x_{ds})] \end{cases} \tag{4.1.10}$$

The values of N_s and x_{ds} can be considered to depend linearly on the mother drop volume (v_m), with slopes S_{Ns} and S_x, respectively:

$$N_s = 1 + Integer[S_{Ns} v_m], \qquad x_{ds} = 1 + S_x v_m \tag{4.1.11}$$

The above model has been successfully used to predict the drop size distribution for a system of *n*-butyl chloride in water in the presence of PVA as the suspending agent (Chatzi and Kiparissides, 1992).

4.1.3 Coalescence

Similar to the rate of drop break up, the rate of drop coalescence can be expressed in terms of collision frequency ($\omega_c(v,u)$) and coalescence efficiency ($\lambda_c(v,u)$):

$$c(v,u) = \omega_c(v,u)\exp[-\lambda_c(v,u)] \tag{4.1.12}$$

Collision frequency

We used the following equation for collision frequency of drops with diameters d_v and d_u, $\omega_c(d_v,d_u)$, where k_c is an adjustable parameter:

$$\omega_c(d_v,d_u)=k_c\frac{\varepsilon^{1/3}}{1+\phi_d}(d_v^2+d_u^2)\sqrt{(d_v^{2/3}+d_u^{2/3})} \qquad (4.1.13)$$

Coalescence efficiency

For the coalescence efficiency term (λ_c) we used the model presented by Alvarez et al. (1994) considering only two efficiency terms, the deformation efficiency (λ_{cd}) and the film drainage efficiency (λ_{cf}); $\lambda_c = \lambda_{cd} + \lambda_{cf}$. In order to calculate the deformation efficiency for drop coalescence it is possible to use the same equations used for break up efficiency with a simple modification.

When two drops collide, the smaller one has a larger energy content and it undergoes a larger deformation (Ivanov et al., 1985). To account for this fact, a mean length for deformation (d_{vu}) in coalescence interpenetration can be defined as:

$$d_{vu}^{-1}(v,u)=(d_v^{-1}+d_u^{-1}) \qquad (4.1.14)$$

Now we can assume that (i) the energy content available for coalescence is $(1/2)u^2(d_{vu})$, and (ii) the energy required to overcome the viscoelasticity and surface-tension resistance is the energy required by a drop of diameter d_{vu} to reach a mean deformation of d_{vu} within a time period $d_{vu}/u(d_{vu})$. Using these assumptions the ratio of required to available energy for coalescence efficiency (λ_{cd}) is obtained by replacing d_v by d_{vu} in equation 4.1.7. With this approach we can use equations 4.1.7 and 4.1.8 to calculate λ_{cd}:

$$\lambda_{cd}(v,u)=a_c\Omega(d_{vu}) \qquad (4.1.15)$$

a_c is an adjustable parameter.

To calculate the film drainage efficiency (λ_{cd}), first consider two drops that approach together. On the verge of coalescence, an unstable film of water is formed with critical tickness h_c and diameter d_{vu} (Ivanov et al., 1985). Then the film breaks and its water is drained by capillary pressure ($2\sigma_d/h_c$). By assuming that the film drainage is fast in comparison with the dynamics of the coalescence process, the capillary pressure over the disc volume ($\pi d^2_{vu}h_c/4$) yields the following energy for film drainage (e_d):

$$e_d = (\pi/2)\sigma_d d_{vu}^2 \qquad (4.1.16)$$

where σ_d is the effective surface tension and, according to Koshy et al. (1988a), can be considered as the difference between the actual and the full coverage value, $\sigma_d = k_\sigma(1-\theta)$ (see equation 4.3.3).

With dividing the drainage energy (equation 4.1.16) by the energy which is available for coalescence, $(1/2)u^2(d_{vu})\rho_d$, we have:

$$\lambda_{cf}(v) = b_c / We_d(d_f) \qquad (4.1.17)$$

$$We_d(d_f) = \rho_w d_f v^2(d_f)/\sigma_d \ , \qquad d_f = (d_v^3 + d_u^3)/d_{vu}^2 \qquad (4.1.18)$$

$We_d(d_f)$ is the film drainage Weber number and d_f is a characteristic drainage length. Considering equations 4.1.15 and 4.1.17 the overall coalescence efficiency will be:

$$\lambda_c(v,u) = a_c\Omega(d_{vu}) - b_c / We_d(d_f) \qquad (4.1.19)$$

4.1.4 Number of Particles and Mean Particle Size

The total number of drops/particles is given by:

$$N_t = \int_0^\infty F(d_v,t)d(d_v) \qquad (4.1.20)$$

The Sauter mean diameter (d_{32}) and the interfacial area per water volume unit (a) can be calculated by the following equations:

$$d_{32} = \frac{\int_0^\infty d_v^3 F(d_v,t)d(d_v)}{\int_0^\infty d_v^2 F(d_v,t)d(d_v)} \qquad (4.1.21)$$

$$a = \frac{6\phi_d}{d_{32}(1-\phi_d)} \tag{4.1.22}$$

4.2 MODELLING OF FREE-RADICAL POLYMERISATION

4.2.1 Kinetics

The basic chemical reactions occurring in a free-radical polymerisation have been schematically presented in chapter 1 (see equations 1.2.1 to 1.2.4). One of the most important mathematical techniques for prediction of the kinetics of free-radical polymerisation reactions is based on the method of moments. We used this method to model the kinetics of suspension polymerisation reactions in which each polymerising drop can be assumed to be a miniature bulk reactor.

The moments of free radicals (λ) and dead-polymer molecules (μ) are defined as:

$$\lambda_i = \sum_{n=1}^{\infty} n^i [\dot{R}_n] \tag{4.2.1}$$

$$\mu_i = \sum_{n=1}^{\infty} n^i [P_n] \tag{4.2.2}$$

where i denotes the degree of the moment. $[\dot{R}_n]$ and $[P_n]$ are the concentrations of growing free radicals and dead polymer chains with n monomer units, respectively. Note that λ_0 is the total free-radical concentration, μ_0 is the total concentration of polymer, and $\lambda_1 + \mu_1$ is the number of moles of monomer which has reacted. To obtain the moments equations first we have to know the mass balances for free radicals and dead polymers using the mechanism of free-radical polymerisation (equations 1.2.1-1.2.4):

$$\frac{1}{V}\frac{d([\dot{R}_0]V)}{dt} = 2fk_d[I] - k_t[\dot{R}_0][M] = 0 \tag{4.2.3}$$

$$\frac{1}{V}\frac{d([\dot{R}_1]V)}{dt} = 2fk_d[I] - k_t[\dot{R}_1]\lambda_0 + (k_f[M] + k_s[S])\lambda_0 \tag{4.2.4}$$

$$\frac{1}{V}\frac{d([\dot{R}_n]V)}{dt} = k_p[M]\left([\dot{R}_{n-1}]-[\dot{R}_n]\right)k_t\lambda_0\lambda_1 - k_t[\dot{R}_n]\lambda_0 - (k_f[M]+k_s[S])[\dot{R}_n] \tag{4.2.5}$$

$$\frac{1}{V}\frac{d([P_n]V)}{dt} = k_{td}[P_n]\lambda_0 + \frac{1}{2}k_{tc}\sum_{m=1}^{n-1}[P_{n-m}][P_m] + (k_f[M]+k_s[S])[P_n] \tag{4.2.6}$$

By multiplying both sides of the above equations by n^0 (for zeroth moment), n^1 (for first moment), or n^2 (for second moment) and summing them over n (n=1 to ∞), one can obtain the differential equations for moments of free radicals and dead polymers. So the zeroth, first and second moments of free radicals (λ_0, λ_1, λ_2) and dead polymers (μ_0, μ_1, μ_2) are obtained as follows:

$$\frac{1}{V}\frac{d(\lambda_0 V)}{dt} = 2fk_d[I] - k_t\lambda_0^2 \tag{4.2.7}$$

$$\frac{1}{V}\frac{d(\lambda_1 V)}{dt} = 2fk_d[I] - k_t\lambda_0\lambda_1 + (k_s[S]+k_p[M])(\lambda_0-\lambda_1) + k_f[M]\lambda_0 \tag{4.2.8}$$

$$\frac{1}{V}\frac{d(\lambda_2 V)}{dt} = 2fk_d[I] - k_t\lambda_0\lambda_2 + k_s[S](\lambda_0-\lambda_2) + k_s[S](\lambda_0-\lambda_2) + k_p[M](2\lambda_1+\lambda_0) + k_f[M](\lambda_0-\lambda_2) \tag{4.2.9}$$

$$\frac{1}{V}\frac{d(\mu_0 V)}{dt} = (k_d + \frac{1}{2}k_{tc})\lambda_0^2 + (k_f[M]+k_s[S])\lambda_0 \tag{4.2.10}$$

$$\frac{1}{V}\frac{d(\mu_1 V)}{dt} = k_t\lambda_0\lambda_1 + (k_f[M]+k_s[S])\lambda_1 \tag{4.2.11}$$

$$\frac{1}{V}\frac{d(\mu_2 V)}{dt} = k_t\lambda_0\lambda_2 + k_{tc}\lambda_1^2 + (k_f[M]+k_s[S])\lambda_2 \tag{4.2.12}$$

The rate of polymerisation (equation 1.2.6) can be rewritten in terms of the zeroth moment of free radicals:

$$R_p = (k_p + k_f)[M]\lambda_0 \tag{4.2.13}$$

4.2.2 Polymer Molecular Weights

In the method of moments cumulative number-average (M_n) and weight-average (M_w) molecular weights of polymer at anytime of polymerisation can be calculated by following expressions where M_m is the molecular weight of monomer.

$$M_n = M_m \frac{\mu_1 + \lambda_1}{\mu_0 + \lambda_0} \quad , \qquad M_w = M_m \frac{\mu_2 + \lambda_2}{\mu_1 + \lambda_1} \tag{4.2.14}$$

4.2.3 Diffusion-Controlled Propagation and Termination

In order to predict the variations of k_t and k_p during the gel and glass effects, respectively, we used the following correlations which were originally proposed by Chiu et al. (1983) and modified later (Baillagou and Soong, 1985b):

$$k_t = \frac{k_{t0}}{1 + k_{t0}\lambda_0 / Ek_{\theta_t}} \tag{4.2.15}$$

$$k_p = \frac{k_{p0}}{1 + k_{p0}\lambda_0 / Ek_{\theta_p}} \tag{4.2.16}$$

$$E = \exp\left(\frac{2.303(1-\phi_p)}{a_E + b_E(1-\phi_p)}\right) \tag{4.2.17}$$

$$k_{\theta_t} = [I]_0 A_{\theta_t} \exp(-E_{\theta_t} / RT), \qquad k_{\theta_p} = A_{\theta_p} \exp(-E_{\theta_p} / RT) \tag{4.2.18}$$

k_{p0} *and* k_{t0} are the values of k_t and k_p at zero conversion, respectively. a_E is a temperature-dependent parameter and b_E is a constant. A and E in equation 4.2.18 are the constant and activation energy for the Arrhenius equation, respectively. A decrease in k_p and k_t starts from the beginning of the reaction but is accelerated at medium and high conversion, respectively. In this model the polymer content (ϕ_p) is the main determining factor in the prediction of the onset of the gel and glass effects. As is seen the gel effect depends on the initial initiator concentration ($[I]_0$) as well as polymer concentration.

4.2.4 Rheological Properties

The viscosity variation of polymer-monomer solution during the polymerisation of MMA is calculated using the following correlation (Baillagou and Soong, 1985b):

$$\mu_d = \mu_m + 2c_p^{1.4}\exp(0.8/V_f) \qquad \text{if} \qquad c_p \le 0.16$$

$$\mu_d = \mu_m + 200c_p^{4.2}\exp(0.8/V_f) \qquad \text{if} \qquad c_p > 0.16 \tag{4.2.19}$$

where μ_m and μ_d are the viscosity of pure MMA and PMMA-MMA solution, respectively. V_f is the free volume of the solution and c_p is the polymer concentration.

4.3 MODELLING OF STABILISER PARTITIONING

Using Langmuir-type interfacial adsorption (Adamson, 1976) for PVA molecules as the suspending agent, the partitioning of PVA molecules and its effect on interfacial tension and drop surface coverage can be calculated by the following equations:

$$c_s = c_{sa} + a\theta c_\infty \tag{4.3.1}$$

$$\theta = \frac{k_a c_{sa}}{1 + k_a c_{sa}} \tag{4.3.2}$$

$$\sigma = \sigma_0 - k_\sigma \theta \tag{4.3.3}$$

where a is the interfacial area per water volume unit, c_s and c_{sa} are the total and aqueous phase concentrations of the suspending agent, respectively, θ is the surface coverage, and c_∞ is the concentration of the suspending agent at θ=1.

4.4 MODELLING OF MONOMER PARTITIONING

In the suspension polymerisation of MMA, with a considerable water solubility of 1.5 wt% at 25°C, interphase mass transfer may be important, especially when a low monomer hold up is used. Kalfas and Ray (1993) proposed a kinetic model considering

the monomer transport from the aqueous phase to the polymerising drops in suspension polymerisation of partially water-soluble monomers (Kalfas et al., 1993; Zhang and Ray, 1997).

It can be easily shown that the aqueous phase becomes saturated with dissolved monomer during the dispersion of the monomer and before the polymerisation reaction can progress much. As the polymerisation begins in the monomer drops, the monomer concentration in the drops decreases from the equilibrium value (with respect to the dissolved monomer in the aqueous phase) forcing transfer of monomer molecules from the aqueous phase to the drops. The rate of monomer transport between two phases can be defined as follows:

$$dW_{m,a}/dt = k_m a_i M_m (c^e_{m,d} - c_{m,d}) \qquad (4.3.4)$$

where $W_{m,a}$ is the weight of dissolved monomer in the aqueous phase. $c^e_{m,d}$ and $c_{m,d}$ are mole concentrations of dissolved monomer in the aqueous phase in equilibrium and non-equilibrium conditions, respectively. k_m is the overall mass transfer coefficient of monomer from the aqueous phase to the drops and M_m is the monomer molecular weight.

The equilibrium concentrations are calculated based on the Flory-Huggins theory of polymer solutions and the modifications by Ugelstad et al. (1980). The free energy of mixing in the two phases is given below:

a) Dispersed phase (drops) containing monomer and polymer

$$(\Delta G_m/RT)_{m,d} = \ln\phi_{m,d} + (1-m_{mp})\phi_{p,d} + \chi_{mp}\phi^2_{p,d} + 2\sigma V_m/r_d RT \qquad (4.3.5)$$

b) Aqueous phase containing water and dissolved monomer

$$(\Delta G_m/RT)_{m,a} = \ln\phi_{m,a} + (1-m_{mw})\phi_{w,a} + \chi_{mw}\phi^2_{w,a} \qquad (4.3.6)$$

where ΔG_m is the difference in Gibbs free energy, R and T are the gas constant and temperature, respectively, and $\phi_{i,j}$ is the volume fraction of species i in phase j. m_{ij} is

the ratio of the molar volumes of species i and j and χ_{ij} is solubility interaction parameter of species i and j. The last term in equation 4.3.5, which accounts for the interfacial tension energy, may be neglected for drops of the size encountered in suspension polymerisation.

The equilibrium concentrations can be obtained by equating the right-hand sides of equations 4.3.5 and 4.3.6.

Two different monomer conversions can be defined here. The first one is the monomer conversion in drops (x_d):

$$x_d = \frac{W_p}{W_p + W_{m,d}} \tag{4.3.7}$$

where W_p is the polymer weight and $W_{m,d}$ is the weight of monomer in drops but the overall monomer conversion, including the monomer dissolved in the aqueous phase, is:

$$x = \frac{W_p}{W_{m0}} \tag{4.3.8}$$

The monomer mass balance is:

$$W_{m0} = W_p + W_{m,d} + W_{m,a} \tag{4.3.9}$$

where W_{m0} is the total weight of initial monomer.

4.5 NUMERICAL SOLUTION OF THE MODEL

4.5.1 Kinetics of Polymerisation

The set of differential equations for free-radical and dead-polymer moments (equations 4.2.7 to 4.2.12) together with the rate of initiator and monomer consumption (equations 1.2.5 and 1.2.6) have been solved by a Runge-Kutta 4th order method.

4.5.2 Aqueous-phase Monomer Concentration

Thermodynamic equilibrium concentrations of monomer in the dispersed phase and the aqueous phase were obtained by equalising the right hand sides of equations 4.3.5 and 4.3.6. A simple trial and error method was used to calculate the equilibrium monomer concentrations starting with a guess for an initial value for $\phi_{m,d}$ until a full agreement between the guessed value and predicted value was obtained. The method converged within a few iterations.

4.5.3 Population Balance Equation (PBE)

The population balance equation (equation 4.1.1) was solved numerically for $F(d_v,t)$. The integro-differential PBE was transformed into a system of differential equations by discretising the range of drop diameters according to the method of classes (Chatzi and Kiparissides, 1992). Thus, the size range was divided into a number of equally-spaced intervals. Up to 100 equally-spaced discretisation points were used for the numerical integration.

A Runge-Kutta 4^{th} order method was used for solving the differential equations over the time. The integral terms in the PBE were approximated using a composite Simpson's rule. For an even number of intervals Simpson's 1/3 rule was applied, while for an odd number of intervals Simpson's 3/8 rule was employed.

4.6 MODEL IMPLEMENETATION

Figure 4.1 illustrates the flow diagram of the model. The model may be used for both reacting and non-reacting dispersions. The kinetic model is used simultaneously with the PBM model when a reacting system (polymerisation) is being studied otherwise only the PBM model is used for non-reacting systems.

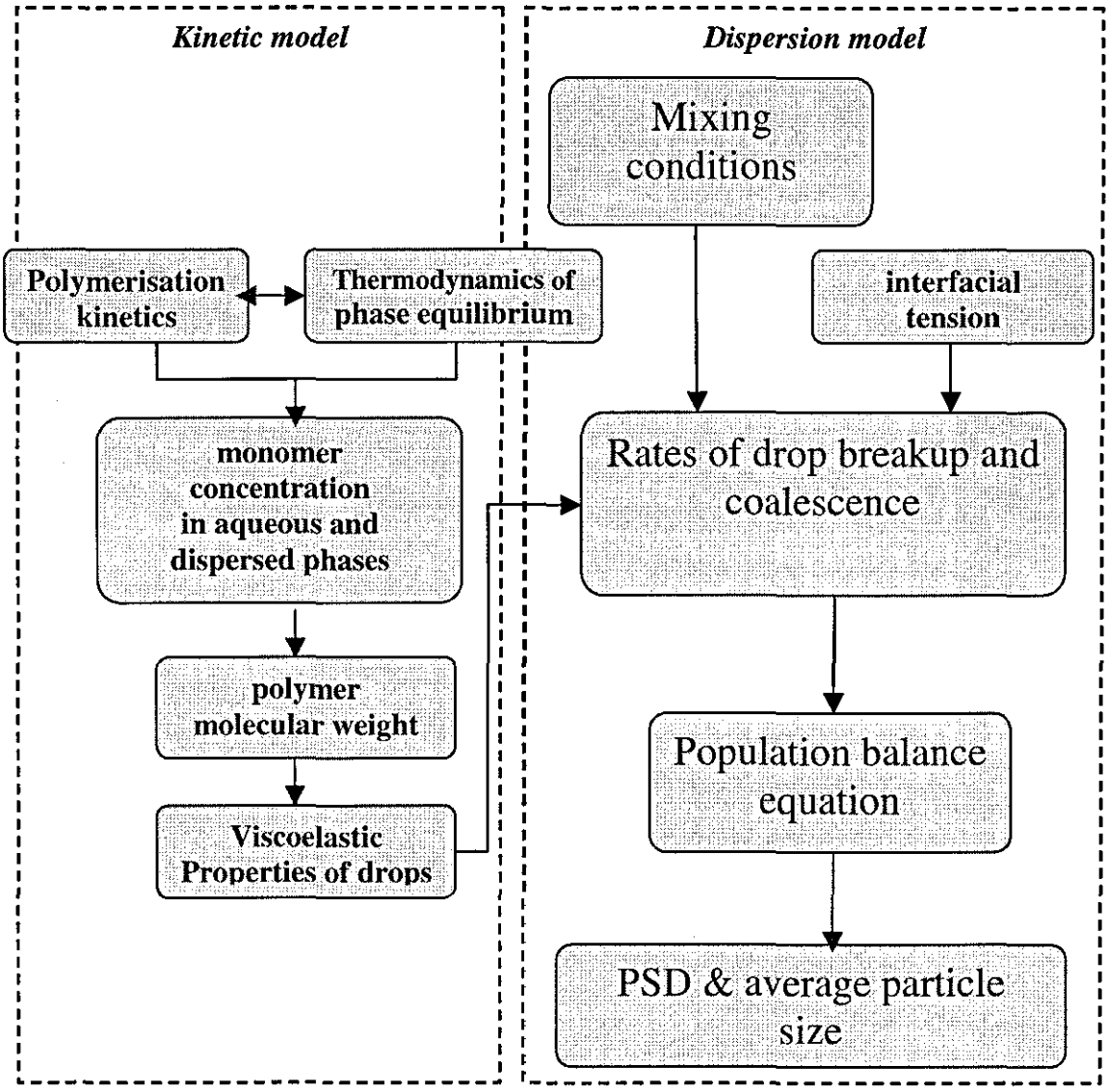

Figure 4.1 Flow diagram of the model.

4.7 MODEL VALIDATION

The validity of the developed model was checked by reproducing the modelling results presented in the paper of Alvarez et al. (1994). They fited their modelling results to Konno's experimental results on the suspension polymerisation of styrene in the presence of PVA as the suspending agent at 70°C using azobis-isobutyronitrile (AIBN) as the initiator (Konno et al., 1982).

We ignored the routine for calculation of mass transfer of monomer (as it is not appreciable for styrene with a very limited water solubility) and considered a binary drop break up ($u(v') = 2$) as Alvarez et al. (1994) did. We also used the same viscosity correlation (see equation 1.3.11) and the physical and kinetic parameters as used by them. Readers are referred to their paper for the constants used.

Figure 4.2 illustrates the experimental results of time evolution of d_{32} (Konno et al., 1982), in comparison with the predicted results by Alvarez et al. (1994) and us. The slight difference between the predictions of the two models is more likely due to the different values of some parameters used (we found errors in some of the correlations and parameters values used by Alvarez et al.). Because the variation of mean particle size with time is the result of interactions between the kinetics of the polymerisation reactions and viscoelasticity of the polymerising drops, as well as the drop break up and coalescence phenomena, we may claim that the different routines and numerical methods used in the developed model are credible and reliable to be used for other suspension polymerisation systems.

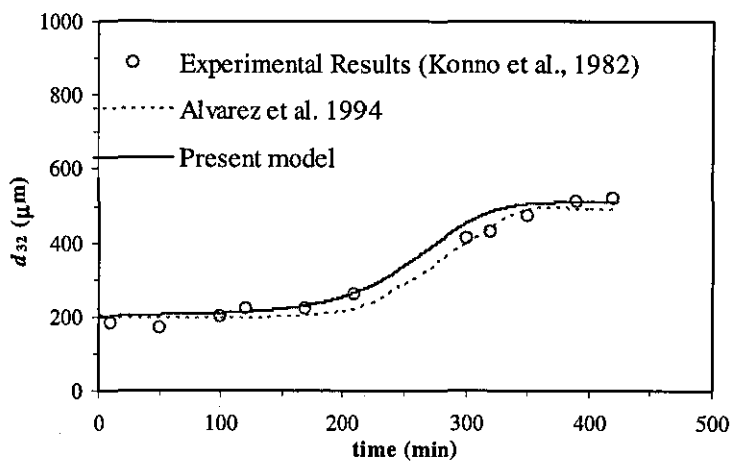

Figure 4.2 Reproducing of modelling results of Alvarez et al. (1994) using the present model.

4.8 APPLICATION OF THE MODEL

4.8.1 Numerical Parameters

Kinetic and Thermodynamic Parameters

The values and expressions used for the physical, kinetic and thermodynamic parameters and constants used for the suspension polymerisation of MMA have been collected in Table 4.2.

Table 4.2 Physical, kinetic and thermodynamic parameters used for modelling of MMA free-radical polymerisation.

Parameter	Value/Expression	Reference
M_m (g/gmol)	100	Brandrup et al. (1999)
ρ_m (g/cm^3)	0.968-0.001225T	Brandrup et al. (1999)
ρ_p (g/cm^3)	1.20	Brandrup et al. (1999)
α_m , α_p (1/°C)	0.001 , 0.00048	Brandrup et al. (1999)
T_{gm} , T_{gp} (°C)	-106 , 114	Brandrup et al. (1999)
μ_m (cp)	$\exp(2.303\times(0.115/V_{fm}-1))$ †	Baillagou and Soong (1985b)
k_d (1/sec)	$2.083\times10^{12}\exp(-14580/T)$ ‡	Brandrup et al. (1999)
k_{p0} (L/mol.sec)	$4.92\times10^{5}\exp(-2189/T)$	Baillagou and Soong (1985b)
k_{t0} (L/mol.sec)	$9.8\times10^{7}\exp(-353/T)$	Baillagou and Soong (1985b)
$k_{\theta p}$ (1/sec)	$3.0233\times10^{13}\exp(-1.17\times10^{5}/RT)$	Baillagou and Soong (1985b)
K_θ (1/sec)	$1.454\times10^{20}\exp(-1.458\times10^{5}/RT)$	Baillagou and Soong (1985b)
a_E	$0.168-8.21\times10^{-6}(T-T_{gp})^2$	Baillagou and Soong (1985b)
b_E	0.03	Baillagou and Soong (1985b)
$C_f (=k_f/k_{p0})$	$8.93\times10^{-4}\exp(-1127/T)$	Baillagou and Soong (1985b)
$C_s (=k_s/k_{p0})$	0.54	Jahanzad et al. (1993)
χ_{mw} , χ_{mp}	4.05 , 1.08	Forcada and Asua (1990)
m_{mw} , m_{mp}	0.87 , 0.5	Forcada and Asua (1990)
k_m	1.0	Zhang and Ray (1997)
s_{eq} (wt%)	1.6 (at 70°C)	Kalfas and Ray (1993)
N_p (eq. 4.1.5)	5	Oldshue (1983)
E_p (g/cm.sec^2)	3.2×10^{10}	Ferry (1980)

† $V_{fm} = 0.025 + \alpha_m (T - T_{gm})$

‡ The Arrhenius equation was derived using the given values for LPO's half lives at different temperatures in Brandrup et al. (1999).

Parameters Obtained Experimentally

Interfacial tensions between MMA and different PVA solutions were determined experimentally. The method and the procedure are explained in Appendix C and the results have been presented in the form of a graph in section 3.1. The values of σ are

shown in Table 4.3. These experimental values were used to find the adsorption parameters in equation 4.1.19. The fitted values for k_a and k_σ are in good agreement with the values found by Lazrak et al. (1998) for the same system (1.5×10^4 and 10.4 for k_a and k_σ, respectively).

The measurements were carried out at 25°C but the measured interfacial tensions were used in the model for simulation of the dispersions and suspension polymerisations at the base temperature of this study (70°C). No correlation was used for temperature dependence of interfacial tension. This has been left for future work.

Table 4.3 Interfacial tensions measured for MMA and different aqueous PVA solutions (at 25°C) and the fitted adsorption parameters.

PVA (g/l)	σ (dyn/cm)
0.0	(σ_0 =) 15.01
0.25	6.05
0.5	4.12
1.0	3.15
2.0	2.50
4.0	2.35
10.0	2.13
k_a (cm^3/g)	1.0×10^4
K_σ (dyn/cm)	13
c_∞ (g/cm^2)	1×10^{-6} †

† Estimated from data reported by Van Den Boomgaard et al. (1978).

Adjustable Parameters

There are totally five adjustable parameter in drop break up and coalescence models used in the present model.

The parameter k_b in the break up frequency model, given in equation 4.1.6, determines the rate of eddy-drop collisions leading to the drop break up. With increasing k_b the frequency of break up increases. The parameter a_b in equation 4.1.7 indicates the efficiency of drop break up. The higher the values of a_b, the lower the required energy for drop deformation leading to a higher probability for drop break up.

The parameter k_c in equation 4.1.13 determines the frequency of drop-drop collision. The collision frequency increases with k_c. The parameters a_c and b_c in equation 4.1.19 indicate the importance of coalescence efficiency. A higher a_c and lower b_c result in a

higher coalescence efficiency due to lower required energy for drop deformation and film drainage processes.

We did not use the satellite formation module for the present study because of ambiguities involved in the direct application of existing models to dispersions with a high viscosity dispersed phase, which may require more elaboration.

In order to estimate the values of the adjustable parameters for suspension polymerisation of MMA, we applied the model to d_{32}-time experimental data of an inviscid non-reacting MMA/water dispersion (ϕ_d=0.05) and found the estimated values for break-up adjustable parameters that give the best fit to the experimental data. Then using these values for a higher dispersed phase hold up (ϕ_d=0.20), the coalescence adjustable values were estimated as well. The adjustable parameters and their fitted values are given in Table 4.4. The fitted values of the adjustable parameters were used, without any alteration, for the modelling of suspension polymerisation of MMA. No optimisation was carried out on parameter fitting due to lack of time. It is obvious that application of an optimisation method on the fitting of a large number of experimental results, which may include the suspension polymerisation runs as well, could substantially improve the accuracy of predictions. However, this will be pursued in the future.

Table 4.4 Comparison of the numerical values for break up and coalescence adjustable parameters obtained by different investigators.

Adjustable parameter	Alvarez et al. (1994)	Maggioris et al. (2000)	This work
k_b (cm^3/g)	0.73	30	0.5
a_b	0.112	14.5	0.03
k_c ($1/cm^3$)	1.37×10^{-5}	7×10^{-12}	1×10^{-7}
a_c	2.62×10^{-3}	1	1×10^{-5}
b_c	3.07	2	3

Table 4.4 also compares the numerical values of the five adjustable parameters obtained by Alvarez et al. (1994), for the suspension polymerisation of styrene, with those obtained by Maggioris et al. (2000), for the suspension polymerisation of vinyl chloride, in the presence of PVA as the suspending agent, and those used in this work, for the suspension polymerisation of MMA.

4.8.2 Model Prediction: Kinetics of polymerisation

Figure 4.3 compares the experimental conversion-time data with the theoretical results for the suspension polymerisation of MMA at the base conditions (70°C, N_I = 500 rpm, ϕ_d = 0.2, LPO = 1 wt%, PVA = 1 g/l). The value of initiator efficiency was adjusted at f = 0.37 to give the best fit to the experimental data. The agreement between the experimental data and model predictions is good. In the following sections, we evaluate the effects of variations of some of the important variables on the kinetics of MMA suspension polymerisation.

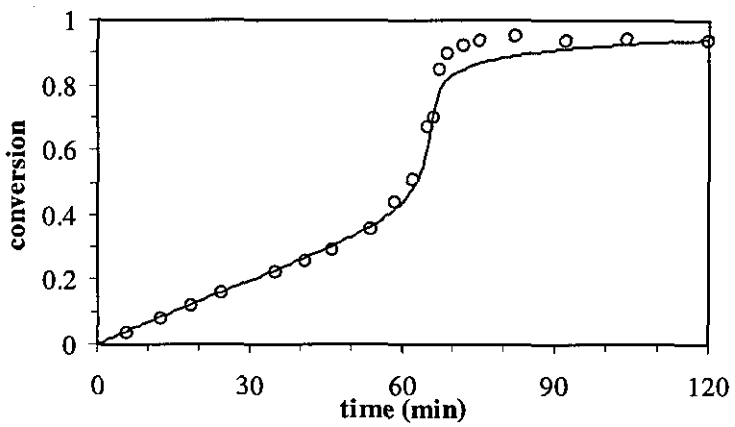

Figure 4.3 Comparison of experimental (symbol) and predicted (line) conversion-time for suspension polymerisation of MMA.

Initiator concentration

Figure 4.4 compares the experimental and theoretical results for conversion-time variations in the suspension polymerisation of MMA (70°C, N_I = 500 rpm, ϕ_d = 0.2, PVA = 1 g/l) with different LPO concentrations. The fit for the lowest LPO concentration used in this research is not as good as those with the highest LPO concentrations. The probable reason might be due to the dissolution of LPO in the water phase, which appears to be more important when the overall concentration of LPO is low.

Reaction temperature

Figure 4.5 compares the experimental and theoretical results for conversion-time variations in the suspension polymerisation of MMA (N_I = 300 rpm, ϕ_d = 0.2, LPO = 1

wt%, PVA = 1 g/l) at different temperatures. Good agreements are observed between the experimental and the theoretical results.

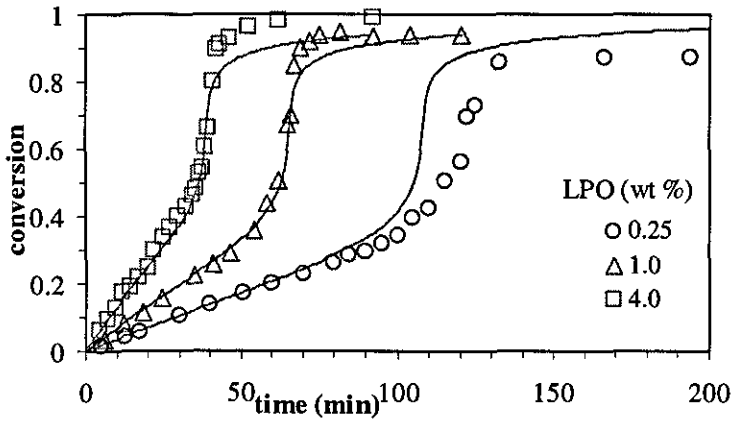

Figure 4.4 Experimental (symbol) and theoretical (line) conversion-time for suspension polymerisation of MMA with different LPO concentrations.

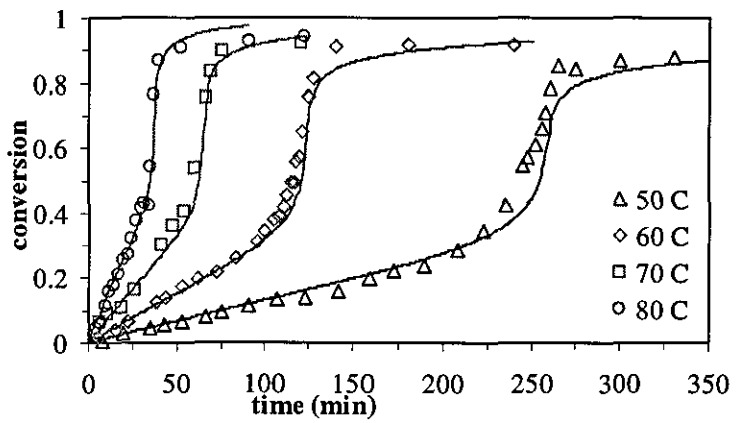

Figure 4.5 Experimental (symbols) and theoretical (lines) conversion-time for suspension polymerisation of MMA at different temperatures.

Monomer hold up

Figure 4.6 compares the experimental and theoretical results for the conversion-time data obtained for the suspension polymerisation of MMA (70°C, N_I = 300 rpm, LPO = 1 wt%, PVA = 1 g/l) with ϕ_d = 0.025 and 0.20. The effect of water solubility of MMA is quite significant for the lower monomer hold up. An advanced gel effect and a lower final conversion are the results of relatively high solubility of MMA in the aqueous phase. The model can predict these effects rather well.

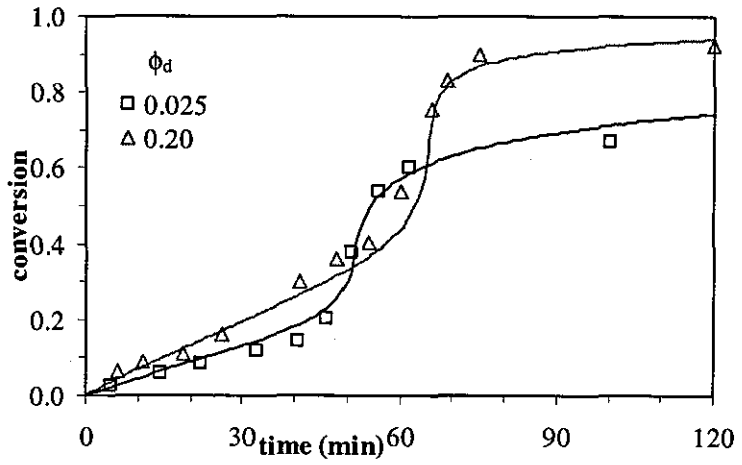

Figure 4.6 Experimental (symbols) and theoretical (lines) conversion-time for suspension polymerisation of MMA with different monomer hold ups.

Monomer concentration in aqueous-phase

Figure 4.7 compares the experimental and theoretical conversion-time for the suspension polymerisation of MMA with $\phi_d = 0.10$ (70°C, $N_I = 300$ rpm, LPO = 1 wt%, PVA = 1 g/l). The experimental and theoretical results for the variations in the MMA concentration in the water phase for this experiment have been compared in *Figure 4.8*. A good agreement is observed between the experimental data and the model predictions.

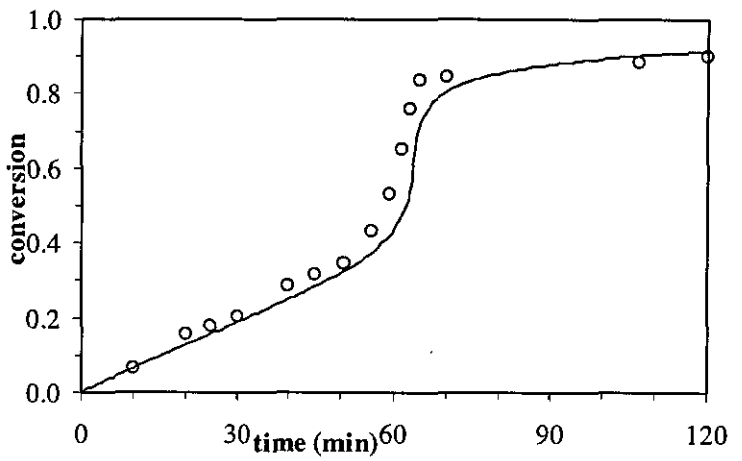

Figure 4.7 Experimental (symbols) and theoretical (line) conversion-time for suspension polymerisation of MMA with $\phi_d = 0.10$.

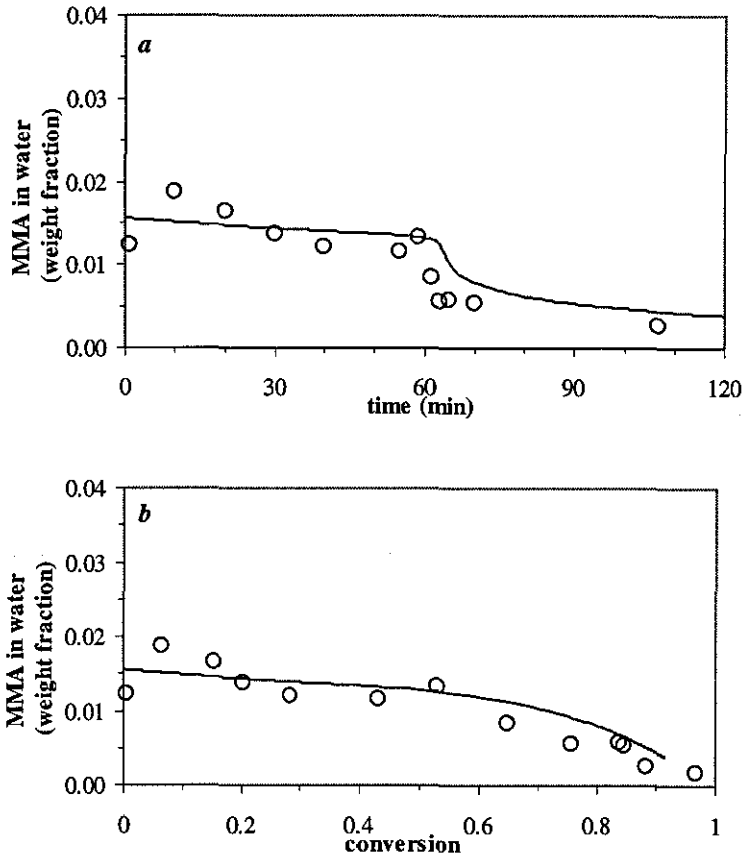

Figure 4.8 Experimental data (symbols) and theoretical predictions (line) of MMA concentration in the aqueous phase in suspension polymerisation of MMA with $\phi_d = 0.10$.

4.8.3 Model prediction: drop/particle size average and distribution

4.8.3.1 Model capabilities

In this section we aim to demonstrate that the model can qualitatively predict the characteristic behaviour of reacting and non-reacting dispersion systems. Some examples of the model capabilities are briefly discussed here.

Figure 4.9 depicts the time evolution of d_{32} for the MMA/water dispersion with different MMA solution viscosities. The MMA solution viscosity can be adjusted by dissolving PMMA in the MMA monomer. The PMMA-MMA solution in fact forms within polymerising drops during the polymerisation reactions. However, in *Figure 4-9* attempts have been made to envisage the effect of viscosity on the drop size variation in a non-reacting system. The characteristic intervals of dispersion, transient stage and quasi steady state, are clearly reproduced by the model. *Figure 4-9* shows that the steady-state d_{32} increases significantly with viscosity. Dispersions with lower viscosity reach the quasi steady state faster. This prediction is in agreement with the experimental results reported in the literature (e.g., Doulah, 1975; Calabrese et al., 1986; Kumar et al., 1991).

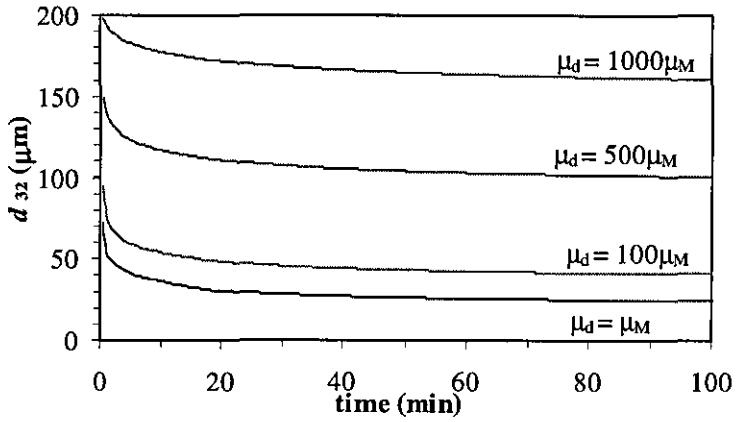

Figure 4.9 The time evolution of d_{32} for (MMA-PMMA)/water dispersions with different dispersed-phase viscosities (T = 70°C, N_I = 500 rpm, ϕ_d = 0.2, PVA = 1 g/l).

Figure 4.10 shows the time evolution of DSD for the MMA/water dispersion. The initial DSDs are broad but narrow with time. Similar evolutions have been obtained in this research and also reported by other investigators.

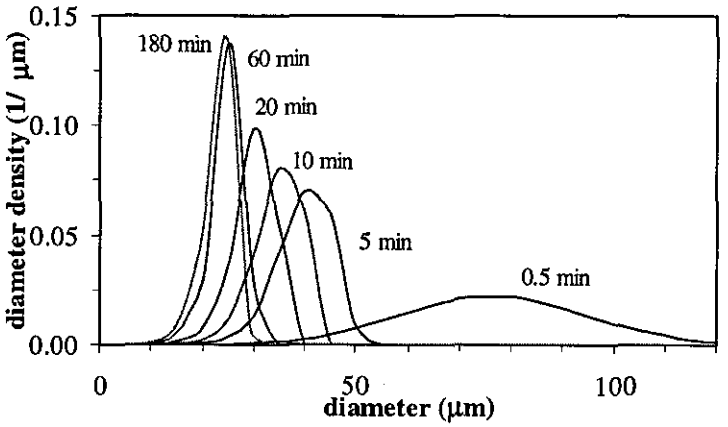

Figure 4.10 The time evolution of DSD for the MMA/water dispersion (for the conditions see the caption of Figure 4.9).

Figure 4.11 demonstrates the final DSDs for the MMA-PMMA/water dispersions. The DSDs become broader with increasing viscosity of the dispersed phase.

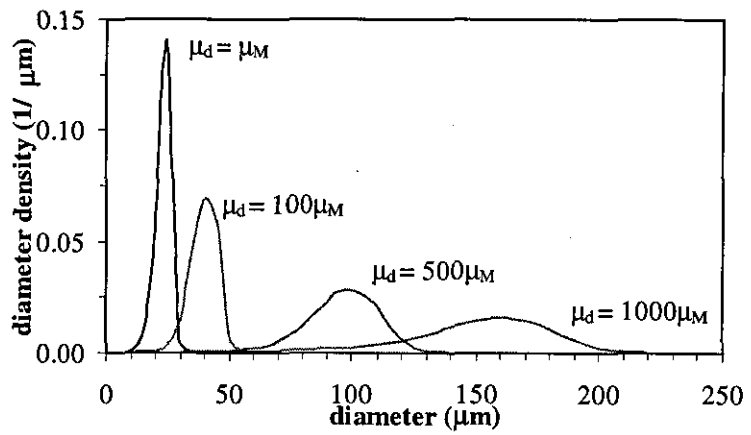

Figure 4.11 Final DSDs for the (MMA-PMMA)/water dispersion with different dispersed phase viscosities.

Figure 4.12 presents the time evolution of d_{32} in a typical MMA suspension polymerisation. The characteristic intervals of suspension polymerisation reactions - transition, quasi steady state, growth, and identification stages - are reproduced by the model as shown in this figure.

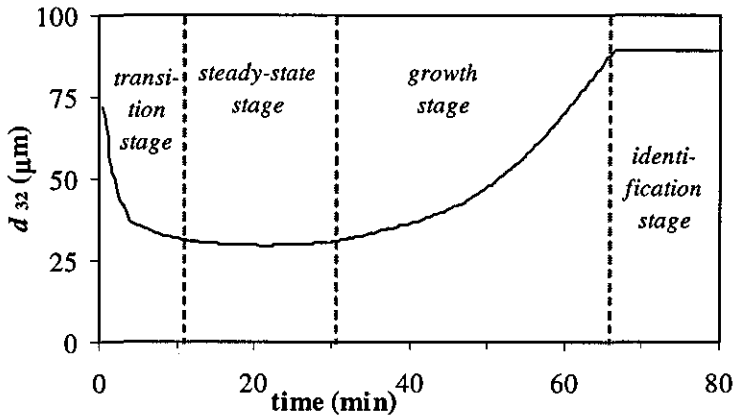

Figure 4.12 The characteristics intervals of the MMA/water dispersion as predicted by the model (T = 70°C, N_I = 500 rpm, ϕ_d = 0.2, LPO = 1 wt%, PVA = 1 g/l).

4.8.3.2 Non-reacting MMA/water dispersion

Figure 4.13 illustrates the experimental results and model predictions (dashed line) for the time variations of Sauter mean diameter for the non-reacting MMA/water dispersion with conditions stated in the caption of this figure. The initial DSD was assumed to be a normal distribution with the average drop size equal to the first experimental measured drop size (at t = 30 sec). The model predicted a very quick transition stage in comparison with the experimental results. Mathematically, it is possible to slow down the approach to the steady state by decreasing the ratio of the rate of drop break up over that of drop coalescence without affecting the steady-state value of drop size. However, this approach is not physically justified as is based on the assumption that a static steady state is prevailing in the dispersion.

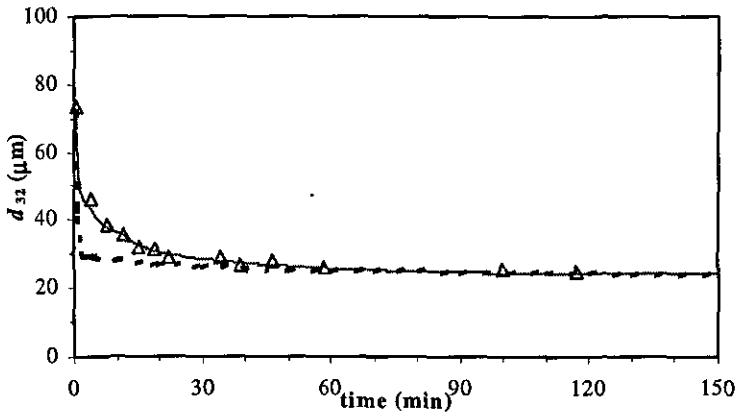

Figure 4.13 The time evolution of d_{32} of the experimental (symbol), predicted (dashed line), and predicted with including the dynamic of the PVA adsorption (solid line): T=70°C, N_I=500 rpm, ϕ_d=0.2, PVA=1 g/l.

There is sufficient evidence available in the literature to indicate that the complete adsorption of polymeric surfactants on the drops is a slow process (Lazrak et al., 1998; Zerfa and Brooks, 1998; Ravera et al., 2000; Diamant et al., 2001). It has been found that the surface coverage of MMA drops by PVA molecules increases with mixing time and takes about 30 min to reach its equilibrium value (Lazrak et al., 1998). The same results have been reported for vinyl chloride drops in the presence of PVA (Zerfa and Brooks, 1998). This means that during the early dispersion, the rate of drop break up and coalescence are low because of poor adsorption of PVA on the surface of drops and subsequently a high interfacial tension. As more PVA molecules are adsorbed on the surface of drops with time, the rate of drop break up is increased but that of drop coalescence is decreased.

In order to incorporate the dynamics of the stabiliser adsorption into the model, we assumed that the drop surface coverage (θ) increases with mixing time to reach to its equilibrium value (θ_{eq}, equation 4.3.2) at t_{eq}. Based on the data reported by Lazrak et al. (1998), the following correlations were used for the time variation of θ:

$$\theta = \theta_{eq}\left(1 + 0.14Ln(t/t_{eq})\right) \qquad \text{for} \quad t \le t_{eq}$$
$$\theta = \theta_{eq} \qquad \text{for} \quad t > t_{eq} \tag{4.8.1}$$

where θ_{eq}=30 min (Lazrak et al., 1998). *Figure 4.14* shows the variation of dimensionless surface coverage (θ/θ_{eq}) with dimensionless time (t / t_{eq}) in accordance to the above equation.

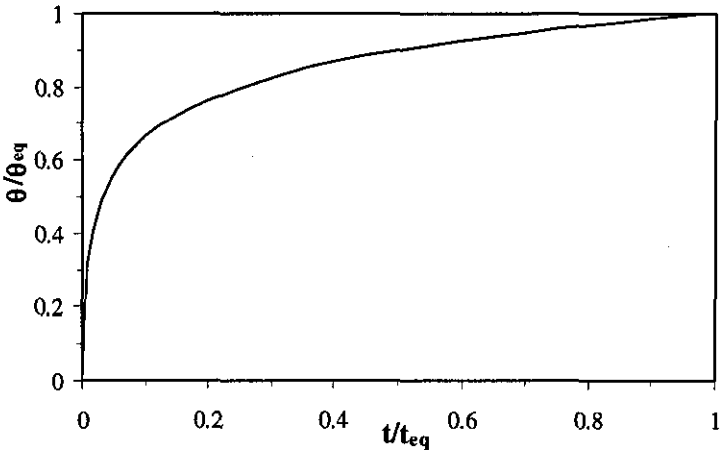

Figure 4.14 The variations of relative surface coverage of drops with relative time.

Figure 4.13 also shows the model prediction using equation 4.8.1 for the same non-reacting MMA/water dispersion. The model predictions fit the experimental data of the transition stage rather well. Therefore, the dynamics of stabiliser adsorption was included in our modelling study.

Figure 4.15 compares the model predictions and the experimental data of the time evolution of d_{32} for dispersions of MMA/water with different PVA concentrations. The model predictions can fairly well fit the experimental data.

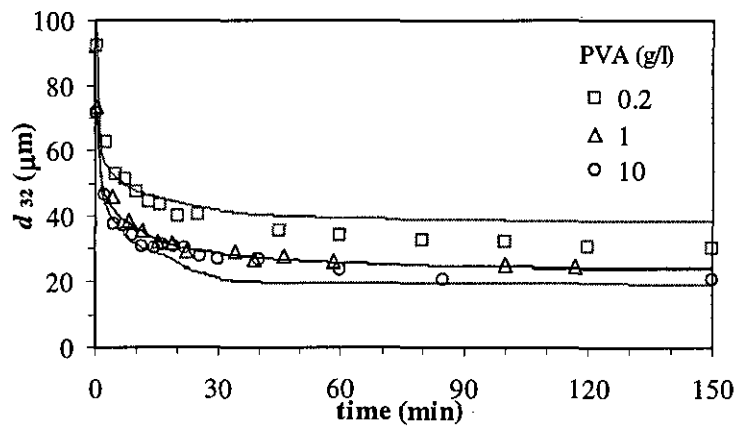

Figure 4.15 The time evolution of experimental (symbols) and predicted (lines) d_{32} for MMA/water dispersions with different PVA concentrations (for other conditions see the caption of Figure 4.13).

Figure 4.16 compares the predicted and experimental steady-state d_{32} for the MMA/water dispersions with different PVA concentrations.

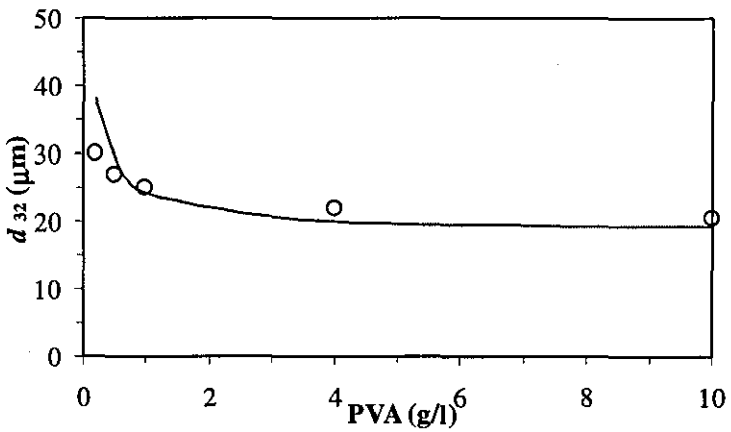

Figure 4.16 Comparison of the experimental (symbol) and predicted (line) steady-state d_{32} with the PVA concentration.

Figure 4.17 compares the time evolution of predicted and experimental DSDs for a typical MMA/water dispersion run. While the average drop sizes are comparable, the predicted distributions are sharper than the experimental. This discrepancy, however, seems not to be a major concern as the broadness of the predicted DSDs can be adjusted by applying a broader standard daughter drop size distribution ($\beta(v',v)$ i.e, equation 4.1.2).

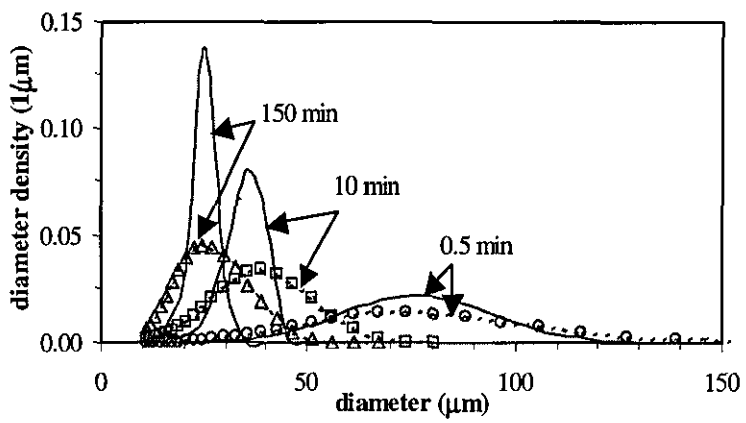

Figure 4.17 Comparison of the experimental (symbol) and predicted (line) DSDs with time (for the conditions see the caption of Figure 4.13).

4.8.3.3 MMA suspension polymerisation

Figure 4.18 illustrates the time evolution of the predicted and experimental d_{32} for the MMA polymerisation runs with different PVA concentrations. The model can satisfactorily reproduce the experimental data.

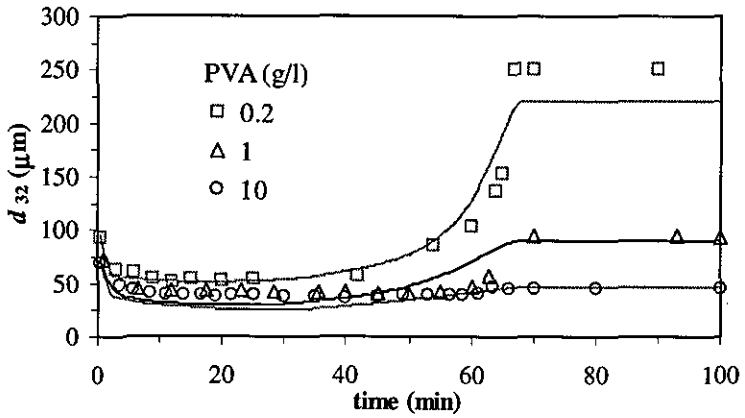

Figure 4.18 Time evolution of experimental (symbols) and predicted (lines) d_{32} for the MMA suspension polymerisations with different PVA concentrations (T = 70°C, N_I = 500 rpm, ϕ_d = 0.2, LPO = 1 wt%).

Figure 4.19 demonstrates the time evolution of predicted and experimental d_{32} for the MMA polymerisation runs with different initiator (LPO) concentrations. The agreement between the model predictions and the experimental data is acceptable, particularly for the higher LPO concentrations. Better agreement may be obtained if the viscosity of the polymerising drops can be better predicted. This requires a more precise conversion-molecular weight-viscosity correlation to be used.

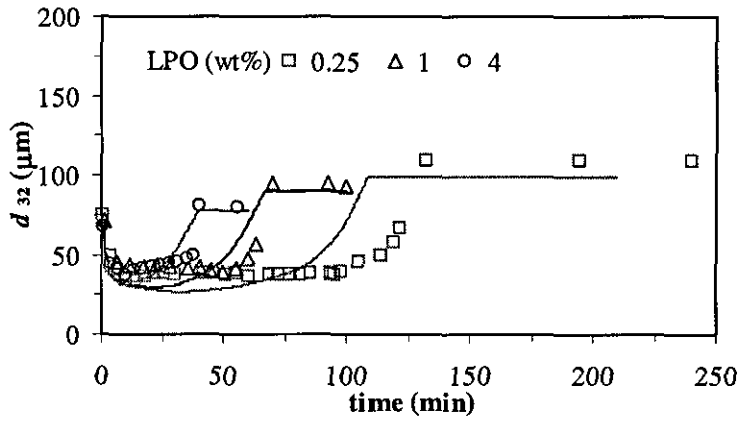

Figure 4.19 Time evolution of experimental (symbols) and predicted (lines) d_{32} for the MMA suspension polymerisations with different LPO concentrations (for other conditions see the caption to Figure 4.18).

Figure 4.20 demonstrates the time evolution of predicted and experimental PSDs for a typical MMA polymerisation run. A good agreement between the model predictions and experimental results is obtained.

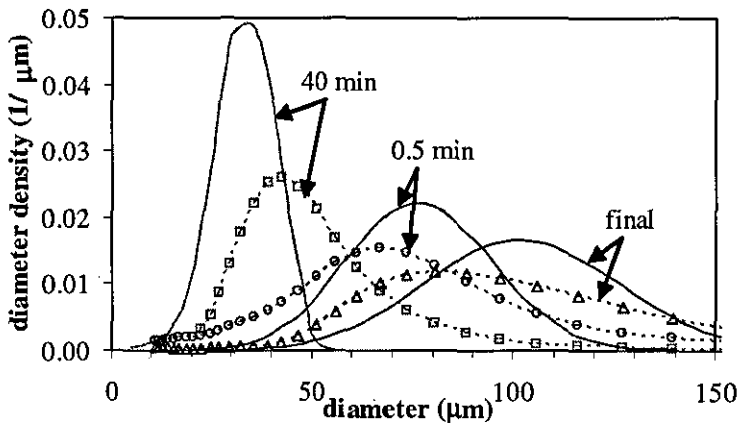

Figure 4.20 Time evolution of experimental (symbols) and predicted (lines) PSD for the MMA suspension polymerisation (T = 70°C, N_I = 500 rpm, ϕ_d = 0.2, LPO = 1 wt%, PVA = 1 g/l).

4.9 CONCLUSIONS

The following conclusions can be drawn from the modelling section:

- The kinetics of suspension polymerisation of MMA was successfully modelled. The model could fairly predict the rate of polymerisation and also the molecular weight and viscosity of the drops with variations in the initiator concentration, monomer concentration, and the reaction temperature.

- The population balance model could qualitatively predict the characteristic behaviour of the evolution of drop size average and distribution in the MMA/water dispersion and the MMA suspension polymerisation reaction.

- The evolution of size variations during the transient stage of mixing was modelled with an assumption that the complete adsorption of PVA on the surface of drops is a slow process.

- The PBM model could successfully reproduce the size variation of drops/particles during mixing (reactions).

- A better agreement between the model predictions and experimental data can be obtained by optimisation and fitting of the adjustable parameters to both experimental d_{32} and PSD, together with application of more specific and tailor-made drop breakage functions and models.

GENERAL CONCLUSIONS

INTODUCTION

The aim of this research work was to obtain a new insight into the evolution of average particle size and distribution in suspension polymerisation reactions. Methyl methacrylate was selected as a model monomer. The comparative study of the MMA suspension polymerisation and MMA/water dispersion was carried out, for the first time, to elaborate on the evolution of drop size distributions. The detailed conclusions have been given in the appropriate sections. Here, the most significant conclusions are highlighted.

1. Kinetics

1.1 rate of Polymerisation

The overall rate of polymerisation during the suspension polymerisation of MMA could be monitored by sampling from the reaction vessel. The polymerisation rate could be divided into three stages:

- *Stage I.* The initial period during which the rate of polymerisation decreased with time.
- *Stage II.* The rate of polymerisation abruptly increased due to the gel effect.
- *Stage II.* The increase in the rate of polymerisation levelled off and final conversion was reached.

The rate of polymerisation in all three stages was shown to be independent of PVA concentration, and the stirring speed, but slightly dependent on monomer hold up. The rate of polymerisation was enhanced with increasing initiator concentration and temperature, as was expected. The concentration of chain transfer agent did not affect the rate of polymerisation during *stage I*, but it reduced the rate of reaction during the next two stages.

1.2 Onset of the gel effect

The onset of the gel effect was advanced, in terms of conversion, with a molecular weight increase. A rise in the molecular weight was induced by a decline in the initiator and chain transfer agent concentrations and the reaction temperature.

2. Evolution of Particle Size Average and Distribution

2.1 Characteristic intervals

It was found that the traditional division of suspension polymerisation processes into three intervals of quasi-steady state, sticky stage, and identification stage is not complete. It was further realised that the kinetics of polymerisation and/or mixing condition can affect such classifications. From the comprehensive experimental results, the characteristic intervals of a typical suspension polymerisation were realised. The understanding of the phenomena occurring in a polymerisation system during each interval will assist to elaborate the evolution of size distributions in these systems. The suspension polymerisation can be characterised by:

- *Transition period* during which PSD narrows dramatically and drop size decreases exponentially due to a higher rate of drop break up, in comparison with drop coalescence, until a steady-state value is reached. For a suspension polymerisation, it was generally accepted that the drop size reaches a steady state in the initial stage of mixing before the onset of the polymerisation reaction. The importance, and even the existence, of the transition stage has been totally ignored in the literature. The results indicate that increasing the impeller speed, monomer hold up, and PVA concentration will lead to a shorter transition period. Increasing the rate of reaction, via increasing initiator concentration, reaction temperature and decreasing inhibitor concentration, will shorten this period.

- *Quasi steady state* during which the rate of drop break up and drop coalescence are almost balanced leading to a steady-state drop size average and distribution. The occurrence of this stage is conditional. Low impeller speed and PVA concentration may remove the quasi steady-state stage completely and drops starts growing considerably after a sharp decrease in size during the transition

stage. Even for non-reacting liquid-liquid dispersions, no real steady state was reached after 3 h of mixing because of continuous drop break up. However, the variation in the average drop size was reduced with time so that a quasi steady state could be assumed. The size of drops is determined as a result of a balance between drop break up and coalescence. During the steady state, the average size of drops remains constant despite a continuous drop breakage and coalescence. This has been called a *dynamic equilibrium*. At a high stabiliser concentration, all stages overlapped so that the drops formed after the transition stage were maintained in the reaction medium and were gradually converted to polymer beads with the least interaction with other particles. This was called a "*static steady state*".

- *Growth stage* during which the rate of drop break up considerably falls below the rate of drop coalescence due to the viscosity build up in drops leading to the drop enlargement and PSD broadening. Traditionally a *critical conversion* or *viscosity* has been used to identify the beginning of the growth stage. Results show that the onset of the growth stage may not be fixed and it depends on the balance of the forces acting on drops. The onset of the growth stage in terms of time was advanced with decreasing stirring speed and PVA concentration and increasing monomer hold up. These variations were associated with a decrease in the rate of drop break up and/or increase in the rate of drop coalescence. The onset of the growth stage in terms of conversion was delayed with increasing initiator concentration because of the formation of a low-molecular-weight polymer. The magnitude of the growth stage became more severe with increasing monomer hold up and decreasing PVA concentration.

- *Identification stage* during which a solid-liquid suspension is attained and PSD and mean particle size remain unchanged afterwards. The onset of this stage appears to be fairly constant for different formulations.

3. Satellite droplets

Satellite droplets were found to form continuously with time in non-reacting systems. A similar behaviour was observed for the reacting systems, but the population of satellite droplets declines significantly after the onset of the growth stage due to instability. With a high concentration of the stabiliser, the growth stage was damped and as a result satellite droplets could have more chance to survive in the system. Water-soluble inhibitors hindered the formation of satellite particles by an emulsion polymerisation mechanism and thus improved the stability of the suspension so that smaller particles could be obtained.

4. Modelling

A population balance model was developed to track the evolution of drop/particle size variation in the course of polymerisation. The time variation in the rheological properties of the polymerising drop was taken into consideration by coupling of the detailed kinetic model of the MMA polymerisation with the population balance model. The following conclusions can be drawn from the modelling section:

- The population balance model developed could qualitatively reproduce the characteristic intervals of non-reacting monomer dispersions (transient and quasi steady-state stages) and reacting monomer dispersions (transition, quasi steady-state , growth and identification stages).

- The transient stage of suspension polymerisation reactions was, for the first time, modelled.

- The agreement between the experimental data and predicted behaviour was, in most cases, satisfactory. The fit can be improved by completion of the model with new routines, in particular for satellite droplet formation, and by optimisation of the adjustable parameters.

RECOMMENDATIONS FOR FURTHER WORK

The results obtained and the conclusions drawn from this research project have increased the understanding of evolution of particle size average and distribution in suspension polymerisation reactions. It is recommended that the following tasks should be undertaken to widen the scope of understanding drop behaviour.

1- Two-stage addition of stabiliser should be implemented for other types of stabilisers as the results appeared to be promising for control of particle size.

2- The effect of viscosity on the evolution of drop size as well as its effect on the formation of satellite droplets should be further investigated.

3- The underlying mechanism for the role of oil-soluble inhibitors in the stability of polymerising drops should be investigated.

4- Research should be directed at more in depth investigation of satellite droplet formation in suspension polymerisation reactors as these tiny off-spec particles were found to be a main cause for the drop instability by adsorbing a large quantity of the stabiliser.

5- The formation of flocculates at high polymer conversion deserves a thorough investigation.

6- Non-homogeneity considerations have to be taken into account since the quality of agitation, especially in large scale reactors, is characterised by the average as well as the local energy dissipation rate. Computational Fluid Dynamics (CFD), coupled with PBM, provides a powerful tool to simulate the turbulent field and to predict the evolution of DSD/PSD in suspension polymerisation reactors. The modelling will be of great potential in resolving of the underlying mechanism of satellite drop formation.

NOMENCLATURE

a	interfacial area per aqueous phase volume unit
a_b, a_c	adjustable parameters of break up and coalescence efficiencies, respectively
b	rate of drop break up, 1/sec (equation 4.1.3)
b_c	adjustable parameter of coalescence efficiency
c	rate of drop coalescence, 1/sec (equation 4.1.12)
c	concentration, kg/m^3
C	constant in equations 1.1.1, 1.1.2, 1.1.7, 1.1.17
C_f	chain-transfer constant of monomer
C_s	chain-transfer constant of chain-transfer agent
d	drop/particle diameter, m
d_{32}	Sauter mean diameter, m
D_I	impeller diameter, m
d_{max}	maximum drop size, m
d_{min}	minimum drop size, m
d_n	number average diameter, m
D_T	tank diameter, m
d_v, d_w	volume and weight average diameters, respectively, m
e	energy, J
E	activation energy, J
E	Young's elasticity modulus
f	initiator efficiency
$F(v,t)$	drop volume distribution
$F(d_v,t)$	drop diameter distribution
F	viscosity parameter defined by equation 1.3.8
G	Gibbs free energy, J (equations 4.3.5, 4.3.6)
I	initiator
k	reaction rate constant, 1/sec
K	constant in equations 1.1.8, 1.1.9, 1.1.12
k_b, k_c	adjustable parameters of break up and collision frequencies, respectively
k_m	overall mass transfer coefficient of monomer from the aqueous phase to the drops
l	macroscale of turbulence, m
$m_{i,j}$	ratio of the molar volumes of species i and j (equations 4.3.5, 4.3.6)
M	monomer

M_m Monomer molecular weight, kg/kgmol

M_n, M_w cumulative number and weight average molecular weights of polymer, kg/kgmol

N number of drops/particles (N_t : total number of drops/particles)

N_I agitation speed, 1/sec

N_p Power Number (equation 4.1.5)

P polymer

R Universal gas constant, J/mol.K

$\overset{\circ}{R}$ free-radical

R_p rate of polymerisation, mol/m^3.sec

Re Reynolds Number

S chain-transfer agent

s_{eq} equilibrium water solubility (wt%)

t time, sec

T temperature, °C

T_g glass-transition temperature, °C

t_i, t_c contact and coalescence times, sec (equation 1.1.10)

u mean turbulent velocity, m/sec (equations 1.1.1, 1.1.2)

u average number of daughter drops formed by breaking of a mother drop

v, v' drop/particle volume, m^3

V volume of the polymerisation locus or dispersed phase, m^3 (equation 1.2.11)

V_e elasticity parameter defined in equation 4.1.8b

V_f free volume of the reaction mixture

V_t total volume of the reactor content, m^3

Vi viscosity group defined by equation 1.1.6

W weight, kg

We Weber Number

x conversion of monomer to polymer

x_{ds} volume ratio of daughter to satellite drops (equations 4.1.10, 4.1.11)

X_n, X_w number and weight average degrees of polymerisation

Y_0 elasticity parameter defined by equation 4.1.8b

Greek letters

α elasticity parameter defined by equation 4.1.8c

α thermal expansion coefficient, 1/°C

β daughter drop volume distribution (equation 1.3.11a)

β polymer molecular weight parameter defined by equation 1.3.2c

ε average energy dissipation rate, m^2/sec^3 (equation 1.1.4)

ε_p volume contraction factor (equation 1.2.10)

ζ viscosity parameter defined by equation 1.3.8

η microscale of turbulence, m (equation 1.1.3)

θ surface coverage of drops/particles (equation 4.1.19b)

Θ elasticity parameter defined by equation 4.1.8c

λ efficiency of drop break up and coalescence

λ moment of free-radical chains, mol/m^3

μ moment of dead-polymer chains, mol/m^3

μ viscosity, kg/m.sec

ν kinematic viscosity, m^2/sec

ρ density, kg/m^3

σ interfacial tension, N/m

σ_v standard deviation (equation 3.1.11)

τ polymer molecular weight parameter defined by equation 1.3.2c

ϕ volume fraction

χ solubility interaction parameter (equations 4.3.5, 4.3.6)

ω drop break up and collision frequency, 1/sec (equations 4.1.6, 4.1.13)

Ω efficiency parameter defined by equation 4.1.7

Subscripts

a aqueous phase

b break up

c coalescence

d dispersed phase - daughter drop – initiation reactions

f transfer to monomer reactions

m monomer

p polymer - propagation reactions

s suspending agent - satellite droplet

t termination reactions

u,v,v' drop/particle volume

REFERENCES

Abrahamson, J. "Collision rates of small particles in a vigorously turbulent fluid." Canadian J. Chem. Eng., 72, 185-193 (1975).

Adams, M.E., Casey, B.S., Mills, M.F., Russell, G.T., Napper, D.H., Gilbert, R.G. "High conversion emulsion, dispersion, and suspension polymerization" Makromol. Chem., Macromol. Symp., 35/36, 1-12 (1990).

Adamson, A.W. "Physical chemistry of surfaces" Wiley, New York (1976).

Alexopoulos, A.H., Maggioris, D., Kiparissides, C. "CFD analysis of turbulence non-homogeneity in mixing vessels: A two-compartment model" Chem. Eng. Sci., 57, 1735-1752 (2002).

Ali, A.M., Yuan, H.H.S., Dickey, D.S., Tatterson, G.B. "Liquid dispersion mechanisms in agitated tanks. I: Pitched-blade turbine" Chem. Eng. Commun., 10(4-5), 205-213 (1981).

Almog, Y., Levy, M. "Effect of initiator on the molecular weight distribution in dispersion polymerization of styrene" J. Polym. Sci., Polym. Chem. Ed., 18, 1-11 (1980).

Alopaeus, V., Koskinen, J., Keskinen, K.I., Majander, J. "Simulation of the population balances for liquid-liquid systems in a nonideal stirred tank. Part 2 - parameter fitting and the use of the multiblock model for dense dispersions" Chem. Eng. Sci., 57(10), 1815-1825 (2002).

Alvarez, J., Alvarez, J.J., and Hernandez, M. "A Population balance approach for the description of particle size distribution in suspension polymerisation reactors." Chem. Eng. Sci., 49(1), 99-113 (1994).

Alvarez, J., Alvarez, J.J., and Martinez, R.E. "Conformation of the particle size distribution in suspension polymerisation. The role of kinetics, polymer viscosity and suspension agent." J. Appl. Polym. Sci., Appl. Polym. Symp., 49, 209-221 (1991).

Arai, K., Konno, M., Matunaga, Y., and Saito, S. "Effect of dispersed-phase viscosity on the maximum stable drop size for breakup in turbulent flow." J. Chem. Eng. Japan, 10(4), 325-330 (1977).

Arshadi, R. "Suspension, emulsion, and dispersion polymerization: A methodological survey." Colloid Polym. Sci., 270, 717-732 (1992).

Azad, A.R.M., Fitch, R.M. "Particle size distribution in suspension polymerizations: Effect of low molecular weight compounds" In Polymer Colloids II, Fitch, R.M. (Ed.), Plenum Press, New York, 95-119 (1978).

Bae, J.H., Tavlarides, L.L. "Laser capillary spectrophotometry for drop-size concentration measurements" A.I.Ch.E. J., 35(7), 1073-1084 (1989).

Baillagou, P.E., Soong, D.S. "A viscosity constitutive equation for PMMA MMA solutions" Chem. Eng. Commun., 33(1-4), 125-1343 (1985a).

Baillagou, P.E., Soong, D.S. "Free-radical polymerization of methyl-methacrylate in tubular reactors" Polym. Eng. Sci., 25(4), 212-231 (1985b).

Bevington, J.C., Hunt, B.J., Warburton, J. "Effects of stabilized radicals upon polymerisations initiated by benzoyl peroxide" Polymer, 44, 3469-3475 (2003).

Bevington, J.C., Warburton, J., Hunt, B.J. "Effects of stabilized radicals upon polymerisations initiated by benzoyl peroxide" J. Macromol. Sci.,, A. Chem., 39(1), 295-303 (2002).

Bhargava, G.S., Khan, H.U., and Bhattacharyya, K.K. "SAN copolymer by suspension polymerisation. II. Bead size distribution and molecular weight." J. Appl. Polym. Sci., 23, 1181-1187 (1979).

Bird, R.B., Armstrong, R.C., Hassager, O. "Dynamics of polymer liquids" Wiley, New York (1977).

Borwankar, R.P., Chung, S.I., Wasan, D.T. "Drop sizes in turbulent liquid-liquid dispersions containing polymeric suspension stabilizers.1. The breakage mechanism" J. Appl. Polym. Sci. ,32(7), 5749-5762 (1986).

Bourne, J.R., Yu, S. "Investigation of micromixing in stirred tank reactors using parallel reactions" Ind. Eng. Chem. Res., 33, 41-55 (1994).

Brandrup, J., Immergut, E.H., Grulke, E.A. (Eds) "Polymer Handbook", 4th Ed., Wiley, New York, II/43 (1999).

Brooks, B.W. "Basic aspects and recent developments in suspension polymerisation." Makromol. Chem., Macromol. Symp., 35/36, 121-140 (1990).

Brown, D.E., Pitt, K., paper presented at CHEMECA, Australia (1970).

Brown, D.E., Pitt, K., Chem. Eng. Sci., 29, 345-350 (1974).

Calabrese, R.V., Chang, T.P.K. and Dang, P.T. "Drop breakup in turbulent stirred-tank contactors. Part I: Effect of dispersed phase viscosity." AIChE J., 32(4), 657-666 (1986a).

Calabrese, R.V., Wang, C.Y., and Bryner, N.P. "Drop breakup in turbulent stirred-tank contactors. Part III: Correlations for mean size and drop size distribution." AIChE J., 32(4), 677-681 (1986b).

Calderbank, P.H., Inst. Chem. Eng., 36, 443 (1958).

Castellanos, J.R., Mendizabal, E., and Puig, J.E. "A quick method for choosing a protecting colloid for suspension polymerization." J. Appl. Polym. Sci., Appl. Polym. Symp., 49, 91-101 (1991).

Chang, T.P.K., Sheu, Y.H.E., Tatterson, G.B., Dickey, D.S. "Liquid dispersion mechanisms in agitated tanks. II: Straight-blade and disk style turbines" Chem. Eng. Commun., 10(4-5), 215-222 (1981).

Chatzi, E.G., Boutris, C.J., Kiparissides, C. "On-line monitoring of drop size distributions in agitated vessels: 2. Effect of stabilizer concentration." Ind. Eng. Chem. Res., 30, 1307-1312 (1991).

Chatzi, E.G., Gavrielides, A.D., Kiparissides, C. "Generalized model for prediction of the steady-state drop size distribution in batch stirred vessels." Ind. Eng. Chem. Res., 28, 1704-1711 (1989).

Chatzi, E.G., and Kiparissides, C. "Drop size distributions in high holdup fraction dispersion systems: effect of the degree of hydrolysis of PVA stabiliser." Chem. Eng. Sci. 49(24B), 5039-5052 (1994).

Chatzi, E.G., and Kiparissides, C. "Dynamic simulation of bimodal drop size distributions in low-coalescence batch dispersion systems." Chem. Eng. Sci., 47(2), 445-456 (1992).

Chatzi, E.G., and Kiparissides, C. "Steady-state drop size distributions in high holdup dispersion systems." AIChE J., 41(7), 1640-1652 (1995).

Chatzi, E.G., Lee, J.M. "Analysis of interactions for liquid-liquid dispersions in agitated vessels" Ind. Eng. Chem. Res., 26, 2263-2267 (1987).

Chen, H.T., Middleman, S., A.I.Ch.E. J., 13, 989 (1967).

Chen, Z., Pauer, W., Moritz, H.U., Pruss, J., Warnecke, H. "Modeling of the suspension polymerisation process using a particle population balance" Chem. Eng. Tech., 22, 609-616 (1999).

Chesters, A.K. "The modelling of coalescence process in fluid-liquid dispersions: A review of current understanding. *Transactions of the Institution of Chemical Engineering* (Part A) 69, 259-270 (1991).

Chiu, W.Y., Carratt, G.M., and Soong, D.S. "A computer model for the gel effect in free-radical polymerization." Macromolecules, 16, 348-357 (1983).

Clark, M.M. "Drop breakup in a turbulent-flow.2. Experiments in a small mixing vessel" Chem. Eng. Sci., 43(3), 681-692 (1988).

Colvin, M., Chung, S.K., Hyson, M.T., Chang, M., Rhim, W.K. "A new method for the production of large spherical monosized polymer particles for biomedical and chromatographic applications" J. Polym. Sci., Part A: Polym. Chem., 28, 2085-2095 (1990).

Coulaloglou, C.A. and Tavlarides, L.L. "Drop size distributions and coalescence frequencies of liquid-liquid dispersions in flow vessels." AIChE J., 22(2),289-297 (1976).

Coulaloglou, C.A. and Tavlarides, L.L. "Description of interaction processes in agitated liquid-liquid dispersions." Chem. Eng. Sci., 32(1),1289-1297 (1977).

Clark, M.M. "Drop breakup in a turbulent flow-II. Experiments in a small mixing vessel" Chem. Eng. Sci., 43(3), 681-692 (1988).

Cui, Y.Q., Van der Lans, R.G.J.M., Noorman, H.J., and Luyben, K.Ch.A.M. "Compartment mixing model for stirred reactors with multiple impellers." Trans. Inst. Chem. Eng., 74, Part A, 261-271 (1996).

Cunningham, M.F. "Microsuspension polymerization of methyl methacrylate." Polym. React. Eng., 7(2), 231-257 (1999).

Cunningham, M.F., Geramita, K., Ma, J.W. "Measuring the effects of dissolved oxygen in styrene emulsion polymerization" Polymer, 41, 5385-5392 (2000).

Cunningham, M.F., Mahabadi, H.K., and Wright, H.M. "Supermicron polymer particles with core-shell type morphology." J. Polym. Sci., Part A: Polym. Chem., 38, 345-351 (2000).

Davies, J.T. "Turbulence phenomena" Academic Press, New York (1972).

Delichatsios, M.A., and Probstein, R.F. "The effect of coalescence and the average drop size in liquid-liquid dispersions." Ind. Eng. Chem. Fundam., 15(2), 134-138 (1976).

Diamant, H., Ariel, G., Andeman, D. "Kinetics of surfactant adsorption: The free energy approach" Colloids and Surfaces, 259, 183-185 (2001).

Dimonie, M.V., Boghina, C.M., Marinescu, N.N. "Inverse suspension polymerization of acrylamide" Eur. Polym. J., 18, 639-645 (1982).

Doulah, M.S. "An effect of holdup on drop sizes in liquid-liquid dispersions." Ind. Eng. Chem. Fundam., 14(2), 137-138 (1975).

Dowding, P.J., Goodwin, J.W., and Vincent, B. "Production of porous Ssspension polymers using a continuous tubular reactor." Colloid and Polymer Science, 278(4), 346-351 (2000).

Dowding, P.J., and Vincent, B. "Suspension polymerisation to form polymer beads." Colloids and Surfaces. A: Physicochemical and Engineering Aspects, 161, 259-269 (2000).

Fan, S., Gretton-Watson, S.P., Steinke, J.H.G., Alpay, E. "Polymerisation of methyl methacrylate in a pilot-scale tubular reactor: modelling and experimental studies" Chem. Eng. Sci., 58, 2479-2490 (2003).

Ferry, J.D. "Viscoelastic properties of polymers", 3rd ed., Wiley, New York (1980).

Fitch, R.M., Prenosil, M.B., Sprick, K.J. "The mechanism of particle formation in polymer hydrosols. 1. Kinetics of aqueous polymerization of methyl methacrylate" J. Polym. Sci., Part C, 27, 95-118 (1969).

Gandhi, K.S., Kumar, R. "An elongational flow model for drop breakage in stirred turbulent dispersions" Chem. Eng. Sci., 45, 2998-3001 (1990).

Godfrey, J.C., Reeve, RN., Grilc, V., Inst. Chem. Eng., Symp. Ser., 89, 107-126 (1984).

Goodall, A.R., and Greenhill-Hooper, M.J. "Characterisation of partially-hydrolysed poly(vinyl acetate)s for use as stabilisers in suspension polymerisation." Makromol. Chem., Makromol. Symp., 35/36, 499-507 (1990).

Hamielec, A.E., and Tobita H. "Polymerization Processes." Ullmann's Encyclopedia of Industrial Chemistry. VCH Publishers Inc., New York, Vol. A21, 305-428 (1992).

Hashim, S. "Drop mixing in suspension polymerisation." Ph.D. thesis, Chemical Engineering Department, Loughborough University, Loughborough, UK (2001).

Hatate, Y., Ikari, A., Kondo, K., Nakashio, F. "Change of size distribution of polymer droplets with time in styrene suspension polymerisation under ultrasonic irradiation" Chem. Eng. Commun., 34, 325-333 (1985).

He, Y., Howes, T., Litster, J.D., and Ko, G.H. "Experimental study of drop-interface coalescence in the presence of polymer stabilisers" Colloids and Surfaces, A: Physicochemical and Engineering aspects, 207, 89-104 (2002).

Hinze, J.O. "Fundamentals of the hydrodynamics mechanism of splitting in dispersion processes." AIChE J., 1, 950-956 (1955).

Hinze, J.O. "Turbulence: an introduction to mechanism and theory." 2nd Ed., McGrow-Hill, Toronto (1987).

Hocq, S., Milot, J.F., Gourdon, C., Casamatta, G. "Electrical-conductivity capillary technique-A new method for bivariate drop-size concentration distribution measurements" Chem. Eng. Sci., 49(4), 481-489 (1994).

Hong, P.O. Lee, J.M. "Changes of the average drop sizes during the initial period of liquid-liquid dispersions in agitated vessels" Ind, Eng. Chem. Proc. Des. Dev., 24, 868-872 (1985).

Howarth,W.J. "Coalescence of drops in a turbulent flow field." Chem. Eng. Sci., 19,33-38 (1964).

Huo, B.P., Campbell, J.D., Penlidis, A., Macgregor, J.F. "Effect of impurities on emulsion polymerization: Case II kinetics" J. Appl. Polym. Sci., 35, 2009-2021 (1987).

Ivanov, I.B., Dimitrov, D.S., Somasundaran, P., Jain, R.K. "Thinning of films with deformable surfaces: diffusional-controlled surfactant transfer" Chem, Eng., Sci., 40, 137-150 (1985).

Jahanzad, F., Kazemi, M.M., Sajjadi, S., Taromi, F.A. "n-Dodecyl mercaptan transfer constant in polymerization of methyl methacrylate" Polymer, 34(16), 3542-3544 (1993).

Jahanzad, F., and Sajjadi, S. "SAN copolymers by suspension polymerisation." Internal report (in Persian), Iran Polymer Institute, Tehran, Iran (2000).

Jo, Y., Park, K., Ahn, J., Ihm, S. "Hollow gelular beads of styrene-divinylbenzene copolymer prepared by suspension polymerisation" Eur. Polym. J., 32(8), 967-972 (1996).

Johnson, G.R. "Effects of agitation during VCM suspension polymerization" J. Vinyl Tech., 2, 138-143 (1980).

Kalfas, G., and Ray, W.H. "Modeling and experimental studies of aqueous suspension polymerization processes. I. Modeling and simulation." Ind. Eng. Chem. Res., 32, 1822-1830 (1993).

Kalfas, G., Yuan, H., and Ray, W.H. "Modeling and experimental studies of aqueous suspension polymerization processes. II. Experiments in batch reactors." Ind. Eng. Chem. Res., 32, 1831-1838 (1993).

Kim, N., Sudol, E.D., Dimonie, V.L., El-Aasser, M.S. "Poly(vinyl alcohol) stabilization of acrylic emulsion polymers using the miniemulsion approach" Macromolecules, 36(15), 5573-5579 (2003).

Kolmogoroff, A.N. "The local structure of turbulence in incompressible viscous fluid for very high Reynolds numbers." C.R. Acad. Sci. USSR, 30, 301 (1941).

Konno, M., Aoki, M., Saito, S. "Scale effect on breakup processin liquid-liquid agitated tanks" J. Chem. Eng. Japan, 16(4), 312-319 (1983).

Konno, M., Arai, K., Saito, S. "The effect of stabilizer on coalescence of dispersed drops in suspension polymerization of styrene." J. Chem. Eng. Japan, 15(2), 131-135 (1982).

Konno, M., Muto, T., Saito, S. "Coalescence of drops in an agitated tank" J. Chem. Eng. Japan, 21(4), 335-338 (1988).

Koshy, A., Das, T.R., and Kumar, R. "Effect of surfactants on drop breakage in turbulent liquid dispersions." Chem. Eng. Sci., 43, 649-654 (1988a).

Koshy, A., Das, T.R., Kumar, R., and Gandhi, K.S. "Breakage of viscoelastic drops in turbulent stirred dispersions." Chem. Eng. Sci., 43, 649-654 (1988b).

Kumar, S., Kumar, R., Gandhi, K.S. "Alternative mechanisms of drop breakage in stirred vessels" Chem. Eng. Sci., 46, 2483-2489 (1991).

Kuriyama, M., Ono, M., Tokanai, H., Konno, H. "The number of daughter drops formed per breakup of a highly viscous mother-drop in turbulent flow" J. Chem. Eng. Japan, 28(4), 477-479 (1995).

Lagisetty, J.S., Das, P.K., and Kumar, R. "Breakage of viscous and non-Newtonian drops in stirred dispersions." Chem. Eng. Sci., 41(1), 65-72 (1986).

Lashares, J.C., Eastwood, C., Martinez-Bazan, C., Montanes, J.L. "A review of statistical models for the break-up of an immiscible fluid immersed into a fully developed turbulent flow" International Journal of Multiphase Flow, 28, 247-278 (2002).

Laso, M., Steiner, L., Hartland, S. "Dynamic simulation of liquid-liquid agitated dispersions.2. Experimental determination of breakage and coalescence rates in a stirred tank" Chem. Eng. Sci., 42(10), 2437-2445 (1987).

Lazrak, N., Le Bolay, N., Ricard, A. "Droplet stabilization in high holdup fraction suspension polymerisation reactors" Eur. Polym. J., 34, 1637-1647 (1998).

Lee, K.C., Song, B.K., Lee, D.J. "Inverse suspension polymerization of acrylamide" Polymer Korea, 25, 460-467 (2001).

Levich, V.G. "Physicochemical hydrodynamics." Prentice-Hall, NJ (1962).

Liu, S., and Li, D. "Drop coalescence in turbulent dispersions." Chem. Eng. Sci., 54, 5667-5675 (1999).

Ma, G.H., Fujuwara, J., Su, Z.G., Omi, S. "Synthesis and characterization of crosslinked uniform polymeric microspheres containing a polyimide prepolymer by a new emulsification process", J. Polym. Sci., Part A: Polym. Chem., 41, 2588-2598 (2003).

Ma, G.H., Su, Z.G., Omi, S., Sundberg, D., Stubbs, J. "Microencapsulation of oil with poly(styrene-N,N-dimethylaminoethyl methacrylate) by SPG emulsification technique: Effects of conversion and composition of oil phase." 266 (2), 282-294 (2003)

Machado R.A.F., Pinto J.C., Araujo P.H.H., Bolzan A. "Mathematical modeling of polystyrene particle size distribution produced by suspension polymerisation" Brazilian J. of Chem. Eng., 17, 395-405 (2000).

Maggioris, D., Goulas, A., Alexopoulos, A.H., Chatzi, E.G., Kiparissides, C. "Prediction of particle size distribution in suspension polymerization reactors: effect of turbulance nonhomogeneity." Chem. Eng. Sci., 55, 4611-4627 (2000).

Maggioris, D., Goulas, A., Alexopoulos, A.H., Chatzi, E.G., Kiparissides, C. "Use of CFD in prediction of particle size distribution in suspension polymer reactors." Computers and Chemical Engineering, 22(Suppl. S), S315-S322 (1998).

Mann, R., Pillai, S.K., El-Hamouz, A.M. Ying, P., Togatorop, A., and Edwards, R.B. "Computational fluid mixing for stirred vessels: progress from seeing to believing." Chem. Eng. J., 59, 39-50 (1995).

Mark, H.F. (editor) "Encyclopedia of polymer science and engineering" Wiley, New York, Vol. 13, 729-733 (1989).

Marten F.L., and Hamielec, A.E. "High-conversion diffusion-controlled polymerization of methyl methacrylate." Am. Chem. Soc. Symp. Ser., 104, 43 (1979).

Marten F.L., and Hamielec, A.E. "High-conversion diffusion-controlled polymerization of styrene." J. Appl. Polym. Sci., 27, 489-505 (1982).

Matsumoto, S., Takeshita, S., Koga, J., Takashima, Y. "A production process for uniform-size polymer particles" J. Chem. Eng. Jpn., 22, 691-693 (1989).

Mendizabal, E., Castellanos-Ortega, J.R., and Puig, J.E. "A method for selecting a polyvinyl alcohol as stabilizer in suspension polymerization." Colloids and Surfaces, 63, 209-217 (1992).

Mighri, F., Carreau, P.J., Aji, A. "Influence of elastic properties on drop deformation and breakup in shear flow" Journal of Rheology, 42(6), 1477-1490 (1998).

Mighri, F., Huneault, M.A. "Drop deformation and breakup mechanism in viscoelastic model fluid systems and polymer blends" Canadian J. Chem. Eng., 80(6), 1028-1035 (2002).

Mikos, A.G., Takoudis, C.G., and Peppas, N.A. "Reaction engineering aspects of suspension polymerization." J. Appl. Polym. Sci., 31, 2647-2659 (1986).

Mlynek, Y., Reshnick, W. "Drop sizes in an agitated liquid-liquid system" A.I.Ch.E. J., 18, 122 (1972).

Munzer M., and Trommsdorff, E. "Polymerization processes." Schildknecht, C.E., Skiest, I., Eds., Wiley, New York, pp.106 (1977).

Nambiar, D.K.R., Kumar, R., Das, T.R., Gandhi, K.S. "A two-zone model for breakage frequency of drops in stirred dispersions." Chem. Eng. Sci., 49(13), 2194-2198 (1994).

Narkis, M. "Size distribution of suspension-polymerized unsaturated polyester beads" J. Appl. Polym. Sci., 23, 2043-2048 (1979).

Ni, X., Brogan, G., Struthers, A., Bennett, D.C., Wilson, S.F. "A systematic study of the effect of geometrical parameters on mixing time in oscillatory baffled reactor" Che. Eng. Res. Des., 76(A5), 635-642 (1998).

Ni, X., Jian, H., Fitch, A. "Evaluation of turbulent integral length scale in an oscillatory baffled column using large eddy simulation and digital particle image velocimetry" Che. Eng. Res. Des., 81(A8), 842-853 (2003).

Ni, X., Johnstone, J.C., Symes, K.C., Grey, B.D., Bennett, D.C. "Suspension polymerisation of acrylamide in an oscillatory-baffled reactor: from drops to particles" A.I.Ch.E. J., 46, 1747-1757 (2001).

Ni, X., Zhang, Y., Mustafa I. "An investigation on droplet size and size distribution in methyl methacrylate suspensions in a batch oscillatory-baffled reactor" Chem. Eng. Sci., 53, 2903--2919 (1998).

Ni, X., Zhang, Y., Mustafa I. "Correlation of polymer article size with droplet size in suspension polymerisation of methyl methacrylate in a batch oscillatory-baffled reactor" Chem. Eng. Sci., 54, 841-850 (1999).

Nishikawa, M., Mori, F., Fujieda, S., and Kayama, T. "Scale-up of liquid-liquid phase mixing vessel" J. of Chem. Eng. of Japan, 20(5), 454-459 (1987).

Nishikawa, M., Mori, M., Kayama, T., Nishioka, S. "Drop size distribution in a liquid-liquid phase mixing vessel." J. Chem. Eng. Japan, 24, 88-94 (1991).

Odian, G. "Principles of polymerization." 3rd Ed., Wiley, New York (1991).

Okaya, T., Suzuki, A., Kikuchi, K. "Importance of grafting in the emulsion polymerization of MMA using PVA as a protective colloid. Effect of initiators" Colloids and Surfaces, A: Physicochemical and Engineering Aspects, 153, 123-125 (1999).

Okubo, M., Yamashita, T., Suzuki, T. "Production of micron-sized monodispersed composite polymer particles by seeded polymerization utilizing the dynamic swelling method." Colloid Polym. Sci., 275(3), 288-292 (1997).

Olayo, R., Garcia, E., Garcia-Corichi, B., Sanchez-Vazquez, L., and Alvarez, J. "Poly(vinyl alcohol) as a stabilizer in suspension polymerization of styrene: The effect of the molecular weight" J. Appl. Polym. Sci., 67, 71-77 (1998).

Oldshue, J.Y. "Fluid mixing Technology" McGrow-Hill, New York (1983).

Omi, S., Katami, K., Yamamoto, A., Iso, M. "Synthesis of polymeric microspheres employing SPG emulsification technique" J. Appl. Polym. Sci., 51, 1-11 (1994).

Pacek, A.W., Man, C.C., and Nienow, A.W. "On the Sauter mean diameter and size distribution in turbulent liquid/liquid dispersions in a stirred vessel." Chem. Eng. Sci., 53(11), 2005-2011 (1998).

Pacek, A.W., Nienow, A.W., Moore, I.P.T. "On the structure of turbulent liquid-liquid dispersed flow in an agitated vessel." Chem. Eng. Sci., 49(20), 3485-3498 (1994).

Park, J.Y., and Blair, L.M. "The effect of coalescence on drop size distribution in an agitated liquid-liquid dispersion" Chem. Eng. Sci., 300, 1057-1064 (1975).

Polacco, G., Palla, M., Semino, D. "Evolution of particle size distribution during suspension polymerisation: theory and experiments" Dynamic and Control of Process Systems, 1-2, 271-276 (1998).

Polacco, G., Semino, D., Rizzo, C. "Feasibility of methyl methacrylate polymerisation for bone cement by suspension polymerisation in a gel phase" J. Mater. Sci.: Mater. Med., 5, 587-591 (1994).

Ravera, F., Ferrari, M., Liggieri, L. "Adsorption and portioning of surfactants in liquid-liquid systems" Advances in Colloid and Interface Science, 88, 129-177 (2000).

Rempp, P., and Merrill, E.D. "Polmyer synthesis." 2nd Rev. Ed., Huthig and Wepf., Basel (1991).

Ross, S.L., Verkhoff, F.H., and Kurl R.L. "Droplet breakage and coalescence processes in an agitated dispersion." Ind. Eng. Chem. Fundam. 17(2), 101-108 (1978).

Rushton, J.H., Costich, E.W., and Everett, H.J. "Power characteristics of mixing impellers: Part I." Chem. Eng. Prog., 46, 395-404 (1950).

Sajjadi, S., and Fazeli, N. "Particle size distribution in suspension polymerisation processes." Internal report (in Persian), Iran Polymer Institute, Tehran, Iran (1994).

Sax, N.I., Lewis, R.J. "Hawley's Condensed Chemical Dictionary" 11th Ed., Van Nostrand Reinhold Co., New York, NY, p. 184 (1989).

Shinnar, R. "On the behaviour of liquid dispersions in mixing vessels." J. Fluid Mech., 10, 259-275 (1961).

Shinnar, R. and Church, J.M. "Predicting particle size in agitated dispersions." Ind. Eng. Chem., 52(3), 253-256 (1960).

Sovova,H. "Breakage and coalescence of drops in a batch stirred vessel- I. Comparison of continuous and discrete models." Chem. Eng. Sci., 36(1),163-171 (1981).

Sprow, F.B. "Distribution of drop size produced in turbulent liquid-liquid dispersion." Chem. Eng. Sci., 22, 435 (1967).

Tanaka, M., Hosogai, K. "Suspension polymerisation of styrene with circular loop reactor" J. Appl. Polym. Sci., 39, 955-966 (1990).

Tavlarides, L.L., and Stamatoudis, M. "The analysis of interphase reactions and mass transfer in liquid-liquid dispersions." Adv. Chem. Eng., 11, 199-273 (1981).

Tsouris, C., Tavlarides, L.L. "Hold-up (volume fraction) measurements in liquid-liquid dispersions using an ultrasonic technique response" Ind. Chem. Eng. Res., 33(3), 748-749 (1994).

Tulig, J.T., Tirrell, M. "Toword a molecular theory of the trommsdorff effect." Macromolecules, 14,1501-1511 (1981).

Ugelstad, J., Mork, P.C., Kaggerud, K.H., Berge, A., Ellingsen, T. "Swelling of oligomer-polymer particles, new methods of preparation of emulsions and polymer dispersions." Adv. Colloid Interface Sci., 13, 101 (1980).

Valadez-Gounzález, A. M.E. Thesis (In Spanish), Unidad de Ciencias Basicas e Ingenieria, Universidad Autonoma Metropolitana, Plantel Iztapalapa, Mexico D.F., Mexico (1988).

Van Den Boomgaard, T., King, T.A., Tadros, T.F., Tang, H., Vincent, B. "The influence of temperature on the adsorption and adsorbed laeyr thickness of various molecular weight fractions of poly(vinyl alcohol) on polystyrene latex particles" Journal of Colloid and Interface Science, 66(1), 68-76 (1978).

Van Heuven, J.W., Beek, W.J., Paper No. 51, Proceeding of International Solvent Extraction Conference, Amsterdam (1971).

Van Heuven, J.W., Hoevenaarj, J.C., Proceeding of 4th International Symposium on Reactor Engineering, Bruxelles (1969).

Villalobos, M.A., Hamielec, A.E., and Wood, P.E. "Bulk and suspension polymerization of styrene in the presence of *n*-pentane. An evaluation of monofunctional and bifunctional initiation." J. Appl. Polym. Sci., 50, 327-343 (1993).

Vivaldo-Lima, E., Wood, P.E., Hamielec, A.E., and Penlidis, A. "An update review on suspension polymerization." Ind. Eng. Chem. Res., 36, 939-965 (1997).

Vivaldo-Lima, E., Wood, P.E., Hamielec, A.E., Penlidis, A. "Calculation of the particle size distribution in suspension polymerization using a compartment-mixing model" The Canadian J. of Chem. Eng., 76, 495-505 (1998).

Wang, Z.P., and Brooks, B.W. "Drop stabilisation by inorganic solids in suspension polymerisation – Modification by electrolytes using a wax model." Polymer Int., 28(3), 239-244 (1992).

Wang, Z.P., and Brooks, B.W. "Drop stabilisation by inorganic solids in suspension polymerisation – Effect of inorganic particle-size using a wax model." Polymer Int., 30(3), 317-326 (1993).

Wedlock, D.J. "Colloid and surface engineering: Applications in the process industries." Edited by Williams, R.A., Butterworth-Heinemann, Oxford (1992).

Yamazaki, N., Naganuma, K., Nagai, M., Ma, G.H., Omi, S. "Preparation of W/O (water-in-oil) emulsions using a PTFE (polytetrafluoroethylene) membrane- A new emulsification device" J. Dispersion Sci. Tech., 24, 249-257 (2003).

Yamazaki, N., Yuyama, H., Nagai, M., Ma, G.H., Omi, S. "Comparison of membrane emulsification obtained using SPG (Shirasu porous glass) and PTFE [poly(tetrafluoroethylene)] membranes" J. Dispersion Sci. Tech., 23, 279-292 (2002).

Yang, B., Takahashi, K., and Takeishi, M. "Styrene drop size and size distribution in an aqueous solution of poly(vinyl alcohol)." Ind. Eng. Chem. Res., 39, 2085-2090 (2000).

Yang, B., Takahashi, K., and Takeishi, M. "Unsteady stirring method used in suspension polymerization of styrene." J. Appl. Polym. Sci., 82, 1873-1881 (2001).

Yuan, H.G., Kalfas, G., and Ray, W.H. "Suspension polymerization." J. Macromol. Sci., Rev. Macromol. Chem. Phys., C31(2&3), 215-299 (1991).

Yuyama, H., Hashimoto, T., Ma, G.H., Nagai, M., Omi, S. "Mechanism of suspension polymerization of uniform monomer droplets prepared by class membrane (Shirasu Porous Glass) emulsification technique" J. Appl. Polym. Sci., 78, 1025-1043 (2000).

Zerfa, M. "Vinyl chloride drop behaviour in suspension polymerisation reactors." Ph.D. thesis, Chemical Engineering Department, Loughborough University, Loughborough, UK (1994).

Zerfa, M., Brooks, B.W. "Experimental investigation of PVA adsorption at the vinyl chloride water interface in monomer suspension." Colloid and Surface A. Physicochemical and Engineering Aspects, 132(2-3), 267-273 (1998).

Zerfa, M., Brooks, B.W. "Prediction of vinyl chloride drop sizes in stabilised liquid-liquid dispersion." Chem. Eng. Sci., 51(12), 3223-3233 (1996).

Zhang, S.X., and Ray, W.H. "Modeling and experimental studies of aqueous suspension polymerization processes. III. Mass transfer and monomer solubility effects." Ind. Eng. Chem. Res., 36, 1310-1321 (1997).

Zhou, G., and Kresta, S.M. "Correlation of mean drop size and minimum drop size with the turbulence energy dissipation and the flow in an agitated tank." Chem. Eng. Sci., 53(11), 2063-2079 (1998).

Zhu, D.W. "Perflourocarbon fluids: universal suspension polymerization media." Macromolecules, 29, 2813-2817 (1996).

APPENDIX A

Experimental Reproducibility

A.1 Conversion

The monomer conversion was measured gravimetrically. *Figure A.1* compares the conversion-time variations of suspension polymerisation of MMA for two runs carried out at the same conditions. The reproducibility is satisfactory.

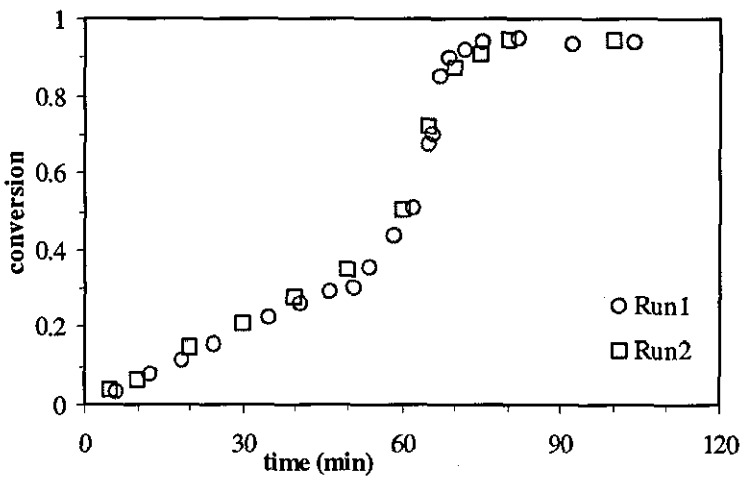

Figure A.1 Conversion-time variations for Run1 and Run2 at the same conditions: T = 70°C, N_I = 300 rpm, ϕ_d = 0.2, LPO = 1 wt%, PVA = 1 g/l.

A.2 Particle Size Distribution

A laser diffraction technique (Malvern, Coulter LS130) was used to measure drop/particle size distribution. The Sauter mean diameter was calculated using the output of the particle sizer. *Figure A.2* compares the time evolution of the Sauter mean diameter and the final PSDs in two runs at the same conditions. Good reproducibility is observed.

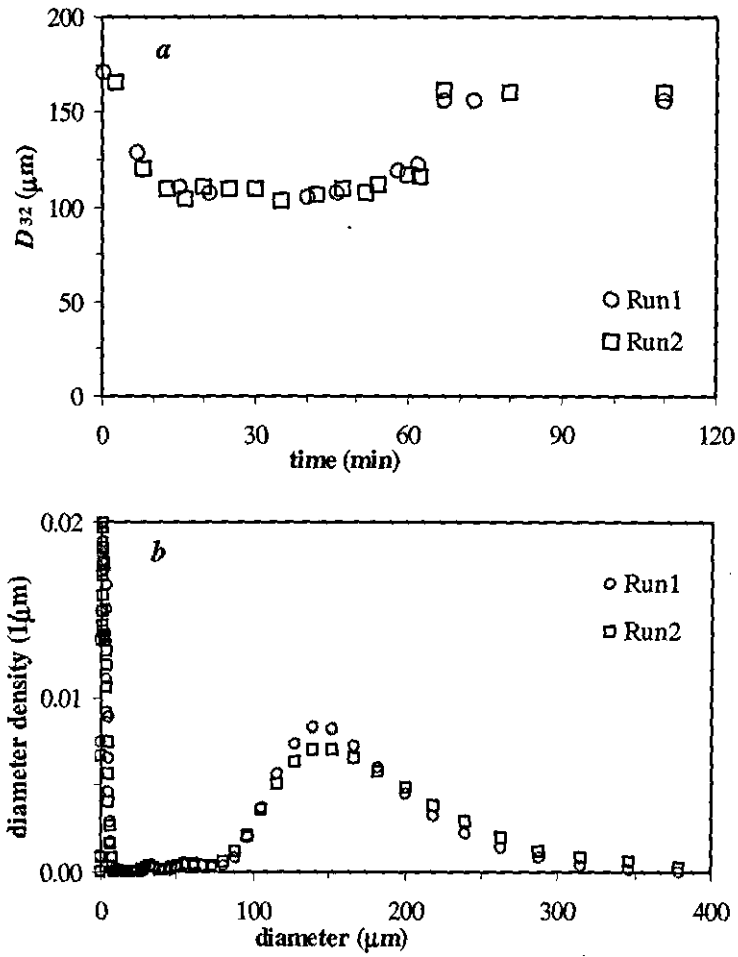

Figure A.2 Comparison of *a*) time evolution of Sauter mean diameter and *b*) final PSDs of Run1 and Run2 at the same conditions mentioned in the caption of Figure A.1.

APPENDIX B

Malvern Particle Sizer

The Laser Diffraction method of measuring particle size takes advantage of an optical principle which dictates that small particles in the path of a light beam scatter the light in characteristic, symmetrical pattern which can be viewed on a screen. Given a certain pattern of scattered light intensity as a function of angle to the axis of the incident beam ('flux pattern'), the distribution of particle sizes can be deduced. *Figure B.1* shows a schematic diagram of light scattering by the small particles in a laser diffraction particle sizer.

The simplest flux pattern, that from a monomodal dispersion of spheres, consists of a central bright spot (known as the Airy disk), surrounded by concentric dark and bright rings whose intensity diminishes further from the centre of the pattern, that is at higher scattering angles. The scattering angle at which the first dark ring, or diffraction minimum, occurs, depends on the size of the particles; the smaller the particle, the higher the angle of the first dark ring (or, alternatively, the larger the size of the Airy disk).

These flux patterns obey the rule of linear superposition. In other words, the pattern from a mixture of two (or more) monomodal dispersions of particles can be constructed by adding the intensity functions of the constituent particles in the mixture. The goal of a Laser Diffraction particle size measurement of course is to measure the flux pattern accurately enough to determine the distribution of particle sizes.

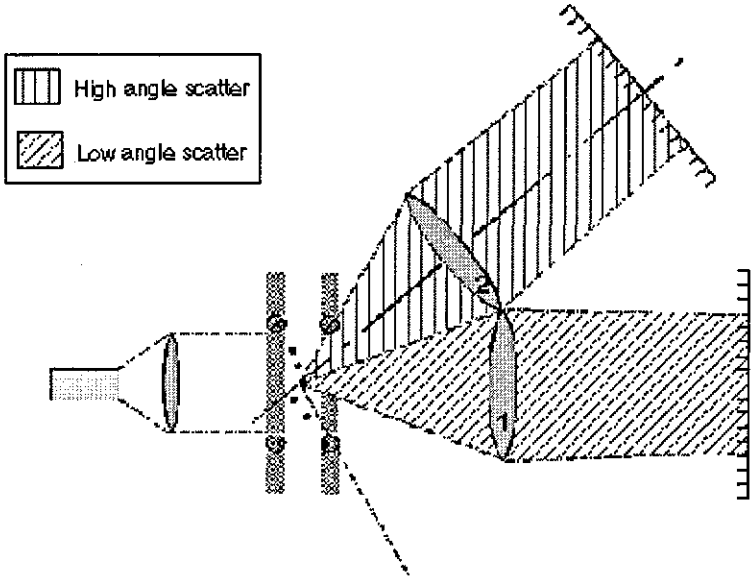

Figure B.1 Schematic diagram of light scattering by small particles.

APPENDIX C

Du Nouy Ring Tensiometry

Du Nouy ring tensiometry is one of the most widely used and effective methods of determining surface and interfacial tensions. The method is to measure the force required to pull a ring from the interface. *Figure C.1* shows the schematic diagram of the Du Nouy ring tensiometer. The ring is hanging on a microbalance. The force is measured directly using the microbalance to determine the apparent weight of a ring of platinum as it is pulled through the liquid-liquid interface.

The surface tension force (F) acts around the perimeter of the ring (on both sides) that is being withdrawn and is equal to the apparent weight force of the ring (mg):

$$F = 4\pi r\gamma = mg$$

where r is the radius of the ring. The interfacial tension (γ) can be easily calculated from the above equation.

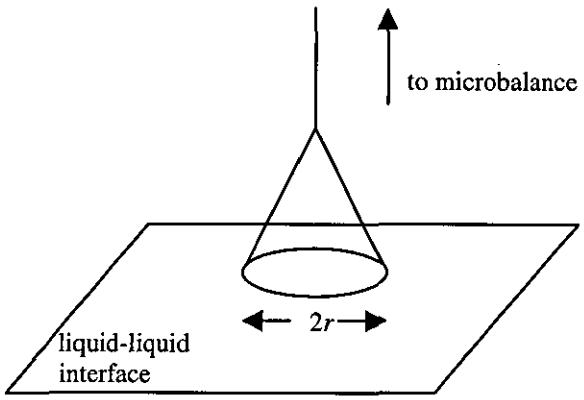

Figure C.1 Schematic diagram of Du Nouy ring tensiometer.

APPENDIX D

Gas-Liquid Chromatography

Gas-liquid chromatography is a method for quantitative and quantitative analysis of different components of mixtures. *Figure D.1* shows a schematic diagram of a typical gas-liquid chromatograph. Carrier gas from a cylinder of compressed gas first passes to a controller, the usual purpose of which is to maintain a constant flow of gas. The gas then passes to the *Column*, at the inlet to which is an *Injector* through which the sample to be analysed can be introduced. The carrier gas then elutes the components of the mixture through the column. At the far end is a device, the *Detector*, the purpose of which is to detect the separate components of the mixture as they emerge one by one. The detector useS some physical or chemical property (for example thermal conductivity) of the vapours by which they can be indicated and, if possible, measured. A further piece of apparatus is a *Flow controller* to measure and control of the rate of flow of gas.

There are two general types of column, *packed* and *capillary*. Capillary columns are more efficient than packed columns.

There are many detectors which can be used in gas-liquid chromatography. Different detectors give different types of selectivity. For example a *Flame Ionisation Detector* (FID) is suitable for detecting organic compounds.

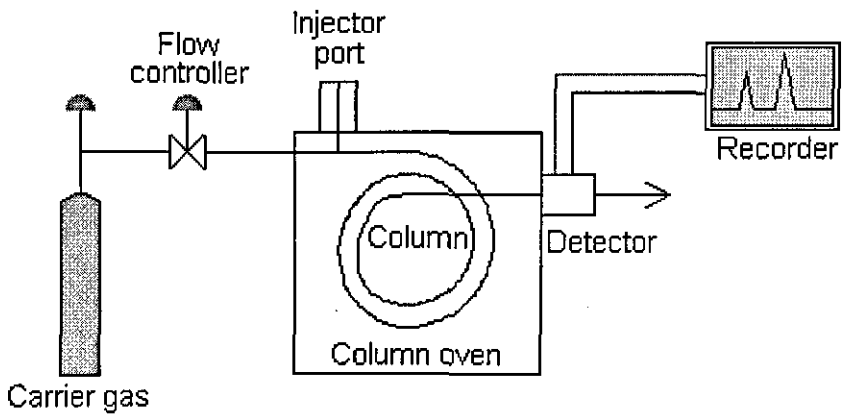

Figure D.1 Schematic diagram of a gas chromatograph

APPENDIX E

Suspension Polymerisation of Styrene

E.1 Introduction

A couple of experiments on the styrene/water dispersion and the styrene suspension polymerisation with PVA as stabiliser were carried out. The objective of this series was to verify that the characteristic intervals found for the MMA suspension polymerisation are universal and can apply to any monomer. It also included the verification of the formation of satellite droplets for a sparingly water-soluble monomer with PVA. In comparison with MMA, the suspension polymerisation of styrene has been more studied in the literature (e.g., Konno et al., 1982; Tanaka and Hosogai, 1990; Villalobos et al., 1993, Olayo et al., 1998;; Yang et al., 2001). A rather low rate of polymerisation for the styrene monomer provides more flexibility in sampling and measuring drop sizes during the polymerisation.

E.2 Experimental

The materials, and the experimental procedure and measurements have been described in detail in chapter 2. Styrene (analytical grade from Aldrich) was distilled under reduced pressure before using. Suspension polymerisation of styrene was carried out at 70°C. Monomer hold up and the agitation speed were 0.20 and 500 rpm, respectively. The concentration of PVA and LPO were 1.0 g/l (based on water phase) and 2.0wt% (based on monomer phase), respectively. Generally the formulation and the polymerisation conditions were similar to those used for the MMA suspension polymerisation. The corresponding non-reacting dispersion of styrene/water was also carried out.

E.3 Results and Discussion

Rate of Polymerisation: Figure E.1 shows the time variations of conversion for the suspension polymerisation of styrene. In comparison with the MMA monomer, the rate of polymerisation was rather low for the styrene monomer due to a low propagation rate constant. A very mild gel effect could be realised within the time interval of 400-450 min.

Mean Particle Size: Figure E.2 shows the time variations of the Sauter mean diameter of daughter drops (D_{32}) for the suspension polymerisation of styrene and the corresponding dispersion. The size of drops was exponentially reduced during the transition stage for both types of processes.

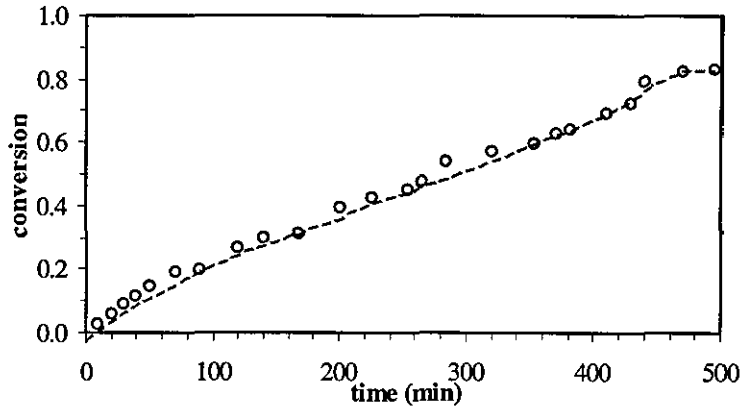

Figure E.1 Conversion-time variations in suspension polymerisation of styrene (for the conditions see section D.1).

The time evolution of D_{32} for the polymerising drops was coincident with that of the non-reacting drops for almost 30 min. This corresponds almost to that at a conversion of 0.10. It seems that the rate of drop break up is not much affected by the viscosity of drops until the conversion reaches 0.10. However, a difference is gradually developed after this conversion; the polymerising drops grow slightly with time, whereas the non-reacting drops remains almost constant in size. The size of polymerising drops shows a steep rise after 420 min (corresponding to the conversion of 0.70) from the start of polymerisation. That marks the onset of the growth stage.

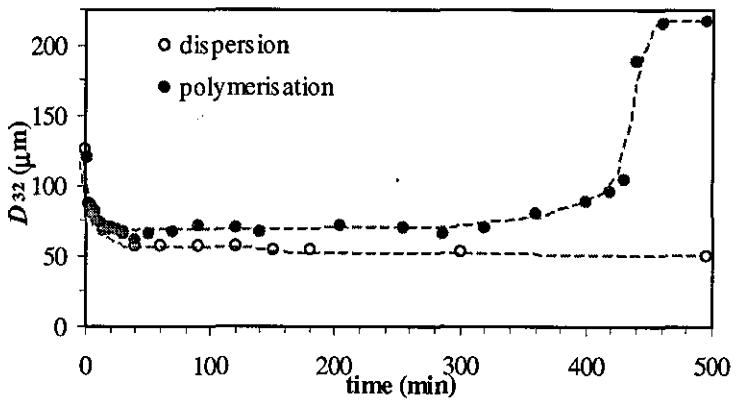

Figure E.2 Variations of D32 with time for suspension polymerisation of styrene and the corresponding dispersion.

It may be concluded that for monomers with a low rate of polymerisation, the transition stage for both polymerising and non-polymerising drops coincide. However, a gap is gradually developed with time during the so-called steady state as a result of growth of the polymerising drops due to the viscosity increase. The gap widens when the growth stage is reached.

Particle Size Distribution: Figure E.3 compares the time evolution of PSD/DSD in both processes. The early distributions were similar, but later distributions were quite different for the reasons explained above. The final PSD from the suspension polymerisation was very broad as a result of continuous drop coalescence during the growth stage.

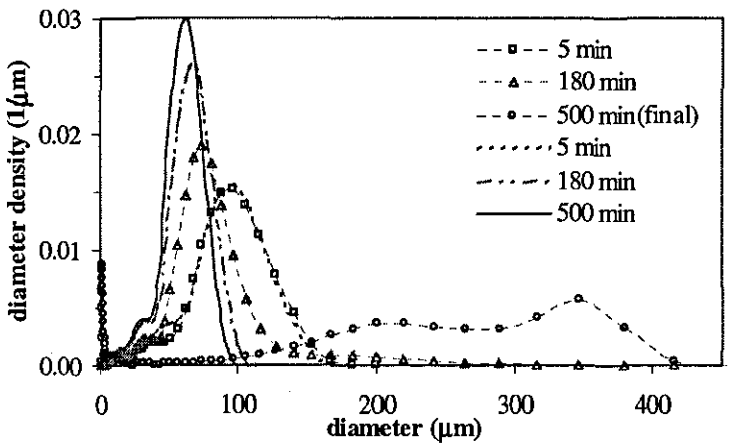

Figure E.3 Comparison of time evolution of PSD/DSD for suspension polymerisation of styrene and the corresponding dispersion (graphs with symbols present suspension polymerisation).

Satellite droplets/particles were also produced in the styrene/water dispersion and polymerisation. *Figure E.4* illustrates the time variations of the volume fraction of satellite droplets (f_{vs}) for the two processes. A close look at this figure reveals two important points:

First, the formation of satellite droplets occurs less frequently for the styrene monomer in comparison with the methyl methacrylate monomer (see *Figure 3.1.6*, chapter 3, for comparison). The higher interfacial tension between styrene and the continuous phase (an aqueous solution of water containing 1.0 g/l of PVA), which is 18.5 dyn/cm at 70°C (Konno et al., 1982), in comparison with that for the MMA system (3.15 dyn/cm at 25°C, see part 3.1, chapter 3), depresses the formation of satellite droplets due to suppression of drop break up. A similar reason can be also put forward for the larger daughter drops obtained for the styrene monomer, in comparison with the MMA monomer.

Second, the evolution of f_{vs} was different for the two monomers. For the styrene monomer f_{vs} increased during the whole course of polymerisation reaction with a rate similar to the rate of

polymerisation (see *Figure E.1*). The formation of satellite particles occurred more extensively during the growth stage where very viscous daughter particles underwent a massive growth. For the MMA monomer, the satellite particles formed during the polymerisation but most of them were lost during the growth stage due to their coalescence/flocculation with large particles. It is not apparent why satellite particles formed in the styrene suspension polymerisation are so stable that can escape coalescence with large particles during the growth stage. We were not able to further explore this finding.

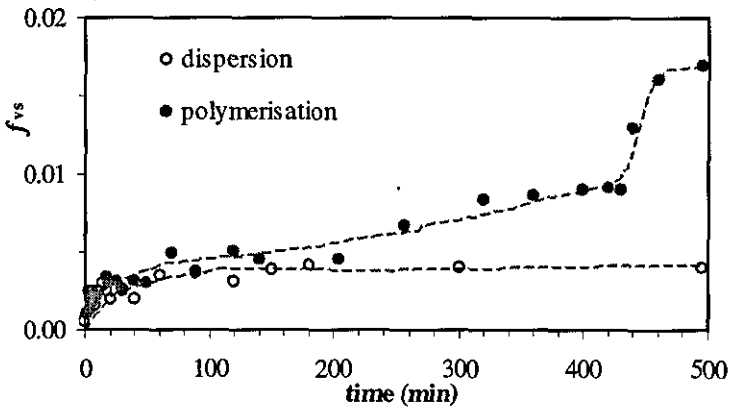

Figure E.4 Variations of fvs with time for suspension polymerisation of styrene and the corresponding dispersion.

APPENDIX F

Micrographs

Figure F.1 Micrographs of drops in the non-reacting dispersion at the following conditions: 70°C, N_I = 500 rpm, ϕ_d = 0.2, PVA = 10 g/l.

scale: 100 μm

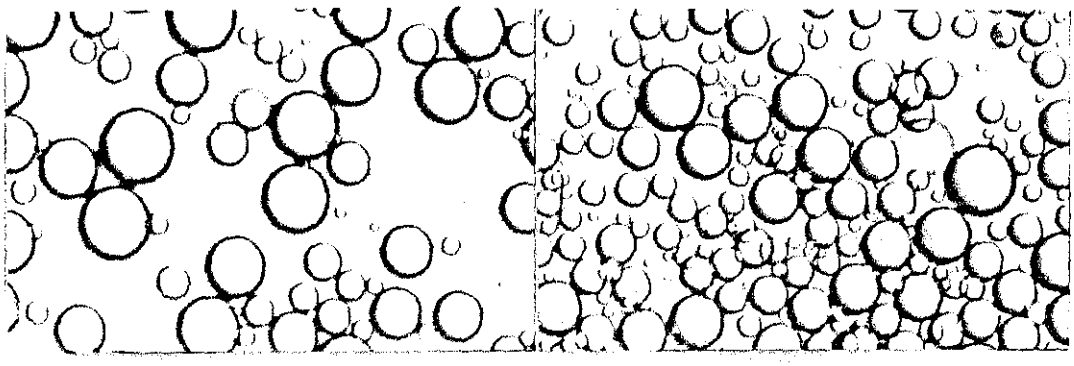

t = 5 min t = 15 min

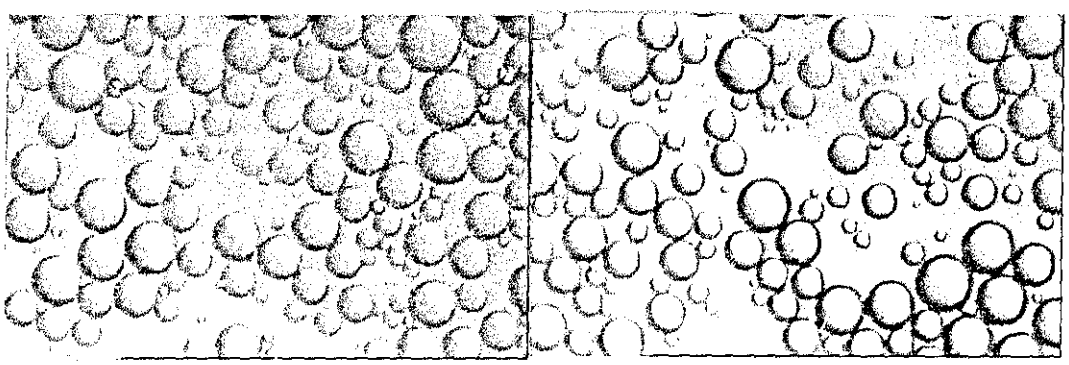

t = 30 min t = 60 min

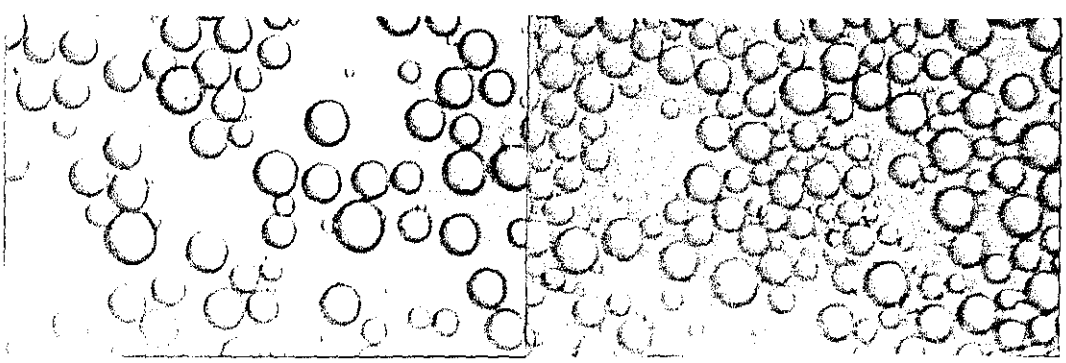

t = 120 min t = 180 min

Figure F.2 Micrographs of the final polymer particles obtained in the suspension polymerisation of MMA at the following conditions:
70°C, N_I = 500 rpm, ϕ_d = 0.2, LPO = 1 wt%, PVA = 10 g/l.

scale: 100 μm

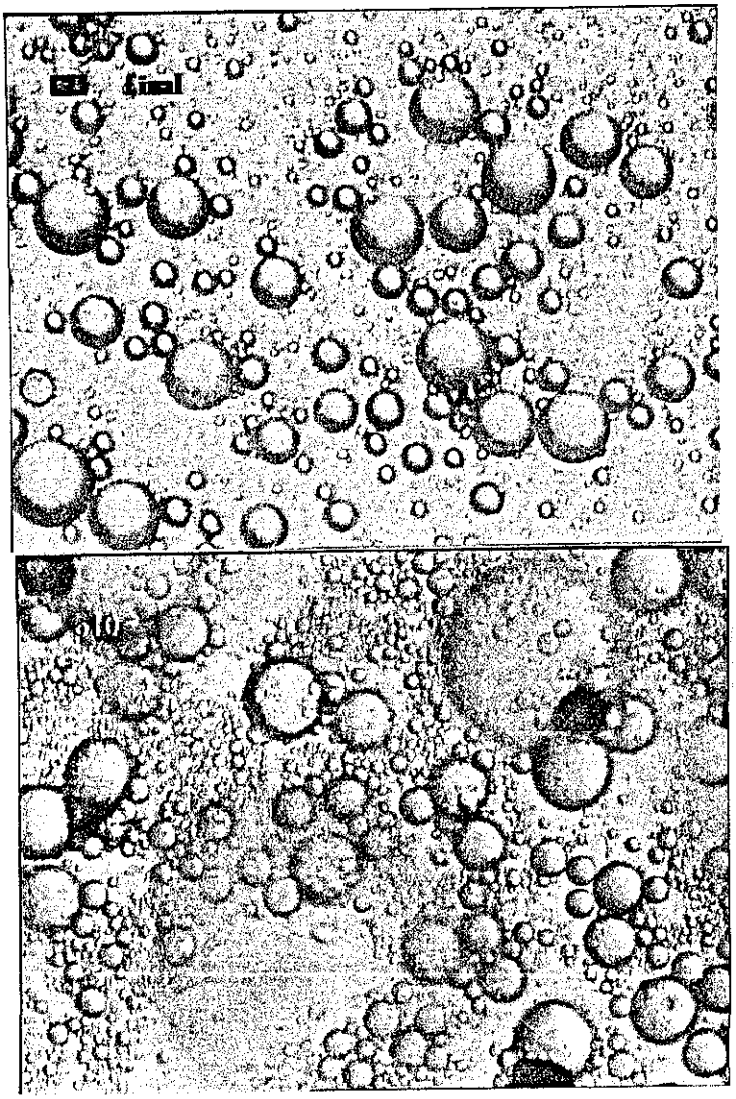

Figure F.3 shows some SEM micrograph of final polymer particles obtained in suspension polymerisation of MMA at the following conditions:

T = 70°C, N_I = 300 rpm, ϕ_d = 0.2, LPO = 1 wt%, PVA = 1 g/l.

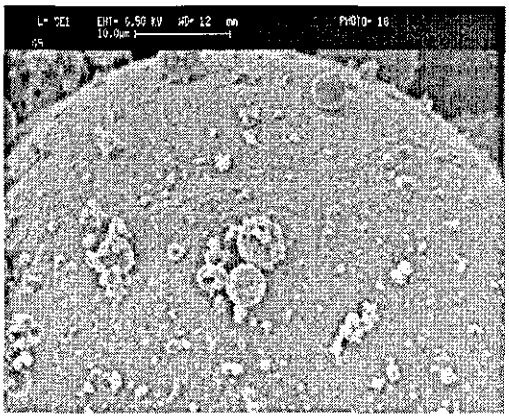

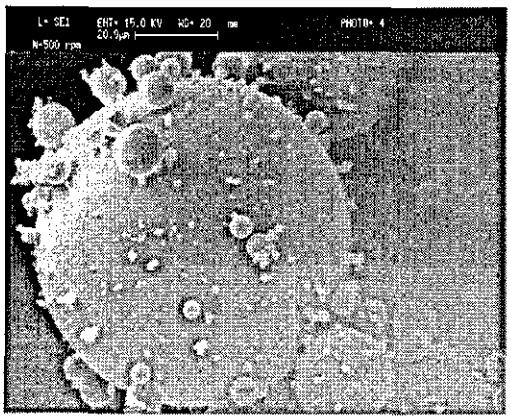

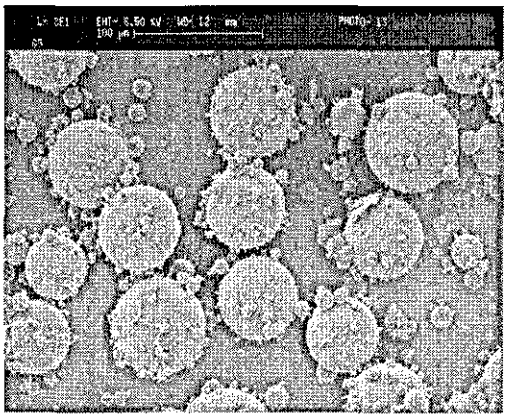

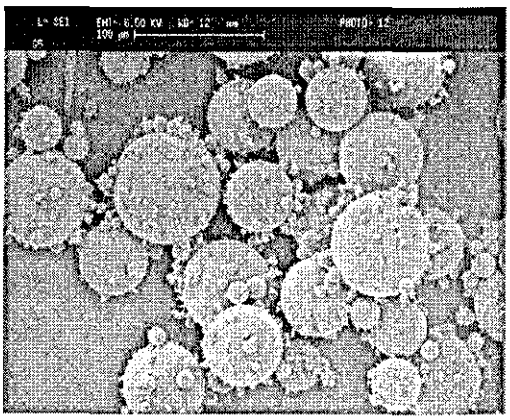

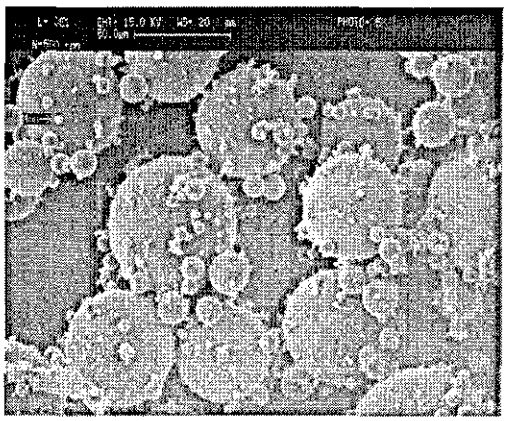

Figure F.4 shows SEM micrographs from final polymer particles obtained in suspension polymerisation of MMA in the presence of hydroquinone (HQ) at the following conditions: T = 70°C, N_I = 300 rpm, ϕ_d = 0.2, LPO = 1 wt%, PVA = 1 g/l.

HQ = 1 g (added to the aqueous phase)

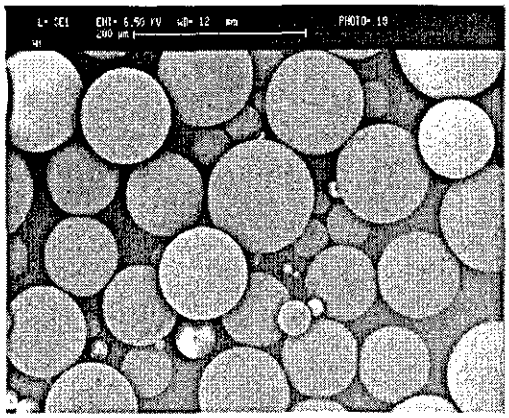

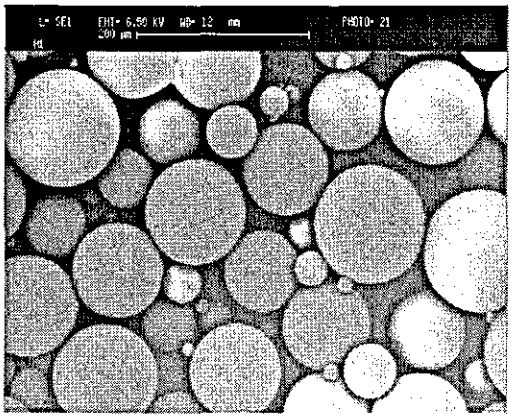

HQ = 4 g (added to the aqueous phase)

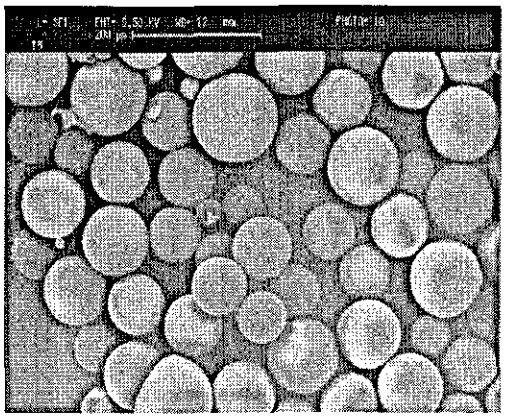

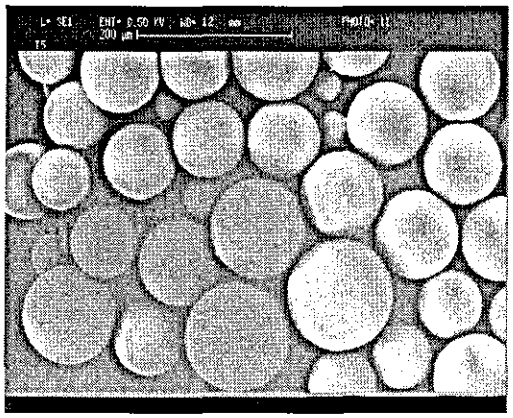

APPENDIX G

(appeared in Macromolecular Symposia, 2004, 206, 255-262)

On the Evolution of Particle Size Average and Size Distribution in Suspension Polymerization Processes

Fatemeh Jahanzad[1], *Shahriar Sajjadi*[2], *Brian W. Brooks*[1]*

[1]Department of Chemical Engineering, Loughborough University, Loughborough, Leicestershire, LE11 3TU, UK
*Email: b.w.brooks@lboro.ac.uk
[2]Division of Engineering, King's College London, London, WC2R 2LS, UK

Summary: The dispersion of methyl methacrylate (MMA) and its suspension polymerization were used as models to elaborate the evolution of particle size average and size distribution in the course of suspension polymerization. The underlying mechanisms for the occurrence of the dynamic and static steady states in the population of drops were defined and their effects on the evolution of drop/particle size average and size distributions were examined. The characteristic intervals of suspension polymerizations (transition, steady-state, growth, and identification) were elaborated. The formation of satellite droplets and their evolution in the course of polymerization were also discussed.

Keywords: suspension polymerization, dispersion, drop break up and coalescence, particle size distribution, steady-state

Introduction

In suspension polymerization, drops of monomer (containing initiator) are dispersed in an aqueous phase, which contains a stabilizer or suspending agent, with the aid of mechanical agitation. As polymerization reactions proceed in the dispersed monomer drops they are gradually converted to polymer particles. The suspending agent prevents excessive coalescence of drops. The product of this process is polymer particles or beads with diameters in the range of 1-5000 μm, depending on the process conditions.

The size of polymer beads is a complex function of drop break up and coalescence rates during the polymerization process. Those rates are affected by several parameters such as the

densities and viscosities of each phase, interfacial tension, type and concentration of suspending agent, dispersed-phase hold up, type of impeller and stirring speed[1-3].

A suspension polymerization can be described as a reactive liquid-liquid dispersion in which the nature of the drops change continuously with time. In a typical liquid-liquid dispersion, the average drop size at first decreases quickly because of a high rate of drop break up in comparison with drop coalescence. Eventually a point is reached when the rates of drop break up and drop coalescence become equal. That leads to the establishment of a so called quasi steady state in drop size and size distribution[4,5].

The evolution of drop size in suspension polymerization is more complex because drop viscosity increases continuously. As the drop viscosity increases, in the course of reaction, the tendency of drops to break up[6-9] and coalesce[10-12] is reduced. This will affect the balance of the rates of the break up and coalescence and may lead to an increase in the size of drops.

Suspension polymerization reactions produce particles with a broad size distribution. This is because different mechanisms for particle formation might coexist in suspension polymerization[13]. Three size classes of particles can be obtained from a suspension polymerization reactor. They are bead particles, satellite particles, and emulsion particles. Satellite particles are the result of the drop break up mechanism and/or nonhomogenities of the system[3]. Experimental evidence and model predictions have been presented to show that drops deform and burst into daughter drops and a number of satellite droplets[14-16]. Emulsion particles are the result of partial dissolution of the initiator in the water phase that gives free radicals that propagate to form new particles in the aqueous phase. These particles are usually smaller than the satellite particles.

In this paper, the characteristics of a model MMA suspension polymerization in the presence of polyvinyl alcohol (PVA) as stabilizer are studied. The evolution of drop/particle size and size distribution is compared with those in the corresponding MMA-water dispersion and some general conclusions are made.

Experimental

MMA (analytical grade from Aldrich) was distilled at reduced pressure. PVA (Mw = 85000-146000, degree of hydrolysis = 87-89% from Aldrich) and lauroyl peroxide (LPO) (97%,

from Aldrich) were used as stabilizer and initiator, respectively, without any further purification. Distilled water was used as continuous phase. The monomer volume fraction was 0.20 and different PVA concentrations were used. The suspension polymerization and dispersion used similar formulation, with the exception that in the suspension polymerization experiments an initiator concentration of 1.0 wt% (based on the monomer phase) was used.

The experiments were carried out using a one-litre jacketed glass reactor equipped with four 90° baffles. A four-paddle impeller was used for agitation. The stirring speed was 500 rpm for all experiments. The temperature of the vessel content was continuously monitored using a thermocouple and controlled within ± 0.5°C of the desired reaction temperature (70 °C). In suspension polymerization experiments nitrogen purging of the aqueous phase was carried out for 30 minutes before the monomer phase was added. Samples were withdrawn at the desired time intervals from the reaction vessel, using a hypodermic syringe, to measure the monomer conversion gravimetrically. Drop/particle size distributions were determined by using a laser diffraction particle sizer (Coulter LS130).

Results and Discussion

Dynamic Steady State

The evolution of the Sauter mean diameter (d_{32}) of the MMA-water dispersion with 0.5 g/l PVA is shown in Figure 1. In the dispersion process (without polymerization), the evolution of drop size can be divided into two stages; *transition* and *steady state*. The steady state drop size distribution in liquid-liquid dispersions will mainly depend on the relative magnitude of the rates of drop break up and coalescence. At steady state, when the rates of drop break up and coalescence are balanced, coalescence removes as many drops from the dispersion as are made via the break up mechanism. This has been called a *dynamic steady state* where individual drops do not retain a unique identity but undergo continuous break up and coalescence.

Figure 1 also illustrates the evolution of d_{32} in the corresponding suspension polymerization with 0.5 g/l PVA. Similar to the dispersion process, during the *transition stage* drops are reduced in size, until they reach an almost constant average size. It can be seen that drops are less severely broken up during the transition stage for the suspension polymerization process

in comparison with the dispersion process. This implies that the formation of even a very small amount of polymer in monomer drops, during the first few minutes of suspension polymerization, suppresses the rate of drop break up and as a result larger drop sizes are formed at the end of this interval. The quasi steady-state drop size is established at a higher value for the suspension polymerization. Enhanced drop stability with adding a very small amount of polymer has been reported by Dowding et al.[11].

According to Figure 1, the particles start to grow at the time of 45 min and a steep rise in the drop size is observed at 60 min. Conversion-time data for this polymerization system shows a steep rise in the rate of polymerization at the time of 60 min, corresponding to the conversion of 0.50 (see the small graph in Figure 3). The acceleration in the rate of polymerization is the result of the gel effect which is caused by the increase in the drop viscosity. It should be noted here that the PVA concentration was found to have no effect on the rate of polymerization or conversion-time curve.

Based on the variations of drop size, as shown in Figure 1, the pattern of variation in drop size with time after the end of the transition stage can be characterised by up to three intervals depending on the polymerization conditions. The first interval is the *steady-state stage* during which a rather constant drop size is maintained by balanced rates of drop break up and coalescence despite an increase in the drop viscosity. A short quasi steady-state stage can be seen for the conditions given in Figure 1. The presence of a quasi steady state for suspension polymerization is not always certain and sometimes that condition is never reached. Even for the dispersion processes there is some reduction in the size of drops with time during the steady-state stage. However, such variations are relatively limited.

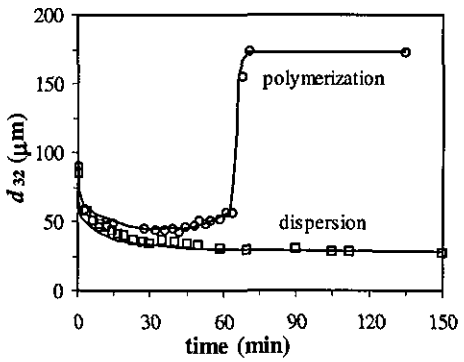

Figure 1- Comparison of evolution of d_{32} in the suspension polymerization of MMA and in the corresponding dispersion ([PVA]=0.5 g/l).

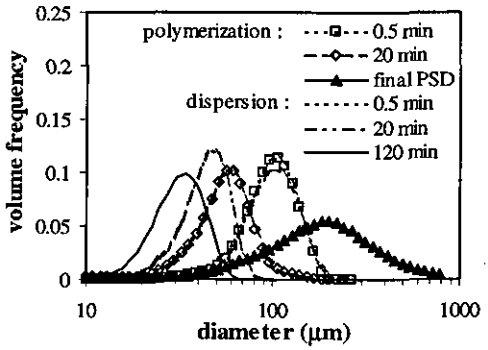

Figure 2- Evoluion of drop/paerticle size distribution for the systems shown in Figure 1.

As the drop viscosity increases, a point is reached where drops can not be easily broken up but they can still undergo coalescence. As a result, drops start growing by coalescence. This interval can be called *growth stage.* This stage has been called the *sticky stage* in the literature perhaps because of the impression that drop coalescence increases with the drop viscosity due to increasing drop tackiness. However, the present authors believe that this is a misleading title because, during this interval, particles are usually more stable against coalescence than in the earlier stage because of reduced mobility of the surface of drops. The viscosity increase in the drops reduces the rate of drop break up more significantly than drop coalescence resulting in an increase in the size of particles [17]. The abrupt increase in the size of drop during the growth stage is a direct result of a sudden viscosity build up in the drops because of the gel effect.

At the end of the growth stage, drops have a very high viscosity and behave like solid particles. These drops cannot coalesce with each other and they keep their identity for the remainder of the process. This has been called *identification point.* Variations in average drop size occur in both the transition stage and the growth stage but sizes remain almost constant during the steady state and during the *identification stage* (i.e., after the indentification point is reached); although some limited flocculation may occur during the identification stage.

Figure 2 shows that the size and size distribution of the reacting and non-reacting drops in the first minutes are similar. Later, during the transition period, the size distribution of both types of drops narrow significantly with time, due to a higher rate of drop break up in comparison with drop coalescence, until a steady-state value is reached. For the dispersion, the size distribution of drops does not change appreciably after the steady-state, but the size distribution of the reacting drops broadens with time when d_{32} changes as shown in Figure 1.

Static Steady State

Figure 3 illustrates the evolution of d_{32} in the suspension polymerization of MMA and in the corresponding MMA dispersion with 10 g/l PVA. For the dispersion process, a similar trend as to that found for 0.5 g/l PVA was obtained. For the suspension polymerization, however, the pattern was different from the suspension polymerization with 0.5 g/l PVA, but it was very similar to that found for the dispersions. In a liquid-liquid dispersion if drops are

reduced to a size that cannot be further broken by agitation and if they are also sufficiently protected against drop coalescence, then drops do not undergo any transformation during mixing and a *static steady-state* may be established. Such a dispersion has been called a *turbulent-stabilized* dispersion by Church and Shinnar[4]. Static steady-state can actually be achieved, or approached, if a high concentration of stabilizer, for example, is used. The resulting drops from such dispersions would be very small. Figure 3 shows that the increase in drop size is very small in the growth stage for the polymerizing drops despite the large increase in the drop viscosity.

Figure 4 depicts the evolution of drop/particle size distribution for conditions corresponding to those shown in Figure 3. For the suspension polymerization, particle growth and PSD broadening occurred to a very limited extent. It is expected that, at a higher PVA concentration, coalescence can be completely removed from the system and the evolution of drop size average and size distribution in suspension polymerizations follow similar trends to those in the corresponding dispersions. The experimental data from Konno et al.[18] for the suspension polymerization of styrene with 10 g/l PVA provides an evidence for such a claim. Although the size measurements with optical microscopy, as used by Konno et al.[18], may not be sufficiently sensitive to small variations in particle size.

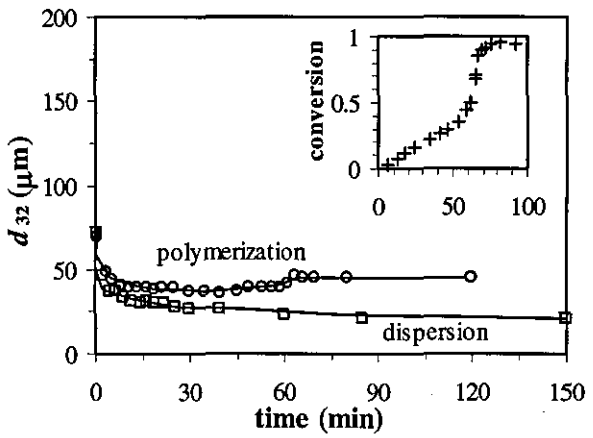

Figure 3- Comparison of evolution of d_{32} in the suspension polymerization of MMA and in the corresponding dispersion ([PVA]=10 g/l).

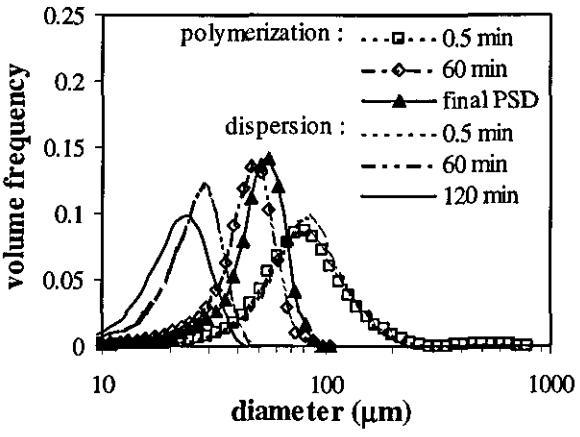

Figure 4- Evolution of drop/particle size distribution for the systems shown in Figure 3.

Satellite Droplets

The size distributions of drops/particles from the suspension polymerizations and dispersions were all bimodal. Figure 5 illustrates a typical PSD measured by using laser diffraction. The drop/particle size distributions included a main or primary peak corresponding to bead drops/particles within the size range of 10-300 μm. That was accompanied by a small secondary peak given by drop/particles with diameters less than 10 μm. The secondary peak is mainly the cumulative result of satellite droplet formation from drop break up but there is a partial contibution from particle formation via dispersion and/or emulsion polymerization mechanisms. Study on the secondary peak has been rarely reported in the literature[19,20]. We used an initiator with very limited water solubility, lauroyl peroxide, to minimize the formation of emulsion particles. The secondary peaks are not shown in Figures 2 and 4 and were ignored in the calculation of d_{32} for simplicity.

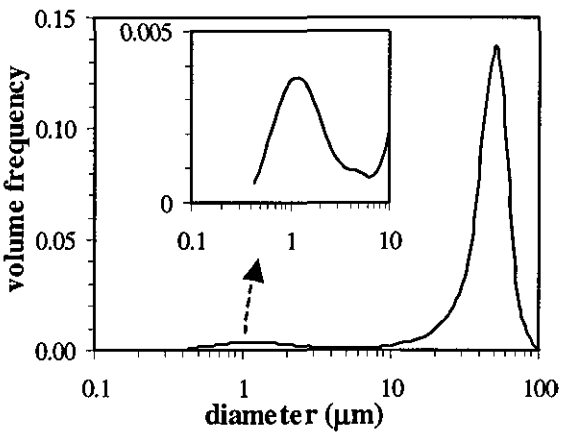

Figure 5- A typical drop size distribution in Suspension polymerization of MMA (t=60 min, [PVA]=10 g/l).

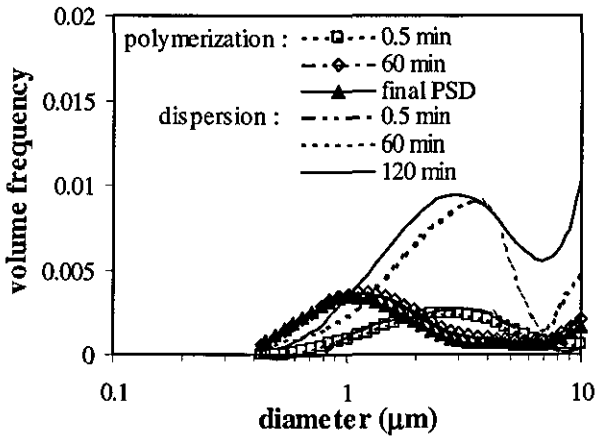

Figure 6- Evolution of satellite size distribution for the systems shown in Figure 5.

Figure 6 illustrates evolution of the size distribution of secondary particles for suspension polymerization of MMA with 10 g/l PVA and for the corresponding dispersion. Satellite droplets were continuously formed with time in the dispersion system. For the polymerization system the satellite size distribution is narrower and smaller in comparison with the corresponding dispersion which can be the result of increasing viscosity in polymerizing drops. In suspension polymerizations with lower PVA concentration the population of

satellite droplets dropped significantly during the growth stage because of coalescence and/or flocculation.

Conclusion

The evolution of drop/particle size distribution in suspension polymerization may pass through four intervals; transition, steady-state, growth and identification stages. As the stability of drops in a suspension polymerization is enhanced, by increasing stabilizer concentration for example, the evolution of drop size distribution approaches that in the corresponding dispersion. That evolution is characterized by a transition stage followed by a steady-state stage. That can only occur if the dynamic steady state can transform to a static one. The size average and distribution of satellite particles obtained via suspension polymerization were smaller and narrower, respectively, than those found in the corresponding dispersion at the conditions of this study. The results suggest that tracking of the evolution of satellite particles could lead to a better understanding of the mechanism of drop formation in suspension polymerization.

References

[1] B.W. Brooks, *Makromol. Chem. Macromol. Symp.* **1990**, 35/36, 121
[2] H.G. Yuan, G. Kalfas, W.H. Ray, *J. Macromol. Sci., Rev. Macromol. Chem. Phys.*, **1991**, C31(2&3), 215.
[3] E. Vivaldo-Lima, P.E. Wood, A.E. Hamielec, A. Penlidis, *Ind. Eng. Chem. Res.* **1997**, 36, 939.
[4] J.M. Church, R. Shinnar, *Ind. Eng. Chem.* **1961**, 53, 479.
[5] P.O. Hong, J.M. Lee, *Ind. Eng. Chem. Process Des. Dev.* **1985**, 24, 868.
[6] J.O. Hinze, *AIChE J.* **1955**, 1, 950.
[7] R.V. Calabrese, T.P.K. Chang, P.T. Dang, *AIChE J.* **1986**, 32(4), 657.
[8] A. Koshy, T.R. Das, R. Kumar, K.S. Gandhi, *Chem. Eng. Sci.* **1988**, 43(10), 2625.
[9] A.N. Sathyagal, D. Ramkrishna, G. Narimhan, *Chem. Eng. Sci.* **1996**, 51(9), 1377.
[10] S. Liu, D. Li, *Chem. Eng. Sci.* **1999**, 54, 5667.
[11] P.J. Dowding, J.W. Goodwin, B. Vincent, *Colloid Polym. Sci.* **2000**, 278, 346.
[12] S. Hashim, B.W. Brooks, *Chem. Eng. Sci.* **2002**, 57(17), 3703.
[13] M.F. Cunningham, *Polym. React. Eng.*, **1999**, 7(2), 231.
[14] G. Narsimhan, D. Ramkrishna, J.P. Gupta, *AIChE J.*, **1980**, 26, 991.
[15] E.G. Chatzi, A.D. Gavrielides, C. Kiparissides, *Ind. Eng. Chem. Res.* **1989**, 28, 1704.
[16] E.G. Chatzi, C. Kiparissides, *AIChE J.*, **1995**, 41(7), 1640.
[17] J. Alvarez, J.J. Alvarez, M.A. Hernandez, *Chem. Eng. Sci.* **1994**, 49(1), 99.
[18] M. Konno, K. Arai, S. Saito, *J. Chem. Eng. Japan* **1982**, 15(2), 131.
[19] G. Polacco, M. Palla, D. Semino, *Polym. Int.* **1999**, 48, 392.
[20] C. Desnoyer, O. Masbernat, C. Gourdon, *Chem. Eng. Sci.* **2003**, 58(7), 1353.